Università degli Studi di Palermo

SCUOLA POLITECNICA

Dipartimento di Ingegneria Civile, Ambientale, Aerospaziale, dei Materiali

Dottorato in Ingegneria Civile e Ambientale

Ingegneria delle Strutture

ciclo XXV

Coor.: Prof. Orazio Giuffrè

PH.D. THESIS

Stochastic dynamic analysis of structures with fractional viscoelastic constitutive laws

Candidato:

Ing. Francesco Paolo Pinnola

Relatori:

Ch.mo Prof. Mario Di Paola

Ch.mo Prof. Pol D. Spanos
(*Rice University*)

S.S.D. ICAR/08

Stochastic dynamic analysis of structures with fractional viscoelastic constitutive laws

Ph.D thesis submitted to the University of Palermo

by

Francesco Paolo Pinnola

Dipartimento di Ing. Civile Ambientale, Aerospaziale, dei Materiali
Università degli Studi di Palermo
Scuola Politecnica
Viale delle Scienze, Ed. 8 - 90128 Palermo

FRANCESCO PAOLO PINNOLA
Palermo, December 2014
e-mail:francesco.pinnola@unipa.it
e-mail:francescopaolopinnola@gmail.com

Thesis of the Ph.D. course in *Structural Engineering*
Dipartimento di Ingegneria Civile Ambientale, Aerospaziale, dei Materiali
Università degli Studi di Palermo
Scuola Politecnica
Viale delle Scienze, Ed.8 - 90128 Palermo, ITALY

Written in LaTeX
Examples and figures made with *Wolfram Mathematica*©

"Quelli che s'innamorano di pratica, sanza scienza, son come 'l nocchiere, ch'entra in navilio sanza timone o bussola, che mai ha certezza dove si vada.
***Sempre la pratica dev'esser edificata sopra la bona teorica**. . . "*[1]

[1] Leonardo Da Vinci (1452-1519).

Contents

Preface xi

Introduction xiii

Notation xxi

1 Special functions and integral transforms 1
- 1.1 Special functions . . . 1
  - 1.1.1 Euler gamma function . . . 1
  - 1.1.2 Mittag-Leffler function . . . 5
  - 1.1.3 Wright function . . . 7
- 1.2 Bessel functions . . . 7
  - 1.2.1 Functions of the first and the second kind . . . 7
  - 1.2.2 Modified Bessel functions . . . 9
- 1.3 Laplace transform . . . 10
  - 1.3.1 Properties of the Laplace transform . . . 11
  - 1.3.2 Application to differential equations . . . 13
- 1.4 Fouirer transform . . . 14
  - 1.4.1 Properties of the Fourier transform . . . 16
  - 1.4.2 Application to differential equations . . . 17
- 1.5 Mellin transform . . . 18
  - 1.5.1 The fundamental strip . . . 19
  - 1.5.2 Properties of the Mellin transform . . . 20

2 Fractional Operators 23
- 2.1 Brief history . . . 23
- 2.2 Fractional derivatives and integrals . . . 25
  - 2.2.1 The Grünwald-Letnikov differintegral . . . 26

2.2.2 The Riemann-Liouville definition . . . 29
2.2.3 Riesz fractional integrals . . . 31
2.2.4 Caputo's approach . . . 31
2.3 Properties of fractional operators . . . 32
2.3.1 The linearity . . . 32
2.3.2 The Leibniz rule . . . 33
2.3.3 The semigroup rule . . . 34
2.4 Laplace transform of fractional operators . . . 35
2.4.1 Laplace transform of Riemann-Liouville fractional derivative . . . 35
2.4.2 Laplace transform of Caputo's fractional derivative . . . 35
2.4.3 Laplace transform of Grünwald-Letnikov fractional derivative . . . 36
2.5 Fourier transform of fractional operators . . . 36
2.5.1 Fourier transform of fractional integral . . . 36
2.5.2 Fourier transform of fractional derivative . . . 37
2.6 Mellin transform of fractional operators . . . 38
2.6.1 Mellin transform of Riemann-Liouville fractional integral 38
2.6.2 Mellin transform of Riemann-Liouville fractional derivative . . . 38
2.6.3 Mellin transform of Caputo's fractional derivative . . . 40
2.7 Some examples of fractional derivatives . . . 40
2.7.1 Unit step function . . . 40
2.7.2 Power-law function . . . 41

3 Linear viscoelastic stress-strain constitutive law 43
3.1 Preliminary remarks . . . 43
3.2 The elastic Hooke's model . . . 44
3.3 The viscous Newton-Petroff model . . . 45
3.4 The viscoelastic model . . . 46
3.4.1 The Maxwell model . . . 46
3.4.2 The Kelvin-Voigt model . . . 48
3.4.3 Other classical models . . . 49
3.5 The creep and the relaxation function . . . 50
3.5.1 The Boltzmann superposition principle . . . 51
3.5.2 Creep and relaxation function for the Maxwell model . . . 54
3.5.3 Creep and relaxation function for the Kelvin-Voigt model 55
3.6 The fractional-order viscoelastic model . . . 56

3.6.1 The Nutting's experience . . . 57
3.6.2 The spring-pot . . . 58
3.6.3 The integral formulation of fractional viscoelasticity . . . 60
3.6.4 The generalized fractional models . . . 63
3.6.5 Characteristic times and apparent modulus . . . 64
3.6.6 Triaxial stress-strain relation . . . 69

4 Mechanical model of fractional viscoelasticity 73
4.1 The mechanical description of fractional law . . . 74
4.2 The discretization of fractional viscoelastic model . . . 78
4.2.1 Discrete model of elasto-viscous material . . . 78
4.2.2 Discrete model of visco-elastic material . . . 80
4.3 The modal analysis of the discrete models . . . 82
4.3.1 Elasto-viscous materials . . . 82
4.3.2 Visco-elastic materials . . . 84
4.3.3 The critical value of $\beta : \beta = 1/2$ . . . 86
4.4 Numerical examples . . . 87
4.5 Conclusions . . . 90

5 Dynamics of structures with fractional viscoelastic behavior 93
5.1 Preliminary remarks . . . 93
5.2 Continuous fractionally damped beam . . . 94
5.2.1 Vibration of Euler-Bernoulli beam modeled using fractional Kelvin-Voigt . . . 94
5.2.2 Numerical solution in the time domain . . . 97
5.2.3 Stochastic analysis in frequency domain . . . 98
5.2.4 Numerical application . . . 99
5.3 Lumped-parameter systems with fractional viscoelastic devices 102
5.3.1 Fractional multi-degree-of-freedom systems . . . 103
5.3.2 State variable analysis of fractional MDOF . . . 104
5.3.3 Numerical applications of fractional SDOF . . . 107
5.3.4 Numerical applications of fractional MDOF . . . 112
5.4 Conclusions . . . 117

6 Stochastic processes represented by fractional calculus 119
6.1 Preliminary remarks . . . 119
6.2 Cross-correlation function by complex fractional moments . . . 120
6.3 Cross-power spectral density function by complex spectral moments . . . 124

6.4 The fractional oscillator under Gaussian white noise 126
6.5 Numerical examples 129
6.5.1 Correlation function of fractional oscillator with $\beta = 1/2$ 129
6.5.2 Two-degree-of-freedom system under white noise 132
6.6 Conclusions 137

Concluding remarks **141**

A Tables of fractional derivatives **145**
A.1 Fractional operators with lower bound $a = -\infty$ 145
A.2 Fractional derivatives with lower bound $a = 0$ 146

B Main used commands in Mathematica **147**
B.1 Special functions 147
B.2 Bessel functions 148
B.3 Integral transforms 148
B.3.1 Laplace transform and its inverse 148
B.3.2 Fourier transform and its inverse 148
B.3.3 Mellin transform and its inverse 148
B.4 Fractional operators 149
B.4.1 Grünwald-Letnikov 149
B.4.2 Riemann-Liouville 149
B.4.3 Caputo 149

C Complex fractional moments **151**
C.1 Properties and relation with fractional calculus 151
C.2 Some exact CSMs for fractional half oscillators 152

Bibliography **155**

Acknowledgements **167**

List of Figures

1.1 Absolute value of the gamma function . . . 2
1.2 Euler gamma function . . . 4
1.3 Bessel function of first kind . . . 8
1.4 Bessel function of second kind . . . 9
1.5 Modified Bessel functions . . . 10

2.1 Fractional derivative of the Unit step function . . . 41

3.1 Hooke's model . . . 45
3.2 Newton-Petroff model . . . 45
3.3 Maxwell model . . . 47
3.4 Kelvin Voigt model . . . 48
3.5 SLS or Zener models . . . 49
3.6 Creep function . . . 51
3.7 Relaxation function . . . 51
3.8 Imposed stress history and corresponded strain . . . 52
3.9 Continuous imposed stress history . . . 53
3.10 Relaxation and creep function for the Maxwell model . . . 55
3.11 Relaxation and creep function of the Kelvin-Voigt model . . . 56
3.12 The spring-pot . . . 59
3.13 Best-fitting of relaxation data of epoxy resin . . . 61
3.14 Best-fitting of creep function of epoxy resin . . . 62
3.15 Normalized characteristic times . . . 66
3.16 Normalized relaxation and creep function . . . 68
3.17 Continuum of Cauchy . . . 69

4.1 Continuous fractional models . . . 76
4.2 Discretized counterpart of the EV model . . . 79

4.3 Discretized counterpart of the VE model 81
4.4 Continuous and discretized fractional axial models. 82
4.5 Kelvin-Voigt elements in modal space (EV) 84
4.6 Kelvin-Voigt elements in modal space (VE) 85
4.7 Creep test of EV model 88
4.8 Creep test of VE model 89
4.9 Power-law function and summation of exponentials 90

5.1 Euler-Bernoulli beam 95
5.2 Cantilever beam 100
5.3 Power spectral density of transversal displacement 101
5.4 Displacement variance 101
5.5 Unit step response of the FSDOF 109
5.6 Displacement variance of FSDOF system. 111
5.7 Fractional two-degree-of-freedom system. 112
5.8 Displacements of the dynamical system 114
5.9 PSDs of the response $X_1(t)$ and $X_2(t)$. 116
5.10 Variances of displacements of two-degree-of-freedom system . 116

6.1 Exact and approximated PSD 131
6.2 Approximated CF by CSMs 132
6.3 PSDs of the response $X_1(t)$ and $X_2(t)$ 136
6.4 CPSD of the response $X_1(t)$ and $X_2(t)$ 137
6.5 CF of the response $X_1(t)$ 138
6.6 CF of the response $X_2(t)$ 138

Preface

This manuscript summarizes my main research activity in this last triennium. It adheres to a common procedure of solving a scientistic problem. That is, introduction to the problem, selection of the mathematical and physical tools to model the problem, proposed solution, and experimental/numerical validation.

The main topics considered are the characterization and the modeling of the mechanical behavior of real materials, and the stochastic dynamics with special regards to the characterization of the stochastic processes. To address these two different kinds of problem an advanced mathematical tool is used. In particular, the differential calculus with non-integer operators offers several new mathematical tools that permit obtaining advanced results.

Therefore, two different topics are studied: mechanical modeling of materials, and stochastic characterization of random process. Both arguments are used in order to pursue one final aim. That is, the *structural dynamics of real structures and structural elements built with advanced material*. This is an important goal that regards many physical and engineering problems. Indeed, in several mechanical and engineering problems it is needed to perform the dynamic analysis of such structures that are increasingly complex, and made with advanced materials. For such structures the classical models and the common tools of the structural dynamics are unable to provide an accurate description of the real problem. Obviously, to perform this kind of dynamical analysis it is necessary to define properly the global model of the structure, to describe correctly the real mechanical behavior of the building materials, and to simulate the external forced processes that load the structures during their life.

The characterization of the mechanical behavior of real building materials is obtained with the aid of recent advanced models which involve fractional operators in the constitutive stress-strain relation. This kind of model

is known as *fractional viscoelasticity*. The choice of this kind of stress-strain model is due to the fact that the fractional viscoelasticity allows to obtain the best agreement with experimental observations for a plethora of materials. After such choice, it is necessary to define the global mechanical model of the structure. In this work both continuous and discretized models of structures with fractional viscoelastic constitutive law are considered.

To complete the dynamic analysis it is needed to represent the real external loads and the corresponding output in terms of displacements of the considered structures. In many cases of engineering interest the external loads are adequately modeled as random processes (earthquake excitation, wind velocity field, ocean-waves actions, impact loading, etc.). To perform this characterization, the classical tools of *stochastic dynamics* are developed by using fractional calculus. In particular, the fractional operators permit obtaining a new stochastic characterization of the inputs (external actions) and outputs (displacements) process.

Declaration

This manuscript contains the main part of my own research performed at the Department of Civil, Environmental, Aerospace and Materials Engineering, University of Palermo, and at the Department of Civil and Environmental Engineering, Rice University; the research was carried out from January 2012 through December 2014. The thesis contains my own results, and where stated, some developments from the work done in collaboration.

Francesco Paolo Pinnola
Palermo, December 2014

Introduction

Aims and reasons

The main purpose of this thesis is to provide a new way to correctly perform stochastic analysis of structures with viscoelastic constitutive law. The reason for this kind of problem relates the fact that structures with viscoelastic materials are built in many areas of mechanical, civil and aerospace engineering. To perform this kind of stochastic analysis there are two fundamental problems. That is, the mechanical description of the viscoelastic phenomenon, and the correct representation of the external loads. Both of these problems are addressed and solved by the proposed modeling that involves some advanced mathematical tools.

The reason to describe materials as viscoelastic is given by the fact that the elastic model, commonly used to describe the mechanical behavior in the classic approach of the mechanics of materials is an idealization of the real mechanical behavior. Indeed, many materials are not completely elastic but have a mechanical behavior intermediate between the purely elastic behavior, that is typical of the solids, and the purely viscous behavior, which is common in the fluids. This phenomenon is known as viscoelastic behavior and is typical of many different materials used in various engineering fields. Moreover, in recent years complex materials, increasingly used in engineering applications, have been obtained with the aid of sophisticated industrial processes aiming to enhance stiffness and strength of materials. For these latter materials the elastic models do not yield an adequate representation of the real mechanical behavior and the modeling through viscoelastic laws is always greater. Besides, the viscoelastic properties cannot be neglected when it is necessary to evaluate the long-term effects in the structures. For example, concrete and some kinds of rocks, that are commonly modeled as elastic-brittle materials, for long observation times they also show viscoelastic behavior. Viscoelas-

tic materials, commonly used in the engineering fields, are woods, pultruded elements, elastomers, fibre-reinforced-polymers, resins, bio-inspired materials, etc.. Other materials which have viscoelastic properties are some kinds of rocks, bitumens, bones, rubbers, biologic tissues, etc..

There are different ways to model the stress-strain relation of the viscoelastic material but the best results, compared to the experimental investigation are given by the use of fractional operators in the stress-strain relation.

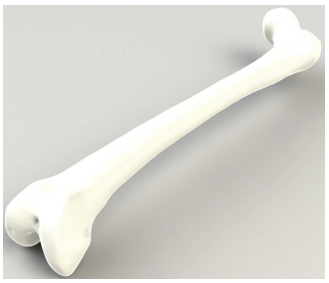
Biological Tissues

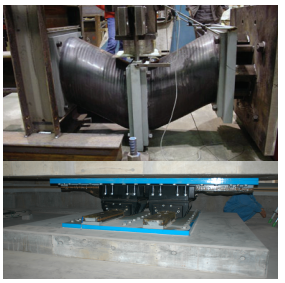
Elastomeric and damped devices


Kolding Bridge


Eyecatcher Building

After the choice of the correct way to model the stress-strain relation (the local model), to perform the dynamic analysis it is necessary to properly model the structure. In other words, it is needed to pass from the local stress-strain relation model to the global load-displacement model. In this manuscript two different global models are considered: the continuous model of the beam, and the discretized multi-degree-of-freedom system with lumped parameters. The first one represents the continuous viscoelastic structural elements (rods, beam, etc.); the second one is capable of describing the structures with viscoelastic devices which can be modeled as frames (building, space frame, etc.).

The last step of the dynamic analysis involves the modeling of the external loads. The choice to perform the dynamic analysis as stochastic is justified by the fact that the external loads acting on the structures are well modeled as random processes. For this reason some tools of the stochastic mechanics will be introduced and developed with the aid of the fractional calculus.

Mathematical tools

In addition to the common tools of the mechanics (eigenvalue analysis, Monte Carlo simulation, step-by-step integration, etc.), an important tool, widely used in this manuscript, is the fractional calculus. It is no more than the

generalization of the ordinary differential and integral calculus to the non-integer derivatives and integrals. The theory of non-integer order derivation goes back to seventeenth century, when in 1695 *Leibniz*, in his letter, asked about the meaning of half derivative to *L'Hôpital*. With this event the study of derivatives and integrals with arbitrary order began, and this study has continued to the end of nineteenth century by *Liouville*, *Grünwald*, *Letnikov* e *Riemann*.

Despite the fact that fractional calculus has existed for more than two hundred years, in the engineering and physics fields its application has been relatively limited. Perhaps, the main reason of this limitation is due to the fact that this kind of operators have no obvious geometrical meaning. This implies that in some physical application there is no obvious mechanical interpretation of the analytical law which involves fractional operators. In the present work this powerful tools is used to describe the viscoelastic stress-strain relation of the real materials, and in stochastic mechanics to perform a new description of the random processes by the complex spectral moments.

Fractional constitutive laws

Several scientists have been experimentally demonstrated that the best way to describe the viscoelastic behavior of real materials is by fractional operators in the stress-strain relation. After an accurate study of the existent results, and with the aid of some experimental investigations performed at the laboratory of the Department of Civil, Environmental, Aerospace and Materials Engineering of University of Palermo, it is possible to assert that the elastic model and the classic models of viscoelasticity are unable to fully describe the viscoelastic phenomenon. For this reason it is needed to introduce an advanced model which involves the fractional differential operators in the stress-strain relation $\sigma(t) - \varepsilon(t)$.

The fractional constitutive law also contains the the perfect elastic model and the purely Newtonian one. Indeed the fractional law contains these two behavior as bounded cases. This kind of model is able to give a good agreement with the experimental observations, and excellent results can be obtained by the best-fitting of experimental test with the aid of few parameters.

Continuous and discrete models

After the choice of the local stress-strain relation, the dynamic analysis of real structures is driven by introducing a proper global model which must be able to describe the behavior in terms of displacements and loads $u(t) - q(t)$.

Two kinds of global models are considered, the continuous systems and the discretized one with lumped parameters. In both cases, the choice of fractional operators in the local stress-strain relation leads to have fractional differential equations in the global displacement-load relations when the dynamic analysis is performed. This kind of differential equations are more difficult to solve respect to the integer-orders one. For this reason new methods to solve this kind of equations are developed and provided in this manuscript.

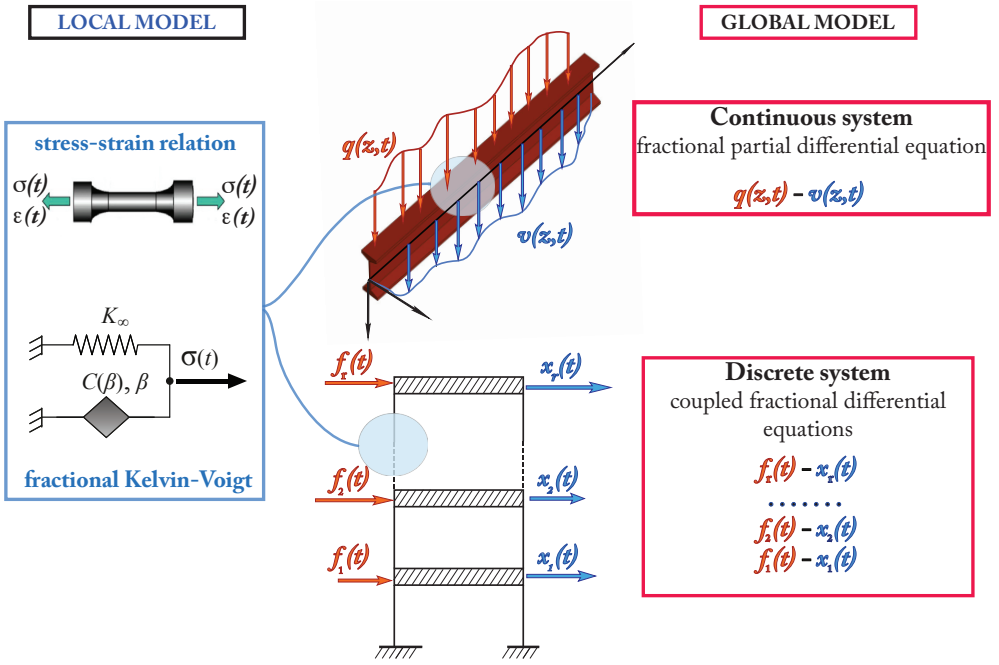

As continuous system, the Euler-Bernoulli beam with fractional dampers is considered; while, as discretized case, the case of shear-type multi-degree-of freedom system with fractional viscoelastic elements is discussed.

The dynamic analysis of a continuous Euler-Bernoulli beam with fractional dampers leads to a partial fractional differential equation in term of

the displacements $u(z,t)$, and the external loads $q(z,t)$ as

$$\rho\frac{\partial^2}{\partial t^2}u(z,t) + C(\beta)J\frac{\partial^4\partial^\beta}{\partial z^4\partial t^\beta}u(z,t) + EJ\frac{\partial^4}{\partial z^4}u(z,t) = q(z,t), \tag{1}$$

where $u(z,t)$ denotes the displacements function in the time t along the beam axis z, J is the moment of inertia of the cross section, ρ is the mass density, $C(\beta)$ and β are characteristic coefficients of the fractional stress-strain relation, and E is the Young's modulus. This problem is solved by the proposed eigenanalysis with the aid of the eigenfunction of the classic elastic Euler-Bernoulli beam and the solution of a set of uncoupled fractional differential equations in the modal space. The analysis is conducted considering both stochastic and deterministic loads. Structural elements that can be modeled as continuous Euler-Bernoulli beams with viscoelastic dampers are the pultruded elements, which are composed by fibers with elastic-brittle behavior into a matrix with pronounced viscoelastic behavior.

The discretized multi-degree-of-freedom system with lumped parameters with fractional viscoelastic elements leads to a set of coupled fractional differential equations that rule the motion of the model as

$$\mathbf{M}\boldsymbol{x}(t) + \sum_{j=1}^{n}\mathbf{C}_j\left(\mathrm{D}^{j\beta}\boldsymbol{x}\right)(t) + \mathbf{K}\boldsymbol{x} = \mathbf{f}(t), \tag{2}$$

where $\mathbf{M}$ and $\mathbf{K}$ are the matrix of mass and stiffness, respectively, $\mathbf{C}_j$ are the matrices that contain the parameters of the fractional viscoelastic elements, $j\beta$ are the fractional orders involved, $\boldsymbol{x}(t)$ represents the vector of nodal displacements, and $\mathbf{f}(t)$ is the vector of the forced loads. In the general case such coupled system cannot be decoupled by the classical methods. For this reason, a novel method based on complex eigenanalysis in the expanded state variables domain.

Stochastic characterization of the response

The external loads in the structures are often well modeled as stochastic processes. In this manner the response in terms of function (in the continuous model) or vector (in the discretized models) displacements is stochastic as well. In order to characterize the response from a stochastic point of view the fractional calculus provides some important tools that are also discussed in

this thesis, with particular emphasis on the characterization of the structures with fractional viscoelastic constitutive law forced by Gaussian white noise.

In particular, with the aid of the complex spectral moments, that are related to the fractional integrals of the power-spectral density function, it is possible to obtain a complete characterization of the stochastic processes. This method is used in conjunction with other results to provide a new description of the stochastic response of the fractional multi-degree-of-freedom system under Gaussian white noise.

Organization of the thesis

This thesis comprises six Chapters. The first two Chapter contain some concepts about the advanced mathematical tools used. In particular, Chapter 1 is devoted to the introduction of some special functions needed to understand the basic concept about the mathematical tools used in fractional calculus. This Chapter also contains the property of the integral transforms.

Chapter 2 introduces the fractional calculus. The fractional derivatives and integrals and their properties are discussed extensively. Particular attention is devoted to this kind of differential calculus since it represents the main used tool in the following Chapters.

Chapter 3 recalls the concepts inherent in the linear stress-strain relations of the viscoelasticity. In particular, the different ways to model this kind of phenomenon, the classic models (Kelvin-Voigt, Maxwell, SLS, etc.), the integral representation of the viscoelasticity and the fractional stress-strain relation are discussed. The capabilities of the fractional model are also shown.

Chapter 4 presents the mechanical interpretation of the fractional stress-strain relation. In particular, with the aid of the recent developments in the fractional viscoelasticity, this Chapter demonstrates that the analytical law which involves fractional operators in the stress-strain constitutive law has a mechanical counterpart. This is an important aspect from an engineering point of view, since it shows that the fractional operators in the mechanical law are more than simple mathematical tools because they also have the corresponding physical meanings.

Chapter 5 discusses the dynamic analysis of real structures with fractional viscoelastic constitutive law. In particular, it deals with two different cases: the continuous structural elements, and the discrete system. In the first part the dynamic analysis of continuous fractional viscoelastic beam is considered.

Whereas, the second part is devoted to the analysis of multi-degree of freedom systems with lumped parameters endowed with fractional viscoelastic devices. For the latter case a new state variable transformation is proposed to simplify the solution. In both cases the forced loads are modeled as stochastic processes and the corresponding responses of the systems (continuous and discrete) are obtained by the step-by-step integration and the Monte Carlo simulation.

In the Chapter 6 a stochastic representation of the random processes by the complex spectral moments is presented. This method is used in conjunction with the expanded state variable analysis, introduced in the previous Chapters, to provide a new representation of the stochastic response of the multi-degree-of-freedom system endowed with fractional viscoelastic devices.

Notation

In order to make easier the reading of this manuscript, it is showed below the mainly used symbols and acronyms (in order of appearance).

$f(t)$	function of the real variable t
$\left(\mathrm{D}^{\alpha}_{a^+}\cdot\right)(t)$	Grünwald-Letnikov fractional differintegral of order α
$\left(D^{\alpha}_{a^+}\cdot\right)(t)$	Riemann-Liouville fractional derivative of order α
$\left(\mathrm{I}^{\alpha}_{a^+}\cdot\right)(t)$	Riemann-Liouville fractional integral of order α
$\left({}_{\mathrm{C}}D^{\alpha}_{a^+}\cdot\right)(t)$	Caputo's fractional derivative of order α
$\left(\mathbf{I}^{\alpha}\cdot\right)(t)$	Riesz fractional integral of order α
$\left(\mathbf{H}^{\alpha}\cdot\right)(t)$	complementary Riesz fractional integral of order α
α or β	real differintegration order
γ	complex integral order
a	lower bound of the fractional operator
t	time variable and/or upper bound
z or s	complex variable
j or i	imaginary unit $j = i = \sqrt{-1}$
$\mathbb{N}$	set of the natural numbers
$\mathbb{Q}$	set of the rational numbers

$\mathbb{R}$	set of the real numbers
$\mathbb{C}$	set of complex numbers
$*$	convolution product
$\mathcal{L}\{\}$ $\mathcal{L}^{-1}\{\}$	Laplace transform operator and its inverse
$\mathcal{F}\{\}$ $\mathcal{F}^{-1}\{\}$	Fourier transform operator and its inverse
$\mathcal{M}\{\}$ $\mathcal{M}^{-1}\{\}$	Mellin transform operator and its inverse
$\mathrm{F}_{\mathcal{L}}(s)$	Laplace transform of $f(t)$
$\mathrm{F}_{\mathcal{F}}(\omega)$	Fourier transform of $f(t)$
$\mathrm{F}_{\mathcal{M}}(s)$	Mellin transform of $f(t)$
$\Re()$	real part of complex number
$\Im()$	imaginary part of complex number
$\Gamma(z)$	Euler gamma function
$\mathrm{E}_{\alpha,\beta}(z)$	Mittag-Leffler function
$W(z,\, \alpha,\, \beta)$	Wright function
$J_\nu(z)$ and $Y_\nu(z)$	first and second kind Bessel functions
$I_\nu(z)$ and $K_\nu(z)$	first and second kind modified Bessel functions
$\delta(t)$	generalized Dirac delta function
$U(t)$	Unit step function
$rect(t)$	rectangular function
$\sigma(t)$	stress history
$\varepsilon(t)$ and $\gamma(t)$	axial and shear strain history
$\Phi(t)$	relaxation function
$\Psi(t)$	creep function

$G(t)$	shear relaxation function
$J(t)$	shear creep function
$\mathbf{T}$	Cauchy stress tensor
$\boldsymbol{\varepsilon}$	deformation tensor
J^{σ}	linear invariant of $\mathbf{T}$
J^{ε}	linear invariant of $\boldsymbol{\varepsilon}$
$\mathbf{T}^{d}$	deviatoric part of the stress tensor
$\boldsymbol{\varepsilon}^{d}$	deviatoric part of the deformation tensor
E	Young's modulus
G	shear modulus
ν	Poisson's ratio
K	bulk modulus
EV	elasto-viscous
VE	visco-elastic
$\mathrm{H}(\omega)$	transfer function
$\mathbf{I}$	identity matrix
$\mathbf{M}$	mass matrix
$\mathbf{C}$	damping matrix
$\mathbf{C}_{\beta}$	matrix of the coefficients of fractional terms with order β
$\mathbf{K}$	stiffness matrix
$\boldsymbol{x}(t)$	vector of displacements $x_j(t)$
FSDOF	fractional single-degree-of-freedom
FMDOF	fractional multi-degree-of-freedom

$\mathbf{H}(\omega)$	transfer matrix
$\mathbf{z}(t)$	vector of state variables $z_j(t)$
$\mathbf{\Phi}$	matrix of eigenvectors
$\boldsymbol{\phi}_j$	j^{th} eigenvector
λ	eigenvalue
$\mathbf{\Psi}$	matrix of complex eigenvectors
$\boldsymbol{\psi}_j$	j^{th} complex eigenvector
$\mathrm{g}(t)$	Green function
$\mathrm{E}[\cdot]$	expectation operator
$W(t)$	Gaussian white noise process
$w_k(t)$	k^{th} realization of the Gaussian white noise
S_0	power spectral density of the Gaussian white noise $W(t)$
$X(t)$	stochastic process
$x_k(t)$	k^{th} realization of the stochastic process $X(t)$
σ_X^2	stationary variance of the stochastic process $X(t)$
$R_X(\tau)$	correlation function of the process $X(t)$
CF	correlation function
$S_X(\omega)$	power spectral density of the process $X(t)$
PSD	power spectral density
$R_{XY}(\tau)$	cross-correlation function of the processes $X(t)$ and $Y(t)$
CCF	cross-correlation function
$S_{XY}(\omega)$	cross-power spectral density of the process $X(t)$ and $Y(t)$
CPSD	cross-power spectral density

$\mathrm{M}_X(\gamma - 1)$	complex moment of order $\gamma - 1$ of the process $X(t)$
CFM	complex fractional moment
$\Lambda_X(-\gamma)$	spectral complex moment of order $-\gamma$ of the process $X(t)$
CSM	complex spectral moment

Chapter 1

Special functions and integral transforms

This Chapter introduces some special functions, the knowledge of which is necessary to fully understand the fractional calculus and the topics reported in what follows.

Further, other concepts about the integral transforms of Laplace, Fourier and Mellin are discussed. In particular, some properties of the mathematical transforms for the ordinary differential calculus are introduced. The knowledge of those properties will expedite the application of the transforms to the fractional differential calculus, that will be discussed in the next Chapter.

1.1 Special functions

Knowledge of some special functions is indispensable to understand fractional calculus. This section reports briefly these special functions and its properties. In particular, the special functions discussed are the Euler gamma function, the Mittag-Leffler, and the Wright functions. Other insights about this argument can be found in [20, 53–55, 64, 77, 83, 91, 99].

1.1.1 Euler gamma function

One of the fundamental special functions of fractional calculus is the Euler gamma function $\Gamma(z)$. This function generalizes the concept of factorial $n!$ for non-integer and/or complex value of n. Indeed, this function was obtained

from an interpolation problem placed in a letter from *Christian Goldbach* (1690-1764) to the young *Leonhard Euler* (1707-1783): *find a simple formula to evaluate the factorials also for non-integer number*.

The gamma function, in the positive half-plane of z, is defined by integral

$$\Gamma(z) := \int_0^\infty e^{-t} t^{z-1}\, dt; \tag{1.1}$$

the integral converges in the right side of the complex plane (that is with $\Re(z) > 0$); indeed, if $z = x + jy$

$$\begin{aligned} \Gamma(x+jy) &= \int_0^\infty e^{-t} t^{x-1+jy}\, dt = \int_0^\infty e^{-t} t^{x-1} e^{jy\log(t)}\, dt \\ &= \int_0^\infty e^{-t} t^{x-1} \left\{\cos\left[y\log(t)\right] + j\sin\left[y\log(t)\right]\right\} dt, \end{aligned} \tag{1.2}$$

the expression in the square brackets is bounded $\forall t$; convergence at infinity is given by e^{-t}, and if $x = \Re(z) > 1$ also the convergence at the origin is provided. The gamma function is a *meromorphic* function, it has simple poles

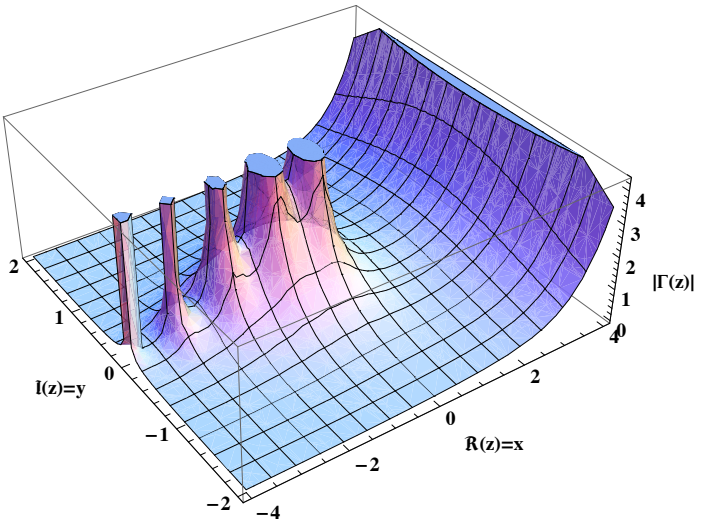

Figure 1.1: Absolute value of the Euler gamma function on the Gauss plane ($|\Gamma(z)|$ for $z \in \mathbb{C}$).

for $x = -n$ (with $n = 1, 2, 3, \dots$) and it is continuous and positive for real and positive values of z (that is for $\Re(z) > 0$). Figure 1.1 shows the absolute value

of gamma function on the Gauss plane ($|\Gamma(z)|$ for $z \in \mathbb{C}$), it can be seen the presence of isolated singularities for $x = -n$.

Another representation of the Euler gamma function has been provided by Gauss, in the form

$$\Gamma(z) := \lim_{n\to\infty} \frac{n! n^z}{z(z+1)\dots(z+n)}. \tag{1.3}$$

From the integral formulation of gamma function in Eq. (1.1) some common integral forms can be readily obtained. The most known one is

$$\sqrt{\pi} = \Gamma\left(\frac{1}{2}\right) = \int_0^\infty t^{-\frac{1}{2}} e^{-t}\, dt. \tag{1.4}$$

The Table 1.1 shows some common values of the Euler gamma function.

$\Gamma(-\frac{3}{2}) = \frac{4}{3}\sqrt{\pi}$	$\Gamma(1) = 1$
$\Gamma(-1) = \pm\infty$	$\Gamma(\frac{3}{2}) = \frac{1}{2}\sqrt{\pi}$
$\Gamma(-\frac{1}{2}) = -2\sqrt{\pi}$	$\Gamma(2) = 1$
$\Gamma(0) = \pm\infty$	$\Gamma(\frac{5}{2}) = \frac{3}{4}\sqrt{\pi}$
$\Gamma(\frac{1}{2}) = \sqrt{\pi}$	$\Gamma(3) = 2$

Table 1.1: Common values of $\Gamma(x)$ for $-\frac{3}{2} \leq x \leq 2$

.

Properties of gamma function

A fundamental property of the gamma function is that

$$\Gamma(z+1) = z\Gamma(z), \tag{1.5}$$

which can be demonstrated by integration by parts. Specifically

$$\Gamma(z+1) = \int_0^\infty e^{-t} t^z \, dt = \left[-e^{-t} t^z \right]_{t=0}^{t=\infty} + z \int_0^\infty e^{-t} t^{z-1} \, dt = z\Gamma(z), \tag{1.6}$$

and by taking into account of Eq. (1.5), and by knowing that $\Gamma(1) = 1$,

$$\begin{aligned} \Gamma(2) &= 1\Gamma(1) = 1 = 1! \\ \Gamma(3) &= 2\Gamma(2) = 2 \cdot 1! = 2! \\ \Gamma(4) &= 3\Gamma(3) = 3 \cdot 2! = 3! \\ &\dots \quad \dots \quad \dots \quad \dots \quad \dots \\ \Gamma(n+1) &= n\Gamma(n) = n \cdot (n-1)! = n! \end{aligned} \tag{1.7}$$

that property can be readily seen in Figure 1.2(a). Indeed, it shows the graph

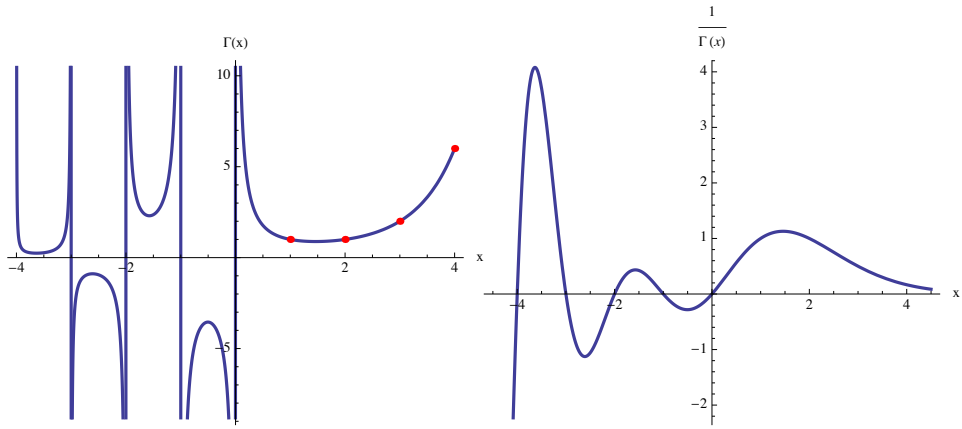

(a) $\Gamma(x)$ **(b)** $\Gamma(x)^{-1}$

Figure 1.2: Euler gamma function and its inverse for $x \in \mathbb{R}$.

of the function $\Gamma(x)$ for $x \in \mathbb{R}$; the red dots have as abscissa $x = n$ (with $n \in \mathbb{N}$) and as ordinate $\Gamma(n) = (n-1)!$.

In the next Chapter, in the definitions of fractional operator, there will be the *inverse gamma function*, that is $\Gamma(x)^{-1}$. The graph of this function for $x \in \mathbb{R}$ is shown in Figure 1.2(b). It can be seen that the trend of the inverse gamma function is oscillating for negative values of x and it tends to zero for $x \to \infty$.

Moreover, observe that the function $\Gamma(z)$ does not have zero finite values, then its inverse is an integer function.

A particular property of the gamma function is given by the relation

$$\Gamma(z)\Gamma(1-z) = \frac{\pi}{\sin \pi z}; \tag{1.8}$$

this Eq. (1.8) is known as *Euler's reflection formula*.

Moreover, the following relation holds:

$$\Gamma(z)\Gamma\left(z+\frac{1}{2}\right) = 2^{1-2z}\sqrt{\pi}\cdot\Gamma(2z); \quad 2z \neq 0, -1, -2, \ldots. \tag{1.9}$$

that is known as *duplication formula*. This formula is a special case of the *multiplication theorem*

$$\Gamma(z)\Gamma\left(z+\frac{1}{m}\right)\Gamma\left(z+\frac{2}{m}\right)\ldots\Gamma\left(z+\frac{m-1}{m}\right) = (2\pi)^{\frac{m-1}{2}} m^{\left(\frac{1}{2}-mz\right)}\Gamma(mz). \tag{1.10}$$

The derivative of gamma function can be expressed by the product of itself and other functions. Indeed,

$$\Gamma'(z) = \Gamma(z)\cdot\psi_0(z),$$

where ψ_0 is the *polygamma function of order 0*. In particular,

$$\Gamma'(1) = -\gamma,$$

where γ is the *Euler-Mascheroni* constant ($\gamma = 0,57721566$).

1.1.2 Mittag-Leffler function

The swedish mathematician *Magnus Gustaf (Götta) Mittag-Leffler* introduced in the 1903 the special function $\mathrm{E}_\alpha(z)$. That function is defined by the power series

$$\mathrm{E}_\alpha(z) := \sum_{k=0}^{\infty} \frac{z^k}{\Gamma(\alpha k+1)}. \tag{1.11}$$

Eq. (1.11) represents the Mittag-Leffler (M-L) function in one-parameter (α) form. Another definition, that plays an important role in the fractional calculus, is the two-parameters M-L function, defined by:

$$\mathrm{E}_{\alpha,\beta}(z) := \sum_{k=0}^{\infty} \frac{z^k}{\Gamma(\alpha k+\beta)}; \quad (\alpha > 0, \ \ \beta > 0). \tag{1.12}$$

From the definition in Eq. (1.12), some particular cases can be readily obtained. Specifically,

$$\mathrm{E}_{1,1}(z) = \sum_{k=0}^{\infty} \frac{z^k}{\Gamma(k+1)} = \sum_{k=0}^{\infty} \frac{z^k}{k!} = e^z, \tag{1.13}$$

$$\mathrm{E}_{1,2}(z) = \sum_{k=0}^{\infty} \frac{z^k}{\Gamma(k+2)} = \sum_{k=0}^{\infty} \frac{z^k}{(k+1)!} = \frac{1}{z} \sum_{k=0}^{\infty} \frac{z^{k+1}}{(k+1)!} = \frac{e^z - 1}{z}, \tag{1.14}$$

and

$$\mathrm{E}_{1,3}(z) = \sum_{k=0}^{\infty} \frac{z^k}{\Gamma(k+3)} = \sum_{k=0}^{\infty} \frac{z^k}{(k+2)!} = \frac{1}{z^2} \sum_{k=0}^{\infty} \frac{z^{k+2}}{(k+2)!} = \frac{e^z - 1 - z}{z^2}. \tag{1.15}$$

For $\alpha = 1$ and generic value of β, M-L becomes:

$$\mathrm{E}_{1,m}(z) = \frac{1}{z^{m-1}} \left\{ e^z \sum_{k=0}^{m-2} \frac{z^k}{k!} \right\}. \tag{1.16}$$

It can be seen that if the parameter $\beta = 1$, the two-parameters M-L function becomes the one-parameter one. Indeed,

$$\mathrm{E}_{\alpha,1}(z) = \sum_{k=0}^{\infty} \frac{z^k}{\Gamma(\alpha k + 1)} \equiv \mathrm{E}_{\alpha}(z). \tag{1.17}$$

As shown in Eqs. (1.13)-(1.15) the M-L function is related to some particular functions for certain values of the parameters α and β. Also the hypergeometric sine and cosine are particular cases of the M-L function:

$$\mathrm{E}_{2,1}(z^2) = \sum_{k=0}^{\infty} \frac{z^{2k}}{\Gamma(2k+1)} = \sum_{k=0}^{\infty} \frac{z^{2k}}{(2k)!} = \cosh(z); \tag{1.18}$$

$$\mathrm{E}_{2,2}(z^2) = \sum_{k=0}^{\infty} \frac{z^{2k}}{\Gamma(2k+2)} = \frac{1}{z} \sum_{k=0}^{\infty} \frac{z^{2k+1}}{(2k+1)!} = \frac{\sinh(z)}{z}. \tag{1.19}$$

Another particular case can be obtained by setting $\alpha = \frac{1}{2}$ and $\beta = 1$:

$$\mathrm{E}_{\frac{1}{2},1}(z) = \sum_{k=0}^{\infty} \frac{z^k}{\Gamma(\frac{k}{2}+1)} = e^{z^2} \mathrm{erfc}(-z), \tag{1.20}$$

where $\mathrm{erfc}(-z)$ represents the *complementary error function*, that is defined as

$$\mathrm{erfc}(z) = \frac{2}{\sqrt{\pi}} \int_z^{\infty} e^{-t^2}\, dt. \tag{1.21}$$

Other properties and applications of M-L function can be found in [6, 55, 64, 74, 91, 99].

1.1.3 Wright function

Useful function to solve the linear fractional differential equation is the *Wright function* [6, 53]. It is closely related to the two-parameters M-L and is defined as

$$W(z;\alpha,\beta) := \sum_{k=0}^{\infty} \frac{z^k}{k!\Gamma(\alpha k+\beta)}; \tag{1.22}$$

for $\alpha = 0$ and $\beta = 1$, the Wright function becomes:

$$W(z;0,1) = \sum_{k=0}^{\infty} \frac{z^k}{k!\Gamma(1)} = \sum_{k=0}^{\infty} \frac{z^k}{k!} = e^z. \tag{1.23}$$

If $\beta = 1-\alpha$ the Wright function becomes the *Mainardi's function* [6, 74]. It is denoted by $M(z;\alpha)$, and defined as

$$W(-z;-\alpha,1-\alpha) = M(z;\alpha) := \sum_{k=0}^{\infty} \frac{(-1)^k z^k}{k!\Gamma[-\alpha(k+1)+1]}. \tag{1.24}$$

1.2 Bessel functions

This section briefly introduces the Bessel functions. The concepts reviewed in this part are needed to understand the some developments in the ensuing Chapters. Other details about this special functions can be found in [29, 56, 88, 96].

1.2.1 Functions of the first and the second kind

The first two kinds of Bessel functions are defined as canonical solutions of the Bessel equation. That is,

$$z^2\frac{d^2y_\nu(z)}{dz^2} + z\frac{dy_\nu(z)}{dz} + (z^2-\nu^2)y_\nu(z) = 0. \tag{1.25}$$

It can be noted that the Eq. (1.25) represents an ordinary differential equation of second order, for which two linear independent solutions must exist at least. Other solutions in a finite domain can be represented by linear combination of the two linear independent solutions. A possible solution of Bessel equation is

$$J_\nu(z) = z^\nu \sum_{k=0}^{\infty} c_k z^k. \tag{1.26}$$

Using the Eq. (1.26) in Eq. (1.25) and placing $\nu \geqslant 0$ yields

$$J_\nu(z) := \left(\frac{z}{2}\right)^\nu \sum_{n=0}^{\infty} \frac{(-1)^n \left(\frac{z}{2}\right)^{2n}}{n!\Gamma(n+\nu+1)} \tag{1.27}$$

The Eq. (1.27), first solution of Eq. (1.25), is known as *Bessel function of first kind*. The Figure 1.3 shows this kind of function for some values of ν.

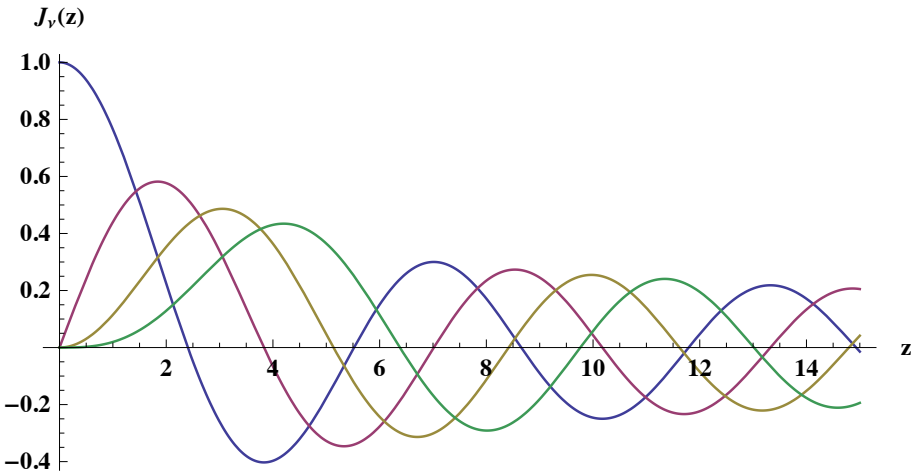

Figure 1.3: Bessel function of first kind for $\nu = 0, 1, 2, 3$.

For non-integer values of ν the function $J_{-\nu}(z)$ becomes the second solution of the Eq. (1.25). This second solution is linear independent by $J_\nu(z)$, it is denoted by $Y_\nu(z)$ and it can be expressed by linear combination of $J_\nu(z)$ and $J_{-\nu}(z)$. Specifically,

$$Y_\nu(z) := \frac{J_\nu(z)\cos(\pi\nu) - J_{-\nu}(z)}{\sin(\pi\nu)}; \tag{1.28}$$

this equation is known as *Bessel function of second kind* or *Neumann function*.

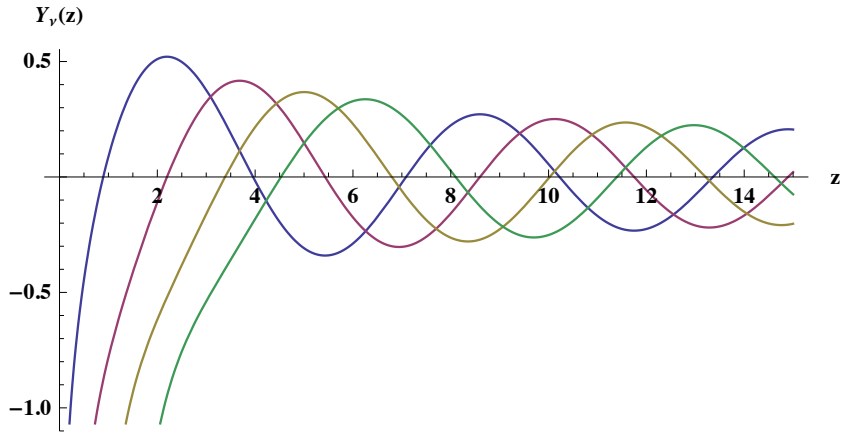

Figure 1.4: Bessel function of second kind for $\nu = 0, 1, 2, 3$.

Figure 1.4 shows the second solution of the Bessel function for certain values of ν. Comparing the two graphs it can be seen that the functions $J_\nu(z)$ have finite values at the origin (for $z = 0$), while the functions $Y_\nu(z)$ have singularities at $z = 0$.

Observe that for the particular case in which $\nu = 1/2$, the linear independent solutions of the Bessel equations becomes

$$J_{\frac{1}{2}}(z) = \frac{\cos(z)}{\sqrt{z}}, \qquad Y_{\frac{1}{2}}(z) = \frac{\sin(z)}{\sqrt{z}}. \tag{1.29}$$

This implies that at least some solutions of the Bessel equation may have oscillating trends, suggesting a similarity between the Bessel functions and the trigonometric functions.

1.2.2 Modified Bessel functions

The adjective “modified" denotes the Bessel functions with imaginary argument. Their equation is obtained by replacing z with jz in the Eq. (1.25). That is,

$$z^2\frac{d^2w_\nu(z)}{dz^2} + z\frac{dw_\nu(z)}{dz} + (z^2 - \nu^2)w_\nu(z) = 0. \tag{1.30}$$

The first solution of the Eq. (1.30) is

$$I_\nu(z) := e^{-j\frac{\pi}{2}\nu}J_\nu(z\,e^{j\frac{\pi}{2}}) = \sum_{k=0}^{\infty}\frac{\left(\frac{z}{2}\right)^{\nu+2k}}{k!\Gamma(k+\nu+1)} \tag{1.31}$$

this solution is known as the *modified Bessel function of the first kind*. Similarly to the previous Bessel function, if ν is non-integer, then $I_{-\nu}(z)$ is linear independent of $I_\nu(z)$. The linear combination of $I_\nu(z)$ and $I_{-\nu}(z)$ permits to obtain the second solution of Eq. (1.30), that is denoted by $K_\nu(z)$ and defined as

$$K_\nu(z) := \frac{\pi\left[I_{-\nu}(z) - I_\nu(z)\right]}{2\sin(\pi\nu)}, \tag{1.32}$$

the Eq. (1.32) is called *modified Bessel function of second kind* or rather *Basset function*. If the first and second kind Bessel function were related to the sine and cosine function, the modified Bessel function are similar to the hypergeometric function $\cosh(z)$ and $\sinh(z)$.

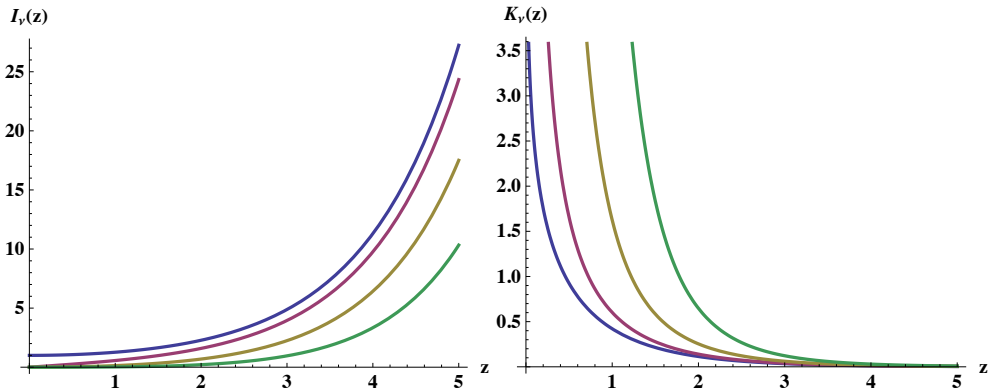

(a) $I_\nu(z)$ **(b)** $K_\nu(z)$

Figure 1.5: Modified Bessel functions for $\nu = 0, 1, 2, 3$.

Figure 1.5 shows the modified Bessel function for $\nu = 0, 1, 2, 3$. Observe that for real and positive values of z the functions $I_\nu(z)$ and $K_\nu(z)$ are real function, but their trends are not oscillating. In particular, $I_\nu(z)$ is a monotonically increased function, that becomes zero for $z = 0$ if $\nu > 0$. While, $K_\nu(z)$ has a singularity at the origin, and tends to zero when $z \to \infty$.

1.3 Laplace transform

The function $\mathrm{F}_\mathcal{L}(s)$ of the complex variable $s = \gamma + j\eta$, defined as

$$\mathrm{F}_\mathcal{L}(s) = \mathcal{L}\{f(t);\, s\} := \int_0^\infty e^{-st} f(t)\, dt \tag{1.33}$$

is known as the *Laplace transform* of the function $f(t)$. This transform allows switching the study of a function in the real variable t to the study in a complex space of variable s.

For the existence of the integral introduced in Eq. (1.33), the function $f(t)$ must be of exponential order α. This means that two positive constants M and T exist, these constants are such that:

$$e^{-\alpha t}|f(t)| \leq M, \quad \forall\, t > T, \tag{1.34}$$

the inequality in Eq. (1.34) implies that the function $f(t)$ must not grow faster then an exponential function of order α when $t \to \infty$.

From the Laplace transform $\mathrm{F}_{\mathcal{L}}(s)$ is possible to obtain the original function $f(t)$ by the *inverse Laplace transform*. Specifically,

$$f(t) = \mathcal{L}^{-1}\{\mathrm{F}_{\mathcal{L}}(s);\ t\} := \frac{1}{2\pi j}\int_{c-j\infty}^{c+j\infty} e^{st}\mathrm{F}_{\mathcal{L}}(s)\ ds, \tag{1.35}$$

where $c \in \Re(s) > c_0$, and c_0 belongs to the right plane of the absolute convergence of the Laplace integral. Observe that $f(t)$, from the inverse Laplace transform, is obtained by performing the integral along the imaginary axis, since the real part of s remains constant.

1.3.1 Properties of the Laplace transform

The Laplace transform of the summation of two functions $f(t)$ and $g(t)$ is equal to the summation of the transformations $\mathrm{F}_{\mathcal{L}}(s)$ and $\mathrm{G}_{\mathcal{L}}(s)$. That is,

$$\mathcal{L}\{f(t) + g(t);\ s\} = \mathrm{F}_{\mathcal{L}}(s) + \mathrm{G}_{\mathcal{L}}(s) \tag{1.36}$$

the Eq. (1.36) is obtained by assuming that for both functions the Laplace transform exists. The Eq. (1.36) represents the property of Laplace transform known as *additivity*.

Consider two function $f(t)$ e $g(t)$, for which the Laplace transform exists; for all $\lambda,\ \mu \in \mathbb{C}$ the following relation holds:

$$\mathcal{L}\{\lambda f(t) + \mu g(t);\ s\} = \lambda\mathcal{L}\{f(t);\ s\} + \mu\mathcal{L}\{g(t);\ s\} = \lambda\mathrm{F}_{\mathcal{L}}(s) + \mu\mathrm{G}_{\mathcal{L}}(s) \tag{1.37}$$

from which is possible to observe that the operator $\mathcal{L}\{\dots\}$ is *linear*.

Consider the *convolution* of two function $f(t)$ e $g(t)$, which are equal to zero for $t < 0$:

$$f(t) * g(t) = \int_0^t f(t-\tau)g(\tau)\ d\tau = \int_0^t f(\tau)g(t-\tau)\ d\tau, \tag{1.38}$$

the Laplace transform of this convolution is equal to the product of the Laplace transform of the two involved functions. That is,

$$\mathcal{L}\{f(t) * g(t);\ s\} = \mathrm{F}_{\mathcal{L}}(s)\mathrm{G}_{\mathcal{L}}(s); \tag{1.39}$$

the Eq. (1.39) holds true provided that $\mathrm{F}_{\mathcal{L}}(s)$ and $\mathrm{G}_{\mathcal{L}}(s)$ exist.

Next, consider the Laplace transform of a derivative of integer order n of the function $f(t)$. That is,

$$\mathcal{L}\{f^{(n)}(t);\ s\} = s^n\mathrm{F}_{\mathcal{L}}(s) - \sum_{r=0}^{n-1} s^{n-r-1}f^{(r)}(0) = s^n\mathrm{F}_{\mathcal{L}}(s) - \sum_{r=0}^{n-1} s^r f^{(n-r-1)}(0); \tag{1.40}$$

the Eq. (1.40) is obtained by integrating by parts under the assumption that the Laplace transform of $f^{(n)}(t)$ exists. The proof of Eq. (1.40) is trivial for $n = 1$:

$$\mathcal{L}\{f'(t);\ s\} = s\mathrm{F}_{\mathcal{L}}(s) - f(0) \tag{1.41}$$

Another property of the Laplace transform $\mathrm{F}_{\mathcal{L}}(s)$ is related to its derivative. Specifically,

$$\begin{aligned}\frac{d}{ds}\mathcal{L}\{f(t);\ s\} = \frac{d}{ds}\mathrm{F}_{\mathcal{L}}(s) = \frac{d}{ds}\int_0^\infty e^{-st}f(t)\,dt = \int_0^\infty \frac{d}{ds}e^{-st}f(t)\,dt \\ = -\int_0^\infty e^{-st}(tf(t))\,dt = -\mathcal{L}\{tf(t);\ s\}.\end{aligned} \tag{1.42}$$

For a fixed value of $s_0 \in \mathbb{C}$, the relation

$$\mathcal{L}\{e^{s_0 t}f(t);\ s\} = \mathcal{L}\{f(t);\ s - s_0\} = \mathrm{F}_{\mathcal{L}}(s - s_0) \tag{1.43}$$

holds. This Eq. (1.43), known as *frequency shifting*, can be readily proved by the definition of Laplace transform:

$$\mathcal{L}\{e^{s_0 t}f(t);\ s\} = \int_0^\infty e^{-st}e^{s_0 t}f(t)\,dt = \mathcal{L}\{f(t);\ s - s_0\}. \tag{1.44}$$

Moreover, for all $t_0 > 0$, if $f(t) = 0$ for all $t < 0$, the following property holds true:

$$\mathcal{L}\{f(t - t_0);\ s\} = e^{-s\,t_0}\mathcal{L}\{f(t);\ s\} = e^{-s\,t_0}\mathrm{F}_{\mathcal{L}}(s) \tag{1.45}$$

the Eq. (1.45) is known as *time shifting*.

For all $a > 0$, the following relation

$$\mathcal{L}\{f(at);\ s\} = \frac{1}{a}\mathcal{L}\left\{f(t);\ \frac{s}{a}\right\} = \frac{1}{a}\mathrm{F}_{\mathcal{L}}\left(\frac{s}{a}\right) \tag{1.46}$$

holds.

1.3.2 Application to differential equations

The Laplace transform allows to solve the differential equations with constant coefficients under assigned initial condition.

A not-homogeneous differential equation of order n, with constant coefficient c_k, can be expressed in the form

$$\sum_{k=0}^{n} C_k \frac{d^k x(t)}{dt^k} = f(t), \tag{1.47}$$

with appended initial conditions:

$$x(0) = x_0;\ x'(0) = x'_0;\ \dots\ x^{(n-1)}(0) = x_0^{(n-1)}; \tag{1.48}$$

for the uniqueness of the solution of the Eq. (1.47) the initial conditions must be n.

By performing the Laplace transform of Eq. (1.47):

$$\mathcal{L}\{x(t);\ s\} = \mathrm{X}_{\mathcal{L}}(s), \tag{1.49}$$

$$\mathcal{L}\{x'(t);\ s\} = s\mathrm{X}_{\mathcal{L}}(s) - x(0) = s\mathrm{X}_{\mathcal{L}}(s) - x_0, \tag{1.50}$$

$$\mathcal{L}\{x''(t);\ s\} = s^2\mathrm{X}_{\mathcal{L}}(s) - sx(0) - x'(0) = s^2\mathrm{X}_{\mathcal{L}}(s) - sx_0 - x'_0, \tag{1.51}$$

and setting

$$\mathcal{L}\{f(t);\ s\} = \mathrm{F}_{\mathcal{L}}(s), \tag{1.52}$$

from Eq. (1.47) is obtained that:

$$\mathrm{X}_{\mathcal{L}}(s)(c_0 + c_1 s + c_2 s^2 + \dots + c_n s^n) - \mathrm{P}_{n-1}(s) = \mathrm{F}_{\mathcal{L}}(s), \tag{1.53}$$

where $\mathrm{P}_{n-1}(s)$ is a polynomial in s of order $n-1$ that contains the summation of all contributions of the initial conditions. Eq. (1.53) yields

$$\mathrm{X}_{\mathcal{L}}(s) = \frac{\mathrm{F}_{\mathcal{L}}(s) + \mathrm{P}_{n-1}(s)}{(c_0 + c_1 s + c_2 s^2 + \dots + c_n s^n)}; \tag{1.54}$$

by performing the inverse Laplace transform of the Eq. (1.54), the solution $x(t)$ of the differential equation (1.47) is given in the form:

$$x(t) = \mathcal{L}^{-1}\{\mathrm{X}_{\mathcal{L}}(s);\ t\} = \frac{1}{2\pi j}\int_{c-j\infty}^{c+j\infty} e^{st}\mathrm{X}_{\mathcal{L}}(s)\ ds. \tag{1.55}$$

Example Consider the homogeneous differential equation

$$x''(t) + 7x'(t) + 8x(t) = 0$$

with the initial conditions:

$$\text{I.C.} \begin{cases} x(0) = 2, \\ x'(0) = 5. \end{cases}$$

By performing the Laplace transform of the given differential equation, one obtains:

$$s^2 \mathrm{X}_{\mathcal{L}}(s) - 2s - 5 + 7s\mathrm{X}_{\mathcal{L}}(s) - 14 + 8\mathrm{X}_{\mathcal{L}}(s) = 0,$$

$$\mathrm{X}_{\mathcal{L}}(s)(s^2 + 7s + 8) - (2s + 19) = 0,$$

$$\mathrm{X}_{\mathcal{L}}(s) = \frac{2s + 19}{(s^2 + 7s + 8)},$$

the solution $x(t)$ is given by the inverse Laplace transform of $\mathrm{X}_{\mathcal{L}}(s)$.

1.4 Fouirer transform

The *Fourier transform* of the continuous and fully integrable function $f(t)$ is defined as

$$\mathrm{F}_{\mathcal{F}}(\omega) = \mathcal{F}\{f(t);\ \omega\} := \int_{-\infty}^{\infty} e^{j\omega t} f(t)\ dt; \tag{1.56}$$

and it permits to express a mathematical function of time t as a function of frequency ω.

Starting from the knowledge of the Fourier transform $\mathrm{F}_{\mathcal{F}}(\omega)$, the function $f(t)$ can be determined by the inverse Fourier transform. That is,

$$f(t) = \mathcal{F}^{-1}\{\mathrm{F}_{\mathcal{F}}(\omega);\ t\} := \frac{1}{2\pi} \int_{-\infty}^{\infty} e^{-j\omega t} \mathrm{F}_{\mathcal{F}}(\omega)\ d\omega. \tag{1.57}$$

Clearly, the Fourier transform is nothing else that a particular case of the Laplace transform, in which the lower bound of the integral has been modified (from 0 to $-\infty$), and the variable $s = -j\omega$ has been introduced.

Some books report other definitions of the Fourier transform and its inverse as

$$\mathrm{F}_{\mathcal{F}}(\omega) = \mathcal{F}\{f(t);\ \omega\} := \frac{1}{2\pi} \int_{-\infty}^{\infty} e^{-j\omega t} f(t)\ dt,$$

$$\mathcal{F}^{-1}\{\mathrm{F}_{\mathcal{F}}(\omega);\ t\} := \int_{-\infty}^{\infty} e^{j\omega t}\mathrm{F}_{\mathcal{F}}(\omega)\ d\omega;$$

or even

$$\mathrm{F}_{\mathcal{F}}(\omega) = \mathcal{F}\{f(t);\ \omega\} := \frac{1}{\sqrt{2\pi}}\int_{-\infty}^{\infty} e^{j\omega t}f(t)\ dt;$$

$$\mathcal{F}^{-1}\{\mathrm{F}_{\mathcal{F}}(\omega);\ t\} := \frac{1}{\sqrt{2\pi}}\int_{-\infty}^{\infty} e^{-j\omega t}\mathrm{F}_{\mathcal{F}}(\omega)\ d\omega.$$

These latter ones are the definition used by the software *Mathematica*©. In the following the definition in Eq. (1.56) for the Fourier transform, and the definition in Eq. (1.57) for the inverse Fourier transform will be used.

The Eq. (1.56) is a complex function of a complex variable, then, by using the Euler formula, it can be distinguished the real from the imaginary part of $\mathrm{F}_{\mathcal{F}}(\omega)$. Specifically,

$$\begin{aligned}\mathcal{F}\{f(t);\ \omega\} &= \int_{-\infty}^{\infty} e^{j\omega t}f(t)\ dt \\ &= \int_{-\infty}^{\infty} \cos(\omega t)f(t)\ dt + j\int_{-\infty}^{\infty} \sin(\omega t)f(t)\ dt.\end{aligned} \tag{1.58}$$

The first part of the Eq. (1.58) is defined as the cosine-transform $\mathcal{F}_c\{f(t);\ \omega\}$ and it represents the real part of the Fourier transform $\Re(\mathcal{F})$. While, the second part, known as the sine-transform $\mathcal{F}_s\{f(t);\ \omega\}$, denotes the imaginary part of the transform $\Im(\mathcal{F})$.

From the Eq. (1.58) some useful observations can be drawn. Specifically, if $f(t)$ is even $\Rightarrow\ \mathcal{F}_s = 0\ \Rightarrow\ \mathrm{F}_{\mathcal{F}}(\omega) = \mathcal{F}_c\{f(t);\ \omega\}$, the Fourier transform is *real* and *even*; and if $f(t)$ is *odd* $\Rightarrow\ \mathcal{F}_c = 0\ \Rightarrow\ \mathrm{F}_{\mathcal{F}}(\omega) = \mathcal{F}_s\{f(t);\ \omega\}$, the Fourier transform is *imaginary* and *odd*.

Example: Consider the generalized *Dirac delta function* $\delta(t)$, by performing the Fourier transform of this function

$$\mathcal{F}\{\delta(t);\ \omega\} = 1,$$

this result cab be obtained by using the Euler formula. Indeed,

$$\int_{-\infty}^{\infty} \delta(t)\cos(\omega t)\ dt + j\int_{-\infty}^{\infty} \delta(t)\sin(\omega t)\ dt,$$

the second part is zero since the $\delta(t)$ is an even function, then for the sampling property of Dirac delta:

$$\big[\cos(\omega t)\big]_{t=0} = 1.$$

1.4.1 Properties of the Fourier transform

The Fourier transform has the *additivity* property

$$\mathcal{F}\{f(t)+g(t);\ \omega\} = \mathrm{F}_{\mathcal{F}}(\omega)+\mathrm{G}_{\mathcal{F}}(\omega), \tag{1.59}$$

under the assumption that for both functions $f(t)$ and $g(t)$ the Fourier transform exists.

Both the operators $\mathcal{F}\{\dots\}$ and $\mathcal{F}^{-1}\{\dots\}$ are *linear*. Thus,

$$\mathcal{F}\{\lambda f(t)+\eta g(t);\ \omega\} = \lambda \mathrm{F}_{\mathcal{F}}(\omega)+\eta \mathrm{G}_{\mathcal{F}}(\omega); \quad \forall \lambda,\ \eta \in \mathbb{C}. \tag{1.60}$$

Consider the Fourier transform of the *convolution*:

$$f(t) * g(t) = \int_{-\infty}^{\infty} f(t-\tau)g(\tau)\,d\tau = \int_{-\infty}^{\infty} f(\tau)g(t-\tau)\,d\tau, \tag{1.61}$$

for two function $f(t)$ and $g(t)$, which are defined in the range $(-\infty,\ \infty)$, the Fourier transform of their convolution is equal to the product of the transforms. That is,

$$\mathcal{F}\{f(t) * g(t);\ \omega\} = \mathrm{F}_{\mathcal{F}}(\omega)\mathrm{G}_{\mathcal{F}}(\omega), \tag{1.62}$$

under the assumption that the transforms $\mathrm{F}_{\mathcal{F}}(\omega)$ and $\mathrm{G}_{\mathcal{F}}(\omega)$ exist. The property in Eq. (1.62) will be useful to obtain the Fourier transform of the fractional operators.

Another useful property is related to the Fourier transform of the derivative of the function $f(t)$. In this regard, considering a continuous and n-derivable function, the Fourier transform yields

$$\mathcal{F}\{f^{(n)}(t);\ \omega\} = (-j\omega)^n \mathrm{F}_{\mathcal{F}}(\omega), \tag{1.63}$$

where n represents the derivation order.

The derivative of the Fourier transform is represented by

$$\mathcal{F}\{t^n f(t);\ \omega\} = (-j)^n \frac{d^n}{d\omega^n}\mathrm{F}_{\mathcal{F}}(\omega); \tag{1.64}$$

note that no all Fourier transforms $\mathrm{F}_{\mathcal{F}}(\omega)$ admit derivative of order n.

Considering $t_0 \in \mathrm{R}$, the Fourier transform yields

$$\mathcal{F}\{f(t+t_0);\ \omega\} = e^{-j\omega t_0}\mathrm{F}_{\mathcal{F}}(\omega), \tag{1.65}$$

while, assuming that $\omega_0 \in \mathrm{C}$, the Fourier transform provides

$$\mathcal{F}\{e^{j\omega_0 t} f(t);\ \omega\} = \mathcal{F}\{f(t);\ \omega + \omega_0\} = \mathrm{F}_{\mathcal{F}}(\omega + \omega_0) \tag{1.66}$$

such expression can be readily proved:

$$\mathcal{F}\{e^{j\omega_0 t} f(t);\ \omega\} = \int_{\mathbb{R}} e^{j\omega_0 t} f(t) e^{j\omega t}\, dt = \int_{\mathbb{R}} f(t) e^{j(\omega+\omega_0)t}\, dt = \mathrm{F}_{\mathcal{F}}(\omega + \omega_0). \tag{1.67}$$

By considering $\forall\ a \in \mathbb{R} \setminus \{0\}$ the relation

$$\mathcal{F}\{f(at);\ \omega\} = \frac{1}{|a|}\mathcal{F}\left\{f(t);\ \frac{\omega}{a}\right\} = \frac{1}{|a|}\mathrm{F}_{\mathcal{F}}\left(\frac{\omega}{a}\right) \tag{1.68}$$

holds true. Other insights and application of this integral transform can be found in [6].

1.4.2 Application to differential equations

Similarly to the case of the Laplace transform, by making the Fourier transform of differential equation in the time domain it is possible to obtain a polynomial equation in the frequency domain, for which the solution is readily evaluated.

Consider the generic solution of non-homogeneous differential equation with constant coefficients. That is,

$$c_0 x(t) + c_1 \frac{d}{dt} x(t) + \cdots + c_n \frac{d^n}{dt^n} x(t) = f(t), \tag{1.69}$$

under the assumptions that the function $f(t)$, the solution $x(t)$ and its derivative, admit the Fourier transform, the Eq. (1.69) in the frequency domain becomes:

$$c_0 \mathrm{X}_{\mathcal{F}}(\omega) + c_1(-j\omega)\mathrm{X}_{\mathcal{F}}(\omega) + c_2(-j\omega)^2\mathrm{X}_{\mathcal{F}}(\omega) + \cdots + c_n(-j\omega)^n\mathrm{X}_{\mathcal{F}}(\omega) = \mathrm{F}_{\mathcal{F}}(\omega) \tag{1.70}$$

from which one obtains

$$\mathrm{X}_{\mathcal{F}}(\omega) = \frac{\mathrm{F}_{\mathcal{F}}(\omega)}{\sum_{k=0}^{n} c_k(-j\omega)^k}, \tag{1.71}$$

the function

$$\mathrm{H}(\omega) = \frac{1}{\sum_{k=0}^{n} c_k(-j\omega)^k}$$

is known as *transfer function*.

If the solution $x(t)$ of the differential equation (1.69) exists, this solution can be obtained by the inverse Fourier transform of $\mathrm{X}_{\mathcal{F}}(\omega)$: +

$$x(t) = \mathcal{F}^{-1}\{\mathrm{X}_{\mathcal{F}}(\omega);\ t\} = \frac{1}{2\pi}\int_{-\infty}^{\infty} \mathrm{F}_{\mathcal{F}}(\omega)\mathrm{H}(\omega)e^{-j\omega t}\,d\omega. \tag{1.72}$$

Note that the inverse Fourier transform does not depend of the initial condition.

1.5 Mellin transform

Another useful mathematical transform is the well known *Mellin transform*. Consider a function $f(t)$ defined in a range $(0,\infty)$, its Mellin transform is

$$\mathrm{F}_{\mathcal{M}}(\gamma) = \mathcal{M}\{f(t);\ \gamma\} := \int_0^{\infty} f(t)t^{\gamma-1}\,dt, \quad \gamma = \rho + j\eta, \tag{1.73}$$

where $\gamma \in \mathbb{C}$. This integral transform has a *power-law* as kernel.

Vice-versa, from the knowledge of transformed function $\mathrm{F}_{\mathcal{M}}(\gamma)$, the given function $f(t)$ can be obtained by performing the inverse Mellin transform. That is,

$$f(t) = \mathcal{M}^{-1}\{\mathrm{F}_{\mathcal{M}}(\gamma);\ t\} := \frac{1}{2\pi j}\int_{\rho-j\infty}^{\rho+j\infty} \mathrm{F}_{\mathcal{M}}(\gamma)t^{-\gamma}\,ds, \quad (0 < t < \infty), \tag{1.74}$$

where $-\rho_1 < \rho < -\rho_2$. This means that ρ must belong to a particular range $(-\rho_1,\ -\rho_2)$, that is known as *fundamental strip* of the Mellin transform. This particular mathematical interval will be discuss in the next subsection.

Observe that the inverse Mellin transform in Eq. (1.74) is performed by integrating the function $\mathrm{F}_{\mathcal{M}}(\gamma)t^{-\gamma}$ along the imaginary axis. Therefore, it can be rewritten as

$$f(t) = \frac{t^{-\rho}}{2\pi}\int_{-\infty}^{+\infty} \mathrm{F}_{\mathcal{M}}(\gamma)t^{-j\eta}\,d\eta; \quad (-\rho_1 < \rho < -\rho_2), \tag{1.75}$$

and that integral does not depend of selected ρ, provided that it belongs to the fundamental strip.

By the definition in Eq. (1.73) it is possible to assert that the gamma function $\Gamma(\gamma)$, for $\rho \geq 0$, can be consider as a particular case of the Mellin transform. Indeed, the Mellin transform of the exponential function e^{-t} leads to:

$$\mathcal{M}\{e^{-t};\ \gamma\} = \int_0^{\infty} e^{-t}t^{\gamma-1}\,dt = \Gamma(\gamma). \tag{1.76}$$

Example: Consider the rectangular function:

$$rect(t) = \begin{cases} 1 & \rightarrow\ 0 < t < 1, \\ \frac{1}{2} & \rightarrow t = 1, \\ 0 & \rightarrow t > 1; \end{cases}$$

its Mellin transform is

$$\mathrm{R}_{\mathcal{M}}(\gamma) = \int_0^{\infty} t^{\gamma-1} rect(t)\ dt;$$

the integral absolutely converges if $\rho > 0$, its solution is

$$\mathrm{R}_{\mathcal{M}}(\gamma) = \left[\frac{t^{\gamma}}{\gamma}\right]_0^1 = \frac{1}{\gamma}.$$

The inverse Mellin transform gives

$$rect(t) = \frac{1}{2\pi j} \int_{\rho-j\infty}^{\rho+j\infty} \frac{1}{\gamma} t^{-\gamma}\ ds; \qquad \rho > 0.$$

1.5.1 The fundamental strip

The integral in Eq. (1.73) converges if $\Re(\gamma) = \rho$ belongs to the *fundamental strip*, that is, if $-\rho_1 < \rho < -\rho_2$. The bounds of the fundamental strip, denoted by ρ_1 e ρ_2, depend on the given function $f(t)$. In particular, ρ_1 represents the order of the given function at the origin, then when $t \rightarrow 0$; while ρ_2 is the order of the function when $t \rightarrow \infty$.

In other words, if the function $f(t)$ is a continuous function in the range $(-\infty,\ \infty)$, and if it is such that

$$\lim_{t\to 0} f(t) = \mathcal{O}\left(t^{\rho_1}\right), \tag{1.77}$$

and

$$\lim_{t\to \infty} f(t) = \mathcal{O}\left(t^{\rho_2}\right), \tag{1.78}$$

then the Mellin transform of the function $f(t)$ exists for any $\gamma \in \mathbb{C}$ such that ρ lies in the fundamental strip. Further, if there is a constant $\mathrm{C} > 0$, such that

$$\int_{-\infty}^{\infty} |\mathrm{F}_{\mathcal{M}}(\rho + j\eta)|\ d\eta < \mathrm{C}, \quad \forall \rho :\ -\rho_1 < \rho < -\rho_2, \tag{1.79}$$

the inverse Mellin transform $\mathrm{F}_{\mathcal{M}}(\gamma)$ exists and the Eq. (1.74) yields the given function $f(t)$.

Example - fundamental strip: Consider the rational function:

$$f(t) = \frac{1}{1+t}.$$

To evaluate the fundamental strip, it is necessary to determine the limits

$$\begin{aligned} &\lim_{t\to 0} \frac{1}{1+t} = 1 \Rightarrow t^{\rho_1} = 1 \Rightarrow \rho_1 = 0, \\ &\lim_{t\to \infty} \frac{1}{1+t} = \frac{1}{\infty} \Rightarrow t^{\rho_2} = \infty^{-1} = 0 \Rightarrow \rho_2 = -1. \end{aligned} \tag{1.80}$$

Then, for the considered function the fundamental strip is $0 \div 1$.

Other examples of Mellin transform of common functions and their fundamental strip can be found in [85, 118].

1.5.2 Properties of the Mellin transform

A fundamental property of the Mellin transform is

$$\mathcal{M}\{t^{\alpha} f(t);\ \gamma\} = \mathcal{M}\{f(t);\ \gamma+\alpha\} = \mathrm{F}_{\mathcal{M}}(\gamma+\alpha). \tag{1.81}$$

Further, consider the *Mellin convolution*:

$$f(t) * g(t) = \int_0^{\infty} f(t\tau) g(\tau)\, d\tau, \tag{1.82}$$

the Mellin transform of this convolution yields

$$\mathcal{M}\left\{\int_0^{\infty} f(t\tau) g(\tau)\, d\tau;\ \gamma\right\} = \mathrm{F}_{\mathcal{M}}(\gamma)\mathrm{G}_{\mathcal{M}}(1-\gamma). \tag{1.83}$$

Moreover, taking into account of the property in Eq. (1.81) yields

$$\mathcal{M}\left\{t^{\lambda}\int_0^{\infty} \tau^{\mu} f(t\tau) g(\tau)\, d\tau;\ \gamma\right\} = \mathrm{F}_{\mathcal{M}}(\gamma+\lambda)\mathrm{G}_{\mathcal{M}}(1-\gamma-\lambda+\mu). \tag{1.84}$$

Another useful property is obtained by making the Mellin transform of the product of the derivative of function $f(t)$ by the variable t. That is,

$$\mathcal{M}\left\{t\frac{d}{dt} f(t);\ \gamma\right\} = -\gamma \mathrm{F}_{\mathcal{M}}(\gamma). \tag{1.85}$$

By integrating repeatedly by parts the following relations about the Mellin transform of the integer-order derivative can be obtained:

$$\begin{aligned}
\mathcal{M}\{f^{(n)}(t);\ \gamma\} &= \int_0^\infty f^{(n)}(t)t^{\gamma-1}\,dt \\
&= \left[f^{(n-1)}(t)t^{\gamma-1}\right]_0^\infty - (\gamma-1)\int_0^\infty f^{(n-1)}(t)t^{\gamma-2}dt \\
&= \left[f^{(n-1)}(t)t^{\gamma-1}\right]_0^\infty - (\gamma-1)\mathcal{M}\left\{f^{(n-1)}(t);\ \gamma-1\right\} \\
&= \cdots \\
&= \sum_{r=0}^{n-1}(-1)^r\frac{\Gamma(\gamma)}{\Gamma(\gamma-r)}\left[f^{(n-r-1)}(t)t^{\gamma-r-1}\right]_0^\infty \\
&\quad + (-1)^n\frac{\Gamma(\gamma)}{\Gamma(\gamma-n)}\mathrm{F}_{\mathcal{M}}(\gamma-n) \\
&= \sum_{r=0}^{n-1}\frac{\Gamma(1-\gamma+r)}{\Gamma(1-\gamma)}\left[f^{(n-r-1)}(t)t^{\gamma-r-1}\right]_0^\infty \\
&\quad + \frac{\Gamma(1-\gamma+n)}{\Gamma(1-\gamma)}\mathrm{F}_{\mathcal{M}}(\gamma-n).
\end{aligned} \tag{1.86}$$

Moreover, if $f(t)$ and $\Re(\gamma)=\rho$ are such that the first part of Eq. (1.86) is equal to zero, the Mellin transform of the integer-order derivative of the function $f(t)$ becomes:

$$\mathcal{M}\{f^{(n)}(t);\ \gamma\} = \frac{\Gamma(1-\gamma+n)}{\Gamma(1-\gamma)}\mathrm{F}_{\mathcal{M}}(\gamma-n). \tag{1.87}$$

For an $a>0$, the following relations holds true:

$$\mathcal{M}\left\{f(at);\ \gamma\right\} = a^{-\gamma}\mathrm{F}_{\mathcal{M}}(\gamma), \tag{1.88}$$

$$\mathcal{M}\left\{f(t^a);\ \gamma\right\} = \frac{1}{a}\mathrm{F}_{\mathcal{M}}\left(\frac{\gamma}{a}\right), \tag{1.89}$$

$$\mathcal{M}\left\{f(t^a);\ \gamma\right\} = \frac{1}{a}\mathrm{F}_{\mathcal{M}}\left(-\frac{\gamma}{a}\right), \tag{1.90}$$

$$\mathcal{M}\left\{t^\alpha f(t^a);\ \gamma\right\} = \frac{1}{a}\mathrm{F}_{\mathcal{M}}\left(\frac{\gamma+\alpha}{a}\right), \tag{1.91}$$

$$\mathcal{M}\left\{t^{\alpha}f(t^{-a});\ \gamma\right\} = \frac{1}{a}\mathrm{F}_{\mathcal{M}}\left(-\frac{\gamma+\alpha}{a}\right). \tag{1.92}$$

Another property is given by the integer-order derivative of the Mellin transform:

$$\mathcal{M}\left\{\log(t)^{n}f(t);\ \gamma\right\} = \mathrm{F}_{\mathcal{M}}{}^{(n)}(\gamma) \quad \text{where } n = 1, 2, 3, \ldots \tag{1.93}$$

The Mellin transform is strictly related to the Fourier transform:

$$\mathcal{M}\left\{\mathcal{F}\left\{f(t);\,\omega\right\};\,\gamma\right\} = \Gamma(\gamma)\cos\left(\frac{\pi\gamma}{2}\right)\mathcal{M}\left\{f(t);\,1-\gamma\right\}. \tag{1.94}$$

Chapter 2

Fractional Operators

"Thus it follows that $d^{1/2}x$ will be equal to $x\sqrt{dx : x}$, an apparent paradox, from which one day useful consequences will be drawn."

G. W. Leibniz, letter to G. A. L'Hôpital
Hannover, Germany, Sept. 30^{th} 1695.

This Chapter deals with the *Fractional Calculus*, a branch of mathematical analysis that extends the classical integro-differential calculus to non-integer order operators. The *fractional operators* represent the core of this Chapter. In particular, the derivatives and integrals of fractional order, their fundamental properties, and some numerical examples about this mathematical tools will be introduced and defined. Moreover, the integral transforms introduced in the previous Chapter will be applied to fractional derivatives and fractional integrals.

The fractional operators introduced in this Chapter are just those required to understand the concepts of fractional viscoelasticity next, but there are other definitions of fractional derivatives and integrals, i.e. the definition of *E.L. Post*, *A. Marchaud*, etc.. Further details can be found in [16, 53–55, 64–66, 77, 83, 91, 99].

2.1 Brief history

As can see from the the epigraph, the first question about the fractional derivative dates back to the classical derivative, when, in the 1695, the German math-

ematician and philosopher *Gottfried Wilhelm von Leibniz* introduced the concept of half-derivative in a letter to his French colleague *Guillaume de L'Hôpital*. After that first idea, the first systematic studies have been made only half century later, and they involved several mathematicians, such as *Fourier*, *Laplace*, *Lacroix* and *Euler*.

Probably, the first one who used fractional calculus in a mathematical problem was *N. H. Abel*. He studied in the 1823 the tautochrone curve by the integral

$$\int_a^t (t-\tau)^{-\frac{1}{2}} f(\tau)\, d\tau,$$

which is similar to the fractional integral that will be introduced by *Riemann* later. But the main breakthrough has been made by the French mathematician *Joseph Liouville*, who in the 1832 formulates the first definition of fractional derivative. He defined a derivative of non-integer order considering an exponential series expansion of the function and operating by a singular element of the summation. In particular, Liouville considered the derivative of exponential function:

$$\frac{\mathrm{d}^n}{dt^n} e^{at} = a^n e^{at} \quad n \in \mathbb{N},$$

and he extended the derivation considering an order $n = \alpha$ with α is a non-integer number, and obtaining

$$\frac{\mathrm{d}^\alpha}{dt^\alpha} e^{at} = a^\alpha e^{at}, \quad \alpha \in \mathbb{R}^+.$$

Subsequently, around the 1835, he expressed the generic function $f(t)$ as a summation of exponential with infinity terms, and he defined the derivative of fractional order as series

$$\left(D^\alpha f\right)(t) = \sum_{j=0}^{\infty} c_j a_j^\alpha e^{a_j t},$$

where $f(t) = \sum_{j=0}^{\infty} a_j^\alpha e^{a_j t}$.

An important contribution was provided in the 1847 by the 22-years-old *George Friedrich Bernhard Riemann*, who introduced a definition of fractional integration by generalizing the Taylor series. That is,

$$\left(\mathrm{I}_{a^+}^\alpha f\right)(t) = \frac{d^{-\alpha}}{dt^{-\alpha}} f(t) = \frac{1}{\Gamma(\alpha)} \int_a^t (t-\tau)^{\alpha-1} f(\tau)\, d\tau.$$

The definitions of Liouville and Riemann have been unified with the aid of Cauchy integration formula in the manuscript of the 1869 by *N. Ya. Sonin* entitled *"On Differentiation with Arbitrary Index"*. This is probably the first document in which the two definitions appear unified. Other contributions to this unification were provided by *A. Krug*, and *Aleksey Vasilievic Letnikov*, the latter one in the 1872 extended the work of Sonin by his paper *"An Explanation of the Theory of Differentiation of Arbitrary Index"*.

Next, during the collaboration with *Letnikov*, in the 1867 *Anton Karl Grünwald* overcame the limits of Liouville definition, obtaining a more complete definition. Indeed, the Grünwald-Letnikov derivative has been obtained with the aid of the *difference quotient*. In the 1930 the mathematician *Emil Leon Post* extended the definition of Grünwald and Letnikov.

Recently, around 1967, *Michele Caputo* provided a new mathematical formulation that represents a good tool to solve some physical problems.

2.2 Fractional derivatives and integrals

By considering the classical derivation and integration operators:

$$\frac{d^n f(t)}{dt^n}; \dots \frac{d^2 f(t)}{dt^2}; \ \frac{df(t)}{dt}; \ f(t); \ \int_a^t f(\tau)\, d\tau; \ \int_a^t \int_a^{\tau_1} f(\tau)\, d\tau\, d\tau_1; \dots \left(\mathrm{I}_{a^+}^n f\right)(t), \tag{2.1}$$

it can be observed that the derivation/integration orders, denoted by n, are all natural numbers ($n \in \mathbb{N}$). The fractional calculus extends these concepts for all $n \in \mathbb{R}$. Indeed, the operators with real order α can be obtained as a sort of interpolation of the sequence of classical operators in Eq. (2.1).

The *fractional derivative* can be denoted by

$$\left(\mathrm{D}_{a^+}^{\alpha} f\right)(t), \tag{2.2}$$

where a is the lower bound, t is the derivation variable and α is the "fractional" order. Another common-used notation is that one provided by *Davis*, for which the derivative is denoted by ${}_a\mathrm{D}_t^{\alpha} f(t)$.

The *fractional integral*, or arbitrary-order integral, corresponds to assume in the previous operator a negative value as order α. This integration operator is denoted by

$$\left(\mathrm{I}_{a^+}^{\alpha} f\right)(t) = \left(\mathrm{D}_{a^+}^{-\alpha} f\right)(t), \tag{2.3}$$

according to the Davis' notation the fractional integral is denoted by ${}_{\mathrm{a}}\mathrm{I}_{\mathrm{t}}^{\alpha} f(t)$.

A *fractional differential equation* is an equation which involves some fractional derivatives. Similarly, in a *fractional integral equation* the fractional integrals appear. A *fractional order system* involves fractional differential/integral equations.

The main definitions of *fractional operators* will be introduced in the next.

2.2.1 The Grünwald-Letnikov differintegral

Starting from the definition of integer-order n derivative the Grünwald-Letnikov definition is readily obtainable. Before this definition, it is needed to introduce an operator that contains derivative and integral at the same time. In this regard, by considering the classical definition of the derivative of a continuous function $f(t)$ as a limit of difference quotient:

$$\frac{df(t)}{dt} = f'(t) := \lim_{h\to 0} \frac{f(t) - f(t-h)}{h}. \tag{2.4}$$

Applying this definition twice, the second order derivative is given as

$$\begin{aligned} \frac{d^2 f(t)}{dt^2} = f''(t) &:= \lim_{h\to 0} \frac{f'(t) - f'(t-h)}{h} \\ &= \lim_{h\to 0} \frac{1}{h}\left[\frac{f(t) - f(t-h)}{h} - \frac{f(t-h) - f(t-2h)}{h}\right] \\ &= \lim_{h\to 0} \frac{f(t) - 2f(t-h) + f(t-2h)}{h^2}. \end{aligned} \tag{2.5}$$

Similarly, the third-order derivative is

$$\frac{d^3 f(t)}{dt^3} = f'''(t) := \lim_{h\to 0} \frac{f(t) - 3f(t-h) + 3f(t-2h) - f(t-3h)}{h^3}. \tag{2.6}$$

Observe that if the derivation order increases, more distant values of the function appear in the calculus. Taking into account that the coefficients in Eqs. (2.4-2.6) follow the *binomial coefficients* rule with alternating signs, the derivative of order n can be found by induction as

$$f^{(n)}(t) = \frac{d^n f(t)}{dt^n} := \lim_{h\to 0} \frac{1}{h^n} \sum_{r=0}^{n} (-1)^r \binom{n}{r} f(t - rh), \tag{2.7}$$

where $\binom{n}{r}$ represents the binomial coefficient:

$$\binom{n}{r} := \frac{n(n-1)(n-2)\dots(n-r+1)}{r!}. \tag{2.8}$$

The Eq. (2.7) is the *generalized integer-order derivative*. Now, in order to obtain the differintegral operator, it is needed to introduce the *generalized integral*. In this regard, consider the definition of integral as Riemann summation:

$$\frac{d^{-1}f(t)}{[d(t-a)]^{-1}} \equiv f^{(-1)}(t) := \int_a^t f(t)\,dt = \lim_{h\to 0}\left[h\sum_{r=0}^{N-1} f(t-rh)\right], \tag{2.9}$$

the integral represents the area under the integrand function, which can be evaluated as summation of N rectangles with infinitesimal base h, and with surface $hf(t)$. The fixed lower bound permits to get an uniques solution of the integral. As was done for the second-order derivative, the second-order integral is

$$\frac{d^{-2}f(t)}{[d(t-a)]^{-2}} \equiv f^{(-2)}(t) := \lim_{h\to 0}\left[h^2\sum_{r=0}^{N-1}(r+1)f(t-rh)\right], \tag{2.10}$$

the third-order becomes

$$\frac{d^{-3}f(t)}{[d(t-a)]^{-3}} \equiv f^{(-3)}(t) := \lim_{h\to 0}\left[h^3\sum_{r=0}^{N-1}\frac{(r+1)(r+2)}{2}f(t-rh)\right], \tag{2.11}$$

and by induction, the *generalized integer-order integral* is

$$\frac{d^{-n}f(t)}{[d(t-a)]^{-n}} \equiv f^{(-n)}(t) := \lim_{h\to 0}\left[h^n\sum_{r=0}^{N-1}\binom{r+n-1}{r}f(t-rh)\right]. \tag{2.12}$$

Now, it is needed the unification of the two operators in Eq. (2.7) and in Eq. (2.12). For the generalized integral, the base h can be expressed as $h = (t-a)/N$, where a is a real constant (the lower bound of the integral). The same expression can be used for the increment h of the derivative operator in Eq. (2.7). Such choice leads to

$$\frac{d^n f(t)}{dt^n} = \lim_{N\to\infty}\left\{\left(\frac{t-a}{N}\right)^{-n}\sum_{r=0}^{N-1}(-1)^r\binom{n}{r}f\left[t-r\left(\frac{t-a}{N}\right)\right]\right\}, \tag{2.13}$$

for the derivative of order n. While the integral of order n is

$$\frac{d^{-n}f(t)}{d(t-a)^{-n}} = \lim_{N\to\infty}\left\{\left(\frac{t-a}{N}\right)^{n}\sum_{r=0}^{N}\binom{r+n-1}{r}f\left[t-r\left(\frac{t-a}{N}\right)\right]\right\}. \quad (2.14)$$

The two definitions in Eq. (2.13) and in Eq. (2.14) are still not unified. In order to do this, it is necessary to use a property of the binomial coefficient. Such coefficient, denoted by $C(n,k)$, is usually defined as

$$C(n,k) = \binom{n}{r} := \frac{n!}{(n-r)!r!}. \quad (2.15)$$

It has the property

$$\binom{n}{r} = \binom{n}{n-r} = (-1)^{r}\binom{r-n-1}{r}, \quad (2.16)$$

and with the aid of such property, it is possible to prove that the derivative in Eq. (2.13) and the integral in Eq. (2.14) are equivalent. Indeed, the relation

$$(-1)^{r}\binom{n}{r} = \binom{r-n-1}{r}, \quad (2.17)$$

holds true for $n \in \mathbb{N}$.

In order to extend the definition of derivation and integration to the *real* and/or *complex* order, it is necessary to generalize the binomial coefficient with the aid of the Euler gamma function. This special function, introduced in the previous Chapter, is strictly related to the binomial coefficients, according to the property in Eq. (1.7). Using such property, the Eq. (2.17) can be expressed through the gamma function as

$$\binom{r-\alpha-1}{r} = \frac{(r-\alpha-1)!}{(-\alpha-1)!r!} = \frac{\Gamma(r-\alpha)}{\Gamma(-\alpha)\Gamma(r+1)}, \quad (2.18)$$

observe that in this latter case the real number $\alpha \in \mathbb{R}$ in the binomial coefficient appears.

The derivation (2.13) and the integration (2.14) for integer-value of the order n have been defined previously. Now, the extension to non-integer order cases can be readily obtained replacing the Eq. (2.18) in the Eq. (2.13). In this way the *Grünwald-Letnikov differintegral* is given as

$$\left(\mathrm{D}^{\alpha}_{a^{+}}f\right)(t) := \lim_{N\to\infty}\left\{\left(\frac{t-a}{N}\right)^{-\alpha}\frac{1}{\Gamma(-\alpha)}\sum_{r=0}^{N-1}\frac{\Gamma(r-\alpha)}{\Gamma(r+1)}f\left[t-r\left(\frac{t-a}{N}\right)\right]\right\}. \quad (2.19)$$

Such definition has some useful advantages respect than the other next definitions. Indeed,

- the integral or the derivative of the function $f(t)$ not explicitly appear;
- it permits to get the approximate numerical solutions of several fractional derivatives and integrals (e.g. see [49]);
- it is readily applicable to various function.

2.2.2 The Riemann-Liouville definition

The definition of integral by *Cauchy* (*Augustin-Louis*, French mathematician and engineering, 1789-1857) is

$$\begin{aligned}\left(\mathrm{I}_{a^+}^{n} f\right)(t) = \frac{d^{-n} f(t)}{d(t-a)^{-n}} &:= \int_a^t \int_a^{\tau_{n-1}} \dots \int_a^{\tau_1} f(\tau)\, d\tau\, d\tau_1 \dots d\tau_{n-1} \\ &= \frac{1}{(n-1)!} \int_a^t (t-\tau)^{n-1} f(\tau)\, d\tau\end{aligned} \tag{2.20}$$

in this way the multiple integral is represented as a convolution integral in which the kernel is $(t-\tau)^{n-1}$. By using the property of the Euler gamma function the Cauchy multiple integral formula can be generalized to the non-integer order case, obtaining the *Riemann-Liouville* (RL) definition. In this regard, by replacing the factorial $(n-1)!$ with the gamma function, and the integer order n with generic order α (real or complex), the following relation holds:

$$\left(\mathrm{I}_{a^+}^{\alpha} f\right)(t) = \frac{d^{-\alpha} f(t)}{d(t-a)^{-\alpha}} := \frac{1}{\Gamma(\alpha)} \int_a^t (t-\tau)^{\alpha-1} f(\tau)\, d\tau. \tag{2.21}$$

The Eq. (2.21) is known as *Riemann-Liouville fractional integral*, since $\Re(\alpha) > 0$, and it holds true for $\alpha \in \mathbb{C}$. According the Davis notation, the integral is also denoted by ${}_a\mathrm{I}_t^{\alpha} f(t)$. In particular, this integral represents the *left-sided integral*, since the lower bound is the parameter a, and then $t > a$. The *right-sided integral* can be obtained chosen as lower bound the integration variable t. That is,

$$\left(\mathrm{I}_{b^-}^{\alpha} f\right)(t) := \frac{1}{\Gamma(\alpha)} \int_t^b (\tau-t)^{\alpha-1} f(\tau)\, d\tau, \tag{2.22}$$

in this case the parameter b is such that $b > t$. For the Davis notation the right-sided integral is also denoted by ${}_t\mathrm{I}_b^{\alpha} f(t)$.

The left-sided (2.21) and right-sided R-L (2.22) integrals with lower/upper bound $\mp\infty$ can be write as convolution

$$\left(\mathrm{I}_{\pm}^{\alpha} f\right)(t) := \frac{1}{\Gamma(\alpha)} \int_{-\infty}^{\infty} \tau_{\pm}^{\alpha-1} f(t-\tau) d\tau = \frac{1}{\Gamma(\alpha)} \int_{0}^{\infty} \tau^{\alpha-1} f(t \pm \tau) d\tau, \quad (2.23)$$

where $\Re(\alpha) > 0$, $\left(\mathrm{I}_{+}^{\alpha} f\right)(t)$ and $\left(\mathrm{I}_{-}^{\alpha} f\right)(t)$ denote the left-sided and right-sided R-L integral, respectively. The Eq. (2.23) represents the fractional integrals on the whole real axis.

The *Riemann-Liouville fractional derivative* can be readily obtained from the definition of R-L fractional integral. In particular, by considering that the derivative of order n can be represented as the derivative of order $n+m$ of the m-order primitive function, the non-integer order the definition is obtained:

$$\left(D_{a^+}^{\alpha} f\right)(t) := \frac{1}{\Gamma(n-\alpha)} \left(\frac{d}{dt}\right)^n \int_a^t \frac{f(\tau)}{(t-\tau)^{\alpha-n+1}} \, d\tau, \quad (2.24)$$

where $(n-1) < \Re(\alpha) < n$. The Eq. (2.24) represents the *left-sided derivative*, since $t > a$. Instead, chosen an upper bound $b : t < b$, the *right-sided derivative* is defined as

$$\left(D_{b^-}^{\alpha} f\right)(t) := \frac{1}{\Gamma(n-\alpha)} \left(-\frac{d}{dt}\right)^n \int_t^b \frac{f(\tau)}{(\tau-t)^{\alpha-n+1}} \, d\tau. \quad (2.25)$$

For the Davis notation the right-sided and left-sided derivative are denoted by ${}_aD_t^{\alpha} f(t)$ and ${}_tD_b^{\alpha} f(t)$ respectively.

In the previous definitions appear the backward difference $(t-\tau)$ in the convolution integral. If the forward difference $(t+\tau)$ is chosen, then another definition, known as *Weil differintegral operator*, is obtained.

Observe that the R-L derivative of a constant is not zero, indeed:

$$D_{0^+}^{\alpha} c = \frac{c\, t^{-\alpha}}{\Gamma(1-\alpha)}. \quad (2.26)$$

The Courant-Hilbert differintegral

Another definition was proposed by *Courant* and *Hilbert* in the 1962. That is,

$$\frac{d^{\frac{1}{2}} f(t)}{d(t-a)^{\frac{1}{2}}} := \frac{1}{\sqrt{\pi}} \frac{d}{dt} \int_a^t \frac{f(\tau)}{\sqrt{t-\tau}} \, d\tau. \quad (2.27)$$

This operator is known as *Courant-Hilbert differintegral*, and it is nothing else that a particular case of Eq. (2.24) with $\alpha = \frac{1}{2}$.

2.2.3 Riesz fractional integrals

The *Riesz fractional integral*, denoted by $(\mathbf{I}^{\alpha} f)(t)$, is defined as

$$(\mathbf{I}^{\gamma} f)(t) := \frac{1}{2\nu_c(\alpha)} \int_{-\infty}^{\infty} \frac{f(\tau)}{|t-\tau|^{1-\alpha}} d\tau, \tag{2.28}$$

where $\nu_c(\alpha) = \Gamma(\alpha)\cos(\alpha\pi/2)$. The Eq. (2.28) holds true for $\Re(\alpha) > 0$, and $\Re(\alpha) \neq 1, 3, 5, \ldots$.

The *complementary Ries integral*, denoted by $(\mathbf{H}^{\alpha} f)(t)$, is defined as

$$(\mathbf{H}^{\gamma} f)(t) = \frac{1}{2\nu_s(\alpha)} \int_{-\infty}^{\infty} \frac{f(\tau)\,\mathrm{sgn}(t-\tau)}{|t-\tau|^{1-\alpha}} d\tau, \tag{2.29}$$

where $\nu_s(\alpha) = \Gamma(\alpha)\sin(\alpha\pi/2)$. The Eq. (2.29) is valid for $\Re(\alpha) > 0$, and $\Re(\alpha) \neq 2, 4, 6, \ldots$.

The Riesz integrals are related to the R-L definitions. Indeed, simple mathematical considerations lead to:

$$(\mathbf{I}^{\alpha} f)(t) = \frac{\Gamma(\alpha)}{2\nu_c(\alpha)} \left[(\mathrm{I}_{+}^{\alpha} f)(t) + (\mathrm{I}_{-}^{\alpha} f)(t) \right], \tag{2.30}$$

$$(\mathbf{H}^{\alpha} f)(t) = \frac{\Gamma(\alpha)}{2\nu_s(\alpha)} \left[(\mathrm{I}_{+}^{\alpha} f)(t) - (\mathrm{I}_{-}^{\alpha} f)(t) \right], \tag{2.31}$$

where $(\mathrm{I}_{+}^{\alpha} f)(t)$ and $(\mathrm{I}_{-}^{\alpha} f)(t)$ are expressed in Eq. (2.23).

2.2.4 Caputo's approach

Another definition has been provided by *Michele Caputo*, and it is applied to solve several physical problems.

The Riemann-Liouville definition represents an accurate mathematica tool, but often it is unsuitable to solve and/or to model real physical problems. In particular, the solution of fractional differential equations with R-L derivatives can be found if the initial conditions are expressed as the involved fractional operators. Such derivatives, having no physical meaning, are unknown in the physical problems, then they do not permit to represent also the initial condition of those problems.

The Caputo's approach [18, 19], overcomes the limitations of the R-L definition. Since, it permits to define the fractional derivative and/or integral of

the function $f(t)$ by using initial conditions expressed as integer-order derivative. In this manner, when there is a fractional differential equation with Caputo's fractional operators, the solution can be evaluated by the knowledge of a certain number of initial conditions expressed as the classical way. To model the mechanical behavior of real materials, the fractional derivation is common used in the rheology. In this physical field there are some problems in which the initial conditions are known in terms of integer-order derivatives (e.g. the deformation rate is the first-order derivative in time of the strain history). The Caputo's formulation permits to solve this kind of problems, providing an accurate modeling of the phenomena.

M. Caputo, around the 1967, provided the following definition of fractional operator:

$$\left({}_{\mathrm{C}}D^{\alpha}_{a^+}f\right)(t) := \frac{1}{\Gamma(n-\alpha)}\int_a^t \frac{f^{(n)}(\tau)}{(t-\tau)^{\alpha+1-n}}\,d\tau, \tag{2.32}$$

which is known as *Caputo's differintegral* and it is valid for $n-1 < \alpha < n$. The Eq. (2.32) is obtained as a kind of interpolation of the integer-order derivative. Indeed, if $\alpha \to n$ the Eq. (2.32) leads to n-order derivative of the function $f(t)$. In this case, the Caputo's derivative of a constant is zero.

In certain cases, in which the function $f(t)$ has particular properties when $t \to -\infty$, and under specific initial conditions, the R-L derivative and the Caputo's one coincide.

2.3 Properties of fractional operators

The properties of classical derivation and integration can be extended to the fractional operators. This shows that the integer-order differential/integral calculus is nothing else that a subset of the fractional calculus.

This section introduces just three fundamental property of the fractional operators, that is, the *linearity* that concerns the summation of two operators; the *Leibniz rule* that affects the product; and the *semigroup property*, which is useful for multiple integration and derivation.

2.3.1 The linearity

The fractional derivative is a linear operator. Considering two function $f(t)$ and $g(t)$, and two parameters $\lambda, \mu \in \mathbb{C}$, the following relation holds:

$$\left(D^{\alpha}\lambda f + \mu g\right)(t) = \lambda\left(D^{\alpha}f\right)(t) + \mu\left(D^{\alpha}g\right)(t), \tag{2.33}$$

this property of fractional derivative is a consequence of its definition.

In order to show this property, consider the Grünwald-Letnikov definition, for which:

$$\begin{aligned}\left(\mathrm{D}^{\alpha}_{a^+}\lambda f+\mu g\right)(t) &= \lim_{\substack{h\to 0\\ nh=t-a}} h^{-\alpha}\sum_{r=0}^{n}(-1)^r\binom{\alpha}{r}\left[\lambda f(t-rh)+\mu g(t-rh)\right]\\ &= \lambda\lim_{\substack{h\to 0\\ nh=t-a}} h^{-\alpha}\sum_{r=0}^{n}(-1)^r\binom{\alpha}{r}f(t-rh)+\mu\lim_{\substack{h\to 0\\ nh=t-a}} h^{-\alpha}\sum_{r=0}^{n}(-1)^r\binom{\alpha}{r}g(t-rh),\end{aligned} \tag{2.34}$$

that leads to

$$\left(\mathrm{D}^{\alpha}_{a^+}\lambda f+\mu g\right)(t)=\lambda\left(\mathrm{D}^{\alpha}_{a^+}f\right)(t)+\mu\left(\mathrm{D}^{\alpha}_{a^+}g\right)(t). \tag{2.35}$$

The property can be proved considering the other definitions.

2.3.2 The Leibniz rule

Take two function $f(t)$ and $\varphi(t)$, the Leibniz rule permits to evaluate the n-derivative of their product:

$$\frac{d^n}{dt^n}[\varphi(t)f(t)]=\sum_{r=0}^{n}\binom{n}{r}\varphi^{(r)}(t)f^{(n-r)}(t), \tag{2.36}$$

where $\binom{n}{r}$ represents the binomial coefficient, and $\varphi^{(r)}(t)$ is the r-order derivative.

In order to demonstrate that the Leibniz rule is still available for fractional operators, let consider the Grünwald-Letnikov derivative of order $\alpha\in\mathbb{R}$:

$$\left(\mathrm{D}^{\alpha}_{a^+}\varphi f\right)(t)=\sum_{r=0}^{n}\binom{\alpha}{r}\varphi^{(r)}(t)\left(\mathrm{D}^{\alpha-r}_{a^+}f\right)(t)-\mathrm{R}^{\alpha}_{n}(t), \tag{2.37}$$

which is obtained under the assumptions that $n\geq\alpha+1$, that the function $f(\tau)$ is continuous in the range $[a,t]$, and that $\varphi(\tau)$ admits $n+1$ continuous derivatives in the domain $[a,t]$. The second term of the Eq. (2.37) is

$$\mathrm{R}^{\alpha}_{n}(t)=\frac{1}{n!\Gamma(-\alpha)}\int_a^t(t-\tau)^{-\alpha-1}f(\tau)\,d\tau\int_\tau^t\varphi^{(n+1)}(\xi)(\tau-\xi)^n\,d\xi, \tag{2.38}$$

and represents a sort of *remainder*, which is due to the fact that the summation in Eq. (2.37) does not have infinite terms, but it is truncated at finite number

n. By using infinite terms in the summation, the Leibniz rule for fractional derivatives becomes:

$$\left(\mathrm{D}^{\alpha}_{a^+}\varphi f\right)(t) = \sum_{r=0}^{\infty}\binom{\alpha}{r}\varphi^{(r)}(t)\left(\mathrm{D}^{\alpha-r}_{a^+}f\right)(t)(t). \tag{2.39}$$

Also in this case, the shown property can be proved by other definitions of fractional derivative.

2.3.3 The semigroup rule

Considering a function $f(t)$, which is integrable for both order α_1 and α_2, with $\Re(\alpha_1) > 0$ and $\Re(\alpha_2) > 0$, then the following relation holds:

$$\left(\mathrm{I}^{\alpha_1}_{a^+}\mathrm{I}^{\alpha_2}_{a^+}f\right)(t) = \left(\mathrm{I}^{\alpha_2}_{a^+}\mathrm{I}^{\alpha_1}_{a^+}f\right)(t) = \left(\mathrm{I}^{\alpha_1+\alpha_2}_{a^+}f\right)(t), \tag{2.40}$$

this property is still available for right-sided integration, then:

$$\left(\mathrm{I}^{\alpha_1}_{b^-}\mathrm{I}^{\alpha_2}_{b^-}f\right)(t) = \left(\mathrm{I}^{\alpha_2}_{b^-}\mathrm{I}^{\alpha_1}_{b^-}f\right)(t) = \left(\mathrm{I}^{\alpha_1+\alpha_2}_{b^-}f\right)(t). \tag{2.41}$$

The Eq. (2.40) is known as *semigroup property*. Observe that the integration is also *commutative*.

Take an $\alpha : \Re(\alpha) > 0$, then:

$$\begin{aligned}\left(D^{\alpha}_{a^+}\mathrm{I}^{\alpha}_{a^+}f\right)(t) &= f(t),\\ \left(D^{\alpha}_{b^-}\mathrm{I}^{\alpha}_{b^-}f\right)(t) &= f(t).\end{aligned} \tag{2.42}$$

The Eqs. (2.42) can be proved by the R-L definition. Indeed, by using this definition from the first of Eqs. (2.42), the following equality holds:

$$\left(D^{\alpha}_{a^+}\mathrm{I}^{\alpha}_{a^+}f\right)(t) = \frac{d^n}{dt^n}\left\{\left(D^{-n+\alpha}_{a^+}\mathrm{I}^{\alpha}_{a^+}f\right)(t)\right\} = f(t), \quad \text{with } n = \Re(\alpha)+1 \tag{2.43}$$

the latter operation, between derivative and integral, is not commutative, therefore:

$$\begin{aligned}\left(\mathrm{I}^{\alpha}_{a^+}D^{\alpha}_{a^+}f\right)(t) &\neq f(t),\\ \left(\mathrm{I}^{\alpha}_{b^-}D^{\alpha}_{b^-}f\right)(t) &\neq f(t).\end{aligned} \tag{2.44}$$

Another particular case can be obtained if $\Re(\alpha) > \Re(\gamma) > 0$:

$$\begin{aligned}\left(D^{\gamma}_{a^+}\mathrm{I}^{\alpha}_{a^+}f\right)(t) &= \left(\mathrm{I}^{\alpha-\gamma}_{a^+}f\right)(t),\\ \left(D^{\gamma}_{b^-}\mathrm{I}^{\alpha}_{b^-}f\right)(t) &= \left(\mathrm{I}^{\alpha-\gamma}_{b^-}f\right)(t)\end{aligned} \tag{2.45}$$

Moreover, considering an $\alpha : \Re(\alpha) > 0$ and an $n \in \mathbb{N}$, then:

$$\begin{aligned} \frac{d^n}{dt^n}\left(D^{\alpha}_{a^+}f\right)(t) &= \left(D^{\alpha+n}_{a^+}f\right)(t), \\ \frac{d^n}{dt^n}\left(D^{\alpha}_{b^-}f\right)(t) &= (-1)^n\left(D^{\alpha+n}_{b^-}f\right)(t). \end{aligned} \tag{2.46}$$

2.4 Laplace transform of fractional operators

In this section the introduced concepts about the Laplace transform are extended to the fractional operators. This mathematical transformation is useful in order to solve the fractional differential equations. For this reason it is commonly used when the fractional calculus is applied to describe physical phenomena.

2.4.1 Laplace transform of Riemann-Liouville fractional derivative

The Laplace transform of the Riemann-Liouville fractional derivative of order $\Re(\alpha) > 0$ with lower bound $a = 0$ is

$$\mathcal{L}\left\{\left(D^{\alpha}_{0^+}f\right)(t);\, s\right\} = s^{\alpha}\mathrm{F}_{\mathcal{L}}(s) - \sum_{r=0}^{n-1} s^r\left[\left(D^{\alpha-r-1}_{0^+}f\right)(t)\right]_{t=0}, \tag{2.47}$$

where $\alpha : n-1 \leq \alpha < n$.

In this mathematical transformation the values of the R-L fractional derivatives at the origin appear. In the physical problems described by fractional differential equations, the R-L formulation cannot be used, since this fractional derivative at the origin have no physical meaning.

2.4.2 Laplace transform of Caputo's fractional derivative

The Laplace transform of the Caputo's fractional derivative leads to:

$$\mathcal{L}\left\{\left({}_{\mathrm{C}}D^{\alpha}_{0^+}f\right)(t);\, s\right\} = s^{\alpha}\mathrm{F}_{\mathcal{L}}(s) - \sum_{r=0}^{n-1} s^{\alpha-r-1}f^{(r)}(0), \tag{2.48}$$

where $\alpha : n-1 \leq \alpha < n$.

Observe that in this case the integer derivatives at the origin appear. This is an important characteristic of this kind of fractional derivatives, since the

Eq. (2.48) can be applied to solve physical problems in which the Caputo's fractional derivatives appear, and when the initial conditions are given in terms of integer derivative. Under a physical point of view, the difference by the Eq. (2.47) and the Eq. (2.48) is crucial, since the integer-order derivative at the origin has a physical meaning (e.g.: if $x(t)$ is the displacement function, $x'(0)$ is the initial velocity, $f''(0)$ is the initial acceleration).

2.4.3 Laplace transform of Grünwald-Letnikov fractional derivative

Applying the Laplace transform to the Grünwald-Letnikov definition, the following relation is given:

$$\mathcal{L}\left\{\left(\mathrm{D}_{0^+}^{\alpha} f\right)(t); s\right\} = \frac{f(0)}{s^{1-\alpha}} + \frac{1}{s^{1-\alpha}}\left[s\mathrm{F}_{\mathcal{L}}(s) - f(0)\right] = s^{\alpha}\mathrm{F}_{\mathcal{L}}(s), \tag{2.49}$$

where $0 \leq \alpha < 1$, and the lower bound is $a = 0$. The assumption about the chosen order is due to the fact that the Laplace transform for $\alpha > 1$ does not exist in this case in classical sense.

2.5 Fourier transform of fractional operators

In some physical problems, expressed by fractional differential equations, is useful to apply the Fourier transform. In this section the previous concepts about this mathematical transformation are extended to fractional derivatives and integrals.

2.5.1 Fourier transform of fractional integral

Considering the R-L fractional integrals on the whole real axis, that is with lower bound $a = -\infty$, and order $\alpha : 0 < \alpha < 1$, the previous definitions leads to:

$$\left(\mathrm{I}_{+}^{\alpha} f\right)(t) = \left(D_{+}^{-\alpha} f\right)(t) := \frac{1}{\Gamma(\alpha)} \int_{-\infty}^{t} (t-\tau)^{\alpha-1} f(\tau) d\tau, \tag{2.50}$$

by performing the Forier transform of (2.50), the following relation holds:

$$\mathcal{F}\left\{\left(D_{+}^{-\alpha} f\right)(t);\ \omega\right\} = (i\omega)^{-\alpha}\mathrm{F}_{\mathcal{F}}(\omega) \tag{2.51}$$

where $\alpha \in \mathbb{R}$.

By using the Eq. (2.51) to left and right-sided fractional integrals $\left(\mathrm{I}_{+}^{\alpha} f\right)(t)$, the Fourier transform becomes:

$$\mathcal{F}\left\{\left(\mathrm{I}_{\pm}^{\alpha} f\right)(t);\, \omega\right\} = (\mp i\omega)^{-\alpha}\, \mathrm{F}_{\mathcal{F}}(\omega)\,, \tag{2.52}$$

where:

$$(\mp i\omega)^{-\alpha} = \left[\cos\left(\frac{\alpha\pi}{2}\right) \pm i\,\mathrm{sgn}(\omega)\sin\left(\frac{\alpha\pi}{2}\right)\right]|\omega|^{-\alpha}\,. \tag{2.53}$$

The Eq. (2.51), obtained from the R-L definition, is still available for the Grünwald-Letnikov $\left(\mathrm{D}_{+}^{-\alpha}\cdot\right)(t)$ and the Caputo's definition $\left({}_{\mathrm{C}}D_{+}^{-\alpha}\cdot\right)(t)$.

For the Riesz fractional integral and its complementary, by performing the Fourier transform to the Eq. (2.30) and Eq. (2.31) and by using the Eq. (2.53), the following relations hold:

$$\mathcal{F}\left\{\left(\mathbf{I}^{\alpha} f\right)(t)\,;\, \omega\right\} = |\omega|^{-\alpha}\, \mathrm{F}_{\mathcal{F}}(\omega)\,, \tag{2.54}$$

$$\mathcal{F}\left\{\left(\mathbf{H}^{\alpha} f\right)(t)\,;\, \omega\right\} = i\,\mathrm{sgn}(\omega)\,|\omega|^{-\alpha}\, \mathrm{F}_{\mathcal{F}}(\omega)\,. \tag{2.55}$$

2.5.2 Fourier transform of fractional derivative

As it was done in the previous case, consider the fractional derivative with lower bound $a = -\infty$:

$$\left(D_{+}^{\alpha} f\right)(t) = \frac{1}{\Gamma(n-\alpha)}\int_{-\infty}^{t} \frac{f^{(n)}(\tau)}{(t-\tau)^{\alpha+1-n}}\, d\tau = \left(D_{+}^{\alpha-n} f^{(n)}\right)(t), \tag{2.56}$$

under the assumption that the function $f(t)$ is derivable n-times, and where $\alpha : n-1 < \alpha < n$.

The Fourier transform of Eq. (2.56), taking into account the Eqs. (2.51) and (1.63), is

$$\mathcal{F}\left\{\left(D_{+}^{\alpha} f\right)(t);\, \omega\right\} = (-i\omega)^{\alpha}\mathrm{F}_{\mathcal{F}}(\omega). \tag{2.57}$$

That expression is common used to solve several physical problem. For example, the equation of the harmonic oscillator with fractional dampers is

$$\ddot{x}(t) + a\left(D_{+}^{\alpha} x\right)(t) + bx(t) = g(t), \tag{2.58}$$

it has been studied by *H. Beyer* and *S. Kempfle* [13], by the Fourier transform.

2.6 Mellin transform of fractional operators

The Mellin transform is the more related to the fractional operators among the all integral transformations. This fact is due to the power-law kernel of this transforms. Indeed, some fractional operators can be considered as Mellin transforms of some particular functions. This section shows how this mathematical transformation modifed the fractional derivatives and integrals in the Mellin domain.

2.6.1 Mellin transform of Riemann-Liouville fractional integral

In order to apply the Mellin transform to the R-L fractional integral, consider the case in which the lower bound is $a = 0$ and take $\tau = t\xi$:

$$\begin{aligned}\left(\mathrm{I}_{+}^{\alpha} f\right)(t) &= \frac{1}{\Gamma(\alpha)} \int_0^t (t-\tau)^{\alpha-1} f(\tau) d\tau = \frac{t^{\alpha}}{\Gamma(\alpha)} \int_0^1 (1-\xi)^{\alpha-1} f(t\xi) d\xi \\ &= \frac{t^{\alpha}}{\Gamma(\alpha)} \int_0^{\infty} f(t\xi) g(\xi)\, d\xi,\end{aligned} \tag{2.59}$$

where

$$g(t) = \begin{cases} (1-t)^{\alpha-1}, & 0 \leq t < 1, \\ 0, & t \geq 1. \end{cases}$$

The Mellin transform of the function $g(t)$ can be expressed by the gamma function:

$$\mathcal{M}\{g(t);\, s\} = \frac{\Gamma(\alpha)\Gamma(s)}{\Gamma(\alpha+s)}. \tag{2.60}$$

Taking into account the Eqs. (1.84), (2.59), and (2.60), the Mellin transform of the fractional integral becomes:

$$\mathcal{M}\left\{\left(\mathrm{I}_{0^+}^{\alpha} f\right)(t);\, s\right\} = \frac{\Gamma(1-s-\alpha)}{\Gamma(1-s)} \mathrm{F}_{\mathcal{M}}(s+\alpha), \tag{2.61}$$

where $\mathrm{F}_{\mathcal{M}}(s)$ denotes the Mellin transform of the function $f(t)$. Observe that Eq. (2.61) can be readily obtained by placing $n = -\alpha$ into the Eq. (1.87).

2.6.2 Mellin transform of Riemann-Liouville fractional derivative

Considering $0 \leq n-1 < \alpha < n$ and $a = 0$, by virtue of the R-L definition in Eq. (2.24) the following relation holds:

$$\left(D_{0^+}^{\alpha} f\right)(t) = \frac{d^n}{dt^n} \left(D_{0^+}^{-n+\alpha} f\right)(t),$$

As was done in the evaluation of the Mellin transform of integer-order derivative, in Eq. (1.86), it can be introduced a function $g(t) = \left(D_{0^+}^{n-\alpha} f\right)(t)$. Moreover, taking into account the previous definition in Eq. (2.61), the Mellin transform of the R-L fractional derivative is given as

$$\begin{aligned}\mathcal{M}\left\{\left(D_{0^+}^{\alpha} f\right)(t);\, s\right\} =& \mathcal{M}\left\{\frac{d^n}{dt^n}\left(D_{0^+}^{\alpha-n} f\right)(t);\, s\right\} = \mathcal{M}\left\{g^{(n)}(t);\, s\right\} \\ =& \sum_{r=0}^{n-1} \frac{\Gamma(1-s+r)}{\Gamma(1-s)}\left[g^{(n-r-1)}(t) t^{s-r-1}\right]_0^{\infty} \\ &+ \frac{\Gamma(1-s+n)}{\Gamma(1-s)} \mathrm{G}_{\mathcal{M}}(s-n) \\ =& \sum_{r=0}^{n-1} \frac{\Gamma(1-s+r)}{\Gamma(1-s)}\left[\frac{d^{n-r-1}}{dt^{n-r-1}}\left(D_{0^+}^{\alpha-n} f\right)(t) t^{s-r-1}\right]_0^{\infty} \\ &+ \frac{\Gamma(1-s+n)\Gamma(1-s+n-n+\alpha)}{\Gamma(1-s)\Gamma(1-s+n)} \mathrm{F}_{\mathcal{M}}(s-n+n-\alpha),\end{aligned} \tag{2.62}$$

or:

$$\begin{aligned}\mathcal{M}\left\{\left(D_{0^+}^{\alpha} f\right)(t);\, s\right\} =& \sum_{r=0}^{n-1} \frac{\Gamma(1-s+r)}{\Gamma(1-s)}\left[\left(D_{0^+}^{\alpha-r-1} f\right)(t) t^{s-r-1}\right]_0^{\infty} + \\ &+ \frac{\Gamma(1-s+\alpha)}{\Gamma(1-s)} \mathrm{F}_{\mathcal{M}}(s-\alpha).\end{aligned} \tag{2.63}$$

If $0 < \alpha < 1$, then the Eq. (2.63) becomes:

$$\mathcal{M}\left\{\left(D_{0^+}^{\alpha} f\right)(t);\, s\right\} = \left[\left(D_{0^+}^{\alpha-1} f\right)(t) t^{s-1}\right]_0^{\infty} + \frac{\Gamma(1-s+\alpha)}{\Gamma(1-s)} \mathrm{F}_{\mathcal{M}}(s-\alpha). \tag{2.64}$$

Moreover, if $f(t)$ and $\Re(s)$ are such that all terms in the square brackets in the Eq. (2.63) become zero, then the Mellin transform takes the following simpler form:

$$\mathcal{M}\left\{\left(\mathrm{D}_{0^+}^{\alpha} f\right)(t);\, s\right\} = \frac{\Gamma(1-s+\alpha)}{\Gamma(1-s)} \mathrm{F}_{\mathcal{M}}(s-\alpha). \tag{2.65}$$

2.6.3 Mellin transform of Caputo's fractional derivative

The Mellin transform of the Caputo's fractional derivative is

$$\begin{aligned}\mathcal{M}\left\{\left({}_{\mathrm{C}}D_{0^+}^{\alpha}f\right)(t);\, s\right\} =& \mathcal{M}\left\{\left({}_{\mathrm{C}}D_{0^+}^{-n+\alpha}f^{(n)}\right)(t);\, s\right\} \\ =& \sum_{r=0}^{n-1}\frac{\Gamma(1-s-n+\alpha+r)}{\Gamma(1-s)}\left[f^{(n-r-1)}(t)t^{s+n-\alpha-r-1}\right]_0^{\infty} \\ &+\frac{\Gamma(1-s+\alpha)}{\Gamma(1-s)}\mathrm{F}_{\mathcal{M}}(s-\alpha),\end{aligned} \tag{2.66}$$

that equation can be proved by the previous case.

If $0<\alpha<1$, Eq. (2.66) becomes:

$$\mathcal{M}\left\{\left({}_{\mathrm{C}}D_{0^+}^{\alpha}f\right)(t);\, s\right\} = \frac{\Gamma(\alpha-s)}{\Gamma(1-s)}\left[f(t)t^{s-\alpha}\right]_0^{\infty} + \frac{\Gamma(1-s+\alpha)}{\Gamma(1-s)}\mathrm{F}_{\mathcal{M}}(s-\alpha)$$

Moreover, if $f(t)$ and $\Re(s)$ are such that the first term of the Eq. (2.66) is equal to zero, the Mellin transform of the Caputo's derivative becomes:

$$\mathcal{M}\left\{\left({}_{\mathrm{C}}D_{0^+}^{\alpha}f\right)(t);\, s\right\} = \frac{\Gamma(1-s+\alpha)}{\Gamma(1-s)}\mathrm{F}_{\mathcal{M}}(s-\alpha). \tag{2.67}$$

2.7 Some examples of fractional derivatives

This section reports some examples of fractional derivatives and integrals of common function. In particular, it will be considered operators with real differintegration order $\alpha \in \mathbb{R}$. More examples can be found in the Appendix.

2.7.1 Unit step function

Consider the *Unit step function*, denoted by $U(t)$, and defined as

$$U(t) = \begin{cases} 0, & t<0, \\ 1, & t>0. \end{cases} \tag{2.68}$$

By the Eq. (2.24), the R-L definition applied to the Unit step function $U(t)$ leads to

$$\left(D_{0^+}^{\alpha}U\right)(t) = \frac{t^{-\alpha}}{\Gamma(1-\alpha)}, \tag{2.69}$$

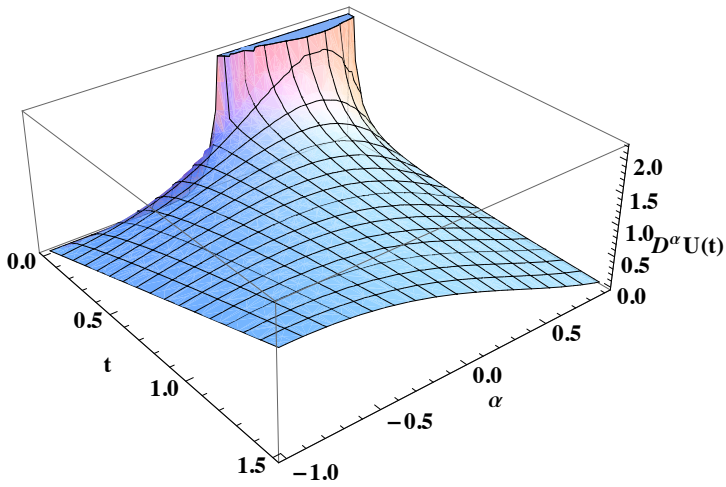

Figure 2.1: Fractional derivative of the Unit step function $U(t)$ with $t \geq 0$, $a = 0$, and differentiation order $-1 < \alpha < 1$.

where the lower bound of the fractional derivative is $a = 0$.

The Figure 2.1 shows the fractional derivative of the function $U(t)$ for $0 < t < 1$, with fractional order $\alpha \in [-1,\ 1]$. It can be observed that for $\alpha = 0$ the graph represents the Unit step function, for $\alpha = 1$ the first-order derivative is shown (the *delta Dirac function*), instead, for $\alpha = -1$ the primitive, i.e. the *ramp function* is given. All fractional values represent the fractional derivative (for $0 < \alpha \leq 1$) or the fractional integral (for $-1 \leq \alpha < 0$).

2.7.2 Power-law function

Consider the following power-law function:

$$f(t) = (t - a)^{\nu}, \tag{2.70}$$

where $\nu \in \mathbb{R}$. By choosing a value n such that $n - 1 \leq \alpha \leq n$, the R-L definition in Eq. (2.24) leads to:

$$\left(D^{\alpha}_{a^+} f\right)(t) = \frac{d^n}{dt^n}\left(D^{-n+\alpha}_{a^+} f\right)(t). \tag{2.71}$$

By placing $\gamma = n - \alpha$ the following relation holds:

$$\left(D^{-\gamma}_{a^+}(t-a)^{\nu}\right)(t) = \frac{\Gamma(1+\nu)}{\Gamma(1+\nu+\gamma)}(t-a)^{\nu+\gamma}, \tag{2.72}$$

and by simple manipulation the equation

$$\left(D_{a^+}^{\alpha}(t-a)^{\nu}\right)(t) = \frac{\Gamma(1+\nu)}{\Gamma(1+\nu-\alpha)}(t-a)^{\nu-\alpha} \tag{2.73}$$

holds true, under the assumptions that $\nu > -1$.

Chapter 3

Linear viscoelastic stress-strain constitutive law

This Chapter introduces some concepts about the linear *viscoelasticity*, with special regard to the classical modeling approach, based on the discrete mechanical models (springs and dashpots). Another formulation, known as *Boltzmann superposition principle*, is also introduced. In the end of the Chapter, the fractional viscoelastic model, based on the fractional calculus, is presented, and the advantages of this kind of modeling are discussed.

3.1 Preliminary remarks

The main characteristic of solids is that they have own shapes, in particular the *elastic* solid shows a deformation if there is an external load, but that deformation disappears when the external load finish, and the solids recover the original shape. Instead, the liquids do not have own shapes, it means that the internal stress does not depend of the deformation (that also is indefinable). In particular, for the *newtonian* liquids the internal stress linear depends on the deformation rate by a characteristic parameters of the liquid (visosity).

The *viscoelasticity* denotes a typical behavior of such materials that shown solid and liquid characteristic at the same time. In other words, the viscoelastic material is characterized by two bounder behavior: the solid-elastic behavior and the liquid-viscous one. This is a common behavior of polymeric materials [43, 62, 78, 92, 106], biological tissues [89, 90, 131], bones [30], mortars [121], resins [43], wood [63], asphalt and bitumen mixture [1, 34], some

kind of rocks [132], ecc.

In the structural engineering the study of the viscoelastic properties of materials is an important research field. This is due to the fact that the viscoelasticity allows to predict the long-time effect in the structures and it also permits to characterize the real stress-strain relation of all construction materials. Moreover, in recent years complex materials, obtained with the aid of sophisticated industrial processes aiming to enhance stiffness and strength of materials, are increasingly used in engineering applications. For this kind of materials the mechanical characterization needs to consider the viscoelastic properties.

In order to describe the viscoelastic behavior is needed to consider the time variable. For this reason it will be introduced the *stress history* and the *strain history*. Moreover, these properties of real materials will be investigated with introducing time dependent measures of stress (relaxation test) and/or strain (creep test).

Any real material shows a time-dependent stress-strain relation, for this reason the viscoelasticity represents an important aspect that cannot be neglected when the mechanical characterization is performed.

3.2 The elastic Hooke's model

The linear elastic stress-strain relation used to describe the mechanical behavior of the solid is

$$\sigma = E\varepsilon, \tag{3.1}$$

where σ represents the stress (*Pascal*), ε denotes the strain, and E is a characteristic coefficient of the material (*Pascal*). The Eq. (3.1), known as *Hooke's law*, is commonly modeled by a perfect spring with constant stiffness E, as represented in Figure 3.1(a).

The Hooke's law represents a stress-strain relation in which the involved mechanical quantities do not depend of the time. Indeed, if the elastic solid is subjected in the time to a constant stress σ, the corresponding deformation ε does not depend by time. Moreover, if the imposed stress goes to zero, the deformation becomes null without loss of energy. This means that the expended work during the loading phase is totally recovered during the unloading phase.

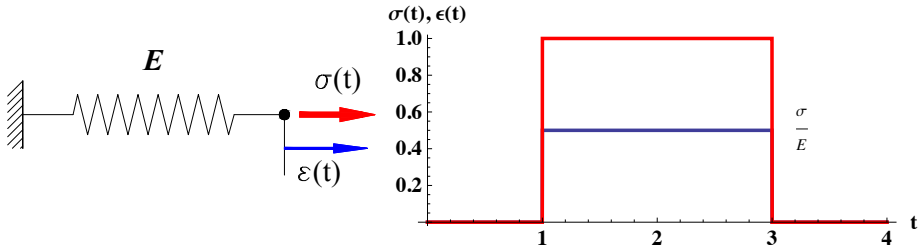

(a) Perfect spring with stiffness E

(b) Constant input load and output

Figure 3.1: Hooke' model.

3.3 The viscous Newton-Petroff model

The viscous model, used to describe the stress-strain relation in the liquid, is represented by the relation

$$\sigma(t) = \mu\dot{\varepsilon}(t), \tag{3.2}$$

where $\sigma(t)$ is the stress history, $\dot{\varepsilon}(t)$ is the strain rate (sec^{-1}), and μ is a characteristic parameter of the liquid, known as viscosity ($Pascal\ sec = 10\ Poise$). The viscosity depends on the material and is also variable with temperature.

The Eq. (3.2) is common represented by a dashpot with viscosity as damping coefficient μ as shown in Figure 3.2(a).

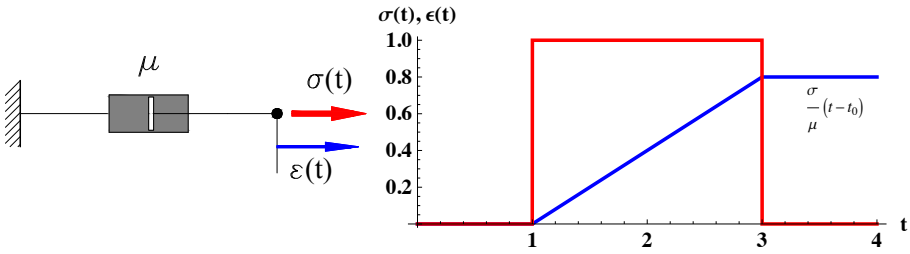

(a) Perfect dashpot with damping coefficient μ

(b) Constant imposed stress and strain

Figure 3.2: Newton-Petroff model.

The Eq. (3.2) is known as *Newton-Petroff law*, and shows that the stress $\sigma(t)$ does not depend of the strain $\varepsilon(t)$ but of its temporal rate. The external

energy is not accumulated by the fluid (that is unable to return to the initial configuration) and then it is entirely converted into heat. In other words, the viscous fluid flows in an irreversible manner under the effect of an external stress.

It should be stated that there are other kinds of fluids, known as *non-Newtonian*, in which there is not a proportional link between the stress $\sigma(t)$ and the deformation rate $\dot{\varepsilon}(t)$.

3.4 The viscoelastic model

The viscoelastic materials have a particular behavior intermediate between the purely elastic one and the perfect Newtonian. All materials are viscoelastic, that is, whether in a solid is applied a constant load can be observed that the corresponding deformation history increases, i.e. it flows (*Creep*), or if it is applied a constant deformation, the stress history decays (*Relaxation*). Obviously, these phenomena are more evident in some materials, like rubbers, polymers, biological tissues, but less evident in other materials, like steel, rocks.

The classical way to describe this particular behavior is by some mechanical models in which there are perfect springs and dashpots assembled each other.

3.4.1 The Maxwell model

The *Maxwell* model is depicted in Figure 3.3(a). It is composed by a perfect spring with stiffness E, and a dashpot with coefficient μ connected in series. Assume with $\varepsilon_e(t)$ the elongation of the spring and with $\varepsilon(t)$ the total elongation of the Maxwell model. The stress-strain relation is given by the following two equations:

$$\sigma(t) = E\varepsilon_e(t), \quad \sigma(t) = \mu[\dot{\varepsilon}(t) - \dot{\varepsilon}_e(t)], \tag{3.3}$$

properly combining the two equations the following relation is obtained:

$$\mu\dot{\sigma}(t) + E\sigma(t) = E\mu\dot{\varepsilon}(t), \tag{3.4}$$

that can be expressed in canonical form

$$\dot{\sigma}(t) + \nu\sigma(t) = E\dot{\varepsilon}(t), \tag{3.5}$$

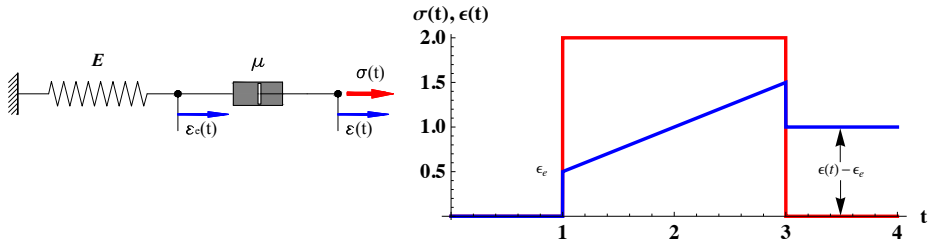

(a) Spring and dashpot connected in series

(b) Constant imposed stress and strain

Figure 3.3: Maxwell model.

where

$$\nu = \frac{E}{\mu} \ (\text{sec}^{-1}).$$

For such equation has to be added the initial condition at $t = 0$ ($\sigma(0) = \sigma_0$). The set of initial condition and the Eq. (3.5) allow to get the stress history caused by an imposed strain history $\varepsilon(t)$. The solution of the differential equation in Eq. (3.5) is the summation of the homogeneous $\sigma_{om}(t)$ and the particular solution $\sigma_p(t)$, the latter depends on the forced strain history $\dot{\varepsilon}(t)$. That is,

$$\sigma(t) = Be^{-\nu t} + \sigma_p(t), \tag{3.6}$$

where B is an integration constant which depends on the initial condition σ_0 and of $\sigma_p(t)|_{t=0}$. Assuming $\dot{\varepsilon}(t) = 0$, $\forall t > 0$, the following relation holds:

$$\sigma(t) = \sigma_0 e^{-\mu t}, \tag{3.7}$$

this equation shows that the stress history decays under a constant strain history, this phenomenon can be experimentally observed. The physics of this system can be summarized as follows: applying a constant deformation in a specimen, at the origin $t = 0$ the spring adsorbs the all stress and assumes a deformation configuration, in which the total strain is elastic $\varepsilon_e(0) = \sigma(0)/E$, in the initial step the dashpot behavior is the same of a rigid element, because the incompressible fluid in the dashpot does not have time to flows inside the chamber. After this step, the fluid inside the dashpot chamber flows, the total deformation remains constant but the elastic deformation $\varepsilon_e(t)$ decays, the spring starts to release the stored energy. At $t = \infty$, the elastic deformation is entirely transferred to the dashpot, thus $\varepsilon_e(t) = 0$.

3.4.2 The Kelvin-Voigt model

Another classical way to model the viscoelastic behavior is by the *Kelvin-Voigt* model. This is obtained by the connection in parallel of a perfect spring with a ideal dashpot. This model is depicted in Figure 3.4(a).

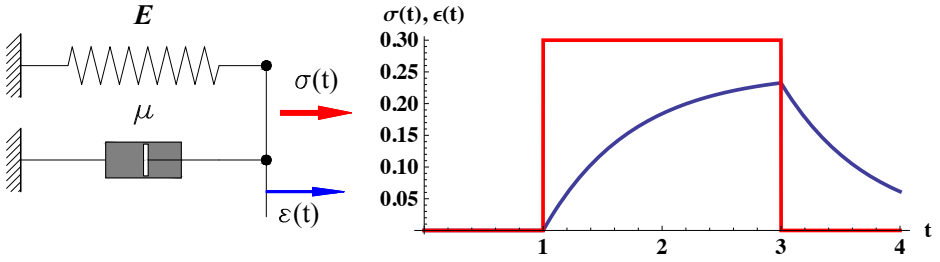

(a) Spring and dashpot connected in parallel

(b) Constant imposed stress and strain

Figure 3.4: Kelvin Voigt model.

In this case the stress in the spring and in the dashpot are different but the deformation is the same. The stress in the spring, denoted by $\sigma_e(t)$, and the stress in the dashpot, denoted by $\sigma_\mu(t)$, are given by the following expression:

$$\sigma_e(t) = E\varepsilon(t), \quad \sigma_\mu(t) = \mu\dot{\varepsilon}(t). \tag{3.8}$$

For the equilibrium the following relation

$$\sigma(t) = \sigma_e(t) + \sigma_\mu(t),$$

holds true, then:

$$\mu\dot{\varepsilon}(t) + E\varepsilon(t) = \sigma(t), \tag{3.9}$$

this equation can be rewritten in the canonical form:

$$\dot{\varepsilon}(t) + \nu\varepsilon(t) = \frac{\sigma(t)}{\mu}. \tag{3.10}$$

The initial condition is $\varepsilon(0) = \varepsilon_0$. Assuming that $\sigma(t) = 0$, the output in terms of deformation history under an imposed stress history at $t = 0$ is $\varepsilon(t) = \varepsilon_0 e^{-\nu t}$.

3.4.3 Other classical models

By increasing the simple elements (spring and dashpot) in the Kelvin-Voigt and/or in the Maxwell model, it is possible to obtain some complex model, that are used to accurately describe the viscoelastic phenomenon. Such models, known as *SLS* (Standard Linear Solid) or *Zener model*, are depicted in Figure 3.5.

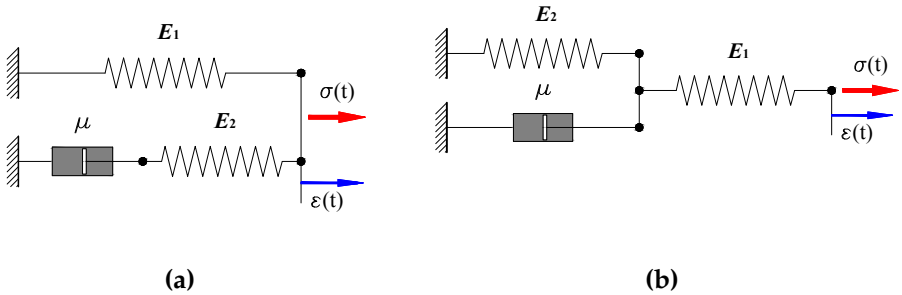

Figure 3.5: Sandard Linear Solid or Zener models.

The model depicted in Figure 3.5(a) is obtained by the connection in parallel of a spring with a Maxwell model. The stress-strain relation is given by the following differential equation:

$$\dot{\sigma}(t) + C\sigma(t) = A\mu\dot{\varepsilon}(t) + CE_1\varepsilon(t), \tag{3.11}$$

where

$$A = \frac{E_1 + E_2}{\mu}, \quad C = \frac{E_2}{\mu}.$$

The model, depicted in Figure 3.5(b), obtained by the connection in series of a spring with a Kelvin-Voigt model, is characterized by the following stress-strain relation:

$$\dot{\sigma}(t) + A\sigma(t) = E_1[\dot{\varepsilon}(t) + C\varepsilon(t)] \tag{3.12}$$

where the coefficients A e C are the same of the previous case.

These two models are more able to describe the experimental results but are more complex because there are more coefficients to calibrate in order to obtain a *best fitting* of experimental data.

Other models can be obtained combining Maxwell and Kelvin-Voigt model, in this casese the stress-strain relation contains a lot of coefficients. The number of parameters increases with the complexity of the model. In the general case the stress-strain relation of this *multi-element models* can be expressed as

$$\sum_{k=0}^{n} a_k \frac{d^k}{dt^k}\sigma(t) = \sum_{k=0}^{m} b_k \frac{d^k}{dt^k}\varepsilon(t) \tag{3.13}$$

where the numbers of parameters m and n depend on the complexity of the model. It can be seen that the Eq.s (3.5), (3.10), (3.11) and (3.12) are particular case of the Eq. (3.13).

Note that the increase of the elements in the model leads to an improvements of the description of the experimental evidence but it also could lead to a loss of the physical meaning of the involved parameters. Indeed, it is possible to obtain negative stiffness and viscosities of some elements in the model from the best-fitting of experimental data. Among the multi-element models the more reliable are those depicted in Figure 3.5(b). Other complex models can be found in [22, 48, 74, 106].

3.5 The creep and the relaxation function

The *creep function* is the response in terms of deformation history under of unitary stress history. Such function, denoted by $\Psi(t)$, is monotonically increasing function. In the linear viscoelasticity field the following relation holds:

$$\varepsilon(t) = \Psi(t)\sigma_0 \tag{3.14}$$

where σ_0 is a constant imposed stress. The function $\Psi(t)$ is the response in terms of strain history for an imposed stress history $\sigma(t) = U(t)$, where $U(t)$ represents the unit step function. In other words the creep function is the unit step response in terms of deformation. Figure 3.6 shows the imposed stress history and the corresponding creep function $\Psi(t)$. This function depends on the considered material.

The *relaxation function*, denoted by $\Phi(t)$, is the stress history caused by an imposed unitary strain history $\varepsilon_0 = 1$. In the linear viscoelasticity the following relation holds:

$$\sigma(t) = \Phi(t)\varepsilon_0 \tag{3.15}$$

where ε_0 is a constant imposed deformation. The function $\Phi(t)$ is the unit step response in terms of stress.

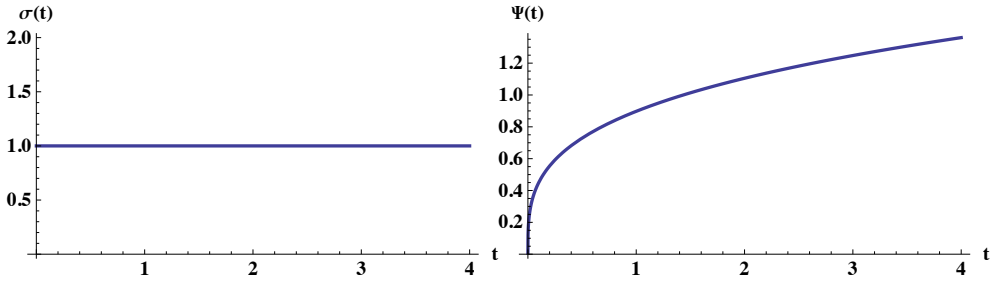

(a) Imposed stress history **(b)** Creep function

Figure 3.6: Creep function.

Figure 3.7 shows the imposed unitary strain history and the corresponding relaxation function $\Phi(t)$. That function is monotonically decreasing function.

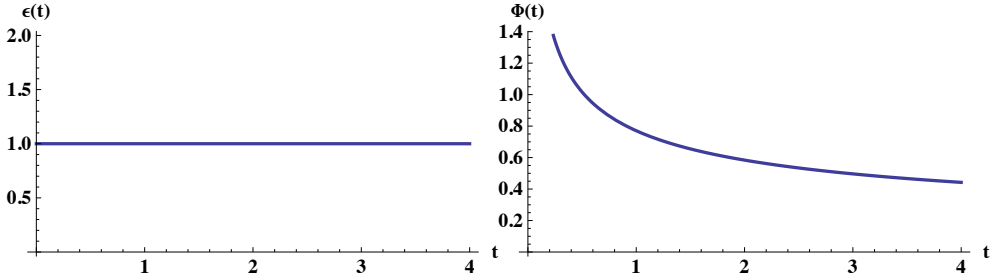

(a) Imposed strain history **(b)** Relaxation function

Figure 3.7: Relaxation function.

The functions $\Phi(t)$ and $\Psi(t)$ contain all informations about the viscoelastic behavior of the materials. It is useful to observe that both creep and relaxation functions are positive $\forall t \geq 0$, while are null for $t < 0$.

3.5.1 The Boltzmann superposition principle

Consider the creep experiment, in which the imposed stress history is like that one shown in Figure 3.8(a). For $t = t_1$ the stress is $\sigma(t) = \sigma_1 H(t - t_1)$, while

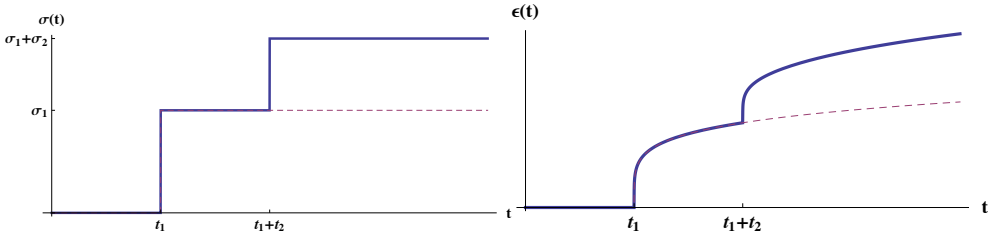

(a) $\sigma(t)$ **(b)** $\varepsilon(t)$

Figure 3.8: Imposed stress history and corresponded strain

for $t > t_2$ the total stress is $\sigma_1 + \sigma_2$, then the imposed stress is

$$\sigma(t) = \sigma_1 H(t - t_1) + \sigma_2 H(t - t_2), \tag{3.16}$$

the creep function $\Psi(t)$ is defined for $t \geq 0$, then the strain response under the imposed stress in Eq. (3.16), depicted in Figure 3.8(a), is given as

$$\varepsilon(t) = \sigma_1 \Psi(t - t_1), \tag{3.17}$$

for all $t: \ t_1 < t < t_2$. For $t > t_2$ the strain history can be obtained considering two contributions:

$$\varepsilon(t) = \sigma_1 \Psi(t - t_1) + \sigma_2 \Psi(t - t_2). \tag{3.18}$$

The Eq. (3.18) is valid if the system is linear, and since $\Psi(t) \neq 0$ for $t \geq 0$, and then $\Psi(t - t_i)$, with $t_i = t_1, t_2$, it is different from zero only if $t \geq t_1$.

The Eq. (3.18) is obtained for two jumps in the imposed stress history. If in the imposed stress history there are n jumps in the time steps $t_1, t_2, \ldots, t_{n-1}$ of $\sigma_1, \sigma_2, \ldots, \sigma_n$, the stress-strain relation becomes:

$$\varepsilon(t) = \sum_{j=1}^{n} \sigma_j \Psi(t - t_j), \tag{3.19}$$

this equation represents the superposition principle that is available in linear viscoelasticity.

If the input in terms of stress history is a continuous law, it is possible to discretize the imposed stress history, considering time increments Δt and stress increments $\Delta\sigma$, as shown in Figure 3.9. Considering infinitesimal in-

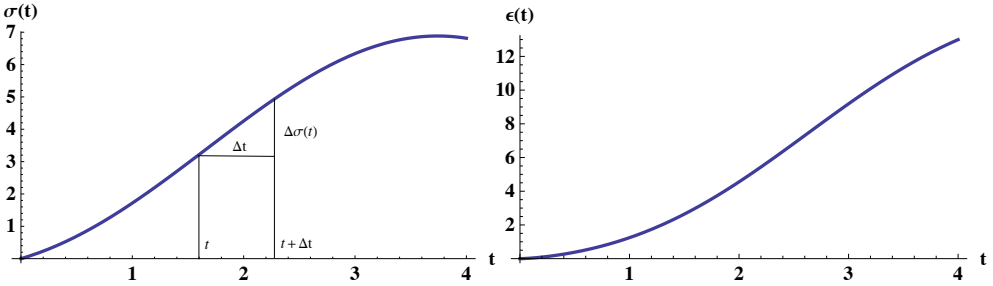

(a) Continuous imposed stress history **(b)** Corresponding strain history

Figure 3.9: Continuous imposed stress history and response.

crements, that is, if $\Delta t \to 0$, then the stress increment becomes infinitesimal $\Delta\sigma \to d\sigma(t)$, and the summation in Eq. (3.19) becomes an integral:

$$\varepsilon(t) = \int_0^t d\sigma(\tau)\Psi(t-\tau) = \int_0^t \dot{\sigma}(\tau)\Psi(t-\tau)\, d\tau. \tag{3.20}$$

If at $t = 0$ the imposed stress is different from zero, i.e. $\sigma(0) = \sigma_0$, the strain history is given as

$$\varepsilon(t) = \int_0^t \dot{\sigma}(\tau)\Psi(t-\tau)\, d\tau + \sigma_0\Psi(t). \tag{3.21}$$

Eq. (3.20) is a convolution (or *faltung*), it represents that the strain-history response at a certain time depends on all the past imposed stress. In other words, the material has memory of the past, then the stress history, as response, is a function of the entire imposed stress history. The Eq. (3.21) represents the *integral formulation of linear viscoelasticity*, introduced by *Ludwig Boltzmann* and *Vito Volterra*.

Consider the relaxation test in which there is an imposed strain history, the corresponding stress history can be found by using the relaxation function and using the same principle. That is,

$$\sigma(t) = \int_0^t \dot{\varepsilon}(\tau)\Phi(t-\tau)\, d\tau + \varepsilon_0\Phi(t) \tag{3.22}$$

where $\varepsilon(0) = \varepsilon_0$ is the initial value at $t = 0$ of the imposed deformation.

The two functions $\Phi(t)$ and $\Psi(t)$ have to be related each other. In order to show this link, consider a quiescent viscoelastic system forced by an imposed

stress history $\sigma(t)$ with $\sigma_0 = 0$, by the Eq. (3.20) the corresponding strain history $\varepsilon(t)$ can be found. After that, by evaluating the derivative of the strain response $\dot{\varepsilon}(t)$ and putting it into the Eq. (3.22) it is possible to found the relaxation function such that restitutes the given imposed $\sigma(t)$. In the Laplace domain the Eq.s (3.21) and (3.22), for $\sigma_0 = 0$ e $\varepsilon_0 = 0$, lead to:

$$\Psi_{\mathcal{L}}(s)\Phi_{\mathcal{L}}(s) = \frac{1}{s^2} \tag{3.23}$$

where $\Psi_{\mathcal{L}}(s)$ and $\Phi_{\mathcal{L}}(s)$ are the Laplace transforms of the creep and relaxation function respectively. The Eq. (3.23) represents the link between the two functions in the Laplace domain, from this relation it is possible to evaluate one of the functions just with the knowledge of the other. In this way, if from the experimental tests the function $\Psi(t)$ is determined, it is possible to obtain the function $\Phi(t)$, and vice-versa.

3.5.2 Creep and relaxation function for the Maxwell model

Consider a constant deformation $\varepsilon(t) = U(t)$, then $\dot{\varepsilon}(t) = \delta(t)$. In this case, the stress history obtained from the Maxwell equation (3.5) represents the *relaxation function* $\sigma(t) = \Phi(t)$, indeed:

$$\dot{\Phi}(t) + \nu\Phi(t) = E\delta(t), \tag{3.24}$$

placing the initial condition:

$$\Phi(0) = \sigma_0 = E,$$

the following relation is obtained

$$\Phi(t) = Ee^{-\nu t}. \tag{3.25}$$

The *creep function* can be obtained from Eq. (3.23) as follows:

$$\Psi(t) = \frac{\nu}{E}t + \frac{1}{E}, \tag{3.26}$$

Therefore, the Boltzmann integrals for the Maxwell models are:

$$\sigma(t) = E\int_0^t e^{-\nu(t-\tau)}\dot{\varepsilon}(\tau)\, d\tau, \tag{3.27}$$

$$\varepsilon(t) = \frac{\nu}{E}\int_0^t \left[(t-\tau) + \frac{1}{\nu}\right]\dot{\sigma}(\tau)\, d\tau. \tag{3.28}$$

Figure 3.10 shows the functions $\Phi(t)$ and $\Psi(t)$ for the Maxwell model. From such Figure can be observed that the relaxation function decays with exponential law, showing an acceptable correspondence with the experimental evidence. Instead, the creep function follows a trend that is not experimentally validated.

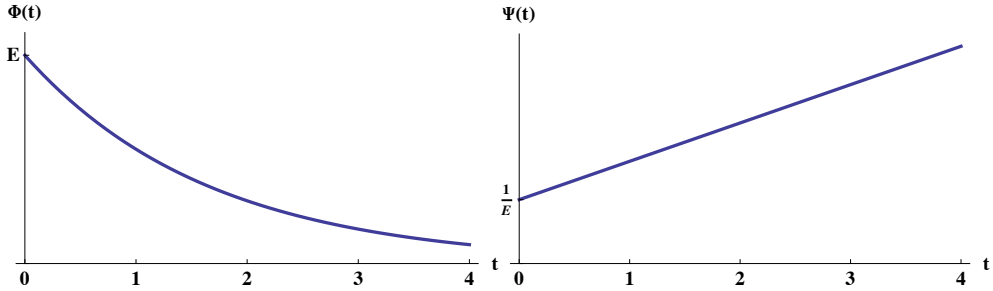

(a) Relaxation function **(b)** Creep function

Figure 3.10: Relaxation and creep function for the Maxwell model.

Observe that the Eq. (3.32) is a convolution integral with exponential kernel. This kind of kernel is common of the ordinary differential equation with integer order operators. At this kind of integer-order differential equation corresponds stress-strain relation with exponential kernel.

3.5.3 Creep and relaxation function for the Kelvin-Voigt model

Consider the creep test in which the imposed stress history is constant. That is, $\sigma(t) = U(t)$. With the aid of the Eq. (3.10), obtained from the Kelvin-Voigt model, and by taking into account that in this case the strain history represents the creep function $\varepsilon(t) = \Psi(t)$, the following differential equation can be readily found:

$$\dot{\Psi}(t) + \nu\Psi(t) = \frac{U(t)}{\mu} \tag{3.29}$$

placing the following initial condition:

$$\Psi(0) = \varepsilon_0 = 0,$$

the following relation holds:

$$\Psi(t) = \frac{1}{E}(1 - e^{-\nu t}); \quad \forall t \geq 0. \tag{3.30}$$

By using the relation in the Laplace domain, in the Eq. (3.23), also the relaxation function is readily found:

$$\Phi(t) = E\left[1 + \frac{\delta(t)}{\nu}\right], \tag{3.31}$$

the Boltzmann superposition integrals for the Kelvin-Voigt model are:

$$\sigma(t) = E\int_0^t \left[1 + \frac{1}{\nu}\delta(t-\tau)\right]\dot{\varepsilon}(\tau)\, d\tau \tag{3.32}$$

$$\varepsilon(t) = \frac{1}{E}\int_0^t \left[1 - e^{-\nu(t-\tau)}\right]\dot{\sigma}(\tau)\, d\tau \tag{3.33}$$

The trend of the functions $\Phi(t)$ and $\Psi(t)$ are depicted in Figure 3.11. In this

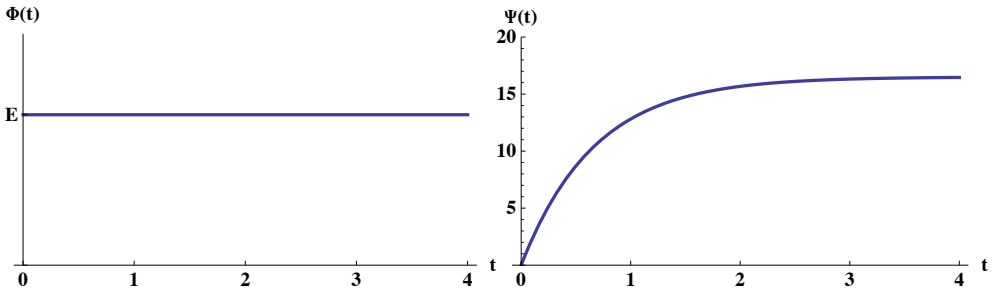

(a) Relaxation function **(b)** Creep function

Figure 3.11: Relaxation and creep function of the Kelvin-Voigt model.

case the creep function increases along as exponential law, showing an agreement with the experimental tests, but the relaxation function is not able to describe the experimental evidence. It follows that also the Kelvin-Voigt is an inconsistent model.

3.6 The fractional-order viscoelastic model

From the previous sections, it is possible to observe that the classic models are not able to completely describe the viscoelastic behavior of real materials. Indeed, the Kelvin-Voigt model is able to describe the creep test, but it is unable

to describe the relaxation phenomenon; vice-versa the Maxwell model well approximates the relaxation tests, but it is unable to describe the creep test. These classic models are needed to describe the same material for the two different tests, creep and relaxation. This is physically unacceptable since leads to have two different models to describe the same material. Moreover, by using as creep function the Kelvin-Voigt function in Eq. (3.30) and as relaxation function that one obtained from Maxwell model in Eq. (3.25) the relation the Laplace domain in Eq. (3.23) is violated.

However, there is another way to describe the viscoelasticity of real materials that is able with a simple model to completely describe this phenomenon and shows a good agreement with the experimental evidence. This more efficient model needs the fractional operators in the stress-strain relation.

3.6.1 The Nutting's experience

The process that has led to the mechanical description of viscoelastic phenomenon has been long. It has regarded some decades and it involved various scientists. Probably, *P. G. Nutting* has produced the first spark, his experimental investigation [82], reported below, has been a relevant source of inspiration for other scientists.

Around the 1921, Nutting focused his experimental observation to the viscoelastic behavior of materials. He conducted several experiments that led him to assert that the two equations used to describe perfectly-elastic solids and perfectly-viscous fluids, seemingly completely different, they actually were two special cases of a single general law. Moreover, he observed that the stress and the strain history during the relaxation and the creep test do not follow an exponential-law, as it is obtained from classic model, but they have power-law trends.

Two different kinds of function have been provided from Nutting's experimentation. The time evolution of displacements u under a constant strength, and the relation between the displacements for the imposed strengths $F(t)$ at a fixed time. The first kind, *dispacement-time* $u - t$ shows a proportional relation between the displacement and the n-order power of the time t^n, that implies a linear relation in the logarithmic scale. That is,

$$\log u \propto \log t$$

where the order n is independent of the imposed strength. From the *displacement-*

strength relation $u - F$ another similar relation has been drawn:

$$\log u \propto \log F$$

then the displacement is proportional to the m^{th} power of the imposed strength F^m.

From the previous results, Nutting proposed a power-law ables to well-represent the mechanical quantity u and F in the time from the experimental evidences. This simple empirical law, appropriate to perform the best-fitting of experimental tests on various materials, is

$$u = at^n F^m \tag{3.34}$$

that represents the evolution in the time t of the displacement u caused by an assigned history load F. The two orders n and m depend on the temperature and are characteristic of the considered material but are independent of the u, t, F and of the geometry of the specimen. The coefficient a depends on the considered material and on the kind of test.

Note that the Hooke's law in Eq. (3.1) is a particular case of the Eq. (3.34) with $n = 0$ and $m = 1$. Instead the law of Newton-Petroff in Eq. (3.2) for the perfectly-viscous fluid is another particular case of the Eq. (3.34) where $n = m = 1$. Nutting also observed that the order n ranges from $0.2 \div 0.91$, and m from $0.75 \div 3.5$. When the order n is close to zero the materials show a solid behavior, on the other hand when n is close to 1 the materials have a behavior similar to the fluids.

Nutting's experience shows how the classic models, even if they are obtained as complex assembly of several classic elements, are not able to describe the viscoelastic behavior of the real materials. Indeed, by the Kelvin-Voigt model or by the Maxwell model is impossible to obtain such kind of relation in Eq. (3.34). In order to solve this problem and to obtain a complete model able to describe both the creep and the relaxation phenomena, in the 1936-1938 *A. N. Gemant* proposes to use the fractional derivative in the stress-strain relation to correctly describe the mechanical behavior of real materials [50, 51].

3.6.2 The spring-pot

In the 50s of the last century, *Scott Blair G. W.* and *Caffyn J. E.* introduce the fractional stress-strain relation in which the fractional derivative appears [109].

This new model, known as *spring-pot*, is able to explain the Nutting's results under mathematical point of view. The representation of this model is depicted in Figure 3.12.

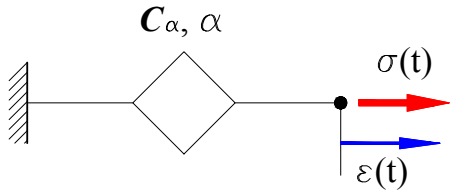

Figure 3.12: The spring-pot.

The stress-strain relation of this kind of model, introduced by Scott Blair [109–111], is

$$\sigma(t) = E\left(D_{0^+}^{\alpha}\varepsilon\right)(t), \tag{3.35}$$

where $\alpha : 0 \leq \alpha \leq 1$ and E are characteristic coefficients of the material.

Later, *A. N. Gerasimov* [52] introduced a similar expression that generalizes the stress-strain relation with the aid of the Caputo's fractional derivative, as follows:

$$\sigma(t) = k\left({}_{\mathrm{C}}D_{+}^{\alpha}\varepsilon\right)(t), \tag{3.36}$$

also in this case $\alpha : 0 \leqslant \alpha \leqslant 1$ and k are characteristic coefficients of the material. Both E in the Eq. (3.35)and k in the Eq. (3.36) have the same mechanical meaning, and they can be defined as *generalized viscosities*. Scott Blair's relation in Eq (3.35) and the Gerasimov's expression in Eq. (3.36) coincide if the considered system is quiescent, that is if $\varepsilon(t) = 0$, $\forall\, t \leqslant 0$.

Another formulation has been introduced from *G. L. Slonimsky* [112]:

$$\varepsilon(t) = \frac{1}{k}\left(\mathrm{I}_{0^+}^{\alpha}\sigma\right)(t), \tag{3.37}$$

where the Riemann-Liouville fractional integral of the stress history $\left(\mathrm{I}_{0^+}^{\alpha}\sigma\right)(t)$ appears. For quiescent system also this expression coincides with the Scott Blair's one.

By using the previous expression is possible to summarize the fractional stress-strain relation of the spring-pot as below:

$$\sigma(t) = C(\alpha)\,({}_{C}D^{\alpha}_{0^+}\varepsilon)\,(t), \tag{3.38}$$

and the inverse relation:

$$\varepsilon(t) = \frac{1}{C(\alpha)}\,(\mathrm{I}^{\alpha}_{0^+}\sigma)\,(t), \tag{3.39}$$

where $C(\alpha)$ e $\alpha : 0 \leqslant \alpha \leqslant 1$ can be obtained from a *best-fitting* of experimental data. It is useful to stress that if the order $\alpha = 0$ the fractional stress-strain relation becomes the Hooke's law in Eq. (3.1), and when $\alpha = 1$ the fractional model returns the Newtonian one in Eq. (3.2).

The order α denotes which phase is predominant in the mechanical behavior of the material. In other words, if α is close to the zero value the material exhibits an elastic predominant phase, vice-versa when α is close to 1 the material is more similar to a newtonian fluid. The coefficient $C(\alpha)$, proportional coefficient between the stress history and the fractional derivative of the strain history, cannot be defined as stiffness E nor as viscosity μ, but it has to follow the following dimensional expression:

$$C(\alpha) = E\eta^{\alpha}, \tag{3.40}$$

where E is the elastic modulus (*Pascal*) and η is a characteristic time of the materials (*sec*).

The relations in Eq.s (3.38) and (3.39) represent a mathematical model that has a perfect correspondence with the experimental results of Nutting. As it will show in the next section, this fractional model of viscoelasticity is able to describe creep and relaxation phenomena, and the obtained creep and relaxation function respect their fundamental relaxation in the Laplace domain.

3.6.3 The integral formulation of fractional viscoelasticity

Another way to obtain the fractional stress-strain relation of the spring-pot in Eq.s (3.38) and (3.39) is by the Boltzmann superposition principle, by choosing the proper Kernel in the convolution integral. According to the Nutting's experience and to the more recent experimental tests [42, 43], the correct way to represent the relaxation function decay as a power-law, therefore:

$$\Phi(t) \propto t^{-\alpha}, \tag{3.41}$$

that is,

$$\Phi(t) = \nu_\alpha t^{-\alpha}, \tag{3.42}$$

where $\alpha : 0 \leqslant \alpha \leqslant 1$ and the coefficient $\nu(\alpha)$ is related to the coefficient $C(\alpha)$ by the following relation:

$$\nu(\alpha) = \frac{C(\alpha)}{\Gamma(1-\alpha)}. \tag{3.43}$$

By taking into account the Eq. (3.40) the relaxation function becomes:

$$\Phi(t) = \frac{C(\alpha)}{\Gamma(1-\alpha)} t^{-\alpha} = \frac{E}{\Gamma(1-\alpha)} \left(\frac{t}{\eta}\right)^{-\alpha}. \tag{3.44}$$

In order to show how this power-law is capable to fit the experimental results, consider the relaxation test of epoxy resin shown in Figure 3.13(a). With the aid of a power-law like the one shown in Eq. (3.42) the best-fitting in Figure 3.13(b).

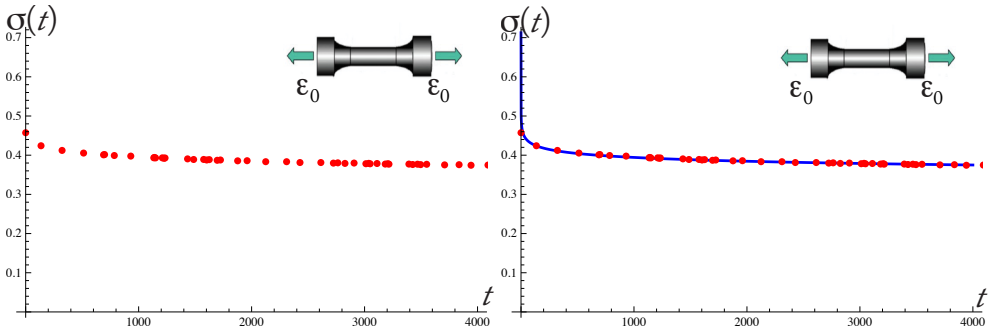

(a) Experimental data of creep test **(b)** Best-fitting with power-law

Figure 3.13: Best-fitting of relaxation data of epoxy resin.

The Figure 3.13(b) show a perfect agreement between the theoretical curve and the experimental results. In particular, in this case the obtained order of the power-law is $\alpha = 0.043$ [43].

By placing the Eq. (3.44) into the kernel of the Boltzmann integral in Eq. (3.22) the following relation holds:

$$\sigma(t) = \frac{C(\alpha)}{\Gamma(1-\alpha)} \int_0^t \dot{\varepsilon}(\tau)(t-\tau)^{-\alpha}\, d\tau = C(\alpha)\, \left({}_C D_{0^+}^{\alpha} \varepsilon\right)(t) \tag{3.45}$$

that is the first fractional relation in Eq. (3.38) of the spring-pot. In other words, if it is placed a power-law in kernel of the Boltzmann superposition integral the fractional operators directly appears, as obtained from Gerasimov.

From the knowledge of the relaxation function, the creep function is directly determined with the aid of the relation in the Laplace domain in Eq. (3.23). The Laplace transform of the power-law relaxation function $\Phi(t)$ in Eq. (3.44) is

$$\Phi_{\mathcal{L}}(s) = C(\alpha)s^{\alpha-1}, \tag{3.46}$$

by the Eq. (3.23) the creep function in the Laplace domain $\Psi_{\mathcal{L}}(s)$ is given as

$$\Psi_{\mathcal{L}}(s) = \frac{1}{C(\alpha)s^{\alpha+1}}, \tag{3.47}$$

by the inverse Laplace transform the creep function is given:

$$\Psi(t) = \mathcal{L}^{-1}\{\Psi_{\mathcal{L}}(s); t\} = \frac{1}{C(\alpha)\Gamma(1+\alpha)}t^{\alpha} = \frac{1}{E\,\Gamma(1+\alpha)}\left(\frac{t}{\eta}\right)^{\alpha}. \tag{3.48}$$

Unlike classical models, also the creep function is still able to describe the real mechanical behavior of material. In order to show this, consider the creep experiment on the same epoxy resin considered before. Figure 3.14(a) shows the experimental data obtained from a creep test. By using the Eq. (3.48) to fit these experimental data the perfect overlap between the experimental results and the theoretical curve is obtained, as shown in Figure 3.14(b).

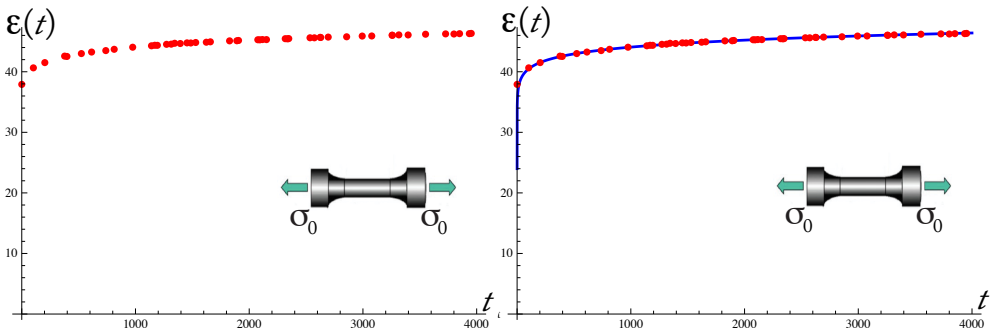

(a) Experimental data of creep test **(b)** Best-fitting with power-law

Figure 3.14: Best-fitting of creep function of epoxy resin.

Also in this case the best-fitting is obtained with the same value of the parameter $\alpha = 0.043$.

The Eq. (3.48) as kernel in the Boltzmann integral in Eq. (3.20) leads to:

$$\varepsilon(t) = \frac{1}{C(\alpha)\Gamma(1+\alpha)} \int_0^t \dot{\sigma}(\tau)(t-\tau)^{\alpha}\, d\tau, \tag{3.49}$$

integrating by parts and by using the property of the Euler gamma function in Eq. (1.5) the following relation holds true:

$$\begin{aligned} \varepsilon(t) &= \frac{\alpha}{C(\alpha)\Gamma(1+\alpha)} \int_0^t \sigma(\tau)(t-\tau)^{\alpha-1}\, d\tau \\ &= \frac{1}{C(\alpha)\Gamma(\alpha)} \int_0^t \sigma(\tau)(t-\tau)^{\alpha-1}\, d\tau = \frac{1}{C(\alpha)} \left(\mathrm{I}_{0^+}^{\alpha}\sigma\right)(t), \end{aligned} \tag{3.50}$$

that is the second fractional relation of the spring-pot in Eq. (3.39), obtained from Slonimsky [112].

The shown treatise proves the capabilities of the fractional model. The spring-pot is able to describe with two parameters $C(\alpha)$ and α two viscoelastic phenomena, the creep and relaxation are captured with the same model. This is a remarkable advantage respect to the other classical models.

3.6.4 The generalized fractional models

The spring-pot represents a generalized model which contains the Hookean and Newtonian behavior as bounded cases. Indeed, if the order of the involved operator is $\alpha = 0$ the spring-pot becomes a perfect spring, and when $\alpha = 1$ the model restitutes the perfect dashpot. By using this new model is possible generalized the other models of classical viscoelasticity. As example, the fractional Maxwell model can be obtained by placing the spring-pot in place of the dashpot, obtaining the following fractional differential equation in the stress-strain relation:

$$\sigma(t) + a_1 \left(D^{\alpha}\sigma\right)(t) = b_0 \left(D^{\alpha}\varepsilon\right)(t), \tag{3.51}$$

where the characteristic parameters of the material are a_1, α, and b_0.

By the same substitution in the Kelvin-Voigt model the generalized Kelvin-Voigt is obtained. The stress-strain relation of this model is

$$\sigma(t) = b_0\varepsilon(t) + b_1 \left(D^{\alpha}\varepsilon\right)(t), \tag{3.52}$$

also in this case the characteristic parameters of the materials are three.

The fractional Zener model, known as 5-parameters model (α, β, a_1, b_0 and b_1), has the following stress-strain relation:

$$\sigma(t) + a_1 \left(D^{\alpha}\sigma\right)(t) = b_0\varepsilon(t) + b_1 \left(D^{\beta}\varepsilon\right)(t), \tag{3.53}$$

usually, the experimental evidence has shown that $\alpha = \beta$. Morevoer, with a thermodynamical approach *R. L. Bagley* and *P. J. Torvik* have proved that the 5-parameters model must have $\alpha = \beta$, in this manner the model becomes the 4-parameters model with the following relation:

$$\sigma(t) + a_1 \left(D^{\alpha}\sigma\right)(t) = b_0\varepsilon(t) + b_1 \left(D^{\alpha}\varepsilon\right)(t), \tag{3.54}$$

where the characteristic parameters are α, a_1, b_0 and b_1.

Generalizing the Eq. (3.13) with fractional operators the generic fractional stress-strain relation of the *fractional multi-elements model* is obtained as

$$\sum_{k=0}^{n} a_k \left(D^{\alpha_k}\sigma\right)(t) = \sum_{k=0}^{m} b_k \left(D^{\beta_k}\varepsilon\right)(t), \tag{3.55}$$

where can be happen that $n = m$, and $\alpha_k = \beta_k$.

3.6.5 Characteristic times and apparent modulus

> *"The mountains flowed before the Lord, the One of Sinai, before the Lord, the God of Israel."*
>
> Bible, Judges 5:5.

Obviously that prophetic phrase, in the Bible, contains a non-scientific message, nevertheless in the 1964 *Markus Reiner* bestows a physical meaning to this expression. Since in that message is summarized the particular behavior that all solids show when the observation times become very long (in this case the observation time becomes timeless "*before the Lord*"). Indeed, also the rocks, that constitute the mountains, flow in a long period. In particular, Reiner in his original paper [93] wrote:

> "*Deborah knew two things. First, that the mountains flow, as everything flows. But, secondly, that they flowed before the Lord, and not before man, for the simple reason that man in his short lifetime cannot see them flowing, while the time of observation of God is infinite. We may therefore well define a non-dimensional number the Deborah number*"

Based on this assertion, to classify the viscoelastic solids, in rheology it is common to use a dimensionless parameter called *Deborah number*, in honor of the homonymous prophetess who uttered the phrase in the epigraph. This number is defined by the ratio of the relaxation time η, which characterizes the fluidity of the material, and the observation time t, characteristic of the experiment:

$$D_e = \frac{\eta}{t}. \tag{3.56}$$

The relaxation time η is a characteristic parameter of the material. It is not easy to found experimentally, and depends on the mechanical model. Usually, it can be see as the ratio between the viscosity $[Pa \cdot sec]$ and the stiffness $[Pa]$ of the material.

$$\eta = \frac{\mu}{E}, \quad [sec]. \tag{3.57}$$

The Deborah's number represents an useful experimental parameter. Indeed, it indicates when the tested material exhibits viscoelastic properties. In other words, it denotes the time, during the experiment, when the solid material start to flow and to show the fluid characteristic. Low values of D_e denote a behavior similar to viscous liquids, while values of D_e tending to infinity describe a material similar to the ideal elastic solids.

The relaxation time is readily evaluable for classic viscoelastic model, but it is not easy to found for the fractional model, since it is inside the parameter $C(\alpha)$ of the fractional differential equation of the spring-pot. Consider the creep and relaxation functions in the Eq.s (3.44) and (3.48) and introduce two characteristic times for both functions, denoted with T_R e T_C, respectively. After that, it is possible to write:

$$\Phi(t) = E\left(\frac{t}{T_R}\right)^{-\alpha} \tag{3.58a}$$

$$\Psi(t) = \frac{1}{E}\left(\frac{t}{T_C}\right)^{\alpha} \tag{3.58b}$$

where the two characteristic times contain η, indeed:

$$T_R = \eta\Gamma(1-\alpha)^{-1/\alpha} \tag{3.59a}$$

$$T_C = \eta\Gamma(1+\alpha)^{1/\alpha} \tag{3.59b}$$

where T_R and T_C denote the *characteristic time of the relaxation* and the *characteristic time of the creep*. In particular, they denote when the rheological behavior

becomes perfectly elastic, then at such times the following proportional relations hold:

$$\sigma(t) = E\left(\frac{t}{T_R}\right)^{-\alpha}\varepsilon(0) = E\varepsilon(0), \quad t = T_R; \tag{3.60a}$$

$$\varepsilon(t) = \frac{1}{E}\left(\frac{t}{T_C}\right)^{\alpha}\sigma(0) = \frac{1}{E}\sigma(0), \quad t = T_C. \tag{3.60b}$$

In the relaxation test for $t < T_R$ the considered material shows a mechanical behavior stiffer than the perfectly elastic one, while for $t > T_R$ the material has a more deformable behavior. An analogous behavior there is in the creep test for T_C. Both the characteristic times contain the time η that is not easy to found, since from the best-fitting of the experimental data is possible to evaluate the parameters α and $C(\alpha)$, into the latter one there is the time η but it is not deducible. By virtue of these observations only the trends of the normalized characteristic times T_R and T_C in η are know, obtaining that:

$$\frac{T_R}{\eta} = \Gamma(1-\alpha)^{-1/\alpha}, \tag{3.61a}$$

$$\frac{T_C}{\eta} = \Gamma(1+\alpha)^{1/\alpha}. \tag{3.61b}$$

Figure 3.15 shows the trends of the normalized characteristic times T_R and T_C

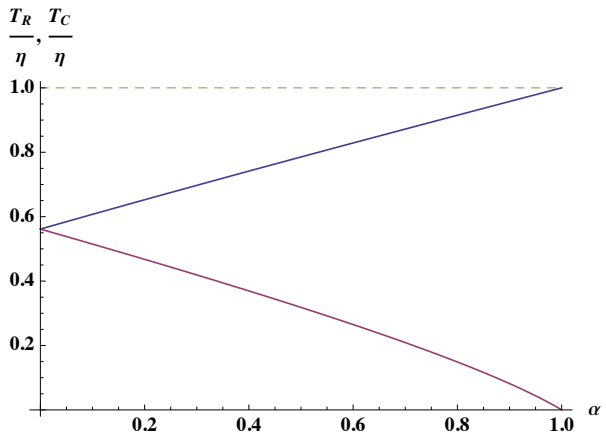

Figure 3.15: Normalized characteristic times.

for $0 \leqslant \alpha \leqslant 1$. Some notable values can be found:

$$\begin{aligned} &\lim_{\alpha\to 0} \frac{T_R}{\eta} = \lim_{\alpha\to 0} \frac{T_C}{\eta} = e^{-\gamma_e} \cong 0.5615, \\ &\lim_{\alpha\to 1} \frac{T_R}{\eta} = 0, \qquad \lim_{\alpha\to 1} \frac{T_C}{\eta} = 1, \end{aligned} \tag{3.62}$$

where γ_e is the Euler-Mascheroni constant ($\gamma_e = 0.57722$). Both functions exhibit quasi-linear trends, then it is possible to rewrite

$$T_C - T_R = \eta \left[\Gamma(1+\alpha)^{1/\alpha} - \Gamma(1-\alpha)^{-1/\alpha}\right] \approx \eta\alpha, \tag{3.63}$$

that expression allows to found the following approximated relations:

$$\begin{aligned} T_R \approx& e^{-\gamma_e}(1+\alpha), \\ T_C \approx& e^{-\gamma_e}(1-\alpha) + \alpha. \end{aligned} \tag{3.64}$$

It is possible to observe that for the purely elastic behavior $\alpha = 0$, the relaxation time coincide with the creep time, and being $\eta = 0$ the system instantly reaches the elastic deformation (or the tension in the relaxation test). Instead, when $\alpha = 1$ the behavior is different for the creep and the relaxation test. Indeed, if the imposed deformation is $\varepsilon(0) = \varepsilon_0$ the corresponded stress will be null $\sigma(t) = \Phi(t)\varepsilon_0 = E(T_R/t)\varepsilon_0 = 0$, instead, if the imposed tension is $\sigma(0) = \sigma_0$ the corresponded deformation will be $\varepsilon(t) = \Psi(t)\sigma_0 = \sigma_0 t/E$, then its linearly increases in the time.

After finding the characteristic times is possible to observe a particular result obtained for the product between the relaxation function $\Phi(t)$ in Eq. (3.44) and the creep function $\Psi(t)$ in Eq. (3.48):

$$\Phi(t)\Psi(t) = \left(\frac{T_R}{T_C}\right)^{\alpha} = \frac{1}{\Gamma(1+\alpha)\Gamma(1-\alpha)} = \frac{\sin(\alpha\pi)}{\alpha\pi}, \tag{3.65}$$

that product is obtained by using the Euler's reflection formula in Eq. (1.8), and it is a function just of the order α. By using the Eq. (3.65) the following relations are found:

$$\Phi(t) = \frac{1}{\Psi(t)}\left(\frac{\sin(\alpha\pi)}{\alpha\pi}\right), \tag{3.66a}$$

$$\Psi(t) = \frac{1}{\Phi(t)}\left(\frac{\sin(\alpha\pi)}{\alpha\pi}\right), \tag{3.66b}$$

these expressions permit to fully characterize the mechanical behavior of real material by the knowledge of the results of one kind of test (creep or relaxation).

Consider the Eq. (3.60a) for $\forall t$, it is possible to define a time-variable elastic modulus that follows the proportional link between the imposed deformation and corresponded stress. Similarly, consider the creep in Eq. (3.60b), it is possible to found another function that permits to hold such proportional relation true, therefore:

$$E_R(t) = E\left(\frac{t}{T_R}\right)^{-\alpha}, \tag{3.67a}$$

$$E_C(t) = E\left(\frac{t}{T_C}\right)^{-\alpha}, \tag{3.67b}$$

where $E_R(t)$ is the *apparent relaxation modulus*, that coincides with the Young's modulus when $t = T_R$; $E_C(t)$ denotes the *apparent creep modulus*, that for $t = T_C$ becomes, also in this case, the Young's modulus. The apparent modulus are functions of the elastic modulus E, that is contained in $C(\alpha)$. This parameter also contains the terms η^α. The two parameters inside $C(\alpha)$, E and η are not separable in the fractional model, but some useful considerations can be drawn by the observation of the normalized curves of the apparent modulus depicted in Figure 3.16. In particular, the Figure 3.16(a) shows the

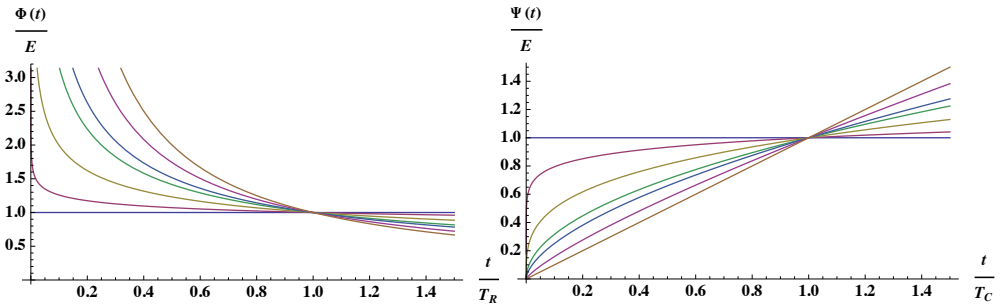

(a) Normalized relaxation function **(b)** Normalized creep function

Figure 3.16: Normalized relaxation and creep function for some values of α.

trend of the relaxation function normalized for t/T_R, while the Figure 3.16(b) shows the creep function normalized for t/T_C. Both curves pass through the point $(1, 1)$ but they have different curvature. Based on this observation two

characteristic points in which the curves have the maximum curvature can be found. Such *knee points* denote two particular times t^*, which indicate a changing in the mechanical behavior of the material. These times are related to the characteristic times T_R and T_C and to the order α by the following relation:

$$\frac{t^*}{T_I} = \left(\frac{\alpha\sqrt{1+2\alpha}}{\sqrt{2+\alpha}} \right)^{\frac{1}{\alpha+1}} \cong \alpha, \tag{3.68}$$

where T_I indicates the generic characteristic time ($I = R$ for the relaxation, and $I = C$ for the creep).

The knee point certainly denotes a changing in the viscoelastic behavior of the material, and represents a characteristic point of the material, on this concept will be back later.

3.6.6 Triaxial stress-strain relation

This section extends the previous uniaxial stress-strain relations to the triaxial case [23, 71, 72, 81, 120]. In order to do this, consider the tridimensional continuous solid with volume V, delimited by the boundary surface S (see Figure 3.17), the Cauchy stress tensor $\mathbf{T}$, and the deformation tensor $\boldsymbol{\varepsilon}$, of a

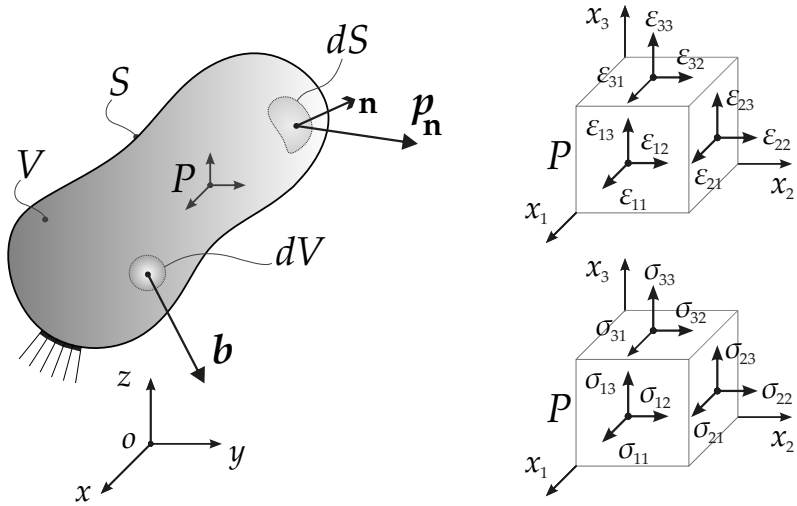

Figure 3.17: Continuum of Cauchy.

generic point $P \in V$ are defined as

$$\mathbf{T} = \begin{bmatrix} \sigma_{11} & \sigma_{12} & \sigma_{13} \\ \sigma_{21} & \sigma_{22} & \sigma_{23} \\ \sigma_{31} & \sigma_{32} & \sigma_{33} \end{bmatrix}, \qquad \boldsymbol{\varepsilon} = \begin{bmatrix} \varepsilon_{11} & \varepsilon_{12} & \varepsilon_{13} \\ \varepsilon_{21} & \varepsilon_{22} & \varepsilon_{23} \\ \varepsilon_{31} & \varepsilon_{32} & \varepsilon_{33} \end{bmatrix}. \tag{3.69}$$

where the terms in the diagonals σ_{ii} and ε_{ii} with $i = 1, 2, 3$ are the axial stresses and axial strains, respectively; instead the other terms σ_{ij} and ε_{ij} with $i, j = 1, 2, 3$ and $i \neq j$ are the shear stresses and shear deformation, respectively. Commonly, another way to denote these latter quantity is $\tau_{ij} = \sigma_{ij}$ for the shear stress, and $2\varepsilon_{ij} = \gamma_{ij}$ for the shear deformation. Moreover, the following relations, for the non-diagonal terms, hold:

$$\sigma_{ij} = \sigma_{j,i}, \qquad \varepsilon_{ij} = \varepsilon_{j,i}, \tag{3.70}$$

from these relations follows that the tensors $\mathbf{T}$ and $\boldsymbol{\varepsilon}$ are symmetric.

Let $\mathrm{J}^{\sigma} = \sigma_{ii}$ and $\mathrm{J}^{\varepsilon} = \sigma_{ii}$ $(i = 1, 2, 3)$ be the linear invariants and $\bar{\mathrm{J}}^{\sigma} = \sigma_{ii}/3$, $\bar{\mathrm{J}}^{\varepsilon} = \varepsilon_{ii}/3$. The Cauchy stress tensor $\mathbf{T}$ and the deformation tensor $\boldsymbol{\varepsilon}$ may be decomposed into the deviatoric part and the volumetric ones as follows

$$\mathbf{T} = \bar{\mathrm{J}}^{\sigma}\mathbf{I} + \mathbf{T}^{d}; \quad \boldsymbol{\varepsilon} = \bar{\mathrm{J}}^{\varepsilon}\mathbf{I} + \boldsymbol{\varepsilon}^{d} \tag{3.71}$$

where $\mathbf{I}$ is the identity matrix. $\mathbf{T}^{d}$ and $\boldsymbol{\varepsilon}^{d}$ are the so called deviatoric part of the stress and strain tensor, respectively.

For linear elastic isotropic material the constitutive law for the volumetric part is written as

$$\mathrm{J}^{\sigma} = 3K\mathrm{J}^{\varepsilon} \tag{3.72}$$

where K is the bulk modulus $K = E/3(1 - 2\nu)$ being E and ν the Young's modulus and the Poisson's ratio, respectively. While for the deviatoric part

$$\mathbf{T}^{d} = 2G\boldsymbol{\varepsilon}^{d} \tag{3.73}$$

where G is the shear modulus $G = E/2(1 + \nu)$.

For a purely viscous Newtonian fluid the volumetric deformation remain constant that is $\dot{\mathrm{J}}^{\varepsilon} = 0$, and then the only significative constitutive equation is

$$\mathbf{T}^{d} = 2G_1\dot{\boldsymbol{\varepsilon}}^{d} \tag{3.74}$$

where G_1 is the coefficient of viscosity of the fluid. For a *purely fractional viscoelastic material*, by denoting $\boldsymbol{\varepsilon}^{d}_{ve}$ the deviatoric part of the purely viscoelastic strain tensor, we assume that Eq. (3.74) is substituted by

$$\mathbf{T}^{d}(t) = 2G_{\beta}\left({}_{\mathrm{C}}D^{\beta}_{0^+}\boldsymbol{\varepsilon}^{d}_{ve}\right)(t) \tag{3.75}$$

where $\left({}_{\mathrm{C}}D^{\beta}_{0^+}\cdot\right)(t)$ is the Caputo's fractional derivative.

For *real viscoelastic material* can be assumed that $\boldsymbol{\varepsilon}^d$ is composed by two terms, the first one is elastic $\boldsymbol{\varepsilon}^d_e$ and the second is the purely viscoelastic one $\boldsymbol{\varepsilon}^d_{ve}$, that is

$$\boldsymbol{\varepsilon}^d = \boldsymbol{\varepsilon}^d_e + \boldsymbol{\varepsilon}^d_{ve}. \tag{3.76}$$

Assuming that $\boldsymbol{\varepsilon}^d_e = \mathbf{T}^d 1/2G$ according to Eq. (3.73), from Eq. (3.76) yields

$$\left({}_{\mathrm{C}}D_{0^+}\boldsymbol{\varepsilon}^d\right)(t) = \left({}_{\mathrm{C}}D^{\beta}_{0^+}\boldsymbol{\varepsilon}^d_e\right)(t) + \left({}_{\mathrm{C}}D^{\beta}_{0^+}\boldsymbol{\varepsilon}^d_{ve}\right)(t) = \frac{1}{2G}\left({}_{\mathrm{C}}D^{\beta}_{0^+}\mathbf{T}^d\right)(t) + \frac{1}{2G_\beta}\mathbf{T}^d(t) \tag{3.77}$$

while for the volumetric component, due to the hypothesis J^ε is constant in time $\left({}_{\mathrm{C}}D^{\beta}_{0^+}\mathrm{J}^\varepsilon\right)(t) = 0$, the constitutive law remains that expressed in Eq. (3.72). The inverse relationship is written in the form

$$\boldsymbol{\varepsilon}^d(t) = \frac{1}{2G}\mathbf{T}^d(t) + \frac{1}{2G_\beta}\left(\mathrm{I}^{\beta}_{0^+}\mathbf{T}^d\right)(t) \tag{3.78}$$

where $\left(\mathrm{I}^{\beta}_{0^+}\mathbf{T}^d\right)(t)$ is the Riemann-Liouville fractional integral.

Chapter 4

Mechanical model of fractional viscoelasticity

The previous Chapter has shown how the fractional viscoelastic model is the best way to fully characterize the real mechanical behavior of materials. The limit of this kind of models is in the mechanical interpretation of the fractional operators. Indeed, this kind of operators do not have a geometric representation, and this aspect directly implies a lack of mechanical meaning when they are used to describe a physical phenomena. This absence for that powerful mathematical model has certainly limited its use in the engineering and mechanical fields. Several works have regarded the mechanical description of the fractional stress-strain relation [7–10, 59, 60, 100–102]. Recently, in [45] the exact mechanical models of such materials have been extensively discussed obtaining two intervals for β: i) Elasto-Viscous (EV) materials for $0 \leq \beta \leq 1/2$; ii) Visco-Elastic (VE) materials for $1/2 \leq \beta \leq 1$. These two ranges correspond to different continuous mechanical models.

In this Chapter a discretization scheme, based upon the continuous models proposed in [91], and useful to obtain a mechanical description of fractional derivative, is presented. It is shown that the discretized models are ruled by a set of coupled first order differential equations involving symmetric and positive definite matrices. Modal analysis shows that fractional order operators have a mechanical counterpart that is ruled by a set of Kelvin-Voigt units and each of them provides a proper contribution to the overall response. The robustness of the proposed discretization scheme is assessed in the Chapter for different classes of external loads and for different values of $\beta \in [0, 1]$.

Many details and extension of this kind of mechanical interpretation of

the mathematical model with fractional operators can be found in [38–40]. Moreover, the continuous and discretized models shown in this Chapter are also used for other physical problem in which fractional operators appear [2, 3].

4.1 The mechanical description of fractional law

According to the previous Chapter the time-dependent behavior of fractional viscoelasticity may be introduced starting from the so-called relaxation function $G(t)$ that represents the stress $\sigma(t)$ for assigned shear strain history $\gamma(t) = U(t)$, being $U(t)$ the unit step function. In virtue of Boltzmann superposition principle the stress-strain constitutive law is given as

$$\sigma(t) = \int_0^t G\,(t-\tau)\; d\gamma(\tau) = \int_0^t G\,(t-\tau)\,\dot{\gamma}(\tau)\,d\tau. \tag{4.1}$$

Eq. (4.1) is valid for $\gamma(0) = 0$. If $\gamma(0) = \gamma_0 \neq 0$, then the additional contribution given as $G(t)\gamma_0$ has to be added in Eq. (4.1). The stress-strain relation described in Eq. (4.1) involves a convolution integral with kernel $G(t)$. In the context of the viscoelastic materials, the functional class of $G(t)$ is of power-law type. That is,

$$G(t) = \frac{C(\beta)}{\Gamma(1-\beta)} t^{-\beta}, \tag{4.2}$$

where $C(\beta)/\Gamma(1-\beta)$ and β are parameters that depend of the materials at hand and may be evaluated by a proper fit of experimental results. Introducing Eq. (4.2) in Eq. (4.1) the stress-strain relation is obtained as

$$\sigma(t) = C(\beta)\left({}_{\mathrm{C}}D^{\beta}_{0^+}\gamma\right)(t), \tag{4.3}$$

where $\left({}_{\mathrm{C}}D^{\beta}_{0^+}\gamma\right)(t)$ is the Caputo's fractional derivative of order β. Advanced engineering materials such as biological polymer, foams and gels show $\beta \in]0,\,1[$.

The reciprocal stress-strain relation may be obtained starting from the creep function $J(t)$, that represents the strain $\gamma(t)$ for the assigned stress history $\sigma(t) = U(t)$. The Boltzmann superposition principle leads to the stress-strain relation in the form:

$$\gamma(t) = \int_0^t J\,(t-\tau)\; d\sigma(\tau) = \int_0^t J\,(t-\tau)\,\dot{\sigma}(\tau)\,d\tau, \tag{4.4}$$

that holds as the initial stress $\sigma(0) = 0$. If $\sigma(0) = \sigma_0 \neq 0$, then the additional contribution $J(t)\sigma_0$ has to be added in Eq. (4.4). Eq. (4.4) is a convolution integral with kernel $J(t)$ and in Laplace domain an algebraic relation among the Laplace transform of relaxation $G_{\mathcal{L}}(s)$ and the Laplace transform of creep $J_{\mathcal{L}}(s)$ function exists as shown in Eq. (3.23). It follows that as $G(t)$ is assigned as in Eq. (4.2), the corresponding creep function $J(t)$ may be readily obtained in the form:

$$J(t) = \frac{t^{\beta}}{C(\beta)\Gamma(1+\beta)}. \tag{4.5}$$

Substitution of such an expression in Eq. (4.4) yields:

$$\gamma(t) = \frac{1}{C(\beta)} \left(\mathrm{I}_{0^+}^{\beta}\sigma\right)(t), \tag{4.6}$$

where $\left(\mathrm{I}_{0^+}^{\beta}\sigma\right)(t)$ is the Riemann-Liouville fractional integral of order β.

Inspection of Eqs. (4.3) and (4.6) reveals that, as soon as we assume that $J(t)$ (or $G(t)$) is of power-law type, then the constitutive law of the materials is ruled by fractional operators, so the name fractional viscoelastic materials.

In a previous study [91] it has been shown that, from a mechanical prospective, it must be distinguished among values of order $\beta = \beta_E \in [0, 1/2]$ and values of order $\beta = \beta_V \in [1/2, 1]$. Such a difference is reflected into the different mechanical models beyond β_E and β_V. In more details there are two different mechanical models that exactly restitute the stress-strain relation expressed in Eq. (4.3) or in Eq. (4.6). As $0 \leq \beta = \beta_E \leq 1/2$ the mechanical model is a massless indefinite fluid column resting on a bed of independent springs as shown in Figure 4.1(a) and in this case is referred so elasto-viscous material. If, instead, $1/2 \leq \beta = \beta_V \leq 1$ the exact mechanical model is represented by indefinite massless shear-type column resting on a bed of independent dashpots as shown in Figure 4.1(b), this model is referred to visco-elastic material.

The correspondence of these mechanical models and fractional order operators has been proved by introducing a z vertical axis as shown in Figure 4.1 and denoting $\sigma(z, t)$ the shear stress (in the fluid or in the cantilever beam) and $\gamma(z, t)$ the normalized displacement field [91]. Moreover let $\sigma(0, t) = \sigma(t)$ and $\gamma(0, t) = \gamma(t)$ the stress applied on the top of the model and the corresponding strain, respectively. The stress-strain relation in Eq. (4.3) is captured by the stress $\sigma(t)$ on the upper lamina and its correspondent transverse displacement $\gamma(t)$ (normalized displacement at the top). All the mechanical characteristics, viscosity of fluid $c_E(z)$ and external stiffness $k_E(z)$ for the

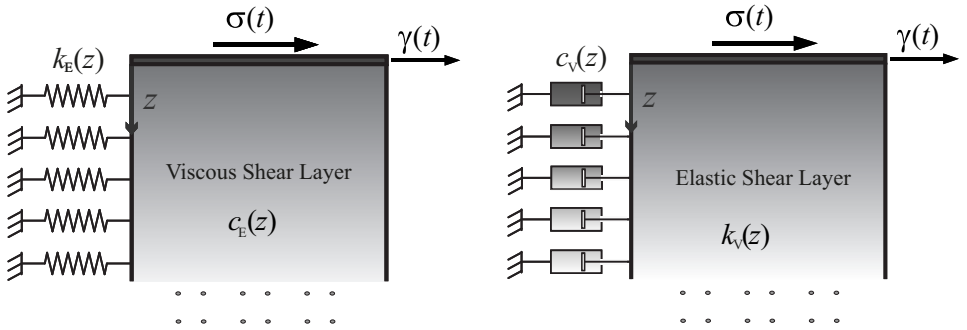

(a) Elasto-Viscous model **(b)** Visco-Elastic model

Figure 4.1: Continuous fractional models.

model in Figure 4.1(a) ($0 \leq \beta \leq 1/2$) as well as shear modulus $k_V(z)$ and external viscous coefficient of external dashpots $c_V(z)$ for the model in Figure 4.1(b) ($1/2 \leq \beta \leq 1$), vary along the z axis with power-law.

In more details, define G_0 and η_0 the reference values of the shear modulus and viscosity coefficient. For the EV materials ($\beta \in [0, 1/2]$) the stiffness and the viscous coefficients decay with power-laws:

$$k_E(z) = \frac{G_0}{\Gamma(1+\alpha)} z^{-\alpha}, \quad c_E(z) = \frac{\eta_0}{\Gamma(1-\alpha)} z^{-\alpha}, \tag{4.7}$$

with $0 \leq \alpha \leq 1$, whereas the VE materials ($\beta \in [1/2, 1]$) the mechanical characteristics of the model in Figure 4.1(b) reads:

$$k_V(z) = \frac{G_0}{\Gamma(1-\alpha)} z^{-\alpha}, \quad c_V(z) = \frac{\eta_0}{\Gamma(1+\alpha)} z^{-\alpha}. \tag{4.8}$$

The governing equation of the continuous model depicted in Figure 4.1(a) is written as

$$\frac{\partial}{\partial z}\left[c_E(z)\frac{\partial \dot{\gamma}(z,\, t)}{\partial z}\right] = k_E(z)\gamma(z,\, t), \tag{4.9}$$

while the equilibrium equation of the continuous model depicted in Figure 4.1(b) is written as

$$\frac{\partial}{\partial z}\left[k_V(z)\frac{\partial \gamma(z,\, t)}{\partial z}\right] = c_V(z)\dot{\gamma}(z,\, t). \tag{4.10}$$

The solution of the differential equations in Eq. (4.9) and (4.10) can be solved by Laplace transform. In this way the solution $\gamma_{\mathcal{L}}(z, s)$ in Laplace domain

involves the modified first and second kind Bessel functions, denoted respectively with $I_\beta(\cdot)$ and $K_\beta(\cdot)$, and defined in Eq. (1.31) and in Eq. (1.32). In particular, for EV case the relation is

$$\gamma_{\mathcal{L}}(z,s) = z^\beta \left[B_{E1} I_\beta \left(\frac{z}{\sqrt{\tau_E(\alpha)s}} \right) + B_{E2} K_\beta \left(\frac{z}{\sqrt{\tau_E(\alpha)s}} \right) \right], \tag{4.11}$$

with $\tau_E(\alpha) = -\eta_0 \Gamma(\alpha)/(\Gamma(-\alpha)G_0)$ and $\beta = (1-\alpha)/2$; while for VE case:

$$\gamma_{\mathcal{L}}(z,s) = z^\beta \left[B_{V1} I_\beta \left(z\sqrt{\tau_E(\alpha)s} \right) + B_{V2} K_\beta \left(z\sqrt{\tau_E(\alpha)s} \right) \right], \tag{4.12}$$

with $\tau_V(\alpha) = -\eta_0 \Gamma(-\alpha)/(\Gamma(\alpha)G_0)$ and $\beta = (1+\alpha)/2$. The constants of integration B_{Ei} and B_{Vi} with $i = 1,2$ are obtained by imposing the following pairs of boundary conditions, for the EV and VE case respectively:

$$\text{(EV)} \begin{cases} \lim\limits_{z\to 0} c_E(z) \dfrac{\partial \dot{\gamma}(z,t)}{\partial z} = \sigma(0,t) = \sigma(t), \\ \lim\limits_{z\to\infty} \gamma(z,t) = 0 \end{cases} \tag{4.13a}$$

$$\text{(VE)} \begin{cases} \lim\limits_{z\to 0} k_V(z) \dfrac{\partial \gamma(z,t)}{\partial z} = \sigma(0,t) = \sigma(t), \\ \lim\limits_{z\to\infty} \gamma(z,t) = 0 \end{cases} \tag{4.13b}$$

and by making the inverse Laplace transform, the fractional stress-strain relation in Eq. (4.6) is obtained, that is to say:

$$\gamma(t) = \frac{1}{C_E(\beta)} \left(\mathrm{I}^\beta_{0^+} \sigma \right)(t) \qquad \text{(EV)} \tag{4.14a}$$

$$\gamma(t) = \frac{1}{C_V(\beta)} \left(\mathrm{I}^\beta_{0^+} \sigma \right)(t) \qquad \text{(VE)} \tag{4.14b}$$

where the coefficients $C_E(\beta)$ and $C_V(\beta)$ are

$$C_E(\beta) = \frac{G_0 \, \Gamma(\beta) \, 2^{2\beta-1}}{\Gamma(2-2\beta)\,\Gamma(1-\beta)} (\tau_E(\alpha))^\beta, \quad 0 \le \beta \le 1/2, \tag{4.15a}$$

$$C_V(\beta) = \frac{G_0 \, \Gamma(1-\beta) \, 2^{1-2\beta}}{\Gamma(2-2\beta)\,\Gamma(\beta)} (\tau_V(\alpha))^\beta, \quad 1/2 \le \beta \le 1. \tag{4.15b}$$

Note that, if the boundary condition applied to the top layer of the model (see Eqs. (4.13a) and (4.13b)), respectively, for EV and VE materials, involves Dirichlet specifics. That is,

$$\begin{cases} \lim_{z\to 0} \gamma(z,t) = \gamma(t), \\ \lim_{z\to\infty} \gamma(z,t) = 0. \end{cases} \tag{4.16}$$

The evaluation of the stress at the top lamina in terms of the transverse displacement field yields:

$$\begin{aligned} \sigma(t) &= C_E(\beta) \left({}_{\mathrm{C}}D^{\beta}_{0^+}\gamma\right)(t) \qquad \text{(EV)} \\ \sigma(t) &= C_V(\beta) \left({}_{\mathrm{C}}D^{\beta}_{0^+}\gamma\right)(t) \qquad \text{(VE)} \end{aligned} \tag{4.17}$$

as reported in [91].

4.2 The discretization of fractional viscoelastic model

The mechanical representation of fractional order operators discussed in previous section may be used to introduce a discretization scheme that corresponds to evaluate fractional derivative. The two cases corresponding to $\beta \in [0,\, 1/2]$ and $\beta \in [1/2,\, 1]$ will be analyzed in this section.

4.2.1 Discrete model of elasto-viscous material

By introducing a discretization of the z-axis as $z_j = j\triangle z$ into to the governing equation of the EV material in Eq. (4.9) yields a finite difference equation of the form:

$$\frac{\triangle}{\triangle z}\left[c_E(z_j)\frac{\triangle\dot{\gamma}(z_j,\, t)}{\triangle z}\right] = k_E(z_j)\gamma(z_j,\, t), \tag{4.18}$$

so that, denoting $k_{Ej} = k_E(z_j)\triangle z$ and $c_{Ej} = c_E(z_j)/\triangle z$ the continuous model is discretized into a dynamical model constituted by massless shear layers, with horizontal degrees of freedom $\gamma(z_j, t) = \gamma_j(t)$, that are mutually interconnected by linear dashpots with viscosity coefficients c_{Ej} and resting on a bed of independent linear springs k_{Ej}.

The stiffness coefficient k_{Ej} and the viscosity coefficient c_{Ej} reads:

$$k_{Ej} = \frac{G_0}{\Gamma(1+\alpha)} z_j^{-\alpha}\triangle z, \quad c_{Ej} = \frac{\eta_0}{\Gamma(1-\alpha)}\frac{z_j^{-\alpha}}{\triangle z}, \tag{4.19}$$

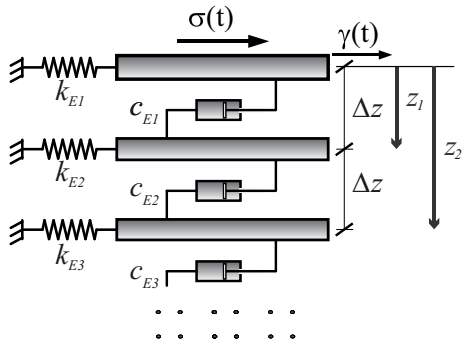

Figure 4.2: Discretized counterpart of the continuous model Figure 4.1(a) EV case.

with $\alpha = 1 - 2\beta$.
The equilibrium equations of the generic shear layer of the model read:

$$\begin{cases} k_{E0}\gamma_1(t) - c_{E0}\triangle\dot{\gamma}_1(t) = \sigma(t), \\ k_{Ej}\gamma_j(t) + c_{Ej-1}\triangle\dot{\gamma}_{j-1}(t) - c_{Ej}\triangle\dot{\gamma}_j(t) = 0, \;\; j = 1, 2, \ldots, \infty, \end{cases} \tag{4.20}$$

where $\gamma_1(t) = \gamma(t)$ and $\triangle\dot{\gamma}_j(t) = \dot{\gamma}_{j+1}(t) - \dot{\gamma}_j(t)$. By inserting Eqs. (4.19) in Eqs. (4.20), at the limit as $\triangle z \to 0$, the discrete model reverts to Eq. (4.9). That is the discretized model presented in Figure 4.2 represents a proper discretization of the continuous EV counterpart.

As soon as z increase $\gamma(z,\, t)$ decay and $\lim_{z\to\infty}\gamma(z,t) = 0$ it follows that only a certain number, say n, of equilibrium equation may be accounted for the analysis. It follows that the system in Eqs. (4.20) may be rewritten in the following compact form:

$$p_E\mathbf{A}\dot{\boldsymbol{\gamma}}(t) + q_E\mathbf{B}\boldsymbol{\gamma}(t) = \mathbf{v}\sigma(t), \tag{4.21}$$

where:

$$p_E = \frac{\eta_0}{\Gamma(1-\alpha)}\triangle z^{-(1+\alpha)}, \qquad q_E = \frac{G_0}{\Gamma(1+\alpha)}\triangle z^{1-\alpha}. \tag{4.22}$$

In Eq. (4.21):

$$\boldsymbol{\gamma}^T(t) = \begin{bmatrix} \gamma_1(t) & \gamma_2(t) & \ldots & \gamma_n(t) \end{bmatrix}, \quad \mathbf{v}^T = \begin{bmatrix} 1 & 0 & 0 & \ldots & 0 \end{bmatrix}, \tag{4.23}$$

where the apex T means transpose. The coefficient matrices $\mathbf{A}$ and $\mathbf{B}$ are

$$\mathbf{A} = \begin{bmatrix} 1^{-\alpha} & -1^{-\alpha} & 0 & \dots & 0 \\ -1^{-\alpha} & 1^{-\alpha}+2^{-\alpha} & -2^{-\alpha} & \dots & 0 \\ 0 & -2^{-\alpha} & 2^{-\alpha}+3^{-\alpha} & \dots & 0 \\ \vdots & \vdots & \vdots & \ddots & \vdots \\ 0 & 0 & 0 & \dots & (n-1)^{-\alpha}+n^{-\alpha} \end{bmatrix}, \tag{4.24}$$

$$\mathbf{B} = \begin{bmatrix} 1^{-\alpha} & 0 & 0 & \dots & 0 \\ 0 & 2^{-\alpha} & 0 & \dots & 0 \\ 0 & 0 & 3^{-\alpha} & \dots & 0 \\ \vdots & \vdots & \vdots & \ddots & \vdots \\ 0 & 0 & 0 & \dots & n^{-\alpha} \end{bmatrix}. \tag{4.25}$$

The matrices $\mathbf{A}$ and $\mathbf{B}$ are symmetric and positive definite (in particular $\mathbf{B}$ is diagonal) and they may be readily constructed for an assigned value of α (depending of the derivative order β) and for a fixed truncation order n. Moreover Eq. (4.21) may now be readily integrated by using standard tools of dynamic analysis how it will be shown later on.

4.2.2 Discrete model of visco-elastic material

As the fractional order derivative is $\beta = \beta_V \in [1/2, 1]$ the mechanical description of the material is the represented by the continuous model depicted in Figure 4.3 and ruled by Eq (4.10).

By introducing a discretization of the z-axis in intervals $\triangle z$ in governing equation of the VE materials in Eq. (4.10) yields a finite difference equation of the form:

$$\frac{\triangle}{\triangle z}\left[k_V(z_j)\frac{\triangle\gamma(z_j,\,t)}{\triangle z}\right] = c_V(z_j)\dot{\gamma}(z_j,\,t), \tag{4.26}$$

that corresponds to a discretized mechanical representation of fractional derivatives. The mechanical model is represented by a set of massless shear layers with state variables $\gamma(z_j,\,t) = \gamma_j(t)$ that are mutually interconnected by linear springs with stiffness $k_{Vj} = k_V(z_j,\,t)/\triangle z$ resting on a bed of independent linear dashpots with viscosity coefficient $c_{Vj} = c_V(z_j,\,t)\triangle z$. Stiffness and dashpot coefficients are

$$k_{Vj} = \frac{G_0}{\Gamma(1-\alpha)}\frac{z_j^{-\alpha}}{\triangle z}, \quad c_{Vj} = \frac{\eta_0}{\Gamma(1+\alpha)}z_j^{-\alpha}\triangle z, \tag{4.27}$$

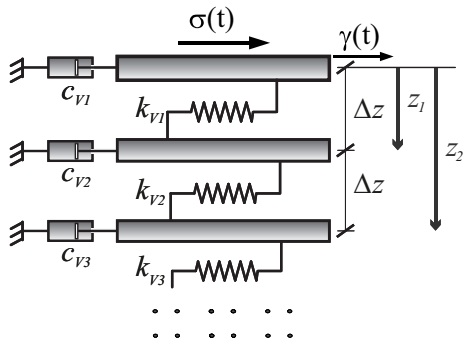

Figure 4.3: Discretized counterpart of the continuous model Figure 4.1(b) VE case.

with $\alpha = 2\beta - 1$.
The set of equilibrium equations reads:

$$\begin{cases} c_{V0}\dot{\gamma}_1(t) - k_{V0}\triangle\gamma_1(t) = \sigma(t), \\ c_{Vj}\dot{\gamma}_j(t) + k_{Vj-1}\triangle\gamma_{j-1}(t) - k_{Vj}\triangle\gamma_j(t) = 0, \quad j = 1, 2, \ldots, \infty. \end{cases} \tag{4.28}$$

Thus, considering the contributions of the first n shear layers the differential equation system may be written as

$$p_V \mathbf{B}\dot{\boldsymbol{\gamma}}(t) + q_V \mathbf{A}\boldsymbol{\gamma}(t) = \mathbf{v}\sigma(t), \tag{4.29}$$

where:

$$p_V = \frac{\eta_0}{\Gamma(1+\alpha)}\triangle z^{1-\alpha}, \quad q_V = \frac{G_0}{\Gamma(1-\alpha)}\triangle z^{-(1+\alpha)}, \tag{4.30}$$

while $\boldsymbol{\gamma}$, $\mathbf{v}$ and the matrices $\mathbf{A}$ and $\mathbf{B}$ have already been defined in sect. 4.2.1.

Up to now, a shear stress and a subsequent shear deformation as in the Couette problem have been considered, but exact governing equations, and then exact mechanical models, for the axial stress and axial deformation are the same how is depicted in Figure 4.4 for both EV and VE case. Also in this case as $\Delta z \to 0$ (continuous problem) both the fractional EV and VE continuous are restored.

In the next section the modal analysis of dynamical system, ruled by Eq. (4.21) and Eq. (4.29), will be performed leading to a set of decoupled system of first order differential equations.

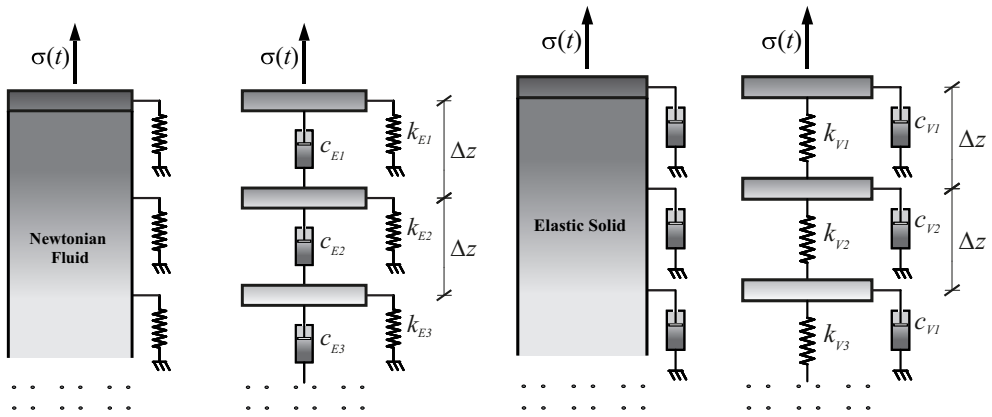

(a) Elasto-Viscous axial model **(b)** Visco-Elastic axial model

Figure 4.4: Continuous and discretized fractional axial models.

4.3 The modal analysis of the discrete models

The observations reported in previous section lead to conclude that, whatever class of viscoelastic materials is considered, the time-evolution of the material system may be obtained by the introduction of a proper set of inner state variables, collected in the vector $\gamma(t)$ and ruled by a set first-order linear differential equations. In this perspective the mechanical response of fractional viscoelastic materials may be obtained in terms of the vector $\gamma(t)$ by means of the decoupling set of eigenmodes of the differential equations system reported in Eq. (4.20) for EV materials or in Eq. (4.28) for VE materials. Since the different mechanical models correspond to Elasto-Viscous and Visco-Elastic materials, as discussed in previous section, these two cases will be dealt separately in the following.

4.3.1 Elasto-viscous materials

The governing equation of EV case is reported in Eq. (4.21). First, consider the homogeneous case with $\sigma(t) = 0$. Performing the coordinate transformation

$$\mathbf{B}^{1/2}\gamma(t) = \mathbf{x}(t), \tag{4.31}$$

and premultiplying by $\mathbf{B}^{-1/2}$, the differential equation for the unknown vector $\mathbf{x}$ is

$$p_E \mathbf{D}\,\dot{\mathbf{x}}(t) + q_E \mathbf{x}(t) = \tilde{\mathbf{v}}\sigma(t), \tag{4.32}$$

where $\tilde{\mathbf{v}} = \mathbf{B}^{-1/2}\mathbf{v}$, $\mathbf{D}$ is the dynamical matrix $\mathbf{D} = \mathbf{B}^{-1/2}\mathbf{A}\,\mathbf{B}^{-1/2}$, defined as

$$\mathbf{D} = \begin{bmatrix} 1 & -\left(\frac{2}{1}\right)^{\frac{\alpha}{2}} & 0 & \dots & 0 & 0 \\ -\left(\frac{2}{1}\right)^{\frac{\alpha}{2}} & 1+\left(\frac{2}{1}\right)^{\alpha} & -\left(\frac{3}{2}\right)^{\frac{\alpha}{2}} & \dots & 0 & 0 \\ 0 & -\left(\frac{3}{2}\right)^{\frac{\alpha}{2}} & 1+\left(\frac{3}{2}\right)^{\alpha} & \dots & 0 & 0 \\ \vdots & \vdots & \vdots & \ddots & \vdots & \vdots \\ 0 & 0 & 0 & \dots & 1+\left(\frac{n-1}{n-2}\right)^{\alpha} & -\left(\frac{n}{n-1}\right)^{\frac{\alpha}{2}} \\ 0 & 0 & 0 & \dots & -\left(\frac{n}{n-1}\right)^{\frac{\alpha}{2}} & 1+\left(\frac{n}{n-1}\right)^{\alpha} \end{bmatrix}, \tag{4.33}$$

$\mathbf{D}$ is symmetric and positive definite. It may be obtained straightforwardly once n and α are fixed. Let $\mathbf{\Phi}$ be the modal matrix whose columns are the orthonormal eigenvectors of $\mathbf{D}$. That is,

$$\mathbf{\Phi}^T\mathbf{D}\,\mathbf{\Phi} = \mathbf{\Lambda}, \qquad \mathbf{\Phi}^T\mathbf{\Phi} = \mathbf{I}, \tag{4.34}$$

where $\mathbf{I}$ is the identity matrix and $\mathbf{\Lambda}$ is the diagonal matrix collecting the eigenvalues $\lambda_j > 0$ of $\mathbf{D}$. The eigenvalues λ_j are ordered in such a way that $\lambda_1 < \lambda_2 < \cdots < \lambda_n$.

Introduce the modal coordinate vector $\mathbf{y}(t)$ defined as

$$\mathbf{x}(t) = \mathbf{\Phi}\,\mathbf{y}(t), \qquad \mathbf{y}(t) = \mathbf{\Phi}^{-1}\,\mathbf{x}(t), \tag{4.35}$$

By placing Eq. (4.35) into Eq. (4.32) and premultiplying for $\mathbf{\Phi}^T$, a decoupled set of differential equations is obtained:

$$p_E\mathbf{\Lambda}\,\dot{\mathbf{y}}(t) + q_E\mathbf{y}(t) = \bar{\mathbf{v}}\sigma(t), \tag{4.36}$$

where $\bar{\mathbf{v}} = \mathbf{\Phi}^T\tilde{\mathbf{v}} = \mathbf{\Phi}^T\mathbf{B}^{-1/2}\mathbf{v} = \mathbf{\Phi}^T\mathbf{v}$. The j^{th} equation of Eq. (4.36) reads:

$$\dot{y}_j(t) + \rho_j\,y_j(t) = \frac{\phi_{1,j}}{p_E\lambda_j}\sigma(t), \qquad j = 1,\,2,\,3,\dots n, \tag{4.37}$$

where $\rho_j = q_E/p_E\lambda_j > 0$ and $\phi_{1,j}$ is the j^{th} element of the first row of the matrix $\mathbf{\Phi}$. Eqs. (4.37) represent a decoupled set of Kelvin-Voigt units, as is shown in Figure 4.5, and the solution of Eq. (4.37) is provided in the form:

$$y_j(t) = y_j(0)\,e^{-\rho_j t} + \frac{\phi_{1,j}}{p_E\lambda_j}\int_0^t e^{-\rho_j(t-\tau)}\sigma(\tau)\,d\tau, \tag{4.38}$$

where $y_j(0)$ is the j^{th} component of the vector $\mathbf{y}(0)$ related to the vector of initial conditions $\boldsymbol{\gamma}(0)$ as

$$\mathbf{y}(0) = \boldsymbol{\Phi}^T \mathbf{B}^{1/2} \boldsymbol{\gamma}(0). \tag{4.39}$$

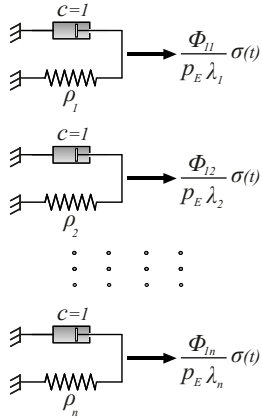

Figure 4.5: Kelvin-Voigt elements in modal space (EV case).

Solution of the differential equation system in Eq. (4.21) may be obtained as the modal vector $\mathbf{y}(t)$, that is evaluated solving Eq. (4.38). From the Eqs. (4.31) and (4.35) the vector $\boldsymbol{\gamma}(t)$ gives

$$\boldsymbol{\gamma}(t) = \mathbf{B}^{-1/2} \boldsymbol{\Phi} \mathbf{y}(t). \tag{4.40}$$

To find the relation among the shear stress and the normalized transverse displacement of the upper lamina, it is necessary to evaluate the first element of vector $\boldsymbol{\gamma}(t)$. That is,

$$\gamma(t) = \mathbf{v}^T \boldsymbol{\gamma}(t). \tag{4.41}$$

4.3.2 Visco-elastic materials

Modal analysis of the differential equations system representing the behavior of VE material is quite similar to previous section. In this case we substitute Eq. (4.31) in Eq. (4.29) and we perform left premultiplication by $\mathbf{B}^{-1/2}$ that reads:

$$p_V \dot{\mathbf{x}}(t) + q_V \mathbf{D}\, \mathbf{x}(t) = \tilde{\mathbf{v}} \sigma(t), \tag{4.42}$$

where **D** is the dynamical matrix defined in previous section. The dynamical equilibrium equation in modal coordinate reads:

$$p_V \dot{\mathbf{y}}(t) + q_V \mathbf{\Lambda}\, \mathbf{y}(t) = \bar{\mathbf{v}} \sigma(t), \tag{4.43}$$

the equilibrium of j^{th} Kelvin-Voigt from Eq. (4.43) is

$$\delta_j \dot{y}_j(t) + y_j(t) = \frac{\phi_{1,j}}{q_V \lambda_j} \sigma(t), \qquad j = 1,\, 2,\, 3, \ldots n, \tag{4.44}$$

where $\delta_j = p_v / q_V \lambda_j > 0$. In this case the problem in the modal coordinates is decomposed in a set of Kelvin-Voigt units as shown in Figure 4.6.

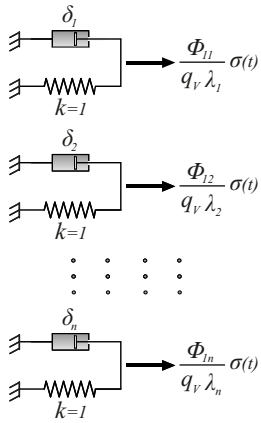

Figure 4.6: Kelvin-Voigt elements in modal space (VE case).

The solution in terms of modal coordinates is

$$y_j(t) = y_j(0)\, e^{-t/\delta_j} + \frac{\phi_{1,j}}{\delta_j\, q_V \lambda_j} \int_0^t e^{-(t-\tau)/\delta_j} \sigma(\tau)\, d\tau. \tag{4.45}$$

The stress-strain relations between shear stress $\sigma(t)$ and normalized displacement $\gamma(t)$ may be obtained as in previous section (see Eq.s (4.38) and (4.41)).

The case of $\beta = 1/2$, that is common to both EV and VE mechanical analogues, is a critical value and some additional considerations may be withdrawn from its analysis as it will be shown in the next section.

4.3.3 The critical value of β : $\beta = 1/2$

The case of $\beta = 1/2$ is of particular interest since eigenvalues and eigenvectors are given in closed form. It follows that the role played by the truncation depth of z and the number of laminae may be evidenced.

The case $\beta = 1/2$ may be treated in two different ways, or by assuming $\beta = 1/2$ starting from the EV case, or by assuming $\beta = 1/2$ starting from the VE case. Starting from the EV-model we get:

$$k_{Ej} = G_0 \triangle z, \qquad c_{Ej} = \frac{\eta_0}{\triangle z}, \tag{4.46}$$

consequently the Eqs. (4.22) take the following form:

$$p_E = \frac{\eta_0}{\triangle z}, \qquad q_E = G_0 \triangle z, \tag{4.47}$$

and the equilibrium equation system in compact form, similarly to the Eq. (4.21), reads:

$$\frac{\eta_0}{\triangle z} \mathbf{A} \dot{\boldsymbol{\gamma}}(t) + G_0 \triangle z \, \mathbf{B} \boldsymbol{\gamma}(t) = \mathbf{v} \sigma(t), \tag{4.48}$$

where the matrices $\mathbf{A}$ and $\mathbf{B}$ assume the following particular form:

$$\mathbf{A} = \begin{bmatrix} 1 & -1 & 0 & \dots & 0 \\ -1 & 2 & -1 & \dots & 0 \\ 0 & -1 & 2 & \dots & 0 \\ \vdots & \vdots & \vdots & \ddots & \vdots \\ 0 & 0 & 0 & \dots & 2 \end{bmatrix}, \tag{4.49}$$

and

$$\mathbf{B} = \mathbf{I}. \tag{4.50}$$

The eigenvalues λ_j and the normalized eigenvectors $\boldsymbol{\phi}_j$ of particular tridiagonal matrix $\mathbf{A}$ can be evaluated with some manipulations from other works [67, 129]. In particular, such eigenvalues and eigenvectors are:

$$\lambda_j = 2 - 2 \cos \left(\frac{2j-1}{2n+1} \pi \right), \quad j = 1, 2 \dots, n \tag{4.51}$$

$$\phi_{k,j} = \sqrt{\frac{4}{2n+1}} \cos \left[\frac{(2j-1)(2k-1)}{2(2n+1)} \pi \right], \quad j, k = 1, 2 \dots, n. \tag{4.52}$$

Using the Eq. (4.52) can be readily calculate the modal matrix $\mathbf{\Phi}$, obtaining the following equation in the modal space:

$$\frac{\eta_0}{\triangle z}\mathbf{\Lambda}\dot{\mathbf{y}}(t) + G_0\triangle z\,\mathbf{y}(t) = \bar{\mathbf{v}}\sigma(t), \tag{4.53}$$

where $\bar{\mathbf{v}} = \mathbf{\Phi}^T\mathbf{v}$ and the j^{th} equation of the system (4.53), corresponding to the equilibrium equation of the j^{th} Kelvin-Voigt unit in the modal space, reads:

$$\dot{y}_j(t) + \frac{G_0\triangle z^2}{\eta_0\lambda_j}\,y_j(t) = \frac{\phi_{1,j}\triangle z}{\eta_0\lambda_j}\sigma(t), \quad j = 1, 2, \ldots, n. \tag{4.54}$$

The solution of j^{th} equation in modal space of **EV**-model is

$$y_j(t) = y_j(0)\,e^{-\frac{G_0\triangle z^2}{\eta_0\lambda_j}t} + \frac{\phi_{1,j}\triangle z}{\eta_0\lambda_j}\int_0^t e^{-\frac{G_0\triangle z^2}{\eta_0\lambda_j}(t-\tau)}\sigma(\tau)\,d\tau, \tag{4.55}$$

and the normalized transverse displacement of the upper lamina is obtained as

$$\begin{aligned}\gamma(t) &= \mathbf{v}^T\mathbf{\Phi}\,\mathbf{y}(t)\\ &= \sum_{j=1}^{n}\left[\phi_{1,j}y_j(0)\,e^{-\frac{G_0\triangle z^2}{\eta_0\lambda_j}t} + \frac{\phi_{1,j}^2\triangle z}{\eta_0\lambda_j}\int_0^t e^{-\frac{G_0\triangle z^2}{\eta_0\lambda_j}(t-\tau)}\sigma(\tau)\,d\tau\right].\end{aligned} \tag{4.56}$$

Exactly the same result is achieved as we work out on the governing equation of the VE material behavior reported in section 4.2.2.

4.4 Numerical examples

In this section a numerical applications is presented for different values of β. Consider that the system is forced by a constant stress case $\sigma(t) = \sigma_0 U(t)$. The fractional integral in Eq. (4.6) may be evaluated in closed form and it returns the creep function given in Eq. (4.5).

In Figure 4.7 the results for $\sigma(t) = \sigma_0 U(t)$ and different values of $\beta \in [0,\, 1/2]$, (EV case) are contrasted with exact solution reported in Eq. (4.6). For this case we select $\triangle z = 0.001$ and $n = 1500$, where $\triangle z$ is the discretization step and n is the number of layers considered (total truncation depth is $\bar{h} = n\triangle z = 1.5$), moreover it is assumed $G_0 = 1$ and $\eta_0 = 1$.

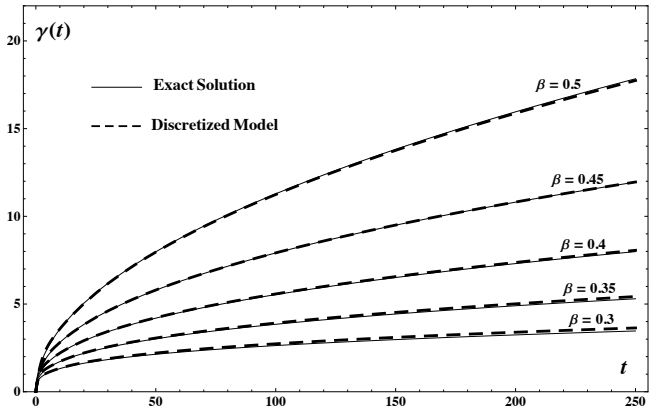

Figure 4.7: Creep test of EV model with $\sigma_0 = 1$: comparison between the exact and approximate solution.

In Figure 4.8 the results for $\sigma(t) = \sigma_0 U(t)$ and different values of $\beta \in [1/2,\ 1]$ (VE case) are contrasted with exact solution in Eq. (4.6), the discretization step selected is $\triangle z = 0.02$, $n = 1500$ (total depth $\bar{h} = 3$). It may be seen that exact solutions are matched with that obtained by the discretization procedure for a large time, moreover for $\beta = 1/2$ the solution obtained with EV case exactly coalesces with that obtained for VE case.

In order to investigate further the role played by truncation depth $\bar{h} = n\triangle z$ and by the number of laminae n, the critical case $\beta = 1/2$ is addressed. The creep function obtained with the discretized model reads:

$$\begin{aligned}\gamma(t) &= \sum_{j=1}^{n}\left[\frac{\phi_{1,j}^2 \triangle z \sigma_0}{\eta_0 \lambda_j}\int_0^t e^{-\frac{G_0 \triangle z^2}{\eta_0 \lambda_j}(t-\tau)} U(\tau)\, d\tau\right] \\ &= \frac{\sigma_0\, n}{G_0\, \bar{h}}\sum_{j=1}^{n}\left[\phi_{1,j}^2\left(1 - e^{\frac{G_0 \bar{h}^2}{\eta_0 \lambda_j n^2} t}\right)\right].\end{aligned} \tag{4.57}$$

Eq. (4.57) shows that the discretized model provides a solution in terms of the sum of exponentials. The sum, tends asymptotically, by increasing the observation time, to the following limit:

$$\lim_{t\to\infty}\gamma(t) = \frac{\sigma_0\, n}{G_0\, \bar{h}}\sum_{j=1}^{n}\phi_{1,j}^2 = a(n, \bar{h}) \tag{4.58}$$

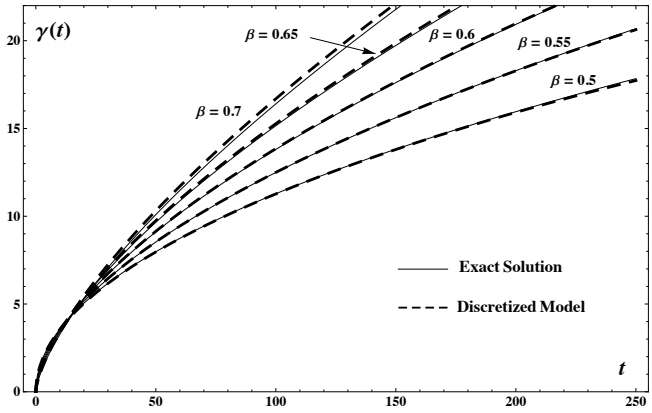

Figure 4.8: Creep test of VE model with $\sigma_0 = 1$: comparison between the exact and approximate solution.

while the exact solution, given by Eq. (4.5) is the power-law type solution:

$$\gamma(t) = \sigma_0 J(t) = \frac{\sigma_0}{G_0\,\Gamma(1.5)} \left(\frac{G_0}{\eta_0} t\right)^{0.5} \tag{4.59}$$

showing that Eq. (4.59) does not denote an asymptotic behavior for $t \to \infty$. It follows that Eq. (4.57) is able to represent the exact solution only for a certain interval of time t^* that depends on the number of laminae as well as on the depth $\bar{h}$ selected for the analysis.

In order to predict a reference time t^* such that the solution obtained by the discretization model and the exact one are nearly coincident, we may refer to Figure 4.9 where the asymptotic value $a(n, \bar{h})$, the discretized solution and that obtained by creep function are reported. We observe that at time $\bar{t}_{n,\bar{h}}$ the exact solution reaches the asymptotic one. In more details placing the equality of the Eq. (4.59) and the asymptotic value $a(n, h)$ we obtain the following limit time $\bar{t}_{n,\bar{h}}$:

$$\bar{t}_{n,\bar{h}} = \left(\frac{\Gamma(1.5) a(n, \bar{h})}{\sigma_0}\right)^2 \eta_0\, G_0. \tag{4.60}$$

The solution obtained by discretization is always smaller than its asymptotic value. It follows that the reference time t^*, at which the response is well approximate, may be expressed in the form:

$$t^* = \nu\, \bar{t}_{n,\bar{h}} \tag{4.61}$$

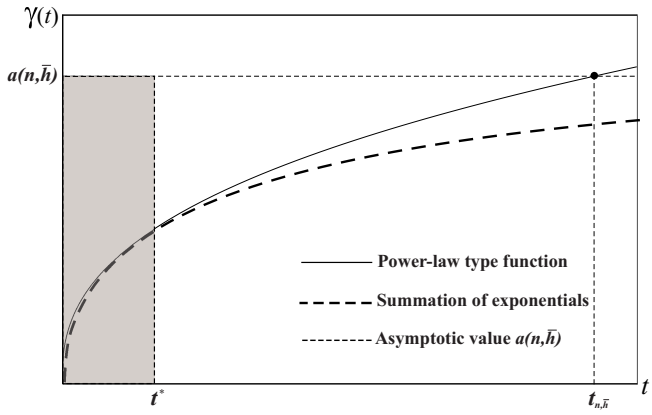

Figure 4.9: Comparison between power-law function and summation of exponentials.

with $\nu \ll 1$. From these observations follows that the larger is the observation time the more the number of layers n and the larger truncation depth $\bar{h}$ will be.

Other examples of the discretized model of the fractional viscoelasticity can be found in [38–40].

4.5 Conclusions

Fractional viscoelastic constitutive laws are characterized by fractional operators of order $\beta : 0 \leq \beta \leq 1$. The order β may be found by creep or relaxation test that exhibit a power-law with exponent β. Two different continuous mechanical models leading to fractional stress-strain relation have been found. For $0 \leq \beta \leq 1/2$ the predominant behavior is the elastic one as compared with the viscous behavior. Its mechanical correspondent is a massless undefined column of Newtonian fluid resting on a bed of independent springs. For $1/2 \leq \beta \leq 2$ the viscous properties are predominant with respect to the elastic ones. Its mechanical correspondent is a massless undefined shear column resting on a bed of independent dashpots. In both cases the various coefficients decay with a power-law that is related to the characteristic value of β.

Discretization leads to an infinite set of coupled differential equations ruled by symmetric and positive definite matrices. As a conclusion, truncation of the depth of the columns and discretization lead always to a set of Kelvin-

Voigt elements in a self-similar arrangement [73]. It follows that the discretization always corresponds to asymptotic value in contrast with the power-law creep function of viscoelastic materials. As a consequence, discretized model produces accurate results only for prescribed observation time. However numerical examples performed for different values of β and different forcing functions produce accurate results in a reasonable long time and then the procedure outlined in the Chapter may be used for fractional calculations.

In this Chapter the physical representation of the fractional constitutive law exists has been found. Therefore, the fractional operator in the stress-strain relation is more than a convenient mathematical tool that permits to obtain a good best-fitting of the experimental results. Indeed, it has an hierarchical mechanical model.

Chapter 5

Dynamics of structures with fractional viscoelastic behavior

5.1 Preliminary remarks

The previous Chapter has shown that the mathematical model of fractional viscoelastic material has a mechanical counterpart. This is an important goal under a physical/engineering point of view. Indeed the existence of a mechanical model of relation with fractional operators means that the fractional stress-strain relation is more than a mathematical tool, but it well describes the physics of the real matter which does not follow the ideal elastic or fluid behavior. After showing that the best way to describe the behavior of real material, and after introducing the mechanical interpretation of this behavior, this Chapter shows the dynamic analysis of such structures builded with viscoelastic material forced by deterministic and stochastic loads.

The dynamic analysis of real structures can be driven by introducing a proper model of that well approximate the behavior in terms of displacement and loads. This kind of problems occurs in many areas of mechanical, civil and aerospace engineering. To perform this analysis is needed to define the local stress-strain relation (depending on the materials which used to build the structures), the global model of the structure, and the description of the external action (load or imposed displacement). Obviously, the considered model to describe the stress-strain relation of the real materials is the fractional one. This chose leads to have the fractional operators also in the equation of motion of the global structure. This global model has been obtained considered the

structures as continuous or discrete. The continuous case, shown in the first part of this Chapter the considered viscoelastic structural element is the Euler-Bernoulli beam with fractional dampers forced by stochastic load. Whereas, as discretized case is considered the case of shear-type multi-degree-of freedom system endowed with fractional viscoelastic elements under deterministic and stochastic loads. As the next sections show, the presence of fractional viscoelastic elements leads to have fractional partial differential equations in the continuous systems, and sets of coupled fractional differential equation in the discretized system with lumped parameters. Both problems are more complicate to solve respect the classic integer-order case, and for this reason is needed to introduce new methods to solve them. In the following these new methods are shown.

5.2 Continuous fractionally damped beam

This section aims at introducing the governing equation of motion of a continuous fractionally damped system under generic input loads, no matter the order of fractional derivative. Moreover, particularizing the excitation as a random noise, the evaluation of the power spectral density performed in frequency domain stresses relevant features of such a system. To asses the accuracy of results the variance response evaluated trough power spectral density function, has been contrasted with Monte Carlo simulations in time domain. In these formulations, the normal-mode approach is used to reduce the differential equation of a fractionally damped continuous beam into a set of infinite equations each of which describes the dynamics of a fractionally damped spring-mass-damper system.

5.2.1 Vibration of Euler-Bernoulli beam modeled using fractional Kelvin-Voigt

Let consider an isotropic homogeneous viscoelastic Euler-Bernoulli beam of length L depicted in Figure 5.1, referred to the axes x, y, z, with origin located at the centroid of the cross section, and x and y are principal axes of inertia of the cross section. All external spatially distributed loads, denoted by $q_y(z,t)$, are assumed to act in y-direction, thus orthogonally to the z-axis.

The dynamic equilibrium equation for vibrations $v(z,t)$ in the y-direction of the length dz of the beam is readily obtained by equating the inertial force to the sum of the forces exerted by the other parts of the beam and the external

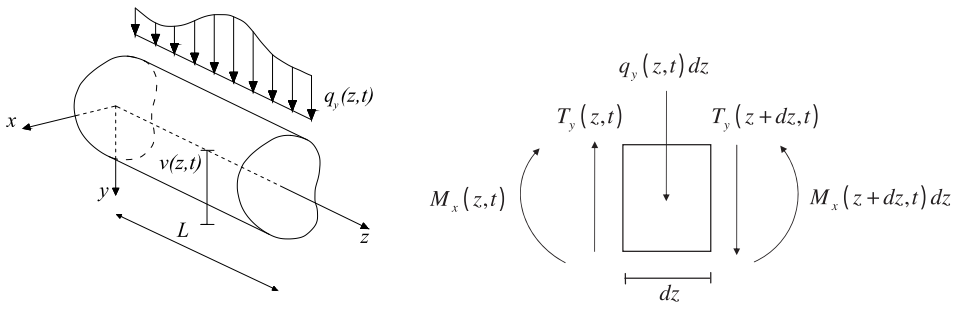

(a) Layout of the beam **(b)** Free body diagram of the beam

Figure 5.1: Euler-Bernoulli beam.

forces Figure 5.1(b):

$$\frac{\partial^2 M_x(z,t)}{\partial z^2} = \rho(z)A(z)\frac{\partial^2 v(z,t)}{\partial t^2} - q_y(z,t), \tag{5.1}$$

where $\rho(z)$ is the mass density of the material, $A(z)$ is the cross sectional area, $M_x(z,t)$ is the bending moment, the latter is related to the shear in the section at abscissa z and at time t $T_y(z,t)$, by the relation:

$$\frac{\partial M_x(z,t)}{\partial z} = T_y(z,t). \tag{5.2}$$

By virtue of the Euler-Bernoulli hypothesis, that is neglecting rotary inertia and shear deformation, the kinematic and the mechanic relations read respectively:

$$\varepsilon(y,z,t) = -y\frac{\partial^2 v(z,t)}{\partial z^2}, \tag{5.3a}$$

$$\sigma(y,z,t) = \frac{M_x(z,t)}{J_x(z)}y, \tag{5.3b}$$

where $J_x(z)$ is the moment of inertia of the cross section with respect to the x-axis.

As aforementioned, this section deals with vibrations of a viscoelastic beam, then to capture the main features of a viscoelastic behavior, like relaxation and creep phenomena, it requires to introduce the proper constitutive law. According to Nutting [82] and Gemant [50, 51], and to the previous Chapters the

more realistic description of creep and/or relaxation is given by a power-law function with real order exponent.

As soon as we assume a power-law function for creep as kernel of Boltzmann integral, the constitutive law, relating axial strain $\varepsilon(y,z,t)$ and the stress $\sigma(y,z,t)$, is ruled by the Riemann-Liouville fractional integral in the stress-strain relation with order equal to that of the power-law, as follows:

$$\varepsilon(y,z,t) = \frac{1}{C(\beta)} \left(\mathrm{I}^{\beta}_{t,0^+} \sigma \right) (y,z,t) \tag{5.4}$$

where $C(\beta,z)$ and $\beta : 0 \leqslant \beta \leqslant 1$ are characteristic parameters of the material.

Vice-versa, starting from the relaxation function, the stress-strain constitutive law is ruled by the Caputo's fractional derivative:

$$\sigma(y,z,t) = C(\beta,z) \left({}_{\mathrm{C}}D^{\beta}_{t,0^+} \varepsilon \right) (y,z,t). \tag{5.5}$$

As the previous Chapter 3 have shown the Eq.s (5.4) and (5.5) represent the stress-strain relation of the spring-pot. Further, viscoelastic behavior is also described using a more general model called fractional Kelvin-Voigt model. By using this latter model, according to the Eq. (3.52), the stress-strain relation in the continuous beam is

$$\sigma(y,z,t) = E(z)\varepsilon(y,z,t) + C(\beta,z) \left({}_{\mathrm{C}}D^{\beta}_{t,0^+} \varepsilon \right) (y,z,t). \tag{5.6}$$

where $E(z)$ is the Young's modulus.

Then, placing the expression of the bending moment $M_x(z,t)$ into Eq. (5.1), and taking into account the Eq.s (5.1)-(5.3b), the following relation holds:

$$\rho(z)A(z)\ddot{v}(z,t) + \frac{\partial^2}{\partial z^2} \left[E(z)J_x(z) \frac{\partial^2 v(z,t)}{\partial z^2} + C(\beta,z)J_x(z) \frac{\partial^{\beta} \partial^2 v(z,t)}{\partial t^{\beta} \partial z^2} \right] = q_y(z,t). \tag{5.7}$$

Notice that Eq. (5.7) covers all cases from a pure classical elastic continuum beam (if the spring-pot is not present) up to the pure fractionally damped continuum beam (if the spring is not present), moreover for the limit cases $\beta = 0$ and $\beta = 1$ the fractional Kelvin-Voigt model reverts to the model with two springs in parallel and to a Kelvin-Voigt model (a spring in parallel with a dashpot) respectively. Once the governing equation of motion has been introduced, the flexural vibrations, solution of this differential equation, are evaluated following the traditional approach:

$$v(z,t) = \sum_{k=1}^{\infty} \xi_k(t)\phi_k(z), \tag{5.8}$$

that represents the displacement function as a linear combination of the normal mode shapes of the undamped free vibration of the system $\phi_k(z)$, dependent on the constraints only (boundary conditions). The coefficients in the linear combination are the modal coordinates $\xi_k(t)$. They are functions of time and take into account the behavior of the fractionally damped model.

5.2.2 Numerical solution in the time domain

Assume that the cross section $A(z)$ of the beam, the elastic modulus $E(z)$, the mass density $\rho(z)$, and the moment of inertia $J_x(z)$, are all constant quantities, then the canonical form of equation of motion in Eq. (5.7) assumes the form:

$$\rho A\ddot{v}(z,t) + EJ_x\frac{\partial^4 v(z,t)}{\partial z^4} + C(\beta)J_x\frac{\partial^\beta\partial^4 v(z,t)}{\partial t^\beta\partial z^4} = q_y(z,t), \tag{5.9}$$

introducing solution in Eq. (5.8) into Eq.(5.9) it leads to:

$$\sum_{k=1}^{\infty}\ddot{\xi}_k(t)\phi_k(z) + \frac{EJ_x}{\rho A}\sum_{k=1}^{\infty}\xi_k(t)\phi_k^{(4)}(z) + \frac{C(\beta)J_x}{\rho A}\sum_{k=1}^{\infty}\left({}_{\mathrm{C}}D_{0^+}^{\beta}\xi_k\right)(t)\phi_k^{(4)}(z) = \frac{q_y(z,t)}{\rho A}, \tag{5.10}$$

then, multiplying both sides of Eq. (5.10) by $\phi_j(z)$ and integrating in dz from 0 to L, the following relation is obtained:

$$\begin{aligned}\sum_{k=1}^{\infty}\ddot{\xi}_k(t)\int_0^L\phi_j(z)\phi_k(z)dz + \frac{EJ_x}{\rho A}\sum_{k=1}^{\infty}\xi_k(t)\int_0^L\phi_j(z)\phi_k^{(4)}(z)dz + \\ + \frac{C(\beta)J_x}{\rho A}\sum_{k=1}^{\infty}\left({}_{\mathrm{C}}D_{0^+}^{\beta}\xi_k\right)(t)\int_0^L\phi_j(z)\phi_k^{(4)}(z)dz = \frac{1}{\rho A}\int_0^L q_y(z,t)\phi_j(z)dz.\end{aligned} \tag{5.11}$$

Taking into account the orthogonality condition

$$\int_0^L\phi_j(z)\phi_k(z)dz = \delta_{jk}, \tag{5.12}$$

where δ_{jk} is the Kronecker delta defined as

$$\delta_{jk} = \begin{cases} 1, & \text{for} \quad j = k, \\ 0, & \text{for} \quad j \neq k, \end{cases} \tag{5.13}$$

the governing differential equation in terms of $y_j(t)$ is obtained as

$$\ddot{\xi}_j(t) + \frac{EJ_x}{\rho A} R_j \xi_j(t) + \frac{C(\beta) J_x}{\rho A} R_j \left({}_{\mathrm{C}}D^{\beta}_{0^+} \xi_j \right)(t) = \frac{1}{\rho A} \int_0^L \phi_j(z) q_y(z,t) dz, \quad (5.14)$$

where $R_j = \int_0^L \phi_j(z) \phi_j^{(4)}(z) dz$.

In time domain, Eq. (5.14) may be solved placing the initial conditions of quiet, and adopting any integration method in conjunction with a discretization form of the fractional derivative. In this regard, according to the works of Schmidt & Gaul [49, 103–105], and Spanos & Evangelatos [115], the fractional operator can be discretized using the definition of Grünwald-Letnikov (GL) in Eq. (2.19) and the properties of binomial coefficient. That is,

$$\left({}_{\mathrm{C}}D^{\beta}_{0^+} \xi_j \right)(t) = \lim_{\Delta t \to 0} \Delta t^{-\beta} \sum_{s=0}^{N} \mathrm{GL}_s \xi_j(t - s\Delta t), \quad (5.15)$$

being GL_s coefficients evaluate with a recursive relation:

$$\mathrm{GL}_s = \frac{s - \beta - 1}{s} GL_{s-1}; \qquad \mathrm{GL}_0 = 1. \quad (5.16)$$

Once the coefficients of the linear combination $\xi_j(t)$ are determined, the fractionally damped beam vibrations may be simply evaluated through Eq. (5.8).

5.2.3 Stochastic analysis in frequency domain

As aforementioned the crux of the determination of the vibrations of a fractionally damped beam is the evaluation of $y_j(t)$. To aim at this, just solve Eq. (5.14) that is valid for arbitrary forcing function, and therefore, it is also useful for random excitation. For instance, dealing with a random ground acceleration $w(t)$, Eq. (5.14) may be rewritten as

$$\ddot{\xi}_j(t) + \frac{EJ_x}{\rho A} R_j \xi_j(t) + \frac{C(\beta) J_x}{\rho A} R_j \left({}_{\mathrm{C}}D^{\beta}_{0^+} \xi_j \right)(t) = -P_j w(t), \quad (5.17)$$

where $P_j = \int_0^L \phi_j(z) dz$ represents the modal participation coefficient. Solution of Eq. (5.17) returns $\xi_j(t)$ in time domain, but it is possible to operate in frequency domain by performing the Fourier transform, therefore:

$$\Xi_{\mathcal{F}j}(\omega) = \mathrm{H}_j(\omega)(-P_j) W_{\mathcal{F}}(\omega) \quad (5.18)$$

where $\mathrm{H}_j(\omega)$ is the transfer function of the viscoelastic system, defined as

$$\mathrm{H}_j(\omega) = \left[-\omega^2 + \frac{EJ_x}{\rho A}R_j + \frac{C(\beta)J_x}{\rho A}R_j(i\omega)^\beta\right]^{-1}. \tag{5.19}$$

Further, assume that $w(t)$ is a realization of the Gaussian white noise process characterized by the following power spectral density (PSD):

$$S_0 = \lim_{\mathrm{T}\to\infty}\frac{1}{2\pi\mathrm{T}}\mathrm{E}\left[W^*_{\mathcal{F}}(\omega,\mathrm{T})W_{\mathcal{F}}(\omega,\mathrm{T})\right], \tag{5.20}$$

where the star means complex conjugate, and $\mathrm{E}[\cdot]$ is the expectation operator. Based on the above considerations, the diagonal elements, of the power spectral density Hermitian matrix of the modal responses $\Xi_{\mathcal{F},j}(\omega)$, are:

$$S_{\Xi_j}(\omega) = \lim_{\mathrm{T}\to\infty}\frac{1}{2\pi\mathrm{T}}\mathrm{E}\left[\Xi^*_{\mathcal{F}j}(\omega,\mathrm{T})\Xi_{\mathcal{F}j}(\omega,\mathrm{T})\right] = \mathrm{H}^*_j(\omega)\mathrm{H}_j(\omega)P_j^2S_0, \tag{5.21}$$

while the elements outside the main diagonal are

$$S_{\Xi_j\Xi_k}(\omega) = \mathrm{H}^*_j(\omega)\mathrm{H}_k(\omega)P_jP_kS_0. \tag{5.22}$$

Finally, since the vibrations of the beam are defined as in Eq. (5.8) the PSD $S_v(\omega,z)$ is

$$S_v(\omega,z) = \lim_{\mathrm{T}\to\infty}\frac{1}{2\pi\mathrm{T}}\mathrm{E}\left[V^*_{\mathcal{F}}(\omega,\mathrm{T};z)V_{\mathcal{F}}(\omega,\mathrm{T};z)\right] = \sum_{k=1}^{\infty}\sum_{j=1}^{\infty}\phi_k(z)\phi_j(z)S_{\Xi_j\Xi_k}, \tag{5.23}$$

and the variance $\sigma_v^2(z)$ of the transversal displacement of the beam is determined according to the relation:

$$\sigma_v^2(z) = \int_{-\infty}^{\infty}S_v(\omega,z)d\omega. \tag{5.24}$$

5.2.4 Numerical application

Previous subsection presented formulations for the deterministic and stochastic of a fractionally damped beam to arbitrary excitations and boundary conditions. For application purposes, in this section a cantilever beam is considered under a Gaussian white noise ground motion with $S_0 = 3\times10^7/2\ \pi\mathrm{N}^2\mathrm{s}$.

Choosing the more general viscoelastic constitutive law, as the fractional Kelvin-Voigt model it is taken that the mass density is $\rho = 500\ \mathrm{kg/m}^3$, the

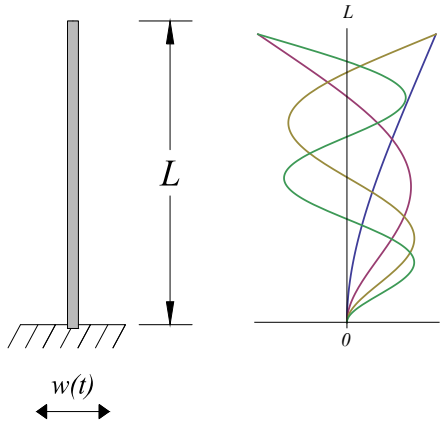

Figure 5.2: Cantilever beam and its eigenfunctions.

length of the beam is $L = 10$ m, the area of rectangular cross-section is $A = 1$ m^2 , the moment of inertia of the cross section with respect to the x-axis is $J_x = 0.021$ m^4. The fractional Kelvin-Voigt model parameters are selected as $\beta = 0.8$, $C(\beta) = 3 \times 10^8$ Ns$^\beta$/m, $E = 150$ GPa. In particular, the last three terms have been deducted from an overlapping of results obtained by Zhu et al. [133]. Then, the first step in developing flexural vibrations is the determination of the particular form of the eigenfunctions $\phi_k(z)$ relative to a cantilever undamped beam, according to Meirovitch [75], is

$$\begin{aligned}\phi_k(z) =& B_k \{[\sin(\lambda_k z) - \sinh(\lambda_k z)]\,[\sin(\lambda_k L) - \sinh(\lambda_k L)] + \\ &+ [\cos(\lambda_k z) - \cosh(\lambda_k z)]\,[\cos(\lambda_k L) - \cosh(\lambda_k L)]\}\,,\end{aligned} \tag{5.25}$$

where λ_k are the eigenvalues of of the cantilever beam while B_k are constants. The layout of the cantilever beam and the trend of its first four eigenfunctions is shown in Figure 5.2, the coefficients B_k are determined fulfilling the orthogonality condition in Eq. (5.12).

Once the eigenfunctions $\phi_k(z)$ are known, it is possible to evaluate coefficients P_j and R_j, after that the stochastic response in terms of PSD $S_v(\omega, z)$ of the transversal displacement through in Eq. (5.23) can be found.

Figure 5.3(a) shows $S_v(\omega, z)$ having considered four eingenfunctions since these results coalesce with those obtained considering forty eingenfunctions. It is apparent that, as we move towards the tip, PSD response values grow; this is more appreciable in Figure 5.3(b) where PSD of the transversal displacement of the beam for fixed cross sections z are depicted, and in Figure 5.4(b)

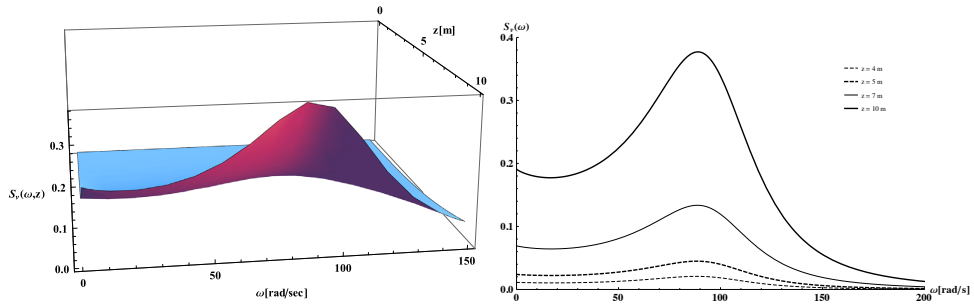

(a) PSD for variable ω and z **(b)** PSD for fixed z

Figure 5.3: Power spectral density of transversal displacement.

where the stationary displacement variance $\sigma_v^2(z)$ at each cross-section has been plotted. In particular the maximum value of $\sigma_v^2(z) = 71$ correspondent to the tip is well contrasted by results of Monte Carlo simulation Figure 5.4(a).

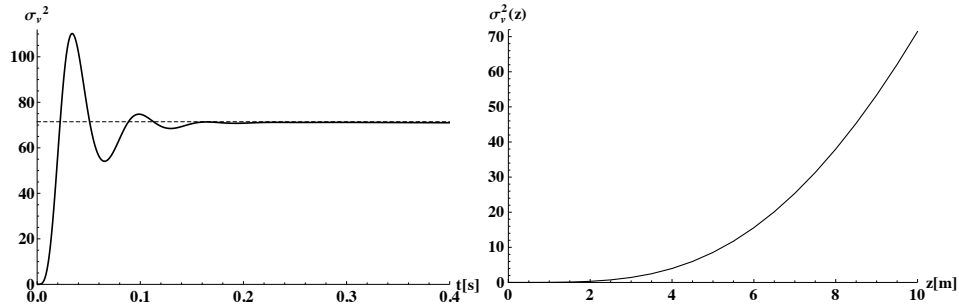

(a) MC simulation (solid line), stationary variance (dashed line) **(b)** Stationary displacement variance

Figure 5.4: Displacement variance

For this purpose the Monte Carlo simulations have been performed integrating Eq. (5.11) via the central difference scheme using a time step $\Delta t = 0.0005\ s$ with a GL discretization of fractional derivative using Eq.s (5.15) and (5.16), retaining 800 terms [47, 115]. White noise samples are obtained by the harmonic superposition method by Shinozuka and Deodatis [107]. Thus, the

generic sample $w_k(t)$ of the excitation process is

$$w_k(t) = \sum_{i=1}^{N} \sqrt{4S_0\Delta\omega}\cos\left(\omega_i t + \phi_i\right), \tag{5.26}$$

where $N = 10000$, $\Delta\omega = 0.01$ and ϕ_i are N realizations of a random variable uniformly distributed in $[0, 2\pi]$.

5.3 Lumped-parameter systems with fractional viscoelastic devices

In this section the dynamic analysis of discretized model with lumped parameters with fractional viscoelastic terms is presented. Usually, this problem is represented by a set of coupled fractional differential equations, and the solution can not readily be found in the general case. This kind of problem that is known as the analysis of fractional multi-degree-of-freedom systems (FMDOF) has been solved in the time domain by using the step-by-step numerical approach [108], and in the frequency domain by using the approximate modal superposition method [69].

The analysis of FMDOF systems has been considered in several articles in which the authors have investigated the improvements of fractional viscoelastic devices in the frame structures [46, 68, 86]. FMDOF systems may also appear in the study of continuous systems with fractional constitutive law like in the previous case and [31, 32, 44]. In fact, this kind of problem leads to a fractional multi-degree-of-freedom system in the discretized form [97, 103–105]. From these articles, it can be concluded that the analysis of FMDOF systems is more cumbersome with respect to the classical one. In certain previous efforts the integration of the equation of motion with fractional terms has been carried by finite difference schemes [83, 84] or by the modified Newmark algorithm [115] and/or by using modal analysis; these approaches often lead to considerable computational burden.

A novel method to perform the analysis of the FMDOF system is presented in this section. The method is derived modifying the traditional complex modal analysis in the state variables domain to obtain a set of uncoupled fractional differential equations. The sole limitation of the presented method regards the involved fractional orders, since the state variable analysis can be performed for FMDOF system only in the case in which all the derivative terms are rational.

5.3.1 Fractional multi-degree-of-freedom systems

The equation of motion of a quiescent single-degree-of-freedom linear fractional system (FSDOF) is

$$m\ddot{x}(t) + c_\beta \left(D_{0^+}^{\beta} x \right)(t) + kx(t) = f(t), \quad t \geqslant 0, \tag{5.27}$$

where $f(t)$ is the forcing function, $x(t)$ is the response of the system, m is the mass, c_β is the coefficient of fractional term, k is th e stiffness, and $\left(D_{0^+}^{\beta} x \right)(t)$ is the fractional derivative of $x(t)$, defined in Eq. (2.24). This kind of dynamical system is known as *fractional oscillator* [70, 80, 116, 130]. The fractional r-degree-of-freedom system is described by a coupled system of fractional differential equations of various FSDOF [68, 86, 97]. This kind of problem can be cast in the form

$$\mathbf{M}\ddot{\boldsymbol{x}}(t) + \sum_{i=1}^{l} \mathbf{C_i} D^{\beta_i} \boldsymbol{x}(t) + \mathbf{K}\boldsymbol{x}(t) = \mathbf{f}(t), \tag{5.28}$$

where $\mathbf{M}$ and $\mathbf{K}$ are the mass and the stiffness matrices; $\mathbf{C_i}$ is the matrix of the coefficients c_{β_i} of the involved fractional terms of order β_i; $\boldsymbol{x}(t)$ is a vector which describes the response of the systems; and $\mathbf{f}(t)$ is the vector of loading.

Consider next the simpler quasi-static problem, in which the terms of the vector $\mathbf{f}(t)$ vary in time slowly to the extent that the inertial force may be neglected. Thus, assuming that the involved fractional terms are all of the same order of derivation β_1, the equation of motion becomes

$$\mathbf{C_1} D^{\beta_1} \boldsymbol{x}(t) + \mathbf{K}\boldsymbol{x}(t) = \mathbf{f}(t). \tag{5.29}$$

This kind of system related to the eigenvectors $\boldsymbol{\phi}_j$ of the matrix

$$\mathbf{K}^{-1}\mathbf{C_1} = \boldsymbol{D}, \tag{5.30}$$

where $\boldsymbol{D}$ is the dynamical matrix. Assume that the modal matrix $\boldsymbol{\Phi}$, where columns are the eigenvectors $\boldsymbol{\phi}_j$, is also normalized with respect to $\mathbf{C_1}$. That is

$$\boldsymbol{\Phi}^{\mathrm{T}}\mathbf{C_1}\boldsymbol{\Phi} = \mathbf{I}, \qquad \boldsymbol{\Phi}^{\mathrm{T}}\mathbf{K}\boldsymbol{\Phi} = \mathbf{U}_{\mathrm{D}}, \tag{5.31}$$

where $\mathbf{I}$ is the identity matrix, and $\mathbf{U}_{\mathrm{D}}$ is a diagonal matrix whose elements are posistive, since $\mathbf{K}$ is positive definite.

Making the modal transformation

$$\boldsymbol{x}(t) = \boldsymbol{\Phi}\boldsymbol{y}(t), \tag{5.32}$$

inserting Eq. (5.32) in Eq. (5.29), and premultiplying by $\boldsymbol{\Phi}^{\mathrm{T}}$, Eq. (5.29) yields

$$\mathbf{I}\, D^{\beta_1}\boldsymbol{y}(t) + \mathbf{U}_{\mathrm{D}}\boldsymbol{y}(t) = \mathbf{g}(t), \tag{5.33}$$

where $\mathbf{g}(t) = \boldsymbol{\Phi}^{\mathrm{T}}\mathbf{f}(t)$ is the forcing vector in the modal space, and $\boldsymbol{y}(t)$ is the vector of the modal displacements that contains the terms $y_j(t)$. Clearly, Eq. (5.33) represents a set of uncoupled differential equations that may be readily solved.

Once $y_j(t)$ is found for $j = 1, 2, \ldots, r$, then $\boldsymbol{x}(t)$ can be obtained using Eq. (5.32). This kind of modal transformation can diagonalize the system in Eq. (5.28) in some particular cases in which all the matrices can be represented by a linear combination of the matrices $\mathbf{K}$ and $\mathbf{C_1}$.

The next section describes a method to decouple the system in Eq. (5.28) in the case in which all the involved matrices are arbitrary. The method is based on a proper transformation/augmentation in the state variables domain of fractional MDOF system.

5.3.2 State variable analysis of fractional MDOF

There are various fractional terms in the Eq. (5.28). By assuming that all fractional orders are rational, it is possible to represent the generic fractional order in Eq. (5.28) as $\beta_i = a_i/b_i$ where $a_i, b_i \in \mathbb{N}$ with $i = 1, 2, \ldots, l$. Thus, the system in Eq. (5.28) can be rewritten as the following sequential linear differential equations of fractional orders:

$$\sum_{j=1}^{n} \mathbf{C_j} D^{j\alpha}\boldsymbol{x}(t) + \mathbf{K}\boldsymbol{x}(t) = \mathbf{f}(t), \tag{5.34}$$

where α is chosen such that $n\alpha$ is equal to the maximum order that appears in the system of equations, and such that all involved orders in Eq. (5.28) can be represented as $\beta_i = d_i\alpha$ where $d_i \in \mathbb{N}$. In this case $n\alpha = 2$ and the corresponding matrix $\mathbf{C_n} = \mathbf{M}$ is the matrix of the mass; all matrices in Eq. (5.34) have dimension $r \times r$. Introducing the vector of state variables

$$\mathbf{z}^{\mathrm{T}}(t) = \left[\boldsymbol{x}^{\mathrm{T}}(t) \;\; D^{\alpha}\boldsymbol{x}^{\mathrm{T}}(t) \;\; D^{2\alpha}\boldsymbol{x}^{\mathrm{T}}(t) \;\; \ldots \;\; D^{\alpha(n-1)}\boldsymbol{x}^{\mathrm{T}}(t)\right], \tag{5.35}$$

and appending to Eq. (5.34) the $n-1$ identities

$$\begin{aligned}
&\sum_{j=1}^{n-1} \mathbf{C}_{j+1} D^{\alpha} D^{(j-1)\alpha} \boldsymbol{x}(t) = \sum_{j=1}^{n-1} \mathbf{C}_{j+1} D^{j\alpha} \boldsymbol{x}(t), \\
&\sum_{j=1}^{n-2} \mathbf{C}_{j+2} D^{\alpha} D^{(j-1)\alpha} \boldsymbol{x}(t) = \sum_{j=1}^{n-2} \mathbf{C}_{j+2} D^{j\alpha} \boldsymbol{x}(t), \\
&\quad \vdots \quad \vdots \quad \vdots \quad \vdots \\
&\mathbf{C}_n D^{\alpha} \boldsymbol{x}(t) = \mathbf{C}_n D^{\alpha} \boldsymbol{x}(t),
\end{aligned} \tag{5.36}$$

then a set of $r \times n$ coupled differential equations is readily cast in the form

$$\mathbf{A} D^{\alpha} \mathbf{z}(t) + \mathbf{B} \mathbf{z}(t) = \mathbf{g}(t), \tag{5.37}$$

where $\mathbf{g}^{\mathrm{T}}(t) = \left[\mathbf{f}^{\mathrm{T}}(t)\ \mathbf{0}\ \ldots\ \mathbf{0}\right]$, $\mathbf{A}$ and $\mathbf{B}$ are symmetric matrices defined as

$$\begin{aligned}
\mathbf{A} &= \begin{bmatrix}
\mathbf{C_1} & \mathbf{C_2} & \ldots & \mathbf{C_{n-1}} & \mathbf{C_n} \\
\mathbf{C_2} & \mathbf{C_3} & \ldots & \mathbf{C_n} & \mathbf{0} \\
\vdots & \vdots & \ddots & \vdots & \vdots \\
\mathbf{C_{n-1}} & \mathbf{C_n} & \ldots & \mathbf{0} & \mathbf{0} \\
\mathbf{C_n} & \mathbf{0} & \ldots & \mathbf{0} & \mathbf{0}
\end{bmatrix}, \\
\mathbf{B} &= \begin{bmatrix}
\mathbf{K} & \mathbf{0} & \ldots & \mathbf{0} & \mathbf{0} \\
\mathbf{0} & -\mathbf{C_2} & \ldots & -\mathbf{C_{n-1}} & -\mathbf{C_n} \\
\vdots & \vdots & \ddots & \vdots & \vdots \\
\mathbf{0} & -\mathbf{C_{n-1}} & \ldots & \mathbf{0} & \mathbf{0} \\
\mathbf{0} & -\mathbf{C_n} & \ldots & \mathbf{0} & \mathbf{0}
\end{bmatrix}.
\end{aligned} \tag{5.38}$$

Next, it is possible to decompose $\mathbf{z}(t)$ in the orthogonal basis of the eigenvectors of $\mathbf{A}$ and $\mathbf{B}$. Specifically, consider the equations

$$\boldsymbol{\Psi}^{\mathrm{T}} \mathbf{A} \boldsymbol{\Psi} = \mathbf{U_D}, \qquad \boldsymbol{\Psi}^{\mathrm{T}} \mathbf{B} \boldsymbol{\Psi} = \mathbf{V_D}, \tag{5.39}$$

where $\mathbf{U_D}$ and $\mathbf{V_D}$ are diagonal matrices. Further, making the complex modal transformation

$$\mathbf{z}(t) = \boldsymbol{\Psi} \boldsymbol{y}(t), \tag{5.40}$$

a new set of decoupled fractional differential equation is derived in the form

$$\mathbf{U_D} D^{\alpha} \boldsymbol{y}(t) + \mathbf{V_D} \boldsymbol{y}(t) = \boldsymbol{\mu}(t), \tag{5.41}$$

where $\boldsymbol{\mu}(t) = \boldsymbol{\Psi}^{\mathrm{T}}\mathbf{g}(t)$. Clearly, once the decoupled set is found, the fractional differential equations can be readily solved. It can be seen that the state variable problem in Eq. (5.37) has a greater number of involved variables with respect to the problem cast in terms of displacements in Eq. (5.34) of the nodal analysis. However, this apparent increase of the computational burden is balanced by the fact that the maximum involved order in the state variable domain is smaller than the maximum order in the nodal analysis. Further, the system in Eq. (5.34) is a set of coupled in the general case, vis-a-vis the system in Eq. (5.37) leads readily to the set of uncoupled equations in Eq. (5.41).

From this result it becomes clear that for application the method it is necessary to modify Eq. (5.28) to obtain the sequential differential form as in Eq. (5.34). To elucidate the procedure for obtaining a sequential differential from the given set of coupled fractional differential equations, consider the dynamical problem in which all of the involved fractional derivatives have the same order β. In this case, the Eq. (5.34) becomes

$$\mathbf{M}\ddot{\boldsymbol{x}}(t) + \mathbf{C}_{\beta}D^{\beta}\boldsymbol{x}(t) + \mathbf{K}\boldsymbol{x}(t) = \mathbf{f}(t); \tag{5.42}$$

the number of terms and the minimum fractional order α in the summation of the Eq. (5.34) depend of the order β. Next, assume that $\beta = 0.5$. In this particular case, also the order $\alpha = \beta$, and the sequential form is given as

$$\sum_{j=1}^{4} \mathbf{C_j} D^{j0.5}\boldsymbol{x}(t) + \mathbf{K}\boldsymbol{x}(t) = \mathbf{f}(t), \tag{5.43}$$

where $\mathbf{C_4} = \mathbf{M}$, $\mathbf{C_3} = \mathbf{C_2} = \mathbf{0}$ and $\mathbf{C_1} = \mathbf{C}_{\beta}$. Clearly, the smaller the order α is, the higher the number of terms is. However, since $\mathbf{C_3} = \mathbf{C_2} = \mathbf{0}$, the system (5.43) can be rewritten as

$$\mathbf{C_4}D^{2}\boldsymbol{x}(t) + \mathbf{C_1}D^{0.5}\boldsymbol{x}(t) + \mathbf{K}\boldsymbol{x}(t) = \mathbf{f}(t). \tag{5.44}$$

Further, taking as the state vector

$$\mathbf{z}^{\mathrm{T}}(t) = \left[\boldsymbol{x}^{\mathrm{T}}(t) \;\; D^{0.5}\boldsymbol{x}^{\mathrm{T}}(t) \;\; D^{1}\boldsymbol{x}^{\mathrm{T}}(t) \;\; D^{1.5}\boldsymbol{x}^{\mathrm{T}}(t)\right], \tag{5.45}$$

and considering Eq. (5.44) and the identity relations in Eqs. (5.36), the following system of fractional differential equations in the state variables domain is found:

$$\mathbf{A}D^{\alpha}\mathbf{z}(t) + \mathbf{B}\mathbf{z}(t) = \mathbf{g}(t), \tag{5.46}$$

where the matrices $\mathbf{A}$ and $\mathbf{B}$ become, for that particular case, as follows

$$\mathbf{A} = \begin{bmatrix} \mathbf{C}_1 & \mathbf{0} & \mathbf{0} & \mathbf{M} \\ \mathbf{0} & \mathbf{0} & \mathbf{M} & \mathbf{0} \\ \mathbf{0} & \mathbf{M} & \mathbf{0} & \mathbf{0} \\ \mathbf{M} & \mathbf{0} & \mathbf{0} & \mathbf{0} \end{bmatrix}, \quad \mathbf{B} = \begin{bmatrix} \mathbf{K} & \mathbf{0} & \mathbf{0} & \mathbf{0} \\ \mathbf{0} & \mathbf{0} & \mathbf{0} & -\mathbf{M} \\ \mathbf{0} & \mathbf{0} & -\mathbf{M} & \mathbf{0} \\ \mathbf{0} & -\mathbf{M} & \mathbf{0} & \mathbf{0} \end{bmatrix}. \tag{5.47}$$

Clearly, Eq. (5.46) can be solved by the complex modal analysis described in Eqs. (5.39-5.41) and the state variables vector $\mathbf{z}(t)$ can be determined. It is worth noting that if in Eq. (5.42) $\alpha = 1$, the vector of state variables is the classical one $\mathbf{z}^{\mathrm{T}}(t) = \left[\boldsymbol{x}^{\mathrm{T}}(t) \;\; \dot{\boldsymbol{x}}^{\mathrm{T}}(t)\right]$.

Obviously, the method is applicable exactly when the involved orders are rational. However, even if in the general case $\alpha \in \mathbb{R}$, it could yield reasonable results by approximating α as fraction. To demonstrate the applicability of the proposed method some numerical results are discussed next.

5.3.3 Numerical applications of fractional SDOF

First, consider the FSDOF system described in Eq. (5.27) forced by deterministic load. This case has been already discussed by Bonilla et al. [14] by using the fractional Wronskian method, and by Suarez and Shokooh [117]. Alternatively, Eq. (5.27) may also be solved by using the Green function $\mathrm{g}(t)$

$$\mathrm{g}(t) = \frac{1}{m}\sum_{j=0}^{\infty} -\frac{1}{j!}\left(\frac{k}{m}\right)^{j} t^{2j+1}\mathrm{E}^{(j)}_{2-\beta,2+j\beta}\left(-\frac{c_\beta}{m}t^{2-\beta}\right), \tag{5.48}$$

where $\mathrm{E}^{(j)}_{\lambda,\mu}(z)$ is the derivative of order j of the two-parameters Mittag-Leffler function that is defined as

$$\mathrm{E}^{(j)}_{\lambda,\mu}(z) = \frac{d^j}{dz^j}\mathrm{E}_{\lambda,\mu}(z) = \sum_{l=0}^{\infty}\frac{(l+j)!z^l}{l!\Gamma(\lambda l+\lambda j+\mu)}. \tag{5.49}$$

Specifically, assuming that the system in Eq. (5.27) is quiescent at $t = 0$, the solution $x(t)$ is given by integral

$$x(t) = \int_0^t \mathrm{g}(t-\tau)f(\tau)d\tau. \tag{5.50}$$

Note that Eq. (5.50) may be computationally demanding since there are two summation with infinity terms as kernel in the convolution integral.

FSDOF under deterministic load

Using the state variable analysis proposed in this section the solution becomes straightforward. To show this, suppose that the involved fractional order is $\beta = 1/2$. Then the minimum fractional order that is involved in the state variable analysis is $\alpha = \beta = 1/2$ and the state variable vector is

$$\mathbf{z}^{\mathrm{T}}(t) = \left[x(t),\ \left(D^{0.5}x\right)(t),\ \dot{x}(t),\ \left(D^{1.5}x\right)(t)\right]. \tag{5.51}$$

Further, the matrices involved in the state variable equations in the Eq. (5.46) become

$$\mathbf{A} = \begin{bmatrix} c_\beta & 0 & 0 & m \\ 0 & 0 & m & 0 \\ 0 & m & 0 & 0 \\ m & 0 & 0 & 0 \end{bmatrix}, \qquad \mathbf{B} = \begin{bmatrix} k & 0 & 0 & 0 \\ 0 & 0 & 0 & -m \\ 0 & 0 & -m & 0 \\ 0 & -m & 0 & 0 \end{bmatrix}. \tag{5.52}$$

Furthermore, performing the state variable analysis, the set of four uncoupled equations

$$u_j\left(D^{\alpha}_{0^+}y_j\right)(t) + v_j y(t) = \mu_j(t), \qquad j = 1,2,3,4, \tag{5.53}$$

is derived. Note that the unit step response of the Eq. (5.53) involves a Mittag-Leffler function, but with only one parameter $\mathrm{E}_\beta(\cdot)$. That is,

$$\mathrm{G}_j(t) = \frac{1}{v_j}\left[1 - \mathrm{E}_\alpha\left(-\frac{v_j}{u_j}t^\alpha\right)\right] = -\frac{1}{v_j}\sum_{k=1}^{\infty}\frac{\left(-v_j/u_j t^\alpha\right)^k}{\Gamma(\alpha k+1)}. \tag{5.54}$$

Clearly, the solution in terms of the modal displacements $y_j(t)$ can be obtained by the Boltzmann superposition integral as

$$y_j(t) = \int_0^t \mathrm{G}_j(t-\tau)\dot{\mu}_j(\tau)d\tau = \int_0^t \mathrm{g}_j(t-\tau)\mu_j(\tau)d\tau, \tag{5.55}$$

where $\mathrm{g}(t)$ is Dirac delta response, in other words the time derivative of $\mathrm{G}(t)$. The displacement $x(t)$ is given as the first term of the state variable vector $\mathbf{z}(t)$ defined in Eq. (5.40). It can be seen that the solution of Eq. (5.55) is more convenient to obtain vis-a-vis Eq. (5.50). If the order of fractional derivative is different than $\beta = 1/2$, the described procedure remains the same. Clearly, the vector of state variables and the matrices $\mathbf{A}$ and $\mathbf{B}$ must be properly changed. For example, consider that the order $\beta = 3/4$; in this case the state variable vector has dimension eight, and the minimum fractional involved order is

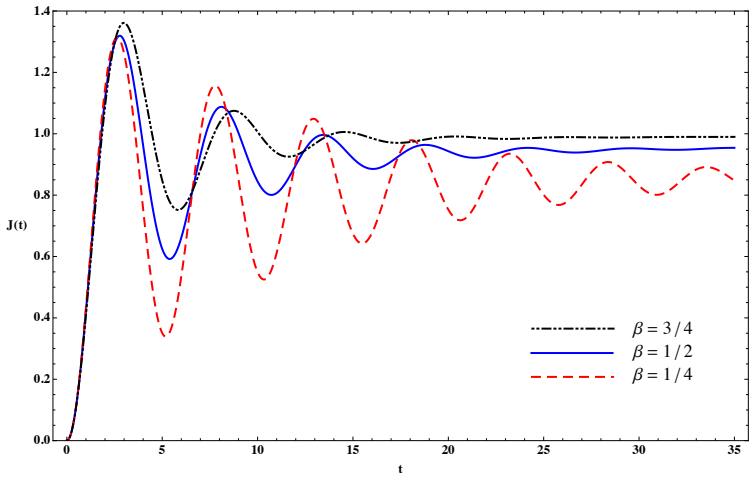

Figure 5.5: Unit step response of the fractional single-degree-of-freedom system.

$\alpha = 1/4$. The matrices **A** and **B** must be generated by the procedure described in Eq.s (5.38).

In the Figure 5.5 the unit step responses of the FSDOF with different fractional differential orders are shown. In particular the chosen coefficients are $m = k = 1$, $c_\beta = 1/2$. Clearly, if the order β is equal to one, the state variable analysis becomes identical to the classic dynamic case, and the state variables become the displacement $x(t)$ and its first derivative $\dot{x}(t)$.

FSDOF under stochastic load

In this section the problem of FSDOF systems driven by stochastic input is carried out in order to show the capabilities of the proposed method also to perform the stochastic analysis in time domain. Consider the case in which the FSDOF in Eq. (5.27) is forced by a zero-mean Gaussian white noise. For this case the state variable vector and the involved matrices are the same described in Eq. (5.51) and Eq. (5.52). In this case, being the displacement a stochastic response process, it will be denoted by the capital letter $X(t)$, while the k^{th} realization of such process will be denoted by $x_k(t)$. Then the procedure to obtain a set of fractional differential equations of order α is still the same of the previous subsection. The solution of j^{th} equation in the complex modal space is readily found by Boltzmann superposition integral in Eq. (5.55). That

is,

$$y_j(t) = \psi_{1j} \int_0^t g_j(t-\tau) w_k(\tau) d\tau, \tag{5.56}$$

where $w_k(t)$ denotes the k^{th} realization of the zero-mean Gaussian white noise process $W(t)$, and ψ_{1j} is the element of the first row and the j^{th} column of modal matrix $\mathbf{\Psi}$. In order to perform the analysis in the time domain the Eq. (5.56) can be solved by step-by-step integration.

Once obtained the solution of the set of fractional differential equations in the complex space the vector of state variable is readily found by the modal transformation in Eq. (5.40). That is,

$$z_j(t) = \sum_{k=1}^{n} \psi_{jk} y_i(t), \qquad k, j = 1, 2, \ldots n, \tag{5.57}$$

where $z_j(t)$ is the j^{th} element of vector $\mathbf{z}(t)$ and n is the number of state variables.

The system is forced by zero-mean Gaussian white noise characterized by the following power spectral density (PSD)

$$S_0 = \lim_{\mathrm{T}\to\infty} \frac{1}{2\pi \mathrm{T}} \mathrm{E}\left[W^*_{\mathcal{F}}(\omega, \mathrm{T}) W_{\mathcal{F}}(\omega, \mathrm{T})\right], \tag{5.58}$$

with $W_{\mathcal{F}}(\omega)$ denoting the truncated Fourier transform of the Gaussian white noise; the asterisk representing complex conjugation; and $\mathrm{E}[\cdot]$ being the expectation operator. The stationary response of the FSDOF system driven by white noise is readily found by spectral analysis, in fact the power spectral density of the response is given as

$$S_X(\omega) = \frac{S_0}{|-m\omega^2 + c_\beta (i\omega)^\beta + k|^2}, \tag{5.59}$$

and the variance σ_X^2 of the displacement $X(t)$ is determined according to the relation

$$\sigma_X^2 = \int_{-\infty}^{\infty} S_X(\omega) d\omega. \tag{5.60}$$

The stationary response in the frequency domain can be used as benchmark for the proposed method. Specifically, using the described modal transformation in the state variable space the set of n solutions in Eq. (5.56) are readily found by step-by-step integration. Subsequently, the displacement response

can be obtained by modal transformation in Eq. (5.57). In this way the stationary and non-stationary response in time domain can be found.

In order to perform this state variable analysis in time domain of FSDOF driven by Gaussian white noise a Monte Carlo simulation is undertaken next. As first step, it is necessary to generate a certain number of random realizations of Gaussian white that forced the system. Later, the response and its statistics can be evaluated.

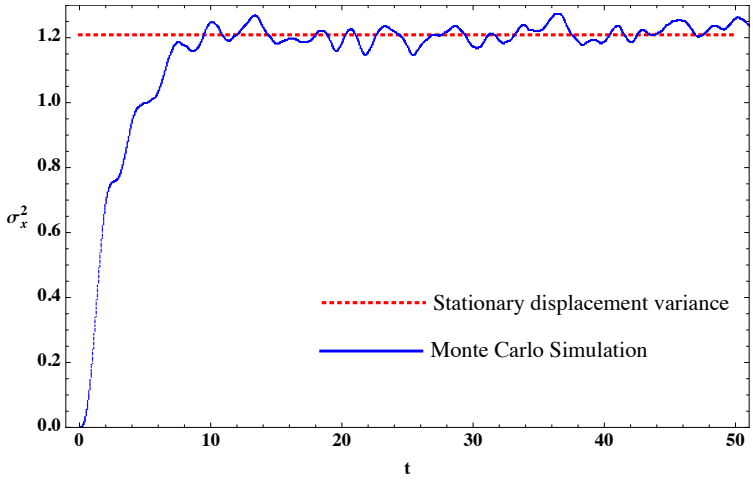

Figure 5.6: Displacement variance of FSDOF system.

Consider, as example, the FSDOF system with the same parameters of the previous section in which the fractional order is $\beta = 1/2$. The chosen parameter to carried out the Monte Carlo simulation are: number of realizations $N = 5000$, $S_0 = 1$, temporal step for the step-by-step integration $\Delta t = 10^{-2}$. Figure 5.6 shows the comparison between the displacement variance obtained by the application the proposed state variable analysis to perform the Monte Carlo simulation and the stationary variance obtained by Eq. (5.60). In particular, for this case, by numerical integration of Eq. (5.60) the stationary variance is $\sigma_X^2 = 1.209$.

The Monte Carlo simulation could be directly performed by the step-by-step integration of the equation of motion in Eq. (5.27), rather than solve four fractional differential equations in the modal space for each realization $x_i(t)$ of the response process $X(t)$. However, this way is not recommended because is not easy to solve the Eq. (5.50) when the involved kernel is that one in

Eq. (5.48). Others possible ways to find the numerical solution $x_i(t)$ of the given problem directly by Eq. (5.27) are by finite differences [83], modified Newmark algorithmic [115], etc.. All of the cited methods can be used in addition to the presented state variable analysis to reduce the computational effort.

5.3.4 Numerical applications of fractional MDOF

Consider the two-degree-of-freedom system in Figure 5.7, which is typical of shear type structures with fractional viscoelastic terms. Next, the preceding concepts of the new complex modal analysis in the state variables domain are used to determine the solution of the fractional multi-degree-of-freedom system. The fractional terms are represented by spring-pots in the figure. The

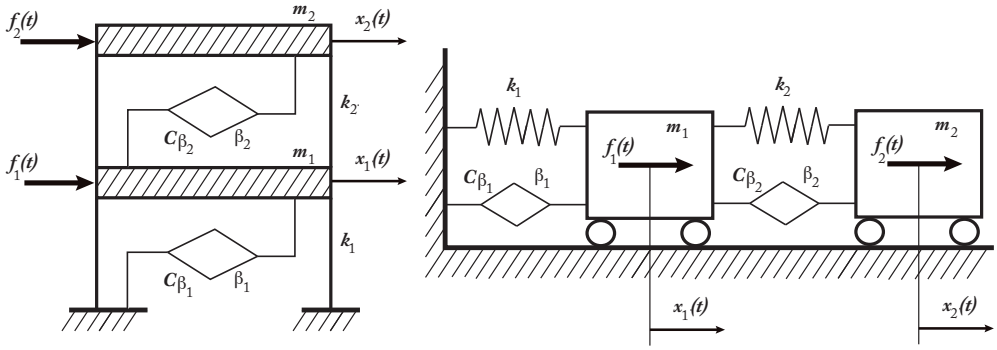

Figure 5.7: Fractional two-degree-of-freedom system.

equations which govern motion of given system in Figure 5.7 are

$$\begin{cases} m_1\ddot{x}_1(t) + c_{\beta_1}\left(D^{\beta_1}x_1\right)(t) - c_{\beta_2}\left(D^{\beta_2}x_2 - x_1\right)(t) + \\ \qquad\qquad + k_1x_1(t) - k_2(x_2 - x_1)(t) = f_1(t), \\ m_2\ddot{x}_2(t) + c_{\beta_2}\left(D^{\beta_2}x_2 - x_1\right)(t) + k_2(x_2 - x_1)(t) = f_2(t), \end{cases} \tag{5.61}$$

where the lumped parameters of the system are the stiffness of the springs k_j; the coefficients of the spring-pots c_{β_j} and their related orders β_j; and the mass of the layers m_j with $j = 1, 2$. Each equation contains both unknowns $x_1(t)$ and $x_2(t)$. The equations are therefore coupled and in this form must be

solved simultaneously. A way to decouple the system by the fractional state variable analysis is shown next.

FMDOF under deterministic load

Consider the case in which $\beta_1 = 3/4$ and $\beta_2 = 1/2$. In this case the coupled equations of motion are the same as expressed in Eq. (5.61). The rational order α that permit to rewrite the set of given equations as the sequential linear differential equations of fractional order in Eq. (5.34) is $\alpha = 1/4$, and the involved matrices in the nodal space are

$$\begin{aligned} \mathbf{K} &= \begin{bmatrix} k_1 + k_2 & -k_2 \\ -k_2 & k_2 \end{bmatrix}, \quad \mathbf{C}_2 = \begin{bmatrix} c_{\beta_2} & -c_{\beta_2} \\ -c_{\beta_2} & c_{\beta_2} \end{bmatrix}, \\ \mathbf{C}_3 &= \begin{bmatrix} c_{\beta_1} & 0 \\ 0 & 0 \end{bmatrix}, \quad \mathbf{C}_8 = \mathbf{M} = \begin{bmatrix} m_1 & 0 \\ 0 & m_2 \end{bmatrix}. \end{aligned} \tag{5.62}$$

Other matrices involved are $\mathbf{C}_1 = \mathbf{C}_4 = \mathbf{C}_5 = \mathbf{C}_6 = \mathbf{C}_7 = \mathbf{0}$; and the vector of state variables is

$$\mathbf{z}^{\mathrm{T}}(t) = \left[\boldsymbol{x}^{\mathrm{T}}(t)\, D^{\frac{1}{4}}\boldsymbol{x}^{\mathrm{T}}(t)\, D^{\frac{1}{2}}\boldsymbol{x}^{\mathrm{T}}(t)\, D^{1}\boldsymbol{x}^{\mathrm{T}}(t)\, D^{\frac{3}{4}}\boldsymbol{x}^{\mathrm{T}}(t) D^{\frac{5}{4}}\boldsymbol{x}^{\mathrm{T}}(t)\, D^{\frac{3}{2}}\boldsymbol{x}^{\mathrm{T}}(t)\, D^{\frac{7}{4}}\boldsymbol{x}^{\mathrm{T}}(t) \right]. \tag{5.63}$$

The dimension of the problem in the state variable domain is $r \times n = 16$. For simplicity, considered that $f_1(t) = 0$ and $f_2(t)$ is

$$f_2(t) = \begin{cases} \sin(t), & 0 < t < 2\pi, \\ 0, & \text{otherwise.} \end{cases} \tag{5.64}$$

Further, the chosen parameters of the two-degree-of-freedom system in Figure 5.7 are $m_1 = 1$, $m_2 = 3/4$, $c_{\beta_1} = c_{\beta_2} = 1$, $k_1 = 3/2$ and $k_2 = 1/2$. These parameters are chosen in order to obtain three matrices of coefficients which are linearly independent. In this case is not possible to decoupled the set of given equations by a simple modal transformation in Eq. (5.32). Therefore, in this case, the presented fractional state variable analysis shows all its potentialities. The uncoupled equations in the modal space are integrated by using the Boltzmann superposition integral in Eq. (5.55). Moreover another approaches to solve the fractional differential equations relies on the Mellin transform has been used. For this example the following parameters of discretized Mellin transform have been chosen: $\rho = 1$, $\bar{\eta} = 100$ and $\Delta\eta = 0.5$ (see the cited articles pertaining to the method [15, 35]). In this manner, the

displacements $x_1(t)$ and $x_2(t)$ are readily determined. The displacements of the two layers obtained by the complex modal analysis are shown in the Figure 5.8. In particular, the figure shows the displacements obtained with the two different methods to integrate the set of uncoupled equations.

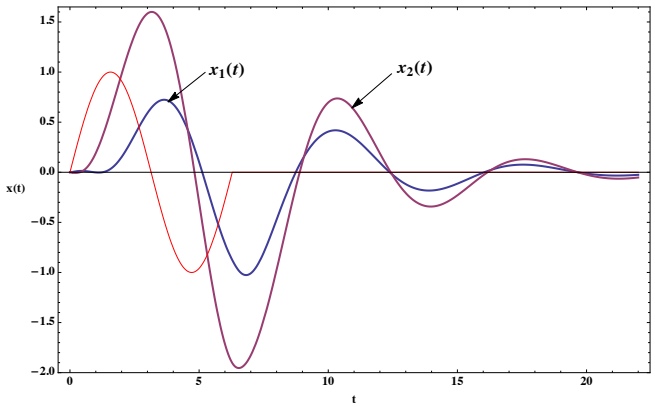

Figure 5.8: Displacements $x_1(t)$ and $x_2(t)$ of the dynamical system.

FMDOF under stochastic input

Next, assume that the fractional two-degree-of-freedom system shown in Figure 5.7 is forced by a stochastic input. In particular, consider that the involved fractional orders are the same in the preciding case and that the $f_1(t) = 0$ and $f_2(t) = W(t)$. Obviously, also in this case, the frequency domain solution is readily obtainable. Specifically, the Fourier transforms of the Eqs. (5.61) yields

$$\mathbf{X}_{\mathcal{F}}(\omega) = \mathbf{H}(\omega)\mathbf{F}_{\mathcal{F}}(\omega) \tag{5.65}$$

where $\mathbf{X}_{\mathcal{F}}(\omega)$ and $\mathbf{F}_{\mathcal{F}}(\omega)$ are the Fourier transforms of the vectors $\boldsymbol{x}(t)$ and $\mathbf{f}(t)$, respectively. Further, the non-diagonal transfer matrix $\mathbf{H}(\omega)$ is defined by its inverse as

$$\begin{aligned}
\mathbf{H}^{-1}(\omega) =& \mathbb{K}(\omega) = \begin{bmatrix} \mathrm{k}_{11} & \mathrm{k}_{12} \\ \mathrm{k}_{21} & \mathrm{k}_{22} \end{bmatrix}, \\
&\mathrm{k}_{11} = k_1 + k_2 + c_{\beta_1}(i\omega)^{\beta_1} + c_{\beta_2}(i\omega)^{\beta_2} - m_1\omega^2, \\
&\mathrm{k}_{21} = \mathrm{k}_{12} = -k_2 - c_{\beta_2}(i\omega)^{\beta_2}, \\
&\mathrm{k}_{22} = k_2 + c_{\beta_2}(i\omega)^{\beta_2} - m_2\omega^2,
\end{aligned} \tag{5.66}$$

where i is the imaginary unit. The terms $(i\omega)^{\beta_j}$ with $j = 1,2$ in Eq. (5.66) are due to the Fourier transform of the fractional operators that are involved in the Eq. (5.61). By this transformation it is clear that the fractional derivative term introduces in the system dynamics both effective damping and effective stiffness frequency dependent terms. In fact, the following relation holds

$$(i\omega)^{\beta} = |\omega|^{\beta}\left[\cos\left(\frac{\beta\pi}{2}\right) + i\,\mathrm{sgn}(\omega)\sin\left(\frac{\beta\pi}{2}\right)\right]. \tag{5.67}$$

The spectral matrix of the inputs is denoted with $\mathbf{S}_f(\omega)$, and based on the preceding assumption it becomes

$$\mathbf{S}_f(\omega) = \begin{bmatrix} 0 & 0 \\ 0 & S_0 \end{bmatrix}, \tag{5.68}$$

where S_0 is expressed in Eq. (5.59).

Based on the above considerations, the spectral matrix $\mathbf{S}_X(\omega)$ of the response can be expressed as

$$\mathbf{S}_X(\omega) = \mathbf{H}^*(\omega)\mathbf{S}_f(\omega)\mathbf{H}^{\mathrm{T}}(\omega), \tag{5.69}$$

where

$$\mathbf{S}_X(\omega) = \begin{bmatrix} S_{X_1}(\omega) & S_{X_1X_2}(\omega) \\ S_{X_2X_1}(\omega) & S_{X_2}(\omega) \end{bmatrix}, \tag{5.70}$$

with the elements of the matrix $\mathbf{S}_X(\omega)$ expressed as

$$S_{X_jX_k}(\omega) = \lim_{\mathrm{T}\to\infty}\frac{1}{2\pi\mathrm{T}}\mathrm{E}\left[X^*_{\mathcal{F},j}(\omega,\mathrm{T})X_{\mathcal{F},k}(\omega,\mathrm{T})\right], \quad j,k = 1,2. \tag{5.71}$$

Similarly to the FSDOF system, the solution in the frequency domain in Eq. (5.71) can be used as a benchmark for the proposed method. In fact, the stationary and non-stationary response can be evaluated by the proposed state variable analysis in addition of the classic Monte Carlo simulation. In particular, the introduced concepts of modal transformation are used to obtain a set of uncoupled differential equations in the state variable domain. For the integration of the equation in the modal space is possible to use the step-by-step integration method showed in the previous section. Similarly to the previous case, the variances obtained by Monte Carlo simulation and fractional state variable analysis are compared to those obtained by numerical integration of the PSDs in Eq. (5.69).

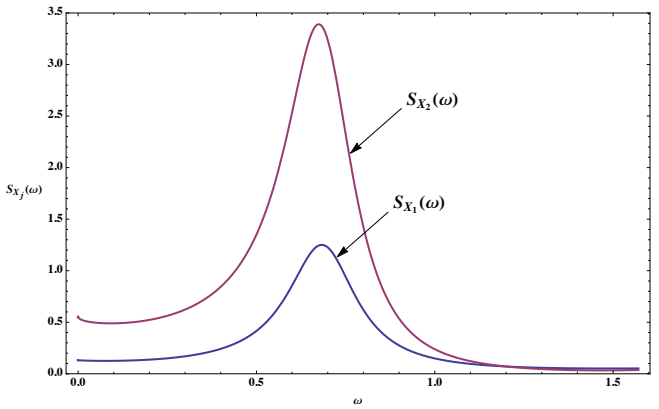

Figure 5.9: PSDs of the response $X_1(t)$ and $X_2(t)$.

The chosen parameters for this examples are $m_1 = 5/4$, $m_2 = 1$, $c_{\beta_1} = 3/4$, $c_{\beta_2} = 1/3$, $\beta_1 = 3/4$, $\beta_2 = 1/2$, $k_1 = 1.8$, and $k_2 = 1$. The parameters for the Monte Carlo simulations are: N = 10^4, $S_0 = 1$, $\Delta t = 10^{-1}$.

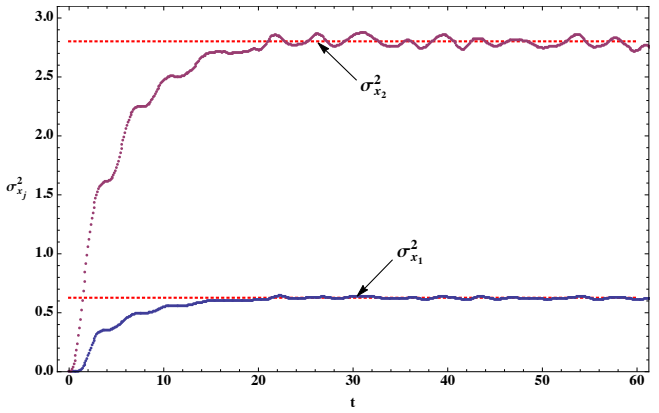

Figure 5.10: Variances of displacements of two-degree-of-freedom system, Monte Carlo simulation (continuous line), Stationary displacement variance (dotted line).

Figure 5.9 shows the PSDs of the displacements that are in the diagonal terms of the matrix $\mathbf{S}_X(\omega)$. Figure 5.10 shows the comparison between the displacement variance obtained by the application of the proposed state vari-

able analysis to perform the Monte Carlo simulation and the stationary variance. For this case, by numerical integration of PSDs in the matrix $\mathbf{S}_X$ the stationary variances are $\sigma^2_{X_1} = 0.627$ and $\sigma^2_{X_2} = 2.802$.

5.4 Conclusions

In the first part of this Chapter the analysis of continuous fractional viscoelastic Euler-Bernoulli beam has been dealt, performing the study either in frequency or in time domain. The viscoelastic behavior has been taken into account by fractional Kelvin-Voigt model that is the proper model for capturing the viscoelasticity phenomena since it exhibits an intermediate behavior between elastic and viscous. Numerical results have been carried out considering a cantilever beam under stochastic loads, no matter the order of fractional derivative, rather so you can appreciate the influence of fractional derivative order beta on PSD response. The latter, stresses the damping effect in reducing PSD amplitude for higher values of the fractional derivative order.

In the second part, the analysis of single-degree and multi-degree-of-freedom systems with fractional viscoelastic elements in the equation of motion have been pursued. This kind of problem is characterized for the presence of a set of coupled fractional differential equations that govern the motion of the system. It has been pointed out that this kind of problem is more complex to solve vis-a-vis the analysis of multi-degree-of-freedom system with integer order derivatives. The analysis has been based on a novel approach using an augmented state variables transformation. The method, based on complex modal analysis in the state variable domain, is applicable if the involved fractional terms have rational order. This assumption is necessary since only in this case it is possible to find an appropriate state variables vector. Note, however, that for engineering applications all real orders can be reasonably approximated by rational orders. By the proposed method the set of coupled fractional differential equations has been decoupled in a proper fractional state variable domain. This transformation has led to a new set of fractional equations which are uncoupled and more convenient to solve. Therefore, a drastic reduction of the computational effort is achieved. To elucidate the applicability of the method several numerical examples have been considered which have confirmed the effectiveness of the method both for deterministic and stochastic system excitations.

Chapter 6

Stochastic processes represented by fractional calculus

6.1 Preliminary remarks

This Chapter deals with the characterization of stochastic processes by the fractional calculus. As it is shown in the previous Chapter, in many cases of engineering and physics interest it is important the characterization of stochastic processes. Usually for Gaussian processes the stochastic characterization is obtained by the correlation function (CF) and by its Fourier transform, namely the power spectral density (PSD). However in many cases, although the PSD is known in analytical form, it is not possible to obtain the analytical form of the correlation function with the inverse Fourier transform operator.

Another way to partly represent the stochastic process is given by the spectral moments (SMs). These quantities are the moments of order $k \in \mathbb{N}$ of the one-sided power spectral density, and they have been introduced by Vanmarcke [119]. These quantities can be used for the prediction of the first excursion failure, fatigue failure, for statistical distribution of peaks and ranges [87] and so on [57, 58, 61]. Many applications and useful information about classical spectral moments can be found in [11, 12, 17, 76, 79, 95, 113, 114]. The limit of these entities is that they are not able to fully represent the stochastic processes. Indeed, the limit of such quantities is due to the fact that for k large the SMs may diverge [25, 87] and then they are not useful quantities for reconstructing the power spectral density.

Recently [25], the representation of the power spectral density and correla-

tion function has been pursued by using complex spectral moments (CSMs). The latter are the spectral moments of complex order $\gamma \in \mathbb{C}$ of the power spectral density. The appealing of such moments is related to the fact that real part of the order $\Re(\gamma)$ remains constant and only the imaginary part $\Im[\gamma]$ runs, then no divergence problems occurs. These complex spectral moments are related to the fractional moments (FMs) of the correlation function, and these latter entities are the Mellin transform [85, 99] of the correlation function. The knowledge of the spectral fractional moments and/or the fractional moments permits to reconstruct the correlation function and the power spectral density in whole domain. This important result has been obtained by using Mellin transform theorem [64, 85, 91, 99]. Moreover, the fractional moments are related to the fractional operator [64, 91, 99] of the correlation function, in particular the Mellin transform is the Riesz complex integral of the correlation function at the origin. This fact permits to interpret the representation of the correlation function by the inverse Mellin transform as a generalized Taylor series.

The capabilities of the fractional moments and complex spectral moments are also applied for the characterization of random variables [24, 26, 37], for the digital simulation of the random processes [27, 98], for the solution of the Fokker-Planck equation [36], Kolmogorov-Feller equation [33] and for the solution of the Einstein-Smoluchowski equation [4].

This Chapter extends the application field of the method in [25]. In particular, in [25] it has been shown how to manipulate SMs in order to characterize the PSD and (symmetric) correlation of a process, while this Chapter shows how to characterize also multivariate processes with complex cross-power spectral density and asymmetric cross-correlation function. Particular attention is devoted to the characterization of the response process of the fractional linear oscillator forced by Gaussian white noise.

6.2 Cross-correlation function by complex fractional moments

Consider $X_1(t)$ and $X_2(t)$ two stationary zero-mean Gaussian random processes, for which the cross-correlation function is denoted by $R_{X_1X_2}(\tau)$, and its Fourier transform, termed as cross-power spectral density function (CPSD), is

$S_{X_1X_2}(\omega)$. The cross-correlation is defined as

$$\begin{aligned} R_{X_1X_2}(\tau) &= \mathrm{E}\left[X_1(t)X_2\left(t+\tau\right)\right] \\ &= \int_{-\infty}^{\infty}\int_{-\infty}^{\infty} p_{x_1x_2}(x_1(t), x_2(t+\tau))x_1x_2dx_1dx_2 \end{aligned} \tag{6.1}$$

where $\mathrm{E}\left[\cdot\right]$ represents the ensemble average. Usually, the cross-correlation is neither even nor odd, so, for simplicity, it is possible to decompose $R_{X_1X_2}(\tau)$ into an even function $u(\tau)$ and an odd function $v(\tau)$ as follows

$$\begin{aligned} R_{X_1X_2}(\tau) &= \frac{1}{2}\left[R_{X_1X_2}(\tau) + R_{X_1X_2}(-\tau)\right] + \frac{1}{2}\left[R_{X_1X_2}(\tau) - R_{X_1X_2}(-\tau)\right] \\ &= u(\tau) + v(\tau). \end{aligned} \tag{6.2}$$

By using the definition in Eq. (1.73), the Mellin transform of the even function $u(\tau)$ for the positive half-plane of τ is

$$\mathrm{M}_{u^+}(\gamma-1) = \mathcal{M}\left\{u(\tau)U(\tau),\, \gamma\right\} = \int_0^{\infty} u^+(\tau)\tau^{\gamma-1}d\tau \tag{6.3}$$

where $U(t)$ is the unit step function and $\gamma \in \mathbb{C}$ with $\gamma = \rho + i\eta$, while for the negative half-plane the Mellin transform leads to

$$\mathrm{M}_{u^-}(\gamma-1) = \mathcal{M}\left\{u(\tau)U(-\tau),\, \gamma\right\} = \int_{-\infty}^{0} u^-(\tau)(-\tau)^{\gamma-1}d\tau. \tag{6.4}$$

The terms $\mathrm{M}_{u^+}(\gamma-1)$ and $\mathrm{M}_{u^-}(\gamma-1)$ may be interpreted as the *Complex Fractional Moments* (CFMs) of half-function $u^+(\tau)$ and $u^-(\tau)$ respectively.

From the Eqs. (6.3) and (6.4) it is noted that $\mathrm{M}_{u^+}(\gamma-1) = \mathrm{M}_{u^-}(\gamma-1)$, because $u(\tau)$ is even. Whereby the $u(\tau)$ may be obtained as the inverse Mellin transform:

$$u(\tau) = \frac{1}{2\pi i}\int_{\rho-i\eta}^{\rho+i\eta} \mathrm{M}_{u^+}(\gamma-1)|\tau|^{-\gamma}d\gamma; \quad \tau \in \mathbb{R}. \tag{6.5}$$

Similarly, it is possible to define the Mellin transform of odd part of cross-correlation $v(\tau)$, for which for the positive half-plane of τ the Mellin transform yields

$$\mathrm{M}_{v^+}(\gamma-1) = \mathcal{M}\left\{v(\tau)U(\tau),\, \gamma\right\} = \int_0^{\infty} v^+(\tau)\tau^{\gamma-1}d\tau \tag{6.6}$$

and for negative value of τ the Mellin transform becomes

$$\mathrm{M}_{v^-}(\gamma-1)=\mathcal{M}\left\{v(\tau)U(-\tau),\,\gamma\right\}=\int_{-\infty}^{0}v^-(\tau)(-\tau)^{\gamma-1}d\tau. \tag{6.7}$$

In this case $\mathrm{M}_{v^+}(\gamma-1)=-\mathrm{M}_{v^-}(\gamma-1)$ because $v(\tau)$ is an antisymmetric function. By using the inverse Mellin transform the given function $v(\tau)$ can be restored by its CFMs, that is

$$v(\tau)=\frac{\operatorname{sgn}(\tau)}{2\pi i}\int_{\rho-i\eta}^{\rho+i\eta}\mathrm{M}_{v^+}(\gamma-1)|\tau|^{-\gamma}d\gamma;\qquad \tau\in\mathbb{R}. \tag{6.8}$$

Based on the previous results and remembering Eq. (6.2) the cross-correlation can be represented in the whole domain by using the CFMs $\mathrm{M}_{u^+}(\gamma-1)$ and $\mathrm{M}_{v^+}(\gamma-1)$ in the following form

$$\begin{aligned}R_{X_1X_2}(\tau)&=\frac{1}{2\pi i}\int_{\rho-i\eta}^{\rho+i\eta}\left[\mathrm{M}_{u^+}(\gamma-1)+\operatorname{sgn}(\tau)\mathrm{M}_{v^+}(\gamma-1)\right]|\tau|^{-\gamma}d\gamma\\&=\frac{|\tau|^{-\rho}}{2\pi}\int_{-\infty}^{\infty}\left[\mathrm{M}_{u^+}(\gamma-1)+\operatorname{sgn}(\tau)\mathrm{M}_{v^+}(\gamma-1)\right]|\tau|^{-i\eta}d\eta\end{aligned} \tag{6.9}$$

In Eq. (6.9) the integral in the inverse Mellin transform is performed along the imaginary axis, then $\rho=\Re(\gamma)$ remains fixed for which $d\gamma=id\eta$. This is possible provided ρ belongs to the so called *fundamental strip* (FS) of the Mellin transform (see Appendix A), since both $\mathrm{M}_{u^+}(\gamma-1)$ and $\mathrm{M}_{v^+}(\gamma-1)$ are holomorph in this strip. It is important to underline that integral in Eq. (6.9) is independent of the value of ρ selected, provided that it belong to the FS.

There is a relation between CFMs and fractional operators. In order to show this relation, consider the Riemann-Liouville integral with complex order γ of a function $f(t)$, defined in Eq. (2.23). This integral at the origin $t=0$ is related to the Mellin transform of the function $f(t)$:

$$\Gamma(\gamma)\left(\mathrm{I}_{\pm}^{\gamma}f\right)(0)=\mathrm{M}_{f^{\pm}}(\gamma-1). \tag{6.10}$$

From Eq. (6.10) and by taking into account the properties between the Riemann-Liouville integral and the Riesz integrals in Eqs. (2.30) and (2.31), it is easy to demonstrate the relation between fractional operators of cross-correlation at the origin and CFMs, indeed

$$\left(\mathbf{I}^{\gamma}R_{X_1X_2}\right)(0)=\frac{\mathrm{M}_{R^+_{X_1X_2}}(\gamma-1)+\mathrm{M}_{R^-_{X_1X_2}}(\gamma-1)}{2\Gamma(\gamma)\cos\left(\frac{\gamma\pi}{2}\right)}=\frac{\mathrm{M}_{u^+}(\gamma-1)}{\Gamma(\gamma)\cos\left(\frac{\gamma\pi}{2}\right)}; \tag{6.11a}$$

$$\left(\mathbf{H}^{\gamma} R_{X_1X_2}\right)(0) = \frac{\mathrm{M}_{R^{+}_{X_1X_2}}(\gamma-1) - \mathrm{M}_{R^{-}_{X_1X_2}}(\gamma-1)}{2\Gamma(\gamma)\sin\left(\frac{\gamma\pi}{2}\right)} = \frac{\mathrm{M}_{v^{+}}(\gamma-1)}{\Gamma(\gamma)\sin\left(\frac{\gamma\pi}{2}\right)}. \quad (6.11b)$$

In this way, the cross-correlation may be expressed in the form:

$$R_{X_1X_2}(\tau) = \frac{|\tau|^{-\rho}}{2\pi}\int_{-\infty}^{\infty}\Gamma(\gamma)\left[\cos\left(\frac{\gamma\pi}{2}\right)\left(\mathbf{I}^{\gamma}R_{X_1X_2}\right)(0) + \right. \\ \left. +\mathrm{sgn}(\tau)\sin\left(\frac{\gamma\pi}{2}\right)\left(\mathbf{H}^{\gamma}R_{X_1X_2}\right)(0)\right]|\tau|^{-i\eta}d\eta. \quad (6.12)$$

The integrals in Eq. (6.9) and Eq. (6.12) may be discretized in order to obtain the approximate form of given function $R_{X_1X_2}(\tau)$, namely

$$\begin{aligned} R_{X_1X_2}(\tau) &\approx \frac{\Delta\eta|\tau|^{-\rho}}{2\pi}\sum_{k=-\mathrm{m}}^{\mathrm{m}}\left[\mathrm{M}_{u^{+}}(\gamma_k-1)+\mathrm{sgn}(\tau)\mathrm{M}_{v^{+}}(\gamma_k-1)\right]|\tau|^{-ik\Delta\eta} \\ &= \frac{\Delta\eta|\tau|^{-\rho}}{2\pi}\sum_{k=-\mathrm{m}}^{\mathrm{m}}\Gamma(\gamma_k)\left[\cos\left(\frac{\gamma_k\pi}{2}\right)\left(\mathbf{I}^{\gamma_k}R_{X_1X_2}\right)(0)+\right. \\ &\quad \left. +\mathrm{sgn}(\tau)\sin\left(\frac{\gamma_k\pi}{2}\right)\left(\mathbf{H}^{\gamma_k}R_{X_1X_2}\right)(0)\right]|\tau|^{-ik\Delta\eta} \end{aligned} \quad (6.13)$$

where the exponent γ is discretized in the form $\gamma_k = \rho + ik\Delta\eta$, $\Delta\eta$ is the discretization step of the imaginary axis, and m is the truncation number in the summation, that is chosen in such a way that any term $n > \mathrm{m}$ in the summation has a negligible contribution. It is to be stressed that CFMs $\mathrm{M}_{u^{+}}$ and $\mathrm{M}_{v^{+}}$ are complex quantities whose real part is even and imaginary part is odd in η axis. This means that $\mathrm{M}_{u^{+}}(\gamma_k-1) = \mathrm{M}^{*}_{u^{+}}(\gamma_{-k}-1)$ and $\mathrm{M}_{v^{+}}(\gamma_k-1) = -\mathrm{M}^{*}_{v^{+}}(\gamma_{-k}-1)$, then the summation of $2m+1$ terms in Eq. (6.13) can be substituted by a summation of $m+1$ terms ($k = 0 \div m$). Note that the Eq. (6.13) is a not-divergent summation, because ρ remains fixed, and this is a very important aspect when it is necessary to restore the given function in a large domain of τ.

By Eq. (6.12) it can be asserted that Eq. (6.13) is a sort of a Taylor series, since knowing the (fractional) operators at the origin of the given function, then the function may be reconstructed. Moreover, Eq. (6.13) does not diverge for $\tau \to \infty$, since the real part of the exponent γ remains fixed and only the imaginary part runs.

Obviously, the representation of the correlation function $R_X(\tau)$ of a single process $X(t)$ is more easy to represent by CFMs. In order to do this be enough

to simplify the Eq.s (6.9) and (6.12) taking into account that the correlation function is symmetric $v(\tau) = 0$, then

$$R_X(\tau) = \frac{|\tau|^{-\rho}}{2\pi} \int_{-\infty}^{\infty} \mathrm{M}_{u^+}(\gamma - 1)|\tau|^{-i\eta} d\eta \approx \frac{|\tau|^{-\rho}\Delta\eta}{2\pi} \sum_{k=-\mathrm{m}}^{\mathrm{m}} \mathrm{M}_{u^+}(\gamma_k - 1)|\tau|^{-ik\Delta\eta}. \tag{6.14}$$

6.3 Cross-power spectral density function by complex spectral moments

In this section the introduced representation by fractional moments will be applied to restore the cross-power spectral density function.

Consider the CPSD; it is denoted by $S_{X_1X_2}(\omega)$ and defined from the cross-correlation by the following definition

$$\begin{aligned} S_{X_1X_2}(\omega) &= \frac{1}{2\pi}\mathcal{F}\left\{R_{X_1X_2}(\tau);\, \omega\right\} = \frac{1}{2\pi}\int_{-\infty}^{\infty} R_{X_1X_2}(\tau) e^{i\omega\tau} d\tau \\ &= \frac{1}{2\pi}\int_{-\infty}^{\infty} R_{X_1X_2}(\tau)\left[\cos(\omega\tau) + i\sin(\omega\tau)\right] d\tau \\ &= \frac{1}{\pi}\left[\int_0^{\infty} u(\tau)\cos(\omega\tau) d\tau + i\int_0^{\infty} v(\tau)\sin(\omega\tau) d\tau\right] \\ &= \frac{1}{2\pi}\left[u_{\mathcal{F}}(\omega) + i v_{\mathcal{F}}(\omega)\right] \end{aligned} \tag{6.15}$$

where $u_{\mathcal{F}}(\omega)$ and $v_{\mathcal{F}}(\omega)$ are the Fourier transform of even part $u(t)$ and odd part $v(t)$ of cross-correlation, respectively, and they represent the real and the imaginary part of CPSD.

Another expression of $S_{X_1X_2}(\omega)$ may be obtained from Eq. (6.9) by using the definition in Eq. (6.15), obtaining the following relationship

$$\begin{aligned} S_{X_1X_2}(\omega) = &\frac{|\omega|^{\rho-1}}{2\pi^2}\int_{-\infty}^{\infty} \Gamma(1-\gamma)\left[\sin\left(\frac{\gamma\pi}{2}\right)\mathrm{M}_{u^+}(\gamma-1) + \right. \\ &\left. + i\,\mathrm{sgn}(\omega)\cos\left(\frac{\gamma\pi}{2}\right)\mathrm{M}_{v^+}(\gamma-1)\right]|\omega|^{i\eta} d\eta \end{aligned} \tag{6.16}$$

which can be discretized as

$$\begin{aligned} S_{X_1X_2}(\omega) \approx &\frac{|\omega|^{\rho-1}\Delta\eta}{2\pi^2}\sum_{k=-\mathrm{m}}^{\mathrm{m}} \Gamma(1-\gamma_k)\left[\sin\left(\frac{\gamma_k\pi}{2}\right)\mathrm{M}_{u^+}(\gamma_k-1) + \right. \\ &\left. + i\,\mathrm{sgn}(\omega)\cos\left(\frac{\gamma_k\pi}{2}\right)\mathrm{M}_{v^+}(\gamma_k-1)\right]|\omega|^{ik\Delta\eta}. \end{aligned} \tag{6.17}$$

As already underlined for Eq. (6.13), since real and imaginary parts of CFMs are even and odd, respectively, summation of $2m+1$ terms can be substituted by a summation of $m+1$ terms.
Another representation of the CPSD is given by the knowledge of *complex spectral moments* (CSMs). These entities are neither else that the spectral counterpart of CFMs. The classical definition of spectral moments has been introduced by [119], and the generalization of these quantities with fractional exponent, just call *complex spectral moments* (CSMs), has been given by [25]. The CSMs are defined as

$$\Lambda_{u^+}(-\gamma) = \int_0^\infty \Re\left\{S_{X_1X_2}(\omega)\right\}\omega^{-\gamma}d\omega = \int_0^\infty u_{\mathcal{F}}(\omega)\omega^{-\gamma}d\omega \tag{6.18a}$$

$$\Lambda_{v^+}(-\gamma) = \int_0^\infty \Im\left\{S_{X_1X_2}(\omega)\right\}\omega^{-\gamma}d\omega = \int_0^\infty v_{\mathcal{F}}(\omega)\omega^{-\gamma}d\omega. \tag{6.18b}$$

By using the definitions of CFMs, in Eqs. (6.3) and (6.6), and using some properties of Fourier transform of fractional operators (see section C.1), may be readily demonstrated that the following identities

$$\begin{aligned} \mathrm{M}_{u^+}(\gamma-1) &= \frac{\Gamma(\gamma)\cos(\gamma\pi/2)}{\pi}\Lambda_{u^+}(-\gamma) \\ \mathrm{M}_{v^+}(\gamma-1) &= \frac{\Gamma(\gamma)\sin(\gamma\pi/2)}{\pi}\Lambda_{v^+}(-\gamma). \end{aligned} \tag{6.19}$$

hold true. This is a very useful result, since in many cases of engineering interest, like wind velocity processes, ocean waves, earthquake processes, and so on, the action in the structures under this kind of processes is defined by the spectral properties in frequency domain rather than by the correlation or cross correlation function in time domain. As a consequence the CFMs, in virtue of Eqs. (6.19), may be easier calculated by Eqs. (6.18) from the knowledge of CSMs.

By using the Eqs. (6.19) the following expression is readily found from Eq. (6.17)

$$S_{X_1X_2}(\omega) = \frac{|\omega|^{\rho-1}}{4\pi^2}\int_{-\infty}^{\infty}\left[\Lambda_{u^+}(-\gamma) + i\mathrm{sgn}(\omega)\Lambda_{v^+}(-\gamma)\right]|\omega|^{i\eta}d\eta \tag{6.20}$$

this expression represents another exact representation of CPSD. In Eq. (6.20) the following properties have been used

$$\cos\left(\frac{\gamma\pi}{2}\right)\sin\left(\frac{\gamma\pi}{2}\right)\Gamma(\gamma)\Gamma(1-\gamma) = \frac{\pi}{2} \tag{6.21}$$

The discretized form of Eq. (6.20) is given as

$$S_{X_1X_2}(\omega) \approx \frac{\Delta\eta|\omega|^{\rho-1}}{4\pi^2} \sum_{k=-\mathrm{m}}^{\mathrm{m}} \left[\Lambda_{u^+}(-\gamma_k) + i\mathrm{sgn}(\omega)\Lambda_{v^+}(-\gamma_k)\right] |\omega|^{i\eta}. \quad (6.22)$$

Because of Eqs. (6.19) the CSMs can be also used to represent the cross-correlation, obtaining the following expression

$$\begin{aligned} R_{X_1X_2}(\tau) =& \frac{|\tau|^{-\rho}}{2\pi^2} \int_{-\infty}^{\infty} \Gamma(\gamma) \left[\cos\left(\frac{\gamma\pi}{2}\right) \Lambda_{u^+}(-\gamma) + \right. \\ & \left. + \mathrm{sgn}(\tau) \sin\left(\frac{\gamma\pi}{2}\right) \Lambda_{v^+}(-\gamma)\right] |\tau|^{-i\eta} d\eta, \end{aligned} \quad (6.23)$$

or in discretized form

$$\begin{aligned} R_{X_1X_2}(\tau) \approx& \frac{\Delta\eta|\tau|^{-\rho}}{2\pi^2} \sum_{k=-\mathrm{m}}^{\mathrm{m}} \Gamma(\gamma_k) \left[\cos\left(\frac{\gamma_k\pi}{2}\right) \Lambda_{u^+}(-\gamma_k) \right. \\ & \left. + \mathrm{sgn}(\tau) \sin\left(\frac{\gamma_k\pi}{2}\right) \Lambda_{v^+}(-\gamma_k)\right] |\tau|^{-ik\Delta\eta}. \end{aligned} \quad (6.24)$$

Then also the CSMs represent another way to describe random process in time and frequency domain. As a conclusion if the CPSD is known then we may evaluate the complex spectral moments Λ_{u^+}, Λ_{v^+} and with these quantities both cross-correlation and CPSD may be readily reconstructed by Eqs. (6.24) and (6.22), respectively. Similarly to the correlation function in the previous section, also in this case the representation of the power spectral density PSD of $X(t)$ is a particular case of the Eq. (6.20). In particular, by placing $v_{\mathcal{F}}(\omega) = 0$, then $\Lambda_{v^+}(-\gamma)$, obtaining that

$$S_X(\omega) = \frac{|\omega|^{\rho-1}}{4\pi^2} \int_{-\infty}^{\infty} \Lambda_{u^+}(-\gamma)|\omega|^{i\eta} d\eta \approx \frac{|\omega|^{\rho-1}\Delta\eta}{4\pi^2} \sum_{-\mathrm{m}}^{\mathrm{m}} \Lambda_{u^+}(-\gamma_k)|\omega|^{ik\Delta\eta}. \quad (6.25)$$

6.4 The fractional oscillator under Gaussian white noise

The concepts about the CFMs and SMs, described in the previous section, can be used to characterize the stochastic response process of the dynamical systems in which fractional operators appear. Consider the equation of motion

of the single-degree of freedom fractional oscillator in Eq. (5.27). If the external force $f(t) = W(t)$ is a zero-mean Gaussian white noise such equation becomes:

$$m\ddot{X}(t) + c_\beta \left(D_{0^+}^{\beta} X \right)(t) + kX(t) = W(t), \quad t \geqslant 0, \tag{6.26}$$

where $X(t)$ denotes the stochastic response process in terms of displacements. In order to fully describe such output response process in probabilistic setting the PSD or the correlation function CF have to be evaluated. For the case of linear systems with integer order operators both PSD and CF are known in closed form. Instead, if fractional order operators are present in the equation of motion, the PSD of the response is already known by the Eq. (5.59), while the CF has to be evaluated in approximated form by the inverse fast Fourier transform of the PSD.

The method to represent the PSD and CF by complex spectral moments presented in the previous sections is also limited, since either if the PSD is given, its spectral moments defined in Eq. (6.18a) cannot be evaluate in closed form by the following integral:

$$\Lambda_X(-\gamma) = \int_0^\infty S_X(\omega)\omega^{-\gamma} d\omega = S_0 \int_0^\infty \frac{\omega^{-\gamma} d\omega}{|-m\omega^2 + c_\beta (i\omega)^\beta + k|^2}. \tag{6.27}$$

The evaluation of this integral gives the fully characterization of the response process $X(t)$, since the knowledge of the complex spectral moments with the aid of the relation in Eq.s (6.19) and Eq. (6.14) also the CF can be reconstructed.

In order to obtain the solution of the integral in Eq. (6.27), the expanded state variable space and the relative complex modal transformation described in the previous Chapter can be useful. Indeed, by the state variable expansion and the modal transformation in Eq. (5.57) the response process can be write as follow:

$$X(t) = \sum_{j=1}^{n} \psi_{1j} Y_j(t), \qquad j = 1, 2, \ldots n, \tag{6.28}$$

in which n is the number of the state variable, which depends on the order α that allows to rewrite the system as sequential linear differential equation, ψ_{1j} is the first term of the j^{th} eigenvector, and $Y_j(t)$ is the stochastic response of the half fractional oscillator in the complex modal domain. The evaluation of

the PSD of the process represented by the Eq. (6.28) yields

$$\begin{aligned} S_X(\omega) &= \lim_{\mathrm{T}\to\infty} \frac{1}{2\pi\mathrm{T}} \mathrm{E}\left[X^*_{\mathcal{F}}(\omega,\mathrm{T}) X_{\mathcal{F}}(\omega,\mathrm{T})\right] \\ &= \sum_{j=1}^{n}\sum_{k=1}^{n} \psi^*_{1j}\psi_{1k} \lim_{\mathrm{T}\to\infty} \frac{1}{2\pi\mathrm{T}} \mathrm{E}\left[Y^*_{\mathcal{F}j}(\omega,\mathrm{T}) Y_{\mathcal{F}k}(\omega,\mathrm{T})\right], \end{aligned} \tag{6.29}$$

in the Eq. (6.29) the PSD and the CPSD of the n half fractional oscillators in the complex modal space are involved. Then, by introducing the following generic CPSD of the processes $Y_j(t)$

$$S_{Y_jY_k}(\omega) = \frac{\psi^*_{1j}\psi_{1k} S_0}{\left[u^*_j(-i\omega)^\alpha + v^*_j\right]\left[u_k(i\omega)^\alpha + v_k\right]}, \tag{6.30}$$

where the apex * denotes the complex conjugate, u_l and v_l with $l = j,k$ denote the diagonal terms of the matrices $\mathbf{U_D}$ and $\mathbf{V_D}$, respectively (see Eq.s (5.39)). By placing the PSD and CPSD, defined in Eq. (6.30), into the Eq. (6.29), the following relation is directly obtained

$$\begin{aligned} S_X(\omega) &= \sum_{j=1}^{n}\sum_{k=1}^{n} \psi^*_{1j}\psi_{1k} S_{Y_jY_k}(\omega) \\ &= S_0 \sum_{j=1}^{n}\sum_{k=1}^{n} \frac{\left(\psi^*_{1j}\psi_{1k}\right)^2}{\left[u^*_j(-i\omega)^\alpha + v^*_j\right]\left[u_k(i\omega)^\alpha + v_k\right]}, \end{aligned} \tag{6.31}$$

the Eq. (6.31) permits to obtain the correlation function of output process of fractional oscillator $X(t)$ as a linear combination of a certain number of output responses of a set of half fractional oscillators. Moreover, the Eq. (6.31) allows to evaluate the SM in Eq. (6.27), indeed the spectral moments of the PSD and CPSD of the half oscillators can be evaluated in closed form, then

$$\begin{aligned} \Lambda_X(-\gamma) &= \sum_{j=1}^{n}\sum_{k=1}^{n} \psi^*_{1j}\psi_{1k} \int_0^\infty S_{Y_jY_k}(\omega)\omega^{-\gamma} d\omega \\ &= S_0 \sum_{j=1}^{n}\sum_{k=1}^{n} \left(\psi^*_{1j}\psi_{1k}\right)^2 \int_0^\infty \frac{\omega^{-\gamma} d\omega}{\left[u^*_j(-i\omega)^\alpha + v^*_j\right]\left[u_k(i\omega)^\alpha + v_k\right]} \\ &= \sum_{j=1}^{n}\sum_{k=1}^{n} \psi^*_{1j}\psi_{1k}\Lambda_{Y_jY_k}(-\gamma). \end{aligned} \tag{6.32}$$

SMs of the fractional half oscillators in Eq. (6.32) depend on the order α, such fractional order permits to rewrite the system as fractional sequential differential equation. Some exact expressions of $\Lambda_{Y_jY_k}(-\gamma)$ for different value of α are reported in the section C.2. After the definition of the SM by the Eq. (6.32) is possible to obtain also the CFM by using the relation in Eq.s (6.19):

$$\begin{aligned} \mathrm{M}_X(\gamma-1) &= \frac{\Gamma(\gamma)}{\pi}\cos\left(\frac{\gamma\pi}{2}\right)\sum_{j=1}^{n}\sum_{k=1}^{n}\psi_{1j}^{*}\psi_{1k}\int_0^{\infty}S_{Y_jY_k}(\omega)\omega^{-\gamma}d\omega \\ &= \frac{\Gamma(\gamma)}{\pi}\cos\left(\frac{\gamma\pi}{2}\right)\sum_{j=1}^{n}\sum_{k=1}^{n}\psi_{1j}^{*}\psi_{1k}\Lambda_{Y_jY_k}(-\gamma). \end{aligned} \tag{6.33}$$

After that, both CF and PSD of the fractional oscillator response process can be handled by the Eq. (6.14) and Eq. (6.25) respectively. In this way, another stochastic characterization of the response of the fractional system is obtained by using an eigenvector expansion in the state variable space and by the introduced concepts about the complex spectral moments.

Obviously, the presented method to evaluate in closed form the spectral moments can be extended to the multi-degree-of-freedom system by using the same concepts in the previous Chapter. The next section shows some numerical examples of the method for the characterization of the response output of single and multi-degree-of-freedom system with fractional derivative driven by Gaussian white noise.

6.5 Numerical examples

The examples in the previous Chapter have shown the way to carry out the stochastic dynamical analysis of the fractional viscoelastic systems with the aid of state variable transformation and Monte Carlo method. In this section a new stochastic characterization of the output response processes of fractional system is presented. In particular, the expanded state variable analysis is used in conjunction with the complex spectral moments in order to find the correlation and the cross-correlation of the response processes of fractional SDOF and MDOF.

6.5.1 Correlation function of fractional oscillator with $\beta = 1/2$

Consider the stochastic fractional differential equation in Eq. (6.26) in which the fractional order is $\beta = 1/2$. In this case the PSD is known in closed form

and it can be obtained from the Eq. (5.59) as follow

$$S_X(\omega) = \frac{S_0}{|-m\omega^2 + c_{1/2}\sqrt{i\omega} + k|^2}, \tag{6.34}$$

while the CF is unknown and can be obtained by the inverse fast Fourier transform or by Monte Carlo simulation. Another way to obtain the CF is by using the method in the previous section, that is, the complex spectral moment representation in conjunction with the fractional state variable analysis.

By using the state variable analysis described in the previous Chapter the order α which permits to obtain the sequential differential system in Eq. (5.34) is $\alpha = \beta = 1/2$. The minimum number of state variable is $n = 4$, and vector $\mathbf{z}$ is

$$\mathbf{z}^{\mathrm{T}}(t) = \left[X(t),\ \left(\mathrm{D}^{(0.5)}X\right)(t),\ \dot{X}(t),\ \left(\mathrm{D}^{(1.5)}X\right)(t)\right], \tag{6.35}$$

the matrices $\mathbf{A}$ and $\mathbf{B}$ are the same in the Eq. (5.52), and the matrix $\mathbf{\Psi}$ is still the same of the previous case, and it represents the matrix of the complex eigenvector of the following matrix

$$\boldsymbol{D} = \mathbf{A}^{-1}\mathbf{B} = \begin{bmatrix} 0 & -1 & 0 & 0 \\ 0 & 0 & -1 & 0 \\ 0 & 0 & 0 & -1 \\ 1/k & 1/c_\beta & 0 & 0 \end{bmatrix}. \tag{6.36}$$

The knowledge of the eigenvectors matrix $\mathbf{\Psi}$ allows to perform the modal transformation in Eq. (5.40) and to obtain the diagonal matrices $\mathbf{U_D}$ and $\mathbf{V_D}$. In this way is possible to rewrite the PSD by the Eq. (6.31) in terms of $Y_j(t)$ as follows:

$$S_X(\omega) = \sum_{j=1}^{4}\sum_{k=1}^{4} \psi_{1j}^*\psi_{1k}S_{Y_jY_k}(\omega) = \sum_{j=1}^{4}\sum_{k=1}^{4} \frac{S_0\left(\psi_{1j}^*\psi_{1k}\right)^2}{\left[u_j^*\sqrt{-i\omega} + v_j^*\right]\left[u_k\sqrt{i\omega} + v_k\right]}, \tag{6.37}$$

and then the spectral moments $\Lambda(-\gamma)$ can be evaluated as

$$\Lambda_X(-\gamma) = \sum_{j=1}^{4}\sum_{k=1}^{4} \psi_{1j}^*\psi_{1k}\Lambda_{Y_jY_k}(-\gamma), \tag{6.38}$$

where, in this case, $\Lambda_{Y_jY_k}(-\gamma)$ is

$$\Lambda_{Y_jY_k}(-\gamma) = S_0\psi_{1j}^*\psi_{1k}\int_0^\infty \frac{\omega^{-\gamma}d\omega}{\left[u_j^*\sqrt{-i\omega}+v_j^*\right]\left[u_k\sqrt{i\omega}+v_k\right]}$$
$$= \frac{S_0\psi_{1j}^*\psi_{1k}2\pi\csc(2\pi\gamma)}{u_j^*u_k\left(v_j^*u_k+iu_j^*v_k\right)}\left\{-v_j^*u_k\left[\frac{(-1)^{\frac{3}{4}}u_j^*}{v_j^*}\right]^{2\gamma}+iu_j^*v_k\left[\frac{(-1)^{\frac{1}{4}}u_k}{v_k}\right]^{2\gamma}\right\} \tag{6.39}$$

where $\gamma = \rho + i\eta$ with $\rho \in (0,1)$. Placing the Eq. (6.39) into the Eq. (6.25) is possible to obtain the PSD in approximate form:

$$S_X(\omega) \approx \frac{|\omega|^{\rho-1}\Delta\eta}{4\pi^2}\sum_{k=-\mathrm{m}}^{\mathrm{m}}\Lambda_X(-\gamma_k)|\omega|^{ik\Delta\eta}. \tag{6.40}$$

In the Figure 6.1 the comparison between the exact PSD of the system and the approximated one obtained by Eq. (6.40) is shown. Such Figure shows the perfect agreement between the exact and approximated solution. For this example the chosen parameters are: $m = k = 1$, $c_{1/2} = 1/4$, and $S_0 = 1$. The discretized parameters are $\rho = 1/8$, $\Delta\eta = 1/5$, and $\mathrm{m} = 500$.

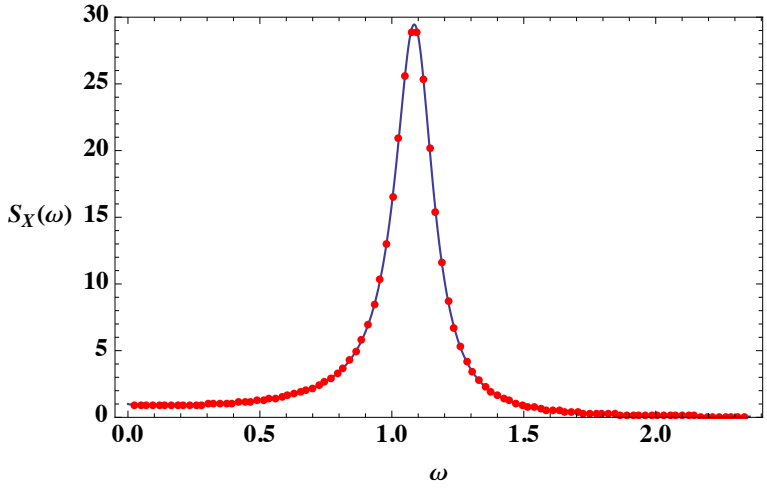

Figure 6.1: Exact (continuous line) and approximated PSD (dotted line).

Moreover, from the knowledge of SMs in Eq. (6.38) is possible to obtain the CFMs by Eq. (6.33), then by using the Eq. (6.14) also the CF of $X(t)$ is given as

$$R_X(\tau) \approx \frac{|\tau|^{-\rho}\Delta\eta}{2\pi^2} \sum_{k=-\mathrm{m}}^{\mathrm{m}} \Lambda_X(-\gamma_k)\Gamma(\gamma_k)\cos\left(\frac{\gamma_k\pi}{2}\right)|\tau|^{-ik\Delta\eta}. \tag{6.41}$$

The approximated CF $R_X(\tau)$ by complex spectral moments is shown in Fig-

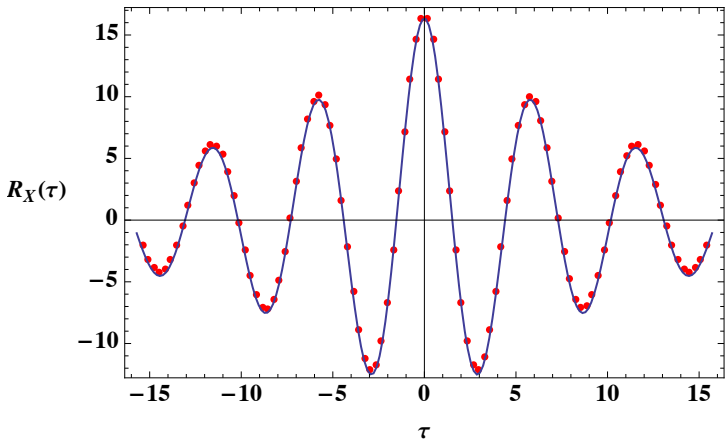

Figure 6.2: Approximated CF by CSMs.

ure 6.2, in which the same parameters for the discretization of the PSD are used. In particular, such Figure shows the comparison between the solution obtained by the Eq. (6.2) in dotted line, and the solution obtained by discretized inverse Fourier transform (see the Appendix B) in continuous line.

Note that the limit for $\gamma \to 0$ of the complex spectral moments is related to the variances of the process, indeed the following relation holds

$$2\lim_{\gamma\to 0}\Lambda_X(-\gamma) = \sigma_X^2 = \int_{-\infty}^{\infty} S_X(\omega)d\omega = R_X(0), \tag{6.42}$$

by the numerical integration of the PSD or by such limit the results is the same, and for this particular case $\sigma_X^2 = 16.3558$.

6.5.2 Two-degree-of-freedom system under white noise

If a multi-degree-of-freedom system is considered, the previous concepts are still valid and the method is the same. Consider two coupled fractional linear

oscillators as the system in Figure 5.7, driven by a zero-mean Gaussian white noise process $W(t)$. The equation of motion in matrix form is

$$\mathbf{M}\ddot{\boldsymbol{x}}(t) + \sum_{j=1}^{l} \mathbf{C}_j D^{\beta_j} \boldsymbol{x}(t) + \mathbf{K}\boldsymbol{x}(t) = \mathbf{f}(t), \tag{6.43}$$

where the vector of the displacements $\boldsymbol{x}(t)$ contains the two response processes as follows

$$\boldsymbol{x}^T(t) = [X_1(t) \;\; X_2(t)]\,. \tag{6.44}$$

Assuming that the forced vector is $\mathbf{f}^T(t) = [0 \;\; W(t)]$, and its spectral matrix, denoted by $\mathbf{S}_f(\omega)$, is the same in Eq. (5.68). In terms of response $X_j(t)$ the spectral matrix is defined as in Eq. (5.70), that is,

$$\mathbf{S}_X(\omega) = \mathbf{H}^*(\omega)\mathbf{S}_f(\omega)\mathbf{H}^{\mathrm{T}}(\omega) = \begin{bmatrix} S_{X_1}(\omega) & S_{X_1X_2}(\omega) \\ S_{X_2X_1}(\omega) & S_{X_2}(\omega) \end{bmatrix}, \tag{6.45}$$

where two terms in the diagonal are the PSD of the process $X_1(t)$ and $X_2(t)$, respectively; whereas the other terms $S_{X_1X_2} = S^*_{X_2X_1}$ are the CPSD of the two process. Also in this case the PSD and CPSD are known in closed form but the CF and CCF can be evaluated in approximated form by the inverse fast Fourier transform or by Monte Carlo simulation. As was done in the previous case, another way to represent both PSD and CF (and the crossed counterparts) is by complex spectral moments. Also in this case the CSMs of the four terms in the matrix $\mathbf{S}_X(\omega)$ cannot be directly evaluated by the Eq. (6.18), but it is necessary to solve this problem by using the state variable domain and the complex modal transformation. In this way is possible to evaluate the four complex spectral moments of the two PSD and the two CPSD. In order to do this, assuming that the involved orders are $\beta_1 = 1$ and $\beta_2 = 1/2$, the Eq. (6.46) can be rewritten in sequential form

$$\sum_{j=1}^{4} \mathbf{C}_j D^{j\frac{1}{2}} \boldsymbol{x}(t) + \mathbf{K}\boldsymbol{x}(t) = \mathbf{f}(t), \tag{6.46}$$

where the involved matrices are $\mathbf{C}_3 = \mathbf{0}$,

$$\mathbf{K} = \begin{bmatrix} k_1 + k_2 & -k_2 \\ -k_2 & k_2 \end{bmatrix}, \mathbf{C}_1 = \begin{bmatrix} c_{1/2} & 0 \\ 0 & 0 \end{bmatrix}, \mathbf{C}_2 = \begin{bmatrix} c_1 & -c_1 \\ -c_1 & c_1 \end{bmatrix}, \mathbf{C}_4 = \begin{bmatrix} m_1 & 0 \\ 0 & m_2 \end{bmatrix}. \tag{6.47}$$

By the aforementioned assumptions the state variable vector is

$$\begin{aligned}\mathbf{z}^{\mathrm{T}}(t) &= \left[z_1^{\mathrm{T}}(t)\, z_2^{\mathrm{T}}(t)\, z_3^{\mathrm{T}}(t)\, z_4^{\mathrm{T}}(t)\right] = \left[\boldsymbol{x}^{\mathrm{T}}(t)\, D^{\frac{1}{2}}\boldsymbol{x}^{\mathrm{T}}(t)\, D^{1}\boldsymbol{x}^{\mathrm{T}}(t)\, D^{\frac{3}{2}}\boldsymbol{x}^{\mathrm{T}}(t)\right] \\ &= [Z_1(t)\, Z_2(t)\, Z_3(t)\, Z_4(t)\, Z_5(t)\, Z_6(t)\, Z_7(t)\, Z_8(t)\,] \\ &= \left[X_1(t)\, X_2(t)\, X_1^{(0.5)}(t)\, X_2^{(0.5)}(t)\, \dot{X}_1(t)\, \dot{X}_2(t)\, X_1^{(1.5)}(t)\, X_2^{(1.5)}(t)\right],\end{aligned} \tag{6.48}$$

then the number of state variable in this case is still $n = 4$ but the dimension of the vector $\mathbf{z}(t)$ is $r \times n = 8$, where $r = 2$ is the number of degrees of freedom of the system. In terms of state variables the spectral matrix $\mathbf{S}_{\mathbf{z}}(\omega)$ contains more terms than $\mathbf{S}_X(\omega)$, indeed, by virtue of Eq. (6.48):

$$\mathbf{S}_{\mathbf{z}}(\omega) = \begin{bmatrix} \mathbf{S}_X(\omega) & \mathbf{S}_{X X^{(\alpha)}}(\omega) & \mathbf{S}_{X\dot{X}}(\omega) & \mathbf{S}_{X X^{(2\alpha)}}(\omega) \\ \mathbf{S}_{X^{(\alpha)} X}(\omega) & \mathbf{S}_{X^{(\alpha)}}(\omega) & \mathbf{S}_{X^{(\alpha)}\dot{X}}(\omega) & \mathbf{S}_{X^{(\alpha)} X^{(2\alpha)}}(\omega) \\ \mathbf{S}_{\dot{X} X}(\omega) & \mathbf{S}_{\dot{X} X^{(\alpha)}}(\omega) & \mathbf{S}_{\dot{X}}(\omega) & \mathbf{S}_{\dot{X} X^{(2\alpha)}}(\omega) \\ \mathbf{S}_{X^{(2\alpha)} X}(\omega) & \mathbf{S}_{X^{(2\alpha)} X^{(\alpha)}}(\omega) & \mathbf{S}_{X^{(2\alpha)}\dot{X}}(\omega) & \mathbf{S}_{X^{(2\alpha)}}(\omega) \end{bmatrix}, \tag{6.49}$$

where each one block has dimension $r = 4$, the dimension of the matrix is $n \times r = 16$, and the first submatrix is $\mathbf{S}_X(\omega)$. In terms of modal coordinates $Y_j(t)$ the matrix in Eq. (6.49) can be rewritten as

$$\begin{aligned}\mathbf{S}_{\mathbf{z}}(\omega) &= \lim_{\mathrm{T}\to\infty} \frac{1}{2\pi \mathrm{T}} \mathrm{E}\left[\mathbf{Z}_{\mathcal{F}}^{*}(\omega)\mathbf{Z}_{\mathcal{F}}^{T}(\omega)\right] \\ &= \lim_{\mathrm{T}\to\infty} \frac{1}{2\pi \mathrm{T}} \mathrm{E}\left[\boldsymbol{\Psi}^{*}\mathbf{Y}_{\mathcal{F}}^{*}(\omega)\left(\boldsymbol{\Psi}\mathbf{Y}_{\mathcal{F}}(\omega)\right)^{T}\right] \\ &= \lim_{\mathrm{T}\to\infty} \frac{1}{2\pi \mathrm{T}} \mathrm{E}\left[\boldsymbol{\Psi}^{*}\mathbf{Y}_{\mathcal{F}}^{*}(\omega)\mathbf{Y}_{\mathcal{F}}^{T}(\omega)\boldsymbol{\Psi}^{T}\right] \\ &= \boldsymbol{\Psi}^{*} \lim_{\mathrm{T}\to\infty} \frac{1}{2\pi \mathrm{T}} \mathrm{E}\left[\mathbf{Y}_{\mathcal{F}}^{*}(\omega)\mathbf{Y}_{\mathcal{F}}^{T}(\omega)\right] \boldsymbol{\Psi}^{T} \\ &= \boldsymbol{\Psi}^{*}\mathbf{S}_{\mathbf{y}}(\omega)\boldsymbol{\Psi}^{T}\end{aligned} \tag{6.50}$$

where $\mathbf{S}_{\mathbf{y}}(\omega)$ is the spectral matrix of the response process $Y_j(t)$ of the set of $n \times r = 16$ half fractional oscillators in the complex modal space. Also in this case the complex spectral moments of any terms of the matrix $\mathbf{S}_{\mathbf{y}}(\omega)$ can be evaluated in closed form while the complex spectral moments of terms of the matrix $\mathbf{S}_X(\omega)$ are unknown.

In order to find the matrix $\boldsymbol{\Psi}$ in Eq. (6.50) it is necessary to find the dynamical matrix $\boldsymbol{D}$ in Eq. (6.36). Taking into account the Eq.s (5.38) the matrices $\mathbf{A}$

and $\mathbf{B}$ become

$$\mathbf{A} = \begin{bmatrix} \mathbf{C}_1 & \mathbf{C}_2 & \mathbf{0} & \mathbf{M} \\ \mathbf{C}_2 & \mathbf{0} & \mathbf{M} & \mathbf{0} \\ \mathbf{0} & \mathbf{M} & \mathbf{0} & \mathbf{0} \\ \mathbf{M} & \mathbf{0} & \mathbf{0} & \mathbf{0} \end{bmatrix}, \quad \mathbf{B} = \begin{bmatrix} \mathbf{K} & \mathbf{0} & \mathbf{0} & \mathbf{0} \\ \mathbf{0} & -\mathbf{C}_2 & \mathbf{0} & -\mathbf{M} \\ \mathbf{0} & \mathbf{0} & -\mathbf{M} & \mathbf{0} \\ \mathbf{0} & -\mathbf{M} & \mathbf{0} & \mathbf{0} \end{bmatrix}, \tag{6.51}$$

in this way, the system in the state variable domain as that one in Eq. (5.37) is obtained. The matrix $\mathbf{\Psi}$ has to contain the eigenvectors of the following matrices:

$$\boldsymbol{D} = \mathbf{A}^{-1}\mathbf{B} = \begin{bmatrix} 0 & 0 & -1 & 0 & 0 & 0 & 0 & 0 \\ 0 & 0 & 0 & -1 & 0 & 0 & 0 & 0 \\ 0 & 0 & 0 & 0 & -1 & 0 & 0 & 0 \\ 0 & 0 & 0 & 0 & 0 & -1 & 0 & 0 \\ 0 & 0 & 0 & 0 & 0 & 0 & -1 & 0 \\ 0 & 0 & 0 & 0 & 0 & 0 & 0 & -1 \\ \frac{k_1+k_2}{m_1} & -\frac{k_2}{m_1} & \frac{c_{1/2}}{m_1} & 0 & \frac{c_1}{m_1} & -\frac{c_1}{m_1} & 0 & 0 \\ -\frac{k_2}{m_2} & \frac{k_2}{m_2} & 0 & 0 & -\frac{c_1}{m_2} & \frac{c_1}{m_2} & 0 & 0 \end{bmatrix}. \tag{6.52}$$

By that modal transformation a set of uncoupled differential equations with complex coefficients of the type in Eq. (5.53) is obtained and the spectral matrix in terms of output of fractional half oscillators in Eq. (6.50) is given. Now the spectral matrix of the processes $Y_j(t)$ can be evaluated, in this case, to complete describe the system it is necessary to define the matrix of complex spectral moments $\mathbf{\Lambda}_{\mathbf{y}}(-\gamma)$. The complex spectral moments of the state variables can also be evaluated as

$$\mathbf{\Lambda}_{\mathbf{z}}(-\gamma) = \mathbf{\Psi}^* \mathbf{\Lambda}_{\mathbf{y}}(-\gamma) \mathbf{\Psi}^T, \tag{6.53}$$

this matrix has the same dimension of $\mathbf{S}_{\mathbf{z}}(\omega)$. All terms of the matrix $\mathbf{\Lambda}_{\mathbf{y}}(-\gamma)$ are defined by the same expression in the previous case (see Eq. (6.39)). In order to fully characterize the two response processes it is needed to evaluate the first block of the matrix $\mathbf{S}_{\mathbf{z}}(\omega)$, that contains the matrix $\mathbf{S}_X$ in Eq. (6.45). The characterization in terms of complex spectral moments is complete given by the first block of $\mathbf{\Lambda}_{\mathbf{z}}(-\gamma)$. That is,

$$\mathbf{\Lambda}_X(-\gamma) = \begin{bmatrix} \Lambda_{X_1}(-\gamma) & \Lambda_{X_1X_2}(-\gamma) \\ \Lambda_{X_2X_1}(-\gamma) & \Lambda_{X_2}(-\gamma) \end{bmatrix}. \tag{6.54}$$

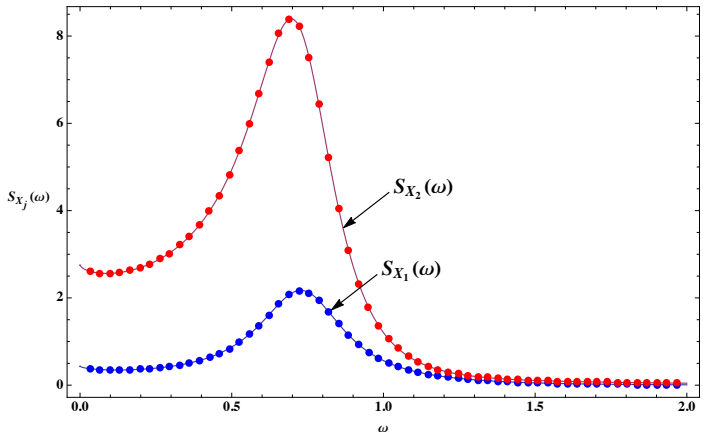

Figure 6.3: PSDs of the response $X_1(t)$ and $X_2(t)$, exact (continuous line) and approximate solution (dotted line).

This four terms of modal coordinates are

$$\Lambda_{X_l X_m}(-\gamma) = \sum_{j=1}^{8}\sum_{k=1}^{8} \psi^*_{lj}\psi_{mk}\Lambda_{Y_j Y_k}(-\gamma)$$
$$= S_0 \sum_{j=1}^{8}\sum_{k=1}^{8} \psi^*_{lj}\psi_{mk}\psi^*_{2j}\psi_{2k}\int_0^\infty \frac{\omega^{-\gamma}d\omega}{\left[u^*_j\sqrt{-i\omega}+v^*_j\right]\left[u_k\sqrt{i\omega}+v_k\right]}, \tag{6.55}$$

where the solution of the integral is the same in Eq. (6.39). Such entities in the Eq. (6.55) are able to represent PSD, and CF by the previous expressions. In particular with the aid of the Eq.s (6.40) and (6.41) the PSDs and CFs can be readily obtained.

Assume as parameters of the system $S_0 = 1$, $k_1 = 3/2$, $k_2 = 1$, $c_1 =$, $c_2 = 1.1$, $m_1 = 2$, $m_2 = 1$, and as parameters of the discretization $\Delta\eta = 1/4$, $\rho = 1/8$ and m $= 100$. The PSDs of the two displacements $X_1(t)$ and $X_2(t)$ are depicted in Figure 6.3. In particular, the continuous lines denote the exact PSDs, the dotted lines represent the approximate solutions obtained by the Eq. (6.40). By using the complex spectral moments also the CPSD $S_{X_1X_2}(\omega)$ can be readily obtained with the evaluation of the complex spectral moments $\Lambda_{X_1X_2}(-\gamma)$ and with the aid of the Eq. (6.22). The real and imaginary part of the CPSD are shown in the Figure 6.4. Also in this case the continuous lines

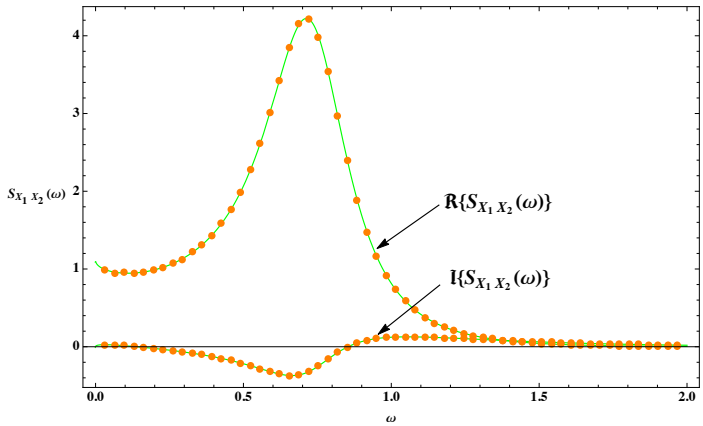

Figure 6.4: Real and imaginary part of CPSD of the response $X_1(t)$ and $X_2(t)$, exact (continuous lines) and approximate solution (dotted lines).

represent the exact solutions, and the dotted lines represent the approximate representations with the complex spectral moments.

As in the previous case, the complex spectral moments permit to obtain also the correlation function. In order to do this, it is necessary to use the Eq. (6.19) to obtain the complex fractional moments of the two correlation functions $R_{X_1}(\tau)$ and $R_{X_2}(\tau)$. In this way also the CFs can be evaluated. The Figure 6.5 and Figure 6.6 show the comparison between the complex fractional moments representation of the correlation functions, obtained by Eq (6.24), and the solution obtained with the discretized inverse Fourier transform.

6.6 Conclusions

A new way to fully represent the CF, CCF, PSD and CPSD by CFMs and/or by CSMs has been pursued in this Chapter. It has been shown how it is possible to evaluate this complex entities starting from the knowledge of the correlation and cross-correlation (CFMs) or by the given PSD or CPSD (CSMs). These entities are strictly related to the Mellin transform and the knowledge of the CFMs permits to restore the correlation and the cross-correlation by the inverse Mellin transform. On the other hand, the inverse Mellin transform of the CSMs yields the CPSD.

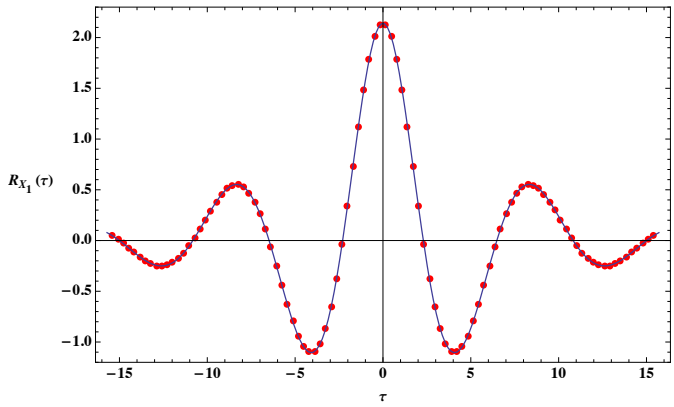

Figure 6.5: CF of the response $X_1(t)$, discretized inverse Fourier transform (continuous lines) and CFMs representation (dotted lines).

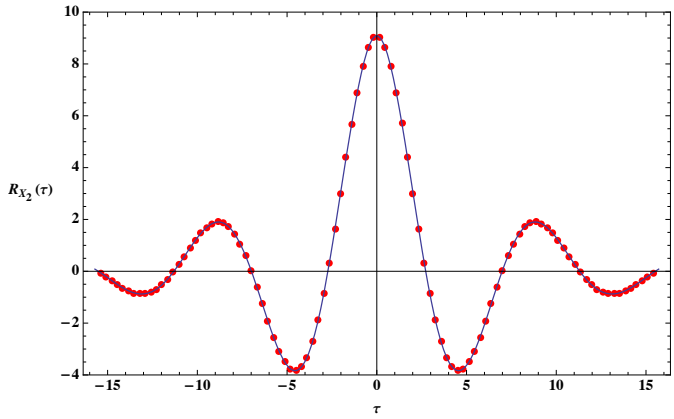

Figure 6.6: CF of the response $X_2(t)$, discretized Fourier transform (continuous lines) and CFMs representation (dotted lines).

It has been shown that both kinds of fractional quantities, CFMs and CSMs, are related by a simple relation obtained by using the properties of the Fourier transform. In other word, the CSMs are nothing else that the spectral counterparts of the CFMs. It means that just the knowledge of one of the two kinds of moments permits to restore the other one and that allows to fully represent both cross-correlation function and CPSD. Then, it is independent the choice to evaluate the CFMs or the CSMs because both quantities have all information in time and in frequency domain. This is a very important result because in many physics and engineering problems is known the CPSD but it is unknown the cross-correlation function and the presented method permits to independently operate.

Many properties in this Chapter have been obtained thanks to the relationships by the Mellin transform and the fractional operators. In particular these relations permit to interpret the discretized inverse Mellin transform as a truncated complex fractional Taylor series. Moreover, this kind of series does not diverge, since the involved quantities have complex fractional order which real part is fixed and just imaginary part runs.

Particular attention has been devoted to the case of fractional systems. Indeed, by the CSMs in conjunction with the expanded state variable analysis, described in the previous Chapter, the characterization of the output response of fractional system under Gaussian white noise has been found. In particular two examples have been reported, the first one is the characterization of the stochastic response of the fractional oscillators, the second example the characterization of two-degree-of-freedom forced by white noise has been considered. The method can be used also to characterize other stochastic process, like the response of classic linear oscillators [5], ocean waves [25], earthquake processes, and wind velocity field [5].

Concluding remarks

This thesis contains some new methods to perform the stochastic dynamic analysis of structures with viscoelastic constitutive law. After the preliminary introduction to this kind of mechanical problem, in the first part of this manuscript, some concepts about the mathematical tools have been provided. In particular, the main properties of the fractional calculus and the integral transforms have been reported.

The concepts inherent the viscoelastic stress-strain relation have been also discussed, and the reasons about the choice of the fractional viscoelastic model for the characterization of the real mechanical behavior of the building materials have been presented. Subsequently, the problems that this choice implies in the global models in terms of displacement-load relation have been introduced. In this regard, some new methods have been developed to perform the stochastic analysis of continuous and discrete fractional viscoelastic systems correctly.

In particular, the analysis of continuous fractional viscoelastic Euler-Bernoulli beam has been pursued, performing the study either in frequency and in time domain. The viscoelastic behavior has been taken into account by using the fractional Kelvin-Voigt model. It is a proper model that is able to capture the viscoelasticity phenomena of a plethora of materials. The fractional stress-strain relation has led to a fractional partial differential equation that rules the motion of the continuous viscoelastic beam. To perform the stochastic analysis of such system a proper eigenanalysis and the Monte Carlo method have been used. Some numerical results have been obtained considering a cantilever beam driven by stochastic loads.

As discrete systems, the fractional oscillator and the fractional multi-degree-of freedom system have been considered. The analysis of this kind of dynamical systems leads to have a set of coupled fractional differential equations that govern the motion. It has been pointed out that this kind of prob-

lem is more complex to solve vis-a-vis the analysis of multi-degree-of-freedom system with integer order derivatives. The analysis has been based on a novel approach using an augmented state variables transformation. The method, based on complex modal analysis in the state variable domain, is applicable if the involved fractional terms have rational order. This assumption is necessary since only in this case it is possible to find an appropriate state variables vector. Note, however, that for engineering applications all real orders can be reasonably approximated by rational orders. By the proposed method the set of coupled fractional differential equations has been decoupled in a proper fractional state variable domain. This transformation has led to a new set of fractional equations which are uncoupled and more convenient to solve. Therefore, a drastic reduction of the computational effort is achieved.

The latter part of the manuscript contains a new characterization of the dynamical response processes of the fractional viscoelastic systems under a stochastic point of view. In particular, a way to fully represent the correlation function and power spectral density (and their crossed counterparts) by the complex spectral moments (CSMs) and/or by the complex fractional moments (CFMs) has been pursued. The way to characterize the stochastic process with the aid of these complex entities it has been shown. Further, the relations between the CFMs and/or the CSMs, the Mellin transform and the fractional Riesz integrals have been introduced to provide some useful consequences. In this manner, it has been shown that the CSMs are nothing else that the spectral counterparts of the CFMs, and they are related by a simple relation. This implies that the choice is independent for evaluating CFMs or CSMs because both quantities have all informations in time and in frequency domain. Some properties of CFMs and CSMs have been obtained thanks to the relationships by the Mellin transform and the fractional operators. In particular, these relation permit to interpret the discretized inverse Mellin transform as a truncated complex fractional Taylor series. This kind of series does not diverge, since the involved quantities have complex fractional order which real part is fixed and just imaginary part runs.

This elegant stochastic characterization has been applied to the case of fractional systems forced by Gaussian white noise. Usually, the normal stationary processes are characterized by the power spectral density, commonly known in closed form, but the correlation can be evaluated only in approximated form by the inverse fast Fourier transform. Using the CSMs in conjunction with the expanded state variable analysis, described in the previous part, the characterization of the output response of fractional system under Gaus-

sian white noise has been found. In this way it has been possible to obtain both the power spectral density and the correlation of the response process of the fractional system. The stochastic responses of single fractional oscillator and multi-degree-of-freedom system endowed with fractional viscoelastic devices have been considered in the numerical examples, in which the capabilities of the fractional calculus have been widely shown.

Appendix A

Tables of fractional derivatives

Some Riemann-Liouville fractional derivatives of common functions are reported below. The chosen differentiation orders are reals $\alpha \in \mathbb{R}$, then the corresponding fractional integral can be readily found placing $-\alpha$ as order in the shown results.

A.1 Fractional operators with lower bound $a = -\infty$

$f(t)$	$\left(D_{+}^{\alpha} f\right)(t), \quad (t > 0, \ \alpha \in \mathbb{R})$
$U(t-b)$	$\begin{cases} \frac{(t-b)^{-\alpha}}{\Gamma(1-\alpha)}, & (t > b) \\ 0, & (0 \leq t \leq b) \end{cases}$
$U(t-b)f(t)$	$\begin{cases} \left(D_{b^{+}}^{\alpha} f\right)(t), & (t > b) \\ 0, & (t \leq b) \end{cases}$
$e^{\lambda t}$	$\lambda^{\alpha} e^{\alpha t} \quad (\lambda > 0)$
$e^{\lambda t+\mu}$	$\lambda^{\alpha} e^{\alpha t+\mu} \quad (\lambda > 0)$
$\sin(\lambda t)$	$\lambda^{\alpha} \sin\left(\lambda t + \frac{\pi\alpha}{2}\right) \qquad (\lambda > 0, \ \alpha > -1)$

$\cos(\lambda t)$	$\lambda^{\alpha}\cos\left(\lambda t+\frac{\pi\alpha}{2}\right) \qquad (\lambda>0,\ \alpha>-1)$

A.2 Fractional derivatives with lower bound $a=0$

$f(t)$	$\left(\mathrm{D}_{0+}^{\alpha}f\right)(t), \quad (t>0,\ \alpha\in\mathbb{R})$
$U(t)$	$\frac{t^{-\alpha}}{\Gamma(1-\alpha)}$
$U(t-b)$	$\begin{cases}\frac{(t-b)^{-\alpha}}{\Gamma(1-\alpha)}, & (t>b)\\ 0, & (0\le t\le b)\end{cases}$
$U(t-b)f(t)$	$\begin{cases}{}_{b}\mathrm{D}_{t}^{\alpha}f(t), & (t>b)\\ 0, & (0\le t\le b)\end{cases}$
$\delta(t)$	$\frac{t^{-\alpha-1}}{\Gamma(-\alpha)}$
t^{η}	$\frac{\Gamma(\eta+1)}{\Gamma(\eta+1-\alpha)}t^{\eta+\alpha} \qquad (\eta>-1)$
$e^{\lambda t}$	$t^{-\alpha}E_{1,1-\alpha}(\lambda t)$
$\cosh\left(\sqrt{\lambda t}\right)$	$t^{-\alpha}E_{2,1-\alpha}(\lambda t^{2})$
$\frac{\sinh\left(\sqrt{\lambda t}\right)}{\sqrt{\lambda t}}$	$t^{1-\alpha}E_{2,2-\alpha}(\lambda t^{2})$
$\ln(t)$	$\frac{t^{-\alpha}}{\Gamma(1-\alpha)}\big(\ln(t)+\psi(1)-\psi(1-\alpha)\big)$
$t^{\gamma-1}\ln(t)$	$\frac{t^{\gamma-\alpha-1}\Gamma(\gamma)}{\Gamma(\gamma-\alpha)}\big(\ln(t)+\psi(\gamma)-\psi(\gamma-\alpha)\big) \quad (\Re(\gamma)>0)$

Appendix B

Main used commands in Mathematica

This Appendix contains some commands of Wolfram Mathematica© used in this thesis. Other details about the special functions, the integral transform, and their commands can be found in [122–128].

B.1 Special functions

Euler gamma function

```
Gamma[x]
Gamma[x+I*y]
Plot[Gamma[x],{x,...,...}]
Plot3D[Abs[Gamma[x+I*y]],{x,...,...},{y,...,...}]
```

Mittag-Lefflerfunction

```
ML[z_]=MittagLefflerE[a,z]
ML[z_]=MittagLefflerE[a,b,z]
```

Wright function

```
W[z_]=Sum[(z^k)/(k!Gamma[a*k+b]),{k,0,Infinity}]
```

B.2 Bessel functions

First and second kind function

```
I[z_]=BesselJ[n, z]
Y[z_]=BesselY[n, z]
```

Modified first and second kind function

```
I[z_]=BesselI[n, z]
K[z_]=BesselK[n, z]
```

B.3 Integral transforms

B.3.1 Laplace transform and its inverse

```
F[s_]=LaplaceTransform[f[t],t,s]
f[t_]=InverseLaplaceTransform[F[s],s,t]
```

B.3.2 Fourier transform and its inverse

```
Fe[om_]=Sqrt[2*Pi]FourierTransform[f[t],t,om]
f[t_]=Sqrt[(2*Pi)^(-1)]InverseFourierTransform[Fe[om],om,t]
```

where `om` $= \omega$ denotes the frequency.

Discretized transform and its inverse

```
Fe[om_]=Dt*Sum[f[j*Dt](Cos[j*Dt*om]+I Sin[j*Dt*om]),{j,-m,m}]
f[t_]=Dom*Sum[F[j*om](Cos[j*Dom*Dt]-I Sin[j*Dom*Dt]),{j,-m,m}]
```

where `Dt` $= \Delta t$ and `Dom` $= \Delta\omega$ are the frequency and the time step, respectively.

B.3.3 Mellin transform and its inverse

```
Fm[s_]=Integrate[f(t)t^(s-1),{t,0,Infinity},
           Assumptions->-a<Re[s]<-b]
f[t_]=1/(2*Pi*I)*Integrate[Fm[s]t^(-s),
           {s,Re[s]-I*Infinity,Re[s]+I*Infinity}]
```

B.4 Fractional operators

B.4.1 Grünwald-Letnikov

```
Limit[(((t-a)/N)^alfa)/(Gamma[-alfa])*Sum[(Gamma[r-alfa])
          /(Gamma[r+1])*f[t-(r(t-a)/N)],{r,0,N-1}],N->Infinity]
```

B.4.2 Riemann-Liouville

```
1/(Gamma[-alfa])Integrate[(t-tau)^(-alfa-1)f[tau],{tau,a,t}]
```

B.4.3 Caputo

```
1/(Gamma[alfa-n])Integrate[(t-tau)^(-alfa+n-1)Dt[f[tau],
          {tau,n}],{tau,a,t}]
```

Appendix C

Complex fractional moments

C.1 Properties and relation with fractional calculus

In this Appendix the concepts about the connection between Mellin and Fourier transform and Riesz fractional integrals will be explained. First the Fourier transform of the Riesz integrals in Eqs. (2.54) and (2.54) are reported

$$\mathcal{F}\{(\mathbf{I}^{\gamma}f)(t);\omega\} = |\omega|^{-\gamma} f_{\mathcal{F}}(\omega), \tag{C.1}$$

$$\mathcal{F}\{(\mathbf{H}^{\gamma}f)(t);\omega\} = i\mathrm{sgn}(\omega)|\omega|^{-\gamma} f_{\mathcal{F}}(\omega) \tag{C.2}$$

Relationships (C.1) and (C.2) can be readily obtained by some simple algebraic manipulation. Now consider that $f(t)$ is a non-symmetric function, then it is possible to divide it into an even function $u(t) = (f(t) + f(-t))/2$ and an odd function $v(t) = (f(t) - f(-t))/2$; taking into account Eqs. (C.1) and (C.2) it is possible to write the Riesz fractional integrals of $f(t)$ in terms of inverse Fourier transform

$$\begin{aligned}(\mathbf{I}^{\gamma}f)(t) &= \frac{1}{2\pi}\int_{-\infty}^{\infty} |\omega|^{-\gamma} f_{\mathcal{F}}(\omega) e^{-i\omega t} d\omega \\ &= \frac{1}{2\pi}\int_{-\infty}^{\infty} |\omega|^{-\gamma} [u_{\mathcal{F}}(\omega)\cos(\omega t) - i\, v_{\mathcal{F}}(\omega)\sin(\omega t)] d\omega\end{aligned} \tag{C.3}$$

$$\begin{aligned}(\mathbf{H}^{\gamma}f)(t) &= \frac{i}{2\pi}\int_{-\infty}^{\infty} \mathrm{sgn}(\omega)|\omega|^{-\gamma} f_{\mathcal{F}}(\omega) e^{-i\omega t} d\omega \\ &= \frac{i}{2\pi}\int_{-\infty}^{\infty} |\omega|^{-\gamma}\mathrm{sgn}(\omega) [v_{\mathcal{F}}(\omega)\cos(\omega t) - i\, u_{\mathcal{F}}(\omega)\sin(\omega t)] d\omega\end{aligned} \tag{C.4}$$

where $u_{\mathcal{F}}(\omega)$ and $v_{\mathcal{F}}(\omega)$ are the Fourier transform of $u(t)$ and $v(t)$, respectively. Since $u(t)$ is a real even function $u_{\mathcal{F}}(\omega)$ is real and even, while since $v(t)$ is a real odd function $v_{\mathcal{F}}(\omega)$ is imaginary and odd. By particularizing Eqs. (C.3) and (C.4) for $t = 0$, one obtains

$$(\mathbf{I}^{\gamma} f)(0) = \frac{1}{2\pi} \int_{-\infty}^{\infty} |\omega|^{-\gamma} u_{\mathcal{F}}(\omega) d\omega = \frac{\Lambda_{u^+}(-\gamma)}{\pi} \tag{C.5}$$

$$(\mathbf{H}^{\gamma} f)(0) = \frac{i}{2\pi} \int_{-\infty}^{\infty} \mathrm{sgn}(\omega) |\omega|^{-\gamma} v_{\mathcal{F}}(\omega) d\omega = i \frac{\Lambda_{v^+}(-\gamma)}{\pi} \tag{C.6}$$

Eq. (C.5) shows that, since Riesz integral is a symmetric operator, it selects in $t = 0$ the real part$u_{\mathcal{F}}(\omega)$ of $f_{\mathcal{F}}(\omega)$ and we can interpret it as the moment of order $-\gamma$ of $u_{\mathcal{F}}(\omega)$, namely $\Lambda_{u^+}(-\gamma)$; analogously for the complementary Riesz integral, Eq. (C.6) show that it select only the imaginary part $v_{\mathcal{F}}(\omega)$ of $f_{\mathcal{F}}(\omega)$ and we can interpret it as the moment of order $-\gamma$ of $v_{\mathcal{F}}(\omega)$, namely $\Lambda_{v^+}(-\gamma)$. On the other hand from Eqs. (2.28) and (2.29)

$$(\mathbf{I}^{\gamma} f)(0) = \frac{1}{2\nu_c(\gamma)} \int_{-\infty}^{\infty} \frac{f(\bar{t})}{|\bar{t}|^{1-\gamma}} d\bar{t} = \frac{1}{\nu_c(\gamma)} \int_0^{\infty} \bar{t}^{\gamma-1} u(\bar{t}) d\bar{t} = \frac{\mathrm{M}_{u^+}(\gamma - 1)}{\nu_c(\gamma)}, \tag{C.7}$$

$$(\mathbf{H}^{\gamma} f)(0) = \frac{1}{2\nu_s(\gamma)} \int_{-\infty}^{\infty} \frac{f(\bar{t})\mathrm{sgn}(\bar{t})}{|\bar{t}|^{1-\gamma}} d\bar{t} = \frac{1}{\nu_s(\gamma)} \int_0^{\infty} \bar{t}^{\gamma-1} v(\bar{t}) d\bar{t} = \frac{\mathrm{M}_{v^+}(\gamma - 1)}{\nu_s(\gamma)}, \tag{C.8}$$

where $\nu_c(\gamma) = \Gamma(\gamma)\cos(\frac{\gamma\pi}{2})$ and $\nu_s(\gamma) = \Gamma(\gamma)\sin(\frac{\gamma\pi}{2})$. Eqs. (C.7) and (C.8) show that Riesz integrals in zero can be related to the Mellin transform of $u(t)$ and $v(t)$; Mellin transforms can be interpreted as moments of order $\gamma - 1$ of the even part $u(t)$ and odd part $v(t)$ of $f(t)$, namely $M_{u^+}(\gamma - 1)$ and $M_{v^+}(\gamma - 1)$, respectively. Then by comparison of Eqs. (C.5) and (C.6) with Eqs.(C.7) and (C.8), relationships (5.34) between moments of order $\gamma - 1$ of $f(t)$ and moments of order $-\gamma$ of its Fourier transform $f_{\mathcal{F}}(\omega)$ are readily found, and here are reported for reading simplicity

$$\begin{aligned} \mathrm{M}_u(\gamma - 1) &= \frac{\nu_c(\gamma)}{\pi} \Lambda_u(-\gamma), \\ \mathrm{M}_v(\gamma - 1) &= \frac{\nu_s(\gamma)}{\pi} \Lambda_v(-\gamma). \end{aligned} \tag{C.9}$$

C.2 Some exact CSMs for fractional half oscillators

As it is shown in the Chapter 6, the complex spectral moments of the response of a fractional oscillator forced by Gaussian white noise is obtained as a sum-

mation of a certain number of CSMs of the response of a set of half fractional oscillators in the complex modal space. The cross power spectral density of this kind of half oscillators is

$$S_{Y_jY_k} = \frac{S_0\psi^*_{1,j}\psi_{1,k}}{\left[u^*_j(-i\omega)^\alpha + v^*_j\right]\left[u_k(i\omega)^\alpha + v_k\right]}, \tag{C.10}$$

the corresponding CSM is defined as

$$\Lambda_{Y_jY_k} = \int_0^\infty S_{Y_jY_k}\omega^{-\gamma}d\omega = a\int_0^\infty \frac{\omega^{-\gamma}d\omega}{\left[u^*_j(-i\omega)^\alpha + v^*_j\right]\left[u_k(i\omega)^\alpha + v_k\right]}, \tag{C.11}$$

where $a = S_0\psi^*_{1,j}\psi_{1,k}$. Some analytical results of the CSMs for different values of the fractional order α are reported below:

$\alpha = 1/2$, $\Re(\gamma) \in (0,1)$

$$\Lambda_{Y_jY_k}(-\gamma) = \frac{a2\pi\csc(2\pi\gamma)}{u_kv^*_j + iu^*_jv_k}\left\{-\frac{v^*_j}{u^*_j}\left[\frac{(-1)^{\frac{3}{4}}u^*_j}{v^*_j}\right]^{2\gamma} + i\frac{v_k}{u_k}\left[\frac{(-1)^{\frac{1}{4}}u_k}{v_k}\right]^{2\gamma}\right\} \tag{C.12}$$

$\alpha = 1/4$, $\Re(\gamma) \in (1/2,1)$

$$\begin{aligned}\Lambda_{Y_jY_k}(-\gamma) = \frac{a4i\pi\csc(4\pi\gamma)}{(-1)^{\frac{1}{4}}u_kv^*_j - u^*_jv_k}\Bigg\{&\left(-\frac{v^*_j}{u^*_j}\right)^3\left[\frac{(-1)^{\frac{7}{8}}u^*_j}{v^*_j}\right]^{4\gamma} + \\ &+ (-1)^{\frac{1}{4}}\left(\frac{v_k}{u_k}\right)^3\left[\frac{(-1)^{\frac{1}{8}}u_k}{v_k}\right]^{4\gamma}\Bigg\}\end{aligned} \tag{C.13}$$

$\alpha = 1/5$, $\Re(\gamma) \in (3/5,1)$

$$\begin{aligned}\Lambda_{Y_jY_k}(-\gamma) = \frac{a5i\pi\csc(5\pi\gamma)}{-(-1)^{\frac{1}{5}}u_kv^*_j + u^*_jv_k}\Bigg\{&\left(\frac{v^*_j}{u^*_j}\right)^4\left[\frac{-(-1)^{\frac{9}{10}}u^*_j}{v^*_j}\right]^{5\gamma} + \\ &+(-1)^{\frac{1}{5}}\left(\frac{v_k}{u_k}\right)^4\left[\frac{(-1)^{\frac{1}{10}}u_k}{v_k}\right]^{5\gamma}\Bigg\}\end{aligned} \tag{C.14}$$

$\alpha = 1/10$, $\Re(\gamma) < 1$

$$\Lambda_{Y_j Y_k}(-\gamma) = \frac{a10i\pi \csc(10\pi\gamma)}{(-1)^{\frac{1}{10}} u_k v_j^* + u_j^* v_k} \left\{ \left(\frac{v_j^*}{u_j^*} \right)^9 \left[\frac{-(-1)^{\frac{19}{20}} u_j^*}{v_j^*} \right]^{10\gamma} + \right. \\ \left. + (-1)^{\frac{1}{10}} \left(\frac{v_k}{u_k} \right)^9 \left[\frac{(-1)^{\frac{1}{20}} u_k}{v_k} \right]^{10\gamma} \right\} \tag{C.15}$$

Bibliography

[1] Aigner, E., Lackner, R., Pichler, C., *Multiscale prediction of viscoelastic properties of asphalt concrete*, Journal of Materials in Civil Engineering, vol. 21 (12), pp. 771-780, 2009.

[2] Ala, G., Di Paola, M., Francomano, E., Li, Y., Pinnola, F.P., *Electrical analogous in viscoelasticity*, Communications in Nonlinear Science and Numerical Simulation, vol. 19 (7), pp. 2513-2527, 2014.

[3] Ala, G., Di Paola, M., Francomano, E., Li, Y., Pinnola, F.P., *Viscoelasticity: An electrical point of view*, International Conference on Fractional Differentiation and Its Applications, ICFDA 2014, 6967407, 2014.

[4] Alotta, G., Di Paola, M., *Probabilistic characterization of nonlinear systems under α-stable white noise via complex fractional moments*, Physica A, vol. 420, pp. 265-276, 2015.

[5] Alotta, G., Di Paola, M., Pinnola, F. P., *Cross-correlation and cross-power spectral density representation by complex fractional moments*, Physical Review E: statistical, nonlinear, and soft matter physics, *article under review*.

[6] Bagarello, F., *Fisica Matematica*, Zanichelli, Bologna, 2007.

[7] Bagley, R. L., Torvik, P., J., *Fractional Calculus - A Different Approach to the Analysis of Viscoelastically Damped Structures*, AIAA Journal, vol. 21 (5), pp. 741-748, 1983.

[8] Bagley, R. L., Torvik, P., J., *On the Appearance of the Fractional Derivative in the Behavior of Real Materials*, Journal of Applied Mechanics, vol. 51, pp. 294-298, 1984.

[9] Bagley, R. L., Torvik, P., J., *On the Fractional Calculus Model of Viscoelastic Behavior*, Journal of Reology, vol. 30 (1), pp. 133-155, 1986.

[10] Bagley, R. L., *Power Law and Fractional Calculus Model of Viscoelasticity*, AIAA Journal, vol. 27 (10), pp. 1412-1417, 1989.

[11] Barbato, M., Conte, J. P., *Spectral characteristics of non-stationary random processes: Theory and applications to linear structural models*, Probabilistic Engineering Mechanics, vol. 23, pp. 416-426, 2008.

[12] Barbato, M., Conte, J. P., *Structural reliability applications of nonstationary spectral characteristics*, Journal of Engineering Mechanics, vol. 137, pp. 371-382, 2011.

[13] Beyer, H., Kemplfe, S., *Definition of Physically Consistent Damping Laws with Fractional Derivates*, ZAMM - Journal of Applied Mathematics and Mechanics, vol. 75 (8), pp. 623-635, 1995.

[14] Bonilla, B., Rivero, M., Trujillo, J. J., *On systems of linear fractional differential equations with constant coefficients*, Applied Mathematics and Computation, vol. 187, pp. 68-78, 2007.

[15] Butera, S., Di Paola, M., *Fractional differential equations solved by using Mellin transform*, Communications in Nonlinear Science and Numerical Simulation, vol. 19, pp. 2220-2227, 2013.

[16] Butzer, P. L., Kilbas, A. A., Truillo, J., *Mellin Transform Analysis and Integration by Parts for Hadamard-Type Fractional Integrals*, Academic-Press, Journal of Analysis and Applications, vol. 270 (1), pp. 1-15, 2001.

[17] Caddemi, S. and Colajanni, P., Muscolino, G., *On the non stationary spectral moments and their role in structural safety and reliability*, Struct. Eng., Mech. and Computation, pp. 1113-1120, 2001.

[18] Caputo, M., *Elasticità e Dissipazione*, Zanichelli, Bologna, 1969.

[19] Caputo, M., *Linear models of dissipation whose Q is almost frequency independent-II*, Geophysical J. Royal Astronomic Society, vol. 13, pp. 529-539, 1967. (Reprinted recently in: Fract. Calc. Appl. Anal., vol. 11 (1), pp. 3-14, 2008).

[20] Carpinteri, A., Mainardi, F., *Fractal and Fractional Calculus in Continuum Mechanics*, CISM Courses and Lectures, Springer, Wien, 1997.

[21] Celauro, C., Di Paola, M., Lo Presti, D., Marino, F., Pirrotta, A., *Modeling of the Viscoelastic Behavior of Paving Bitumen Using Fractional Derivatives*, Meccanica dei Materiali e delle Strutture, vol. 1 (2), pp. 38-51, 2009.

[22] Christensen, R., *Theory of Viscoelasticity: An Introduction*, Elsevier, 1982.

[23] Corradi Dell'Acqua, L., *Meccanica delle Strutture: il comportamento dei corpi continui*, vol. 1, McGraw-Hill, Milano, 2010.

[24] Cottone, G., Di Paola, M., *On the use of fractional calculus for the probabilistic characterization of random variables*, Probabilistic Engineering Mechanics, vol. 24, pp. 321-330, 2009.

[25] Cottone, G., Di Paola, M., *A new representation of power spectral density and correlation function by means of fractional spectral moments*, Probabilistic Engineering Mechanics, vol. 25, pp. 348-353, 2010.

[26] Cottone, G., Di Paola, M. and Metzler, R., *Fractional calculus approach to the statistical characterization of random variables and vectors*, Physica A, vol. 389, pp. 909-920, 2010.

[27] Cottone, G., Di Paola, M., *Fractional spectral moments for digital simulation of multivariate wind velocity fields*, Journal of Wind Engineering and Industrial Aerodynamics, vol. 99, pp. 741-747, 2011.

[28] Cottone, G., Di Paola, M., Butera, S., *Stochastic dynamics of nonlinear system with a fractional power-law nonlinear term: The fractional calculus approach*, Probabilistic Engineering Mechanics, vol. 26, pp. 101-108, 2011.

[29] Courant, R., Hilbert, D., *Methods of Mathematical Physics vol. I*, McGraw-Hill, London, 1980.

[30] Deseri, L., Di Paola, M., Zingales, M., Pollaci, P., *Power-law hereditariness of hierarchical fractal bones*, International Journal for Numerical Methods in Biomedical Engineering, vol. 29 (12), pp. 1338-1360, 2013.

[31] Di Lorenzo, S., Pinnola, F. P., Pirrotta, A., *On the dynamics of fractional visco-elastic beams*, ASME 2012 International Mechanical Engineering Congress & Exposition, Houston, vol. 4, pp. 1273-1282, 2012.

[32] Di Lorenzo, S., Di Paola, M., Pinnola, F. P., Pirrotta, A., *Stochastic response of fractionally damped beams*, Probabilistic Engineering Mechanics, vol. 35, pp. 37-43, 2013.

[33] Di Matteo, A. and Di Paola, M., Pirrotta, A., *Probabilistic characterization of nonlinear systems under Poisson white noise via complex fractional moments*, Nonlinear Dynamics, vol. 77, pp. 729-738, 2014.

[34] Di Mino, G., Airey, G., Di Paola, M., Pinnola, F. P., D'Angelo, G., Lo Presti, D., *Linear and nonlinear fractional hereditary constitutive laws of asphalt mixtures*, Journal of Civil Engineering and Management, *article in press*, doi: 10.3846/13923730.2014.914104.

[35] Di Paola, M., *Complex fractional moments and their use for the solution of the Fokker Planck equation*, Vienna Congress on Recent Advances in Earthquake Engineering and Structural Dynamics (VEESD 2013), Paper No. 463, 2013.

[36] Di Paola, M., *Fokker planck equation solved in terms of complex fractional moments*, Probabilistic Engineering Mechanics, vol. 38, pp. 70-76, 2014.

[37] Di Paola, M., Pinnola, F. P., *Riesz Fractional Integrals and Complex Fractional Moments for the Probabilistic Characterization of Random Variables*, Probabilistic Engineering Mechanics, vol. 29, pp. 149-156, 2012.

[38] Di Paola, M., Pinnola, F. P., Zingales, M., *Fractional multi-phase hereditary materials: Mellin transform and multi-scale fractances*, European Congress on Computational Methods in Applied Sciences and Engineering (ECCOMAS 2012), e-Book Full Papers, pp. 4735-4745, 2012.

[39] Di Paola, M., Pinnola, F. P., Zingales, M., *A Discrete Mechanical Model of Fractional Hereditary Materials*, Meccanica: an International Journal of Theoretical and Applied Mechanics, vol. 48 (7), pp. 1573-1586, 2013.

[40] Di Paola, M., Pinnola, F. P., Zingales, M., *Fractional differential equations and related exact mechanical models*, Computers and Mathematics with Applications, vol. 66 (5), pp. 608-620, 2013.

[41] Di Paola, M., Pirrotta, A., *Fractional Calculus - Application to Visco-Elastic Solids*, Meccanica dei Materiali e delle Strutture, vol. 1 (2), pp. 52-62, 2009.

[42] Di Paola, M., Pirrotta, A., Valenza, A., *Visco-elastic behavior through fractional calculus: an easier method for best fitting experimental results*, Mechanics of materials, vol. 43, pp. 799-806, 2011.

[43] Di Paola, M., Fiore, V., Pinnola, F. P., Valenza, A., *On the influence of the initial ramp for a correct definition of the parameters of fractional viscoelastic materials*, Mechanics of Materials, vol. 69, pp. 63-70, 2014.

[44] Di Paola, M., Heuer, R., Pirrotta, A., *Fractional visco-elastic Euler-Bernoulli beam*, International Journal of Solids and Structures, vol. 50, pp. 3505-3510, 2013.

[45] Di Paola, M., Zingales, M., *Exact mechanical models of fractional hereditary materials*, Journal of Rheology, vol. 56 (5), pp. 983-1004, 2012.

[46] Escobedo-Torres, J., Ricles, J. M., *The fractional order elastic-viscoelastic equations of motion: Formulation and solution method*, Journal of Intelligent Material Systems and Structures, vol. 29, pp. 489-502, 1998.

[47] Evangelatos, G. I., Spanos, P. D., *An accelerated Newmark scheme for integrating the equation of motion of nonlinear systems comprising restoring elements governed by fractional derivatives*, Recent advances in mechanics, part 1, pp. 159-177, 2011.

[48] Flügge, W., *Viscoelasticity*, Blaisdell Publishing Company, Waltham, 1967.

[49] Gaul, L., Schmidt, A., *FE Implementation of Viscoelastic Constitutive Stress-Strain Relations Involving Fractional Time Derivatives*, A. A. Balkema Publisher, Constitutive Models for Rubber II, pp. 79-89, Tokyo, 2001.

[50] Gemant, A., *A Method of Analyzing Experimental Results Obtained from Elasto-Viscous Bodies*, Physics, vol. 7, pp. 311-317, 1936.

[51] Gemant, A., *On Fractional Differentials*, The Philosophical Magazine, vol. 25, pp. 540-549, 1938.

[52] Gerasimov, A. N., *A generalization of linear laws of deformation and its application to inner friction problems*, Prikl. Mat. Mekh., vol. 12, pp. 251-259, 1949, (in Russian).

[53] Gorenflo, R., Luchko, Y., Mainardi, F., *Analytical properties and applications of the Wright function*, Fractional Calculus and Applied Analysis, vol. 2 (4), pp. 383-414, 1999.

[54] Gorenflo, R., Mainardi, F., *Fractional Calculus: integral and differential equations of fractional order*, da Carpinteri e Mainardi [20].

[55] Gorenflo, R., Mainardi, F., *On Mittag-Leffler-Type Functions in Fractional Evolution Processes*, Journal of Computational and Applied Mathematics, vol. 118 (1-2), pp. 283-299, 2000.

[56] Gradshteyn, I. S., Ryzhik, I. M.,*Table of Integrals, Series, and Products*, Daniel Zwillinger, 2000.

[57] Gzyl, H., Inverardi, P. N., Tagliani, A., Villasana, M., *Maxentropic solution of fractional moment problems*, Applied Mathematics and Computation, vol. 173 (1), pp. 109-125, 2006.

[58] Gzyl, H., Tagliani, A., *Hausdorff moment problem via fractional moments*, Applied Mathematics and Computation, vol. 216 (11), pp. 3319-3328, 2010.

[59] Heymans, N., Bauwens, J. C., *Fractal rheological models and fractional differential equations for viscoelastic behavior*, Rheological Acta, vol. 33, pp. 210-219, 1994.

[60] Hilfer, R., Application of Fractional Calculus in Physics, World Scientific, Singapore, 2000.

[61] Inverardi, P. N., Petri, A., Pontuale, G., Tagliani, A., *Stieltjes moment problem via fractional moments*, Applied Mathematics and Computation, vol. 166 (3), pp. 664-667, 2005.

[62] Jones, R. M., *Mechanics of Composite Materials*, Taylor & Francis, Philadelphia, 1999.

[63] Kelley, S. S., Rials, T. G., Glasser, W. G., *Relaxation behaviour of the amorphous behaviour the amorphous components of wood*, Journal of Materials Science, vol. 22, pp. 617-624, 1987.

[64] Kilbas, A. A., Srivastave, H. M., Trujillo, J. J., *Theory and Applications of Fractional Differential Equations*, Elsevier, Amsterdam, 2006.

[65] Kilbas, A. A., Trujillo, J. J., *Differential equations of fractional order:methods results and problem I*, Applicable Analysis, vol. 78 (1-2), pp. 153-192, 2001.

[66] Kilbas, A. A., Trujillo, J. J., *Differential equations of fractional order:methods results and problem II*, Applicable Analysis, vol. 81 (2), pp. 435-493, 2002.

[67] Kouchi, S., *Eigenvalues and eigenvectors of tridiagonal matrices*, Electronic Journal of Linear Algebra, vol. 15, pp. 115-133, 2006.

[68] Lewandowski, R.,Pawlak, Z., *Dynamic analysis of frames with viscoelastic dampers modelled by rheological models with fractional derivatives*, vol. 330, pp. 923-936, 2011.

[69] Li, L., Hu, Y., Wang, X, *Improved approximate methods for calculating frequency response function matrix and response of MDOF systems with viscoelastic hereditary terms*, Journal of Sound and Vibration, vol. 332, pp. 3945-3956, 2013.

[70] Li, M., Lim, S. C., Chen, S., *Exact Solution of Impulse Response to a Class of Fractional Oscillators and Its Stability*, Mathematical Problems in Engineering, Article ID 657839, 2011.

[71] Luongo, A., Paolone, A., *Scienza delle Costruzioni: il continuo di Cauchy*, vol. 1, Casa Editrice Ambrosiana, Milan, 2005.

[72] Malvern, L. E., *Introduction to the Mechanics of a Continuous Medium*, Prentice-Hall, Inc., Englewood Cliffs (NJ), 1969.

[73] Mandelbrot, B. B., *The Fractal Geometry of Nature*, W. H. Freeman & Co., New York, 1982.

[74] Mainardi, F., *Fractional Calculus and Waves in Linear Viscoelasticity*, Imperial College Press-World Scientific Publishing Co. Pte. Ltd., London, 2010.

[75] Meirovitch, L., Principles and Techniques of Vibrations, Prentice-Hall International, Inc., New Jersey, 1997.

[76] Michaelov, G. and Sarkani, S. and Lutes, L., *Spectral characteristics of nonstationary random processes response of a simple oscillator*, Structural Safety, vol. 21, pp. 245-267, 1999.

[77] Miller, K. S., Ross, B., *An Introduction to the Fractional Calculus and Fractional Differential Equations*, Wiley-InterScience, New York, 1993.

[78] Müller, S., Kästner, M., Brummund, J., Ulbricht, V., *A nonlinear fractional viscoelastic material model for polymers*, Computational Materials Science, vol. 50, pp. 2938-2949, 2011.

[79] Muscolino, G., *Non-stationary pre-envelope covariances of non-classically damped systems*, Journal of Sound and Vibration, vol. 149, pp. 107-123, 1991.

[80] Narahari Achar, B.N., Hanneken, J.W., Enck, T., Clarke, T., *Dynamics of the fractional oscillator*, Physica A, vol. 297, pp. 361-367, 2001.

[81] Noll, W., *A new mathematical theory of simple materials*, Archive for Rational Mechanics and Analysis, vol. 48 (1), pp. 1-50, 1972.

[82] Nutting, P. G., *A New General Law of Deformation*, Journal of the Franklin Institute, vol. 191, pp. 679-685, 1921.

[83] Oldham, K. B., Spainer, J., *The Fractional Calculus: Theory and applications of differentiation and integration to arbitrary order*, Academic Press, New York, 1974.

[84] Ostalczyk, P. W., *A Note on the Grünwald-Letnikov Fractional-Order Backward-Difference*, Physica Scripta, vol. 136, 2009.

[85] Paris, R. B. and Kaminski, D., *Asymptotics and Mellin-Barnes Integrals*, Cambridge University Press, New York, 2001.

[86] Pawlak, Z., Lewandowski, R., *The continuation method for the eigenvalue problem of structures with viscoelastic dampers*, vol. 125, pp. 53-61, 2013.

[87] Petrucci, G. and Di Paola, M. and Zuccarello, B., *On the characterization of dynamic properties of random processes by spectral parameters*, Journal of Applied Mechanics, vol. 67, pp. 519-526, 2000.

[88] Pinsky, M. A., *Partial Differential Equations and Boundary-Value Problems*, WCB McGraw-Hill, Boston, 1998.

[89] Pioletti, D. P., Rakotomanana, L. R., Benvenuti, J.-F., Leyvraz, P.-F., *Viscoelastic constitutive law in large deformations: Application to human knee ligaments and tendons*, Journal of Biomechanics, vol. 31 (8), pp. 753-757, 1998.

[90] Pioletti, D. P., Rakotomanana, L. R., *Non-linear viscoelastic laws for soft biological tissues*, Source of the Document European Journal of Mechanics, A/Solids, vol. 19 (5), pp. 749-759, 2000.

[91] Podlubny, I., *Fractional differential equations*, Academic Press, San Diego, 1999.

[92] Pokrovkii, V. N., *The Mesoscopic Theory of Polymer Dynamics*, Springer, Springer Series in Chemical Physics, vol. 95, 2nd Ed., pp. 256, 2010.

[93] Reiner, M., *The Deborah number*, Phys. Today, vol. 17, pp. 62, 1964.

[94] Riande, E., Dìaz-Calleja, R., Prolongo, M. G., Masegosa, R. M., Salom, C., *Polymer Viscoelasticity, stress and strain in practice*, Marcel Dekker, Inc., New York, 2000.

[95] Roberts, J. B., Spanos, P. D., *Random Vibration and Statistical Linearization*, Dover Publication, Inc., New York, 1999.

[96] Rossetti, C., *Metodi Matematici per la Fisica*, Libreria Editrice Universitaria Levrotto & Bella, Torino, 1982.

[97] Rossikhin, Y. A., Shitikova, M. V., *A new method for solving dynamic problems of fractional derivative viscoelasticity*, International Journal of Engineering Science, vol. 39, pp. 149-176, 2001.

[98] Runtemund, K and Cottone, G. and Müller, G., *Treatment of arbitrarily autocorrelated load functions in the scope of parameter identification*, Computer and Structures, vol. 126, pp. 29-40, 2013.

[99] Samko, G. S., Kilbas, A. A., Marichev, O. I., *Fractional Integrals and Derivatives: Theory and Applications*, New York (NY): Gordon and Breach, 1993.

[100] Schiessel, H., Blumen, A., *Hierarchical Analogues to Fractional Relaxation Equations*, Journal of Physics A: Mathematical and General, vol. 26, pp. 5057-5069, 1993.

[101] Schiessel, H., Blumen, A., *Mesoscopic Pictures of the Sol-Gel Transition: Ladder Models and Fractal Network*, Macromolecules, vol. 28, pp. 4013-4019, 1995.

[102] Schiessel, H., Metzeler, R., Blumen, A., Nonnenmacher, T. F., *Generalized Viscoelastic Models: their Fractional Equations with Solutions*, Journal of Physics A: Mathematical and General, vol. 28, pp. 6567-6584, 1995.

[103] Schmidt, A., Gaul L., *Finite element formulation of viscoelastic constitutive equations using fractional time derivatives*, Nonlinear Dynamics, vol. 29 (1), pp. 37-55, 2002.

[104] Schmidt, A., Gaul, L., *On a critique of a numerical scheme for the calculation of fractionally damped dynamical systems*, Mechanics Research Communications, vol. 33 (1), pp. 99-107, 2006.

[105] Schmidt, A., Gaul, L., *On the numerical evaluation of fractional derivatives in multi-degree-of-freedom systems*, Signal Processing, vol. 86 (10), pp. 2592-2601, 2006.

[106] Shawn, M. T., Macknight, W. J., *Itroduction to Polymer Viscoelasticity*, Wiley-InterScience, Hoboken, New Jersey, 2005.

[107] Shinozuka, M., Deodatis, G., *Stochastic process models for earthquake ground motion*, Probabilistic Engineering Mechanics, vol. 3, pp. 114-123, 1998.

[108] Singh, M.P., Chang, T.-S., Nandan, H., *Algorithms for seismic analysis of MDOF systems with fractional derivatives*, Engineering Structures, vol. 33, pp. 2371-2381, 2011.

[109] Scott Blair, G. W., Caffyn, J. E., *An application of the theory of quasi-properties to the treatment of anomalous strain-stress relations*, The Philosophical Magazine, vol. 40 (300), pp. 80-94, 1949.

[110] Scott Blair, G. W., *The subjective assessment of the consistency of materials in relation to physical measurements*, The Journal of Society of Cosmetic Chemist, vol. 17, pp. 45-56, 1966.

[111] Scott Blair, G. W., *Psychorheology: Links Between the Past and the Present*, Journal of Texture Studies, vol. 5, pp. 3-12, 1974.

[112] Slonimsky, G. L., *On the law of deformation of highly elastic polymeric bodies*, Dokl. Akad. Nauk SSSR, vol. 140 (2), pp. 343-346, 1961, (in Russian).

[113] Spanos, P. D., Miller, M., *Linear system spectral moments determination*, Proceeding of the Sixth Spec. Conf. on Prob. Mech. Struct. and Geo. Rel., ASCE, Denver, 1992.

[114] Spanos, P. D., Miller, S., *Hilbert transform generalization of a classical random vibration integral*, Journal of Applied Mechanics, vol. 61, pp. 575-581, 1994.

[115] Spanos, P. D., Evangelatos, G. I., *Response of a non-linear system with restoring forces governed by fractional derivatives-Time domain simulation and statistical linearization solution*, Soil Dynamics and Earthquake Engineering, vol. 30, pp. 811-821, 2010.

[116] Stanislavsky, A. A., *Fractional oscillator*, Physical review E: statistical, nonlinear, and soft matter physics, vol. 70, pp. 051103-1-051103-6, 2004.

[117] Suarez, L. E., Shokooh, A., *An Eigenvectors Expansion Method for the Solution of Motion Containing Fractional Derivatives*, Journal of Applied Mechanics, vol. 64, pp. 629-635, 1997.

[118] Szpankowski, W., *Average Case Analysis of Algorithms on Sequences*, John Wiley & Sons, inc., New York, 2001.

[119] Vanmarcke, E., *Properties of spectral moments with applications to random vibrations*, Journal of Engineering Mechanics, vol. 98, pp. 425-446, 1972.

[120] Viola, E., *Scienza delle Costruzioni: teoria dell'elasticità*, vol. 1, Pitagora Editrice, Bologna, 1990.

[121] Wang, F.-Z., Liu, Z.-C., Hu, S.-G., *Influence of loading rate on compressive strength of CA mortar*, Beijing Gongye Daxue Xuebao - Journal of Beijing University of Technology, vol. 34 (10), pp. 1059-1065, 2008.

[122] Weisstein, E. W., *Binomial Coefficient*, http//mathworld.wolfram.com/BinomialCoefficient.html, da Wolfram MathWorld.

[123] Weisstein, E. W., *Gamma Function*, http://mathworld.wolfram.com/GammaFunction.html, da Wolfram MathWorld.

[124] Weisstein, E. W., *Fourier Transform*, http://mathworld.wolfram.com/FourierTransform.html, da Wolfram MathWorld.

[125] Weisstein, E. W., *Laplace Transform*, http://mathworld.wolfram.com/LaplaceTransform.html, da Wolfram MathWorld.

[126] Weisstein, E. W., *Mellin Transform*, http://mathworld.wolfram.com/MellinTransform.html, da Wolfram MathWorld.

[127] Weisstein, E. W., *Mittag-Leffler Function*, http://mathworld.wolfram.com/Mittag-LefflerFunction.html, da Wolfram MathWorld.

[128] Weisstein, E. W., *Wright Function*, http://mathworld.wolfram.com/WrightFunction.html, da Wolfram MathWorld.

[129] Wen-Chyuan Yueh, *Eigenvalues of several tridiagonal matrices*, Applied Mathematics E-Notes, vol. 5, pp. 66-74, 2005.

[130] Yuan, L., Agrawal, O. P., *A numerical scheme for dynamic system containing fractional derivatives*, Journal of Vibration and Acoustic, vol. 124 (2), pp. 321-324, 2002.

[131] Zhang, M., Nigwekar, P., Castaneda, B., Hoyt, K., Joseph, J. V., Di Sant'Agnese, A., Messing, E. M., Strang, J. G., Rubens, D. J., Parker, K. J., *Quantitative Characterization of Viscoelastic Properties of Human Prostate Correlated with Histology*, Ultrasound in Med. & Biol., vol. 34 (7), pp. 1033-1042, 2008.

[132] Zhou, H., Wang, C. P., Han, B. B., Duan Z. Q., *A Creep Constitutive Model for Salt Rock Based on Fractional Derivatives*, International Journal of Rock Mechanics and Mining Sciences, vol. 48 (1), pp. 116-121, 2011.

[133] Zhu, Z. Y., Li, G. G., Cheng, C. J., *A numerical method for fractional integral with application*, Applied Mathematics and Mechanics, vol. 24, pp. 373-384, 2003.

Acknowledgements

I am immensely grateful to my mentor, Prof. Mario Di Paola, for his wise guide, his teaching capabilities, and his scientific character. His suggestions were fundamental in my research path. He was able to instill in me such curiosity, and desire for learning and knowledge, that made this period fruitful, interesting and unforgettable.

A great thanks goes to my illustrious supervisor, Prof. Pol D. Spanos from Rice University, for his hospitality during my time in Houston. His precious suggestions improved this thesis significantly, and the meaningful meetings permitted to develop some important topics in my research activities.

I wish to thank Prof. Antonina Pirrotta, Prof. Massimiliano Zingales, Prof. Giuseppe Failla, Prof. Antonino Valenza, and Dr. Vincenzo Fiore for their support in many occasions, thanks to them I found an inspiring and charming research group. Thanks to my colleagues Pietro, Gioacchino, Gianluca, Salvo, Alberto, and Emma for the scientific discussions, collaborations, and friendly moments. I am also thankful to all Ph.D. advisor board and to the members of the Department of Civil, Environmental, Aerospace, and Materials Engineering. For their help and patience I have to thank Ruggero Garaffa and Maria Rita Cinà of the Department Library.

An important and invaluable thanks is addressed to my parents for their constant support and encouragement, and to Fabio and Graziamaria for having always believing in me.

Last but not the least, a special thanks goes to Lorenza, who shared every moment during these years supporting and challenging me always with love, to her this manuscript is dedicated.

Francesco Paolo Pinnola
Palermo, December 2014